

Structure and Evolution of Galaxies

Tsutomu T. TAKEUCHI

*Division of Particle and Astrophysical Science,
Nagoya University*

Second Cosmology School, Kielce

Nagoya



Nagoya



Nagoya



Nagoya



Contents

Part I: Galaxy Structure

1. Elliptical Galaxy
2. Spiral Galaxy

Part II: Galaxy Evolution

3. Luminosity Function of Galaxies
4. Chemical Evolution of Galaxies

Part III: Formation of Structures and Galaxies

5. Structure Formation I
6. Structure Formation II
7. Galaxy Formation

Part I: Galaxy Structure

1. Elliptical Galaxy

1.1 Self-gravitating system

1.2 Stellar dynamics

1.3 Structure and classification of elliptical galaxies

1.4 Mass of elliptical galaxies

1.5 Scaling relations for elliptical galaxies

1.1 Self-gravitating system

Virial theorem of N -body system

The equation of motion of N -body system is

$$m^i \ddot{x}_\beta^i = - \frac{\partial}{\partial x_\beta^i} \sum_{(j \neq i)}^N \Phi^{(ij)}, \quad \beta = 1, 2, 3; \quad i = 1, 2, \dots, N \quad (1)$$

where a gravitational potential made by these particles themselves is

$$\Phi^{(ij)} = -Gm^i m^j |\vec{x}^j - \vec{x}^i|^{-1}$$

Multiplying x_α^i on both sides yields

$$\sum_i m^i x_\alpha^i \ddot{x}_\beta^i = - \sum_{(i, j \neq i)} x_\alpha^i \frac{\partial}{\partial x_\beta^i} \Phi^{(ij)} \quad (2)$$

Virial theorem of N -body system

The rhs of eq. (2) is a potential-energy tensor

$$W_{\alpha\beta} \equiv - \sum_{(i,j \neq i)} x_{\alpha}^i \frac{\partial}{\partial x_{\beta}^i} \Phi^{(ij)} = \sum G m^i m^j \frac{x_{\alpha}^i (x_{\beta}^j - x_{\beta}^i)}{|\vec{x}^j - \vec{x}^i|^3} \quad (3)$$

Since eq. (3) is symmetric under an interchange between i and j , we obtain

$$W_{\alpha\beta} = -\frac{1}{2} G \sum_{(i,j \neq i)} m^i m^j \frac{(x_{\alpha}^j - x_{\alpha}^i)(x_{\beta}^j - x_{\beta}^i)}{|\vec{x}^j - \vec{x}^i|^3}$$

Also, the above is symmetric for α and, β , the rhs of eq. (2) is also symmetric. Then, it leads

$$\sum_i m^i x_{\alpha}^i \ddot{x}_{\beta}^i = \frac{1}{2} \sum m^i (x_{\alpha}^i \ddot{x}_{\beta}^i + \ddot{x}_{\alpha}^i x_{\beta}^i) = \frac{1}{2} \frac{d^2 I_{\alpha\beta}}{dt^2} - 2K_{\alpha\beta} \quad (4)$$

Virial theorem of N -body system

Thus, we obtain the so-called “tensor virial theorem”

$$\frac{1}{2} \frac{d^2 I_{\alpha\beta}}{dt^2} = 2K_{\alpha\beta} + W_{\alpha\beta} \quad (5)$$

where

$$I_{\alpha\beta} \equiv \sum m^i x_{\alpha}^i x_{\beta}^i, K_{\alpha\beta} \equiv \frac{1}{2} \sum m^i \dot{x}_{\alpha}^i \dot{x}_{\beta}^i$$

If we take the trace of eq.(5), we have the scalar virial theorem

$$\ddot{I} = 2K + W$$

$$I = \frac{1}{2} \sum m^i |\vec{x}^i|^2, W = -\sum_{i>j} Gm^i m^j / |\vec{x}^j - \vec{x}^i| \approx -\frac{GM^2}{2R},$$

$$K = \frac{1}{2} \sum m^i |\dot{\vec{x}}^i|^2 \approx \frac{MV^2}{2}$$

Virial theorem of N -body system

In the case of virial equilibrium, we have

$$2K + W = 0 \quad (6)$$

Recall that the total energy of the system is

$$E = K + W \quad (7)$$

Therefore, we have

$$E = -K = \frac{W}{2} \quad (8)$$

The specific heat of a self-gravitating system

This implies that **if we take away the energy from the system, the kinetic energy *increases*.**

$$E = -K = \frac{W}{2} \quad (8)$$

Namely, the specific heat of the system is negative.

The specific heat of a self-gravitating system

This implies that **if we take away the energy from the system, the kinetic energy *increases*.**

$$E = -K = \frac{W}{2} \quad (8)$$

Namely, **the specific heat of the system is negative.**

This leads to a very important conclusion that a self-gravitating system does not have an equilibrium.

The specific heat of a self-gravitating system

This implies that **if we take away the energy from the system, the kinetic energy *increases*.**

$$E = -K = \frac{W}{2} \quad (8)$$

Namely, **the specific heat of the system is negative.**

This leads to a very important conclusion that a self-gravitating system does not have an equilibrium.

Because of this special property, structures spontaneously emerge in self-gravitating system (self-organization)!

This is called the gravothermal catastrophe.

Virial equilibrium and dynamical timescale

In the case of virial equilibrium, we have

$$2K + W = 0$$

Then,

$$V^2 \approx \frac{GM}{R}$$

In this case, the dynamical timescale is evaluated by

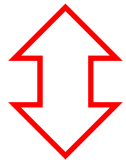
$$\begin{aligned} t_{\text{cross}} \text{ (crossing time)} &\approx R / V \approx \left(\frac{R^3}{GM} \right)^{\frac{1}{2}} \\ &\approx \frac{1}{\sqrt{G\rho}} \approx t_{\text{dyn}} \text{ (dynamical time)} \end{aligned}$$

1.2 Stellar dynamics

Large stellar system as a collisionless system

Collisional system

The system where the two-body interaction is working effectively within a timescale under consideration (in our case, **the age of the Universe**).



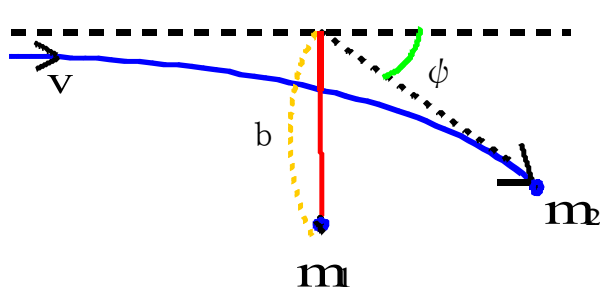
Collisionless system

The system where the two-body interactions does not work effectively.

But what timescale should we use to evaluate the effect of collision?

Relaxation time

For this purpose, we estimate **“the two-body relaxation time”** of the system. We set as follows:



$$\tan\left(\frac{\psi}{2}\right) = \frac{G(m_1 + m_2)}{v^2 b}$$
$$\frac{\Delta v}{v} = 2 \sin\left(\frac{\psi}{2}\right)$$

A number of scattering of stars with velocity $(v, v+dv)$ and impact parameter $(b, b+db)$ in a time interval dt is expressed as

$$2\pi b f(v, t) v dt db dv$$

Then, we evaluate an accumulated effect of small angle scatterings with a mean square velocity change Δv^2 ($\Delta v \ll v$).

Relaxation time

The amount of Δv is evaluated as

$$\frac{\Delta v}{v} \approx \Psi \approx \frac{4Gm}{v^2 b} \rightarrow (\Delta v)^2 \approx \frac{16G^2 m^2}{v^2 b^2}$$

Then, the amplitude of a velocity change is given by

$$(\Delta v)^2 \times 2\pi b f(v, t) v dt db dv = 32\pi G^2 m^2 \frac{1}{v} \frac{1}{b} f(v) dt db dv$$

By using these equations, we estimate the accumulated effect by evaluating $\int dt db dv$

Relaxation time

Since

$$\int_0^{\infty} v^{-1} f(v) dv = n \langle v^{-1} \rangle, \quad \int_{b_1}^{b_2} \frac{db}{b} = \ln \left(\frac{b_2}{b_1} \right)$$

Here, $b_2 = R$ (system size) and let $b_1 =$ impact parameter of 90° scattering, then

$$\tan \left(\frac{\pi}{4} \right) = 1 = \frac{2Gm}{v^2 b} \rightarrow b = \frac{2Gm}{v^2}$$

Thus we obtain

$$\ln \left(\frac{b_2}{b_1} \right) = \ln \left(\frac{Rv^2}{2Gm} \right)$$

Using virial equilibrium, we see

$$v^2 \approx \frac{GmN}{R},$$

Relaxation time

Hence,

$$\ln\left(\frac{b_2}{b_1}\right) = \ln\left(\frac{N}{2}\right)$$

Thus, we obtain

$$\left(\frac{\Delta v}{v}\right)^2 \approx 32\pi G^2 m^2 n v^{-3} \ln\left(\frac{N}{2}\right) t$$

By using this relation, we can estimate the relaxation time, t_{relax} , in which $\Delta v/v = 1$,

$$t_{\text{relax}} = \frac{v^3}{32\pi G^2 m^2 n \ln\left(\frac{N}{2}\right)} = \frac{v^3 R^3}{24G^2 m M \ln\left(\frac{N}{2}\right)} = \frac{0.04N}{\ln\left(\frac{N}{2}\right)} t_{\text{cross}}$$

(the second step we have used $M = 4\pi m n R^3/3$, and the third step $v^2 = GmN/R$).

Astrophysical examples

Globular clusters

$$N \sim 10^5-6, R \sim 20\text{pc}, v \sim 10\text{kms}^{-1}$$

$$t_r \sim 10^8 \text{ yr} \ll 10^{10} \text{ yr} (\sim \text{the age of the Universe})$$

\Rightarrow collisional system.



ω Centauri

Elliptical galaxies

$$N \sim 10^{10-12}, R \sim 10-100\text{kpc}, v \sim 200\text{kms}^{-1}$$

$$t_r \sim 10^{18} \text{ yr} \gg 10^{10} \text{ yr}$$

\Rightarrow collisionless system!



M87

Basic equation: collisionless Boltzmann equation (CBE)

Fluid:

local equilibrium \ll dynamical time \ll global equilibrium

\Rightarrow can be described only as a function of position.

Stellar system:

dynamical time \ll local equilibrium \sim global equilibrium

\Rightarrow depends on position and motion independently (6-dim phase space)

\Rightarrow described by probability distribution function (DF) or phase density function $f(\vec{x}, \vec{v}, t)$.

This is related to density as

$$\rho(\vec{x}) = \int d^3v f(\vec{x}, \vec{v})$$

Basic equation: collisionless Boltzmann equation (CBE)

Collisionless system:

A point in the phase space does not jump but moves smoothly, *i.e.*, the “phase fluid” conserves mass. Hence, the distribution function (DF) conserves along a streamline.

$$\frac{df}{dt} = \frac{\partial f}{\partial t} + \frac{\partial}{\partial \vec{w}} (f \dot{\vec{w}}) = 0, \vec{w} = (\vec{x}, \vec{v})$$

$$\left(\text{cf. fluid: } \frac{d\rho}{dt} = \frac{\partial \rho}{\partial t} + \frac{\partial}{\partial \vec{x}} (\rho \dot{\vec{x}}) = 0 \right)$$

$$\rightarrow \frac{\partial f}{\partial t} + \vec{v} \frac{\partial}{\partial \vec{x}} f - \frac{\partial \Phi}{\partial \vec{x}} \frac{\partial f}{\partial \vec{v}} = 0.$$

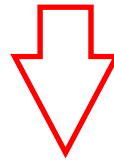
And density should suffice Poisson eq. at the same time

$$\nabla \Phi = 4 \pi G \rho = 4 \pi G \int d^3 \vec{v} f(\vec{x}, \vec{v})$$

Jeans equation

Then, we derive **Jeans equation** to describe stellar system.
We multiply $v_i^l v_j^m v_k^n$ on both sides of the CBE and integrate over velocity (to obtain moment equations):

$$\frac{\partial f}{\partial t} + \vec{v} \cdot \frac{\partial f}{\partial \vec{x}} - \frac{\partial \Phi}{\partial \vec{x}} \cdot \frac{\partial f}{\partial \vec{v}} = 0$$



$$\int v_i^l v_j^m v_k^n \frac{\partial f}{\partial t} d^3 v + \int v_i^l v_j^m v_k^n \vec{v} \cdot \frac{\partial f}{\partial \vec{x}} d^3 \vec{v} - \frac{\partial \Phi}{\partial \vec{x}} \int v_i^l v_j^m v_k^n \frac{\partial f}{\partial \vec{v}} d^3 \vec{v} = 0,$$

$$\overline{\rho v_i^l v_j^m v_k^n} \equiv \int v_i^l v_j^m v_k^n f d^3 \vec{v}$$

Jeans equation: continuum equation (zeroth order)

$$\int \frac{\partial f}{\partial t} d^3\vec{v} + \int \vec{v} \cdot \frac{\partial f}{\partial \vec{x}} d^3\vec{v} - \frac{\partial \Phi}{\partial \vec{x}} \cdot \int \frac{\partial f}{\partial \vec{v}} d^3\vec{v} = 0$$

1. **First term: by definition, $\rho = \int f d^3\vec{v}$,**
2. **Use $\vec{v} \equiv \frac{1}{\rho} \int \vec{v} f d^3\vec{v}$,**
3. **By using the divergence theorem, the volume integral is transformed into a surface integral, and let $f \rightarrow 0$ rapidly as $|\vec{v}| \rightarrow \infty$.**

Thus we have the continuum equation

$$\frac{\partial \rho}{\partial t} + \frac{\partial(\rho \vec{v})}{\partial \vec{x}} = 0 \quad (6)$$

Jeans equation: equation of motion (first order)

$$\frac{\partial(\rho\bar{v}_l)}{\partial t} + \sum_k \frac{\partial(\rho\overline{v_k v_l})}{\partial x_k} + \rho \frac{\partial\Phi}{\partial x_l} = 0 \quad (7)$$

Defining a velocity dispersion tensor as

$$\sigma_{kl}^2 = \overline{(v_k - \bar{v}_k)(v_l - \bar{v}_l)} = \overline{v_k v_l} - \bar{v}_k \bar{v}_l \quad (8)$$

and using the continuum equation [eq. (5)], we obtain

$$\rho \frac{\partial\bar{v}_l}{\partial t} + \rho \sum_k \bar{v}_k \frac{\partial\bar{v}_l}{\partial x_k} = -\rho \frac{\partial\Phi}{\partial x_l} - \frac{\partial(\rho\sigma_{kl}^2)}{\partial x_k} \quad (9)$$

Here we used

$$\int v_i \frac{\partial f}{\partial v_j} d^3\vec{v} = -\int \frac{\partial v_i}{\partial v_j} f d^3\vec{v} = -\delta_{ij} \rho$$

Jeans equation

Equation (9) is called **Jeans equation**

$$\rho \frac{\partial \bar{v}_l}{\partial t} + \rho \sum_k \bar{v}_k \frac{\partial \bar{v}_l}{\partial x_k} = -\rho \frac{\partial \Phi}{\partial x_l} - \frac{\partial (\rho \sigma_{kl}^2)}{\partial x_k}$$

This is similar to **Euler equation** for fluid mechanics:

1. Lhs is a Lagrange differential of mean velocity along with a streamline.
2. First term of rhs is the gravitation.
3. Second term of rhs corresponds to pressure gradient, but different from ordinary fluid, it is **anisotropic** tensor.

To know σ_{kl}^2 , we need the next-order moment eq.

⇒ We adopt some assumption to solve this equation.

1.3 Structure and classification of elliptical galaxies

Introduction: ellipticals as complicated system

Until the late 1970s, it was believed that elliptical galaxies are simple systems: gas-free, disk-free, rotationally flattened ellipsoids of very old stars. In the last 20 years, most of these assumptions turned out to be wrong or only crude approximations:

- 1. Massive ellipticals are not flattened by rotation, but are anisotropic.**
- 2. Ellipticals do have an interstellar medium, but it is hot $T > 10^6\text{K}$.**
- 3. A significant fraction of ellipticals exhibits kinematic peculiarities (like counter-rotating cores) which point to a 'violent' formation process.**
- 4. Low mass ellipticals seem to contain intermediate age stars.**
- 5. All ellipticals and bulges seem to contain supermassive black holes amounting to about 0.2% of their mass.**

Classification of ellipticals

1. Normal ellipticals

- i. Giant elliptical(gE's),
- ii. E's,
- iii. compact elliptical (cE's),
- iv. (S0 galaxies).

Absolute magnitude range: $M_B = -23 \sim -15$.

2. Dwarf elliptical(dE's)

Comparing with cE's, they have

- a. smaller surface brightness,
- b. more metal-poor

3. cD galaxies

- a. have absolute magnitude $M_B \sim -25$
- b. usually located near cluster center
- c. have extended diffuse envelope
- d. have high M/L

Classification of ellipticals

4. Blue compact dwarf galaxies (BCDs)

have $B - V = 0.0 \sim 0.3$,

very gas-rich

often with intense star formation (in this sense, they are not exactly ellipticals).

5. Dwarf spheroidal galaxy

have very low luminosity ($M_B \sim -8$),

have very low surface brightness.

1



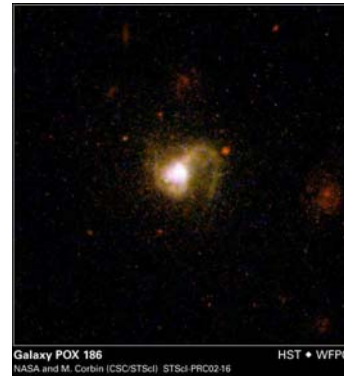
2



3



4



5



Structure: de Vaucouleurs profile

Profiles of E's and cD's obey **de Vaucouleurs law**.

$$I(r) = I_e \cdot 10^{-3.33((r/r_e)^{1/4}-1)}$$

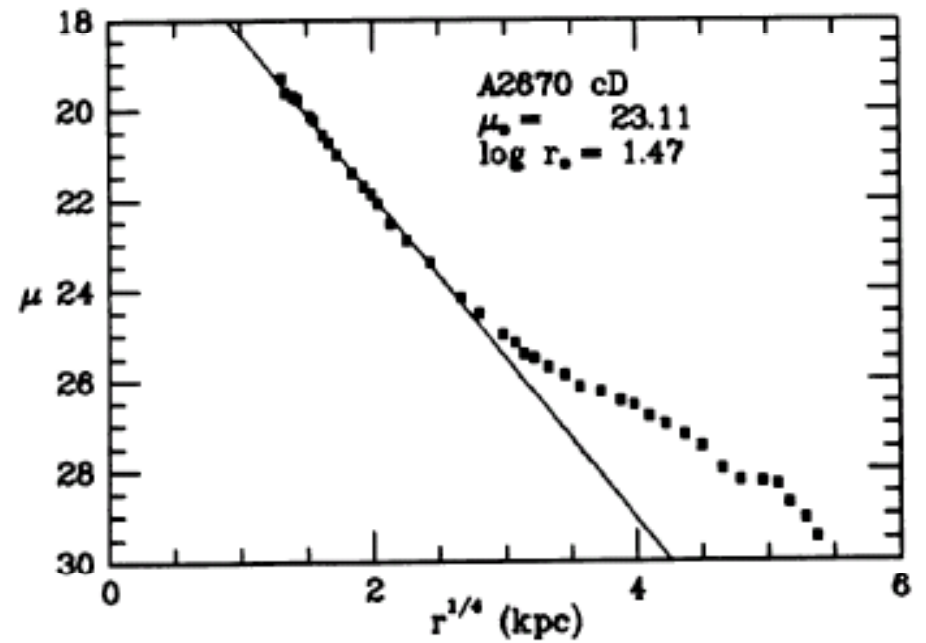
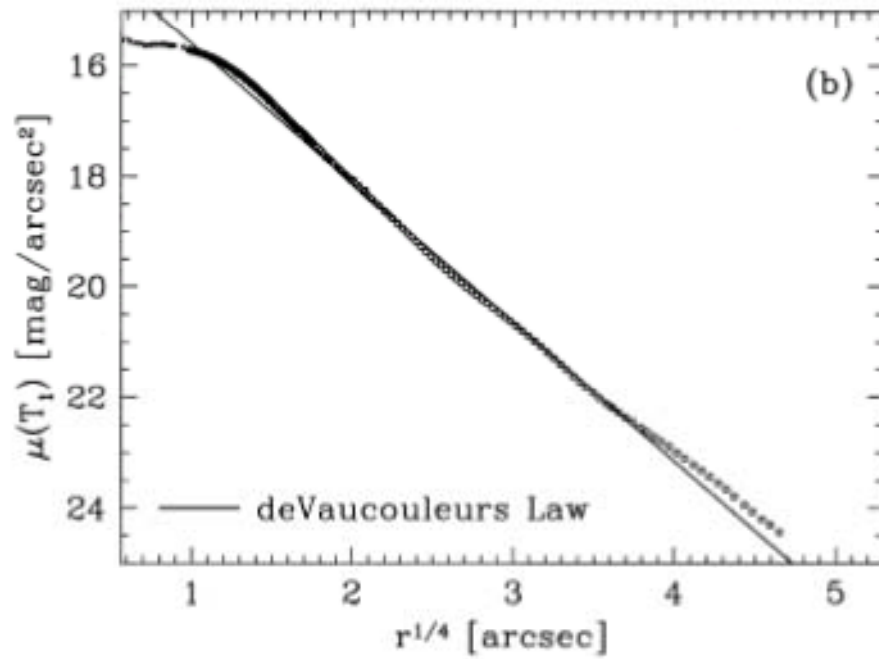
Also, R_e and M_B are related

\Rightarrow average surface brightness μ_{ave} and M_B are also related: Kormendy relation

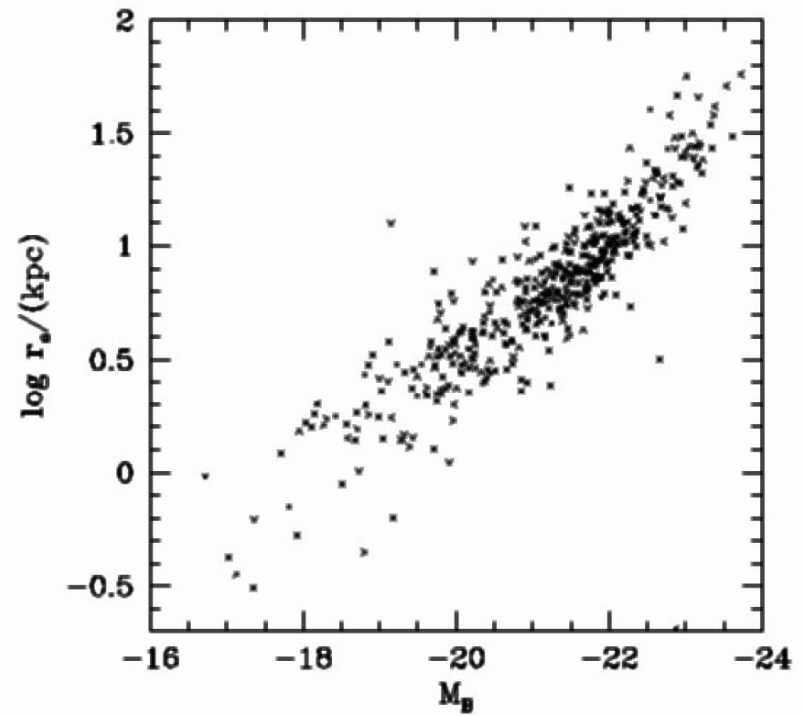
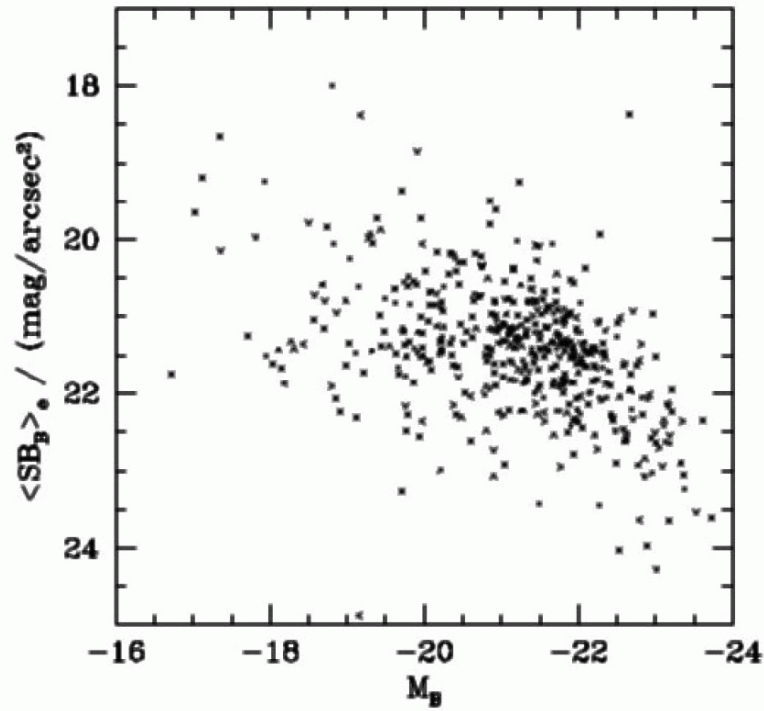
Specific features for each type:

1. Normal E's best fit de Vaucouleurs profile.
2. Profiles of higher and lower luminosity E's decline slower and faster at large r . Especially, cD's only obey at the innermost part.
3. dE's are better described by an exponential profile.

Structure: de Vaucouleurs profile



Structure: Kormendy relation



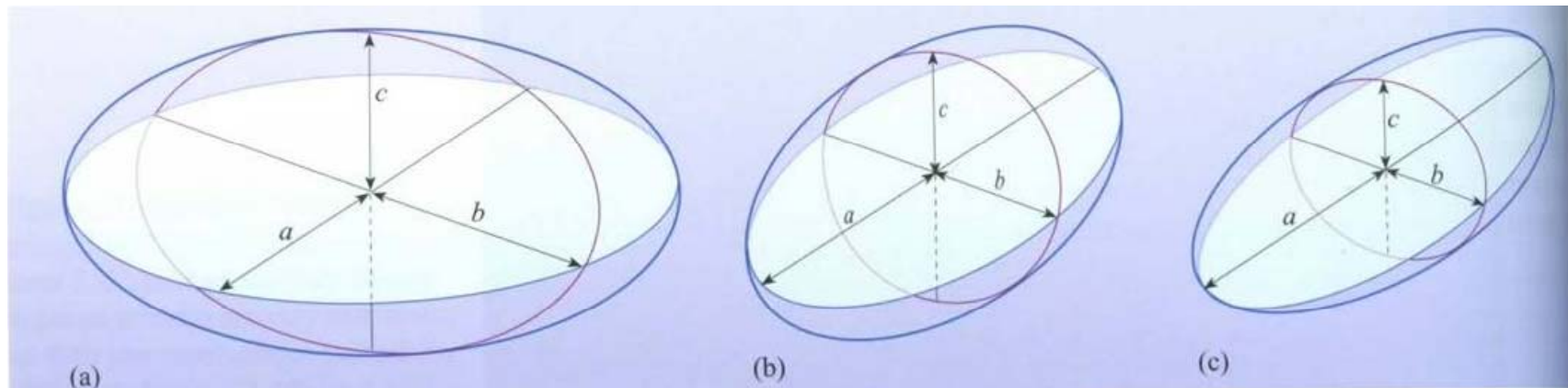
Structure: three dimensional properties

Isophotes are to the first order elliptical

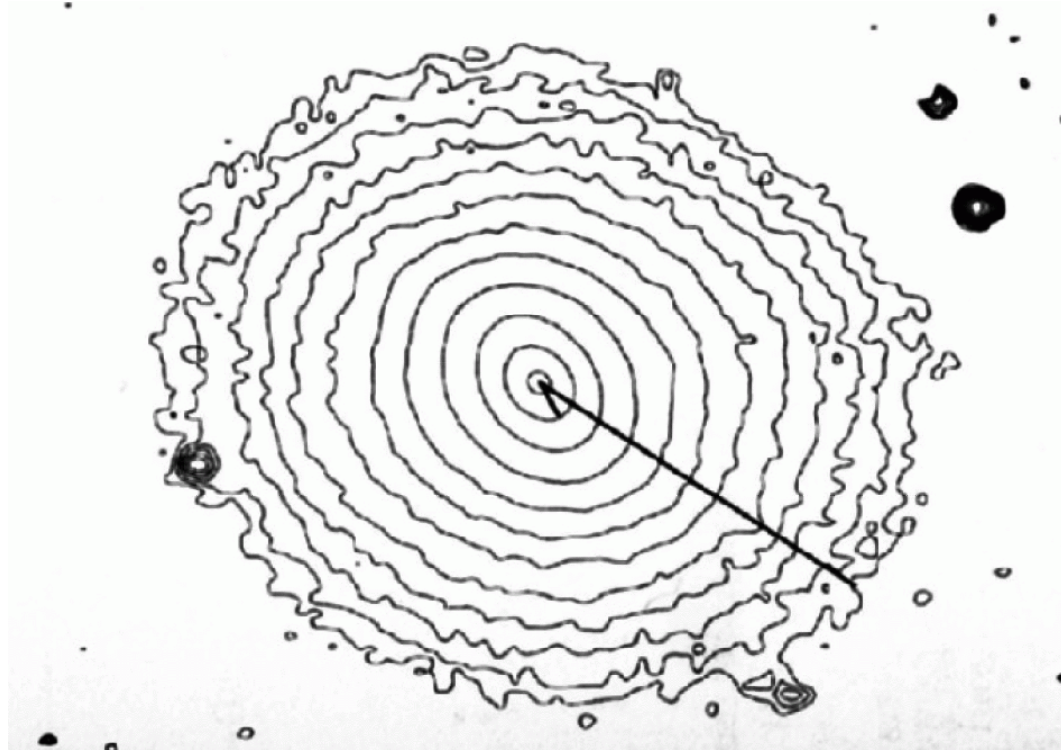
→ the density is constant on ellipsoids, i.e. the possible shapes are:

1. oblate ($a = b > c$, rotationally symmetric ellipsoid, like a pancake)
2. prolate ($a > b = c$, like a lemon)
3. triaxial ($a \neq b \neq c$, ellipsoid, like a box with smoothed edges)

All are projection of three-dimensional density profiles.



Structure: projection of three dimensional profile



Since the three-dimensional structure is triaxial, the projected profile has an axial twist.

Structure: isophotal shape

Isophotes are generally not exactly elliptical. The “boxiness” or “diskiness” of isophotes is usually quantified by measuring a quantity denoted a_3 . First the ellipse $Re(\varphi)$ is fitted to the isophote. For each angle φ , one determines the distance

$$\delta(\varphi) = Ri(\varphi) - Re(\varphi)$$

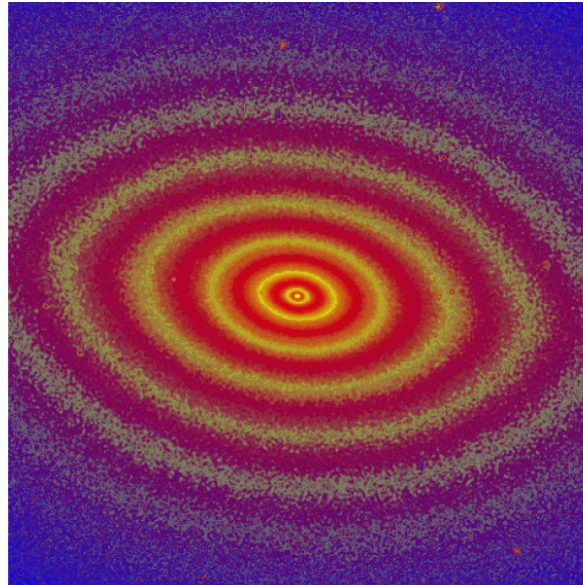
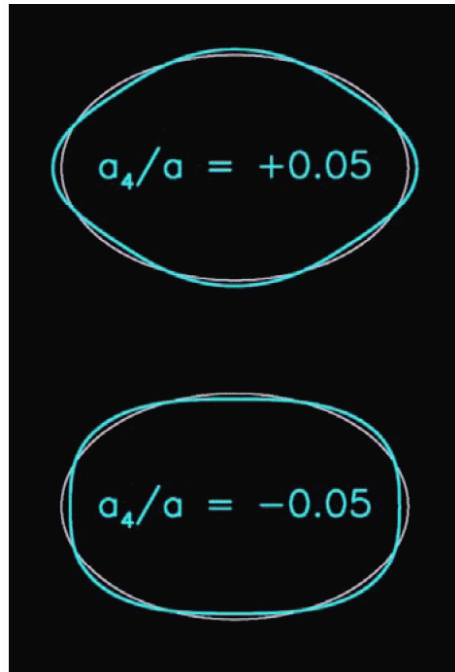
between the radii of corresponding points on the ellipse and on the isophote. Then one expresses the function $\delta(\varphi)$ as a Fourier series:

$$\delta(\varphi) = \bar{\delta} + \sum_{n=1}^{\infty} a_n \cos(n\varphi) + \sum_{n=1}^{\infty} b_n \sin(n\varphi)$$

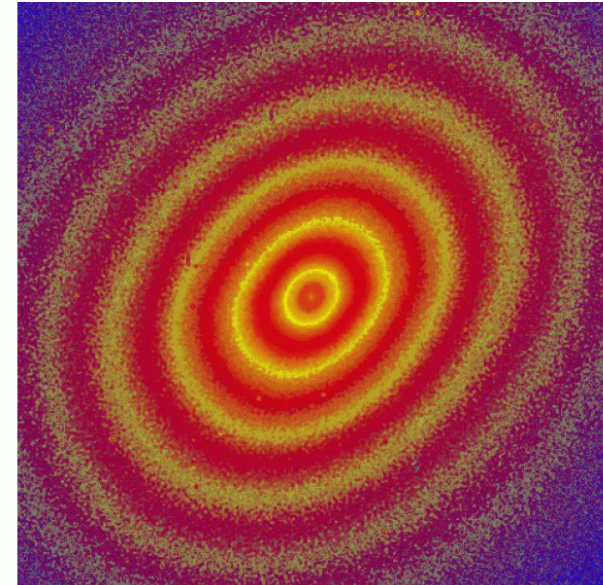
$a_4 < 0$: boxy isophotes,

$a_4 > 0$: diskiness isophotes.

Structure: isophotal shape



NGC 821: $a_4/a \sim +0.02$, diskly



NGC 2300: $a_4/a \sim -0.02$, boxy

Structure: what determines the shape of ellipticals?

Brightness profile is determined by the distribution of orbits of stars. If the velocity distribution is anisotropic, the stellar distribution does not become spherically symmetric.

If statistical properties of the distribution of stellar orbits is independent of time, it is a static system. Though elliptical galaxies are collisionless system, i.e., two-body relaxation does not take place, elliptical galaxies have some homogeneous properties as we have seen:

- 1. de Vaucouleurs profile**
- 2. Not rotationally supported**
- 3. Triaxial ellipsoidal figure**

⇒ Even if without knowing the details of dynamical structure, we imagine that a certain “relaxation” occurs.

What is it?

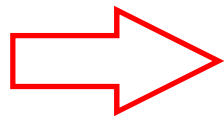
Relaxation for collisionless system?: violent relaxation

What made collisionless system “relaxed”? Lynden-Bell (1967) proposed a possible mechanism referred to as “violent relaxation”.

We start from the collisionless Boltzmann eq.

$$\frac{\partial f}{\partial t} + \vec{v} \cdot \frac{\partial f}{\partial \vec{x}} - \frac{\partial \phi}{\partial \vec{x}} \cdot \frac{\partial f}{\partial \vec{v}} = 0$$

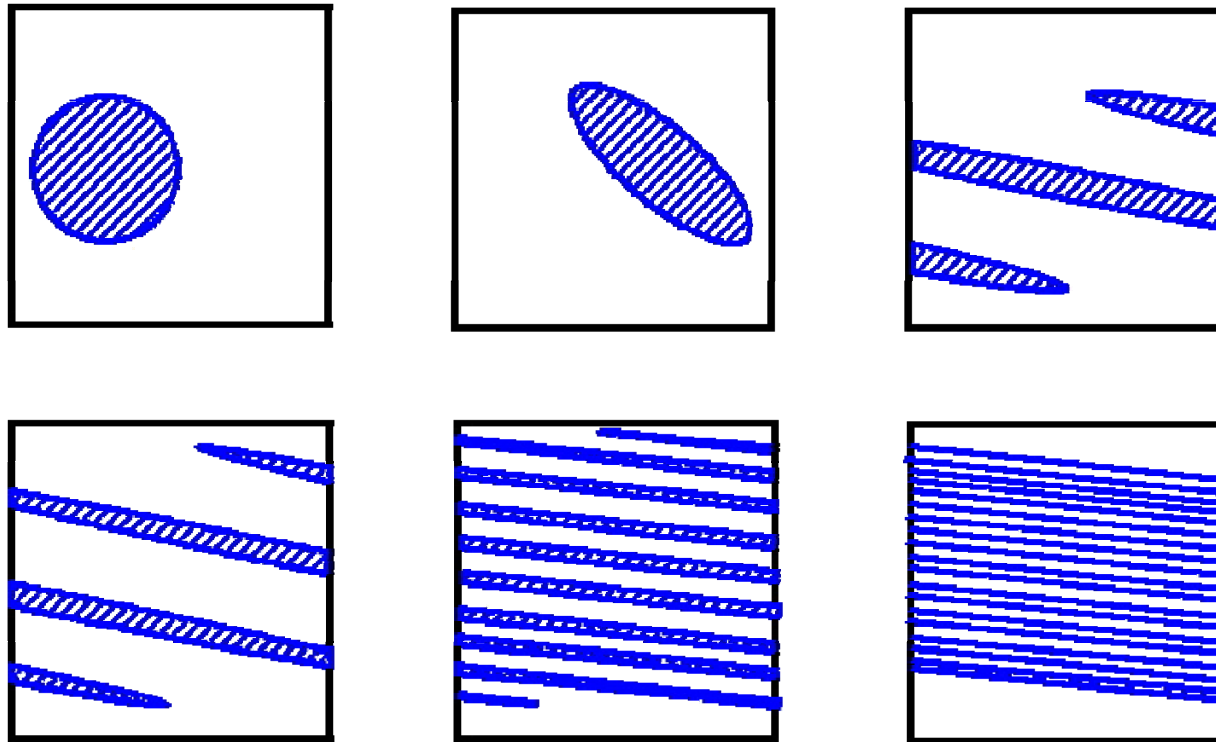
The potential part changes violently both in space and time.



Microscopically it causes a **phase mixing**. Of course the DF, f , conserves, but it becomes smaller and smaller in scale. Then, macroscopically the coarse-grained DF \bar{f} goes to an “equilibrium”

Relaxation for collisionless system?: violent relaxation

Mixing of phase distribution by a violent change of the mean gravitational field in space and time, similar to the mechanism that a chaos occurs.



The resulting distribution is referred to as Lynden-Bell distribution.

Relaxation for collisionless system?: violent relaxation

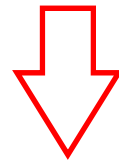
In the context of statistical mechanics, Lynden-Bell distribution is regarded as **the fourth distribution**:

	Particle	
Exclusion	Indistinguishable	Distinguishable
Without	B-E distribution	M-B distribution
With	F-D distribution	Lynden-Bell distribution

Relaxation for collisionless system?: violent relaxation

However...

This distribution was not perfectly reproduced by numerical experiments. **Even worse, some fundamental problems as a consistent theory were pointed out.**



Relaxation process of collisionless system still remains as an open problem.

Different derivation of the theory was proposed (Nakamura 2000). Since this is also closely related to a long-standing problem in plasma physics (collisionless space plasma often shows Maxwellian distribution, known as Langmuir's paradox: Langmuir 1928).

1.4 Mass of elliptical galaxies

Mass of elliptical galaxies: classical observation

$M/L \sim 5$ at center of ellipticals; this does not require additional mass.

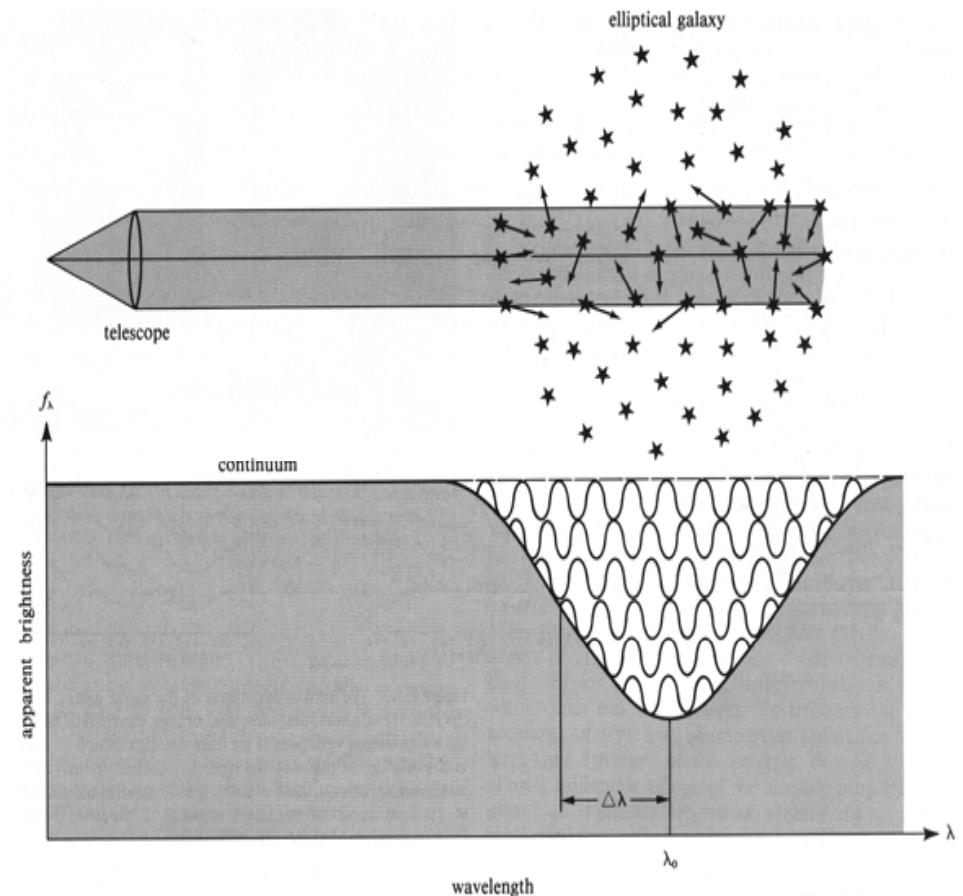
However, from the velocity dispersions of planetary nebulae or stars, a whole elliptical galaxy was found to be $M/L > 10$ for.

Since the M/L of globular clusters is $\sim 1-2$, and $\sim 2-3$ for old galaxies assuming a normal initial mass function (IMF), we found that **elliptical galaxies are more massive than we thought.**

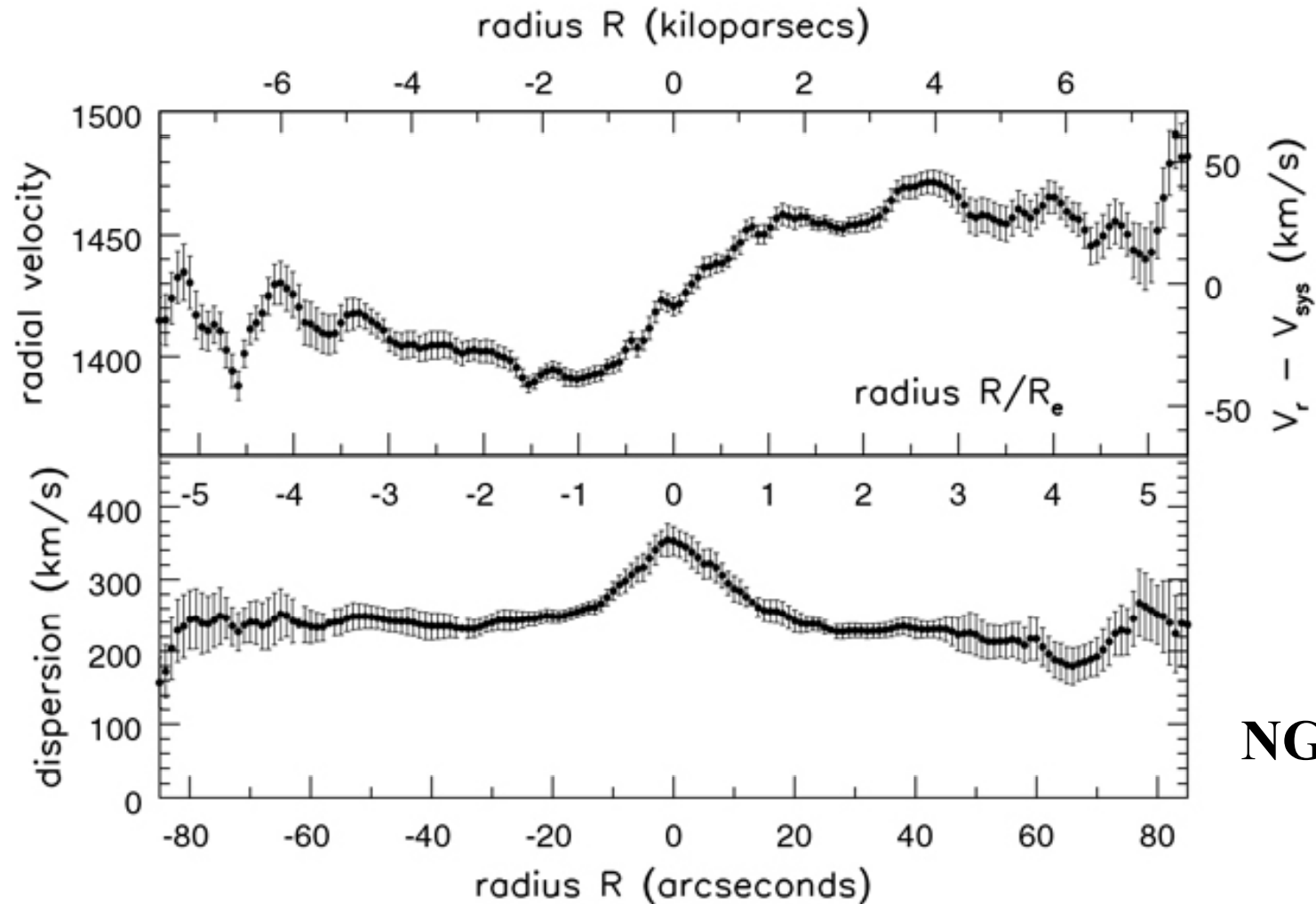
Mass of elliptical galaxies: classical observation

The measurement of a mean star velocity in an elliptical galaxy:
the Doppler broadening of the absorption lines of a galaxy
⇒ dispersion of the star velocity along the line of sight

$$\frac{\Delta\lambda}{\lambda_0} = \sqrt{\frac{1 - (v/c)}{1 + (v/c)}}$$



Mass of elliptical galaxies: classical observation



NGC 1399

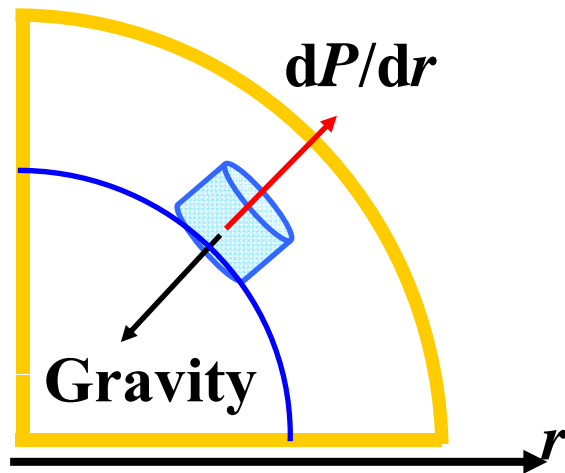


Fig 6.12 (A. Graham) 'Galaxies in the Universe' Sparke/Gallagher CUP 2007

Mass of elliptical galaxies: X-ray observation

Since elliptical galaxies have hot X-ray gas, this can be used to estimate their mass reliably.

Assume a hydrostatic equilibrium.



$$\frac{dP}{dr} = -\rho(r) \frac{GM(r)}{r^2}$$

Using the equation of state (ideal gas),

$$P = nk_B T = \frac{\rho}{\mu m_p} k_B T$$

We obtain

$$M(<r) = r \frac{k_B T}{G \mu} \left(-\frac{d \ln \rho}{d \ln r} - \frac{d \ln T}{d \ln r} \right)$$

Mass of elliptical galaxies: X-ray observation

From X-ray observation, we can obtain $n(r)$ and $\rho(r)$. By assuming some simplifying scaling,

$$n \propto r^{-\alpha}$$

$$\mathcal{E} \propto n_p^2 \propto r^{-2\alpha}$$

$$I_X \propto R^{1-2\alpha}$$

we obtain

$$M(< r) \simeq 4 \cdot 10^{11} M_{\odot} \cdot \left(\frac{T}{10^7 K} \right) \cdot \left(\frac{r}{10 kpc} \right)$$

and this yields a consistent mass estimate with velocity dispersion observation with Jeans equation.

Typically $M_{\text{dyn}} \sim 10^{11-13} M_{\text{sun}}$, suggesting dark matter.

1.5 Scaling relations

Faber-Jackson relation

A relation between galaxy luminosity vs. velocity dispersion at the center.

From the virial theorem (assuming a constant surface brightness B):

$$2 \times \frac{3}{2} M = 2\pi \frac{I_0 R_0^2}{R_0^2} \sigma^2 = \frac{GM^2}{R}$$

$$L = 4\pi R^2 B$$

$$\Rightarrow L \approx \sigma^4$$

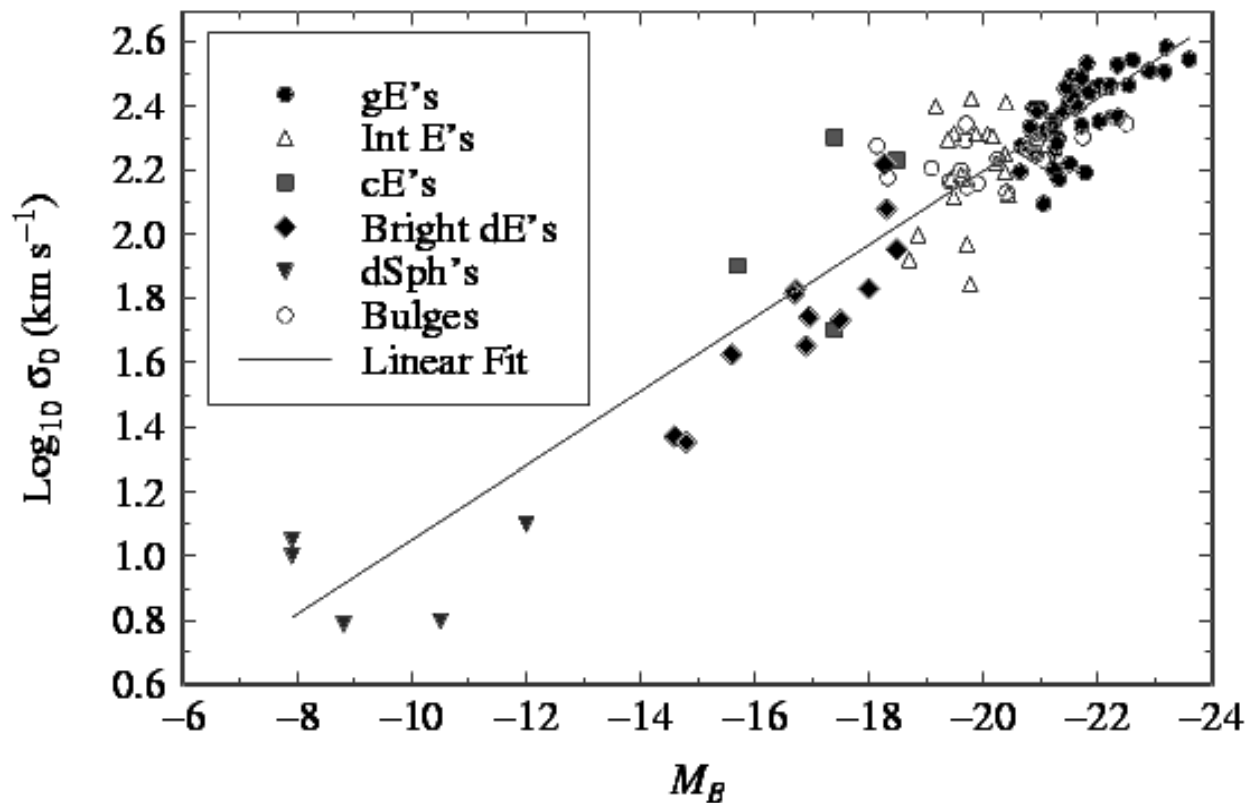
In practice, B is not constant

\Rightarrow the power index takes a value between 3 and 5.

Faber-Jackson relation

Since a luminosity of a galaxy is determined by using a velocity dispersion which can be directly measured, this relation is used to estimate a distance to a galaxy without going through the Hubble constant.

However in practice, the dispersion is pretty large (~ 2 mag).



The fundamental plane relation

Since the dispersion in the Faber-Jackson relation is large, people tried to consider **a second parameter** to introduce (Dressler 1987; Djorgowski & Davis 1987; and others).
parameter space

We operate now in the 3-D space:

R – radius,

I – luminosity,

σ – velocity dispersion,

or additionally (more dimensions)

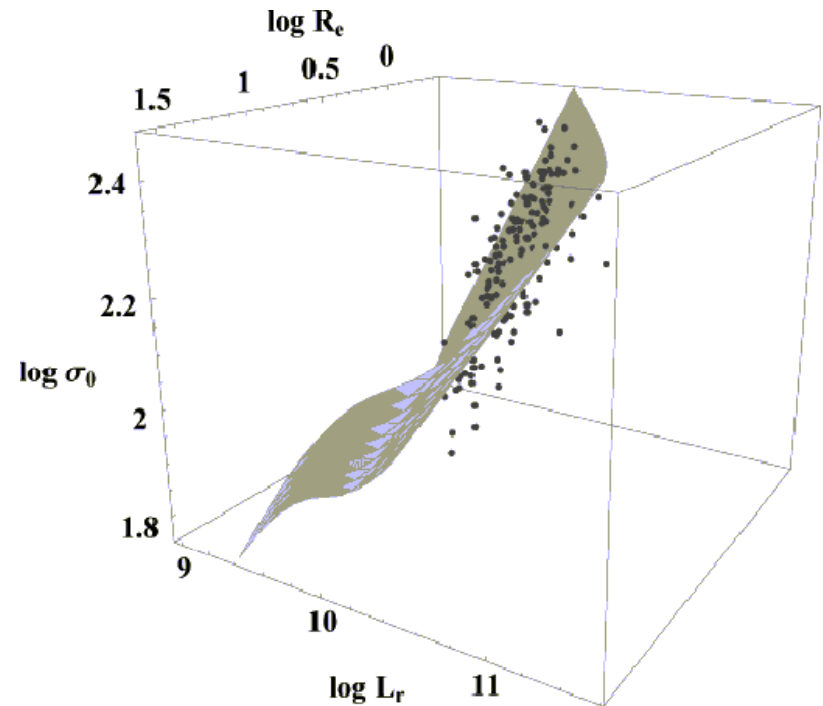
μ – surface brightness and other parameters

Empirical relations \Rightarrow a plane in the 3D space (or even with more dimensions).

The fundamental plane relation

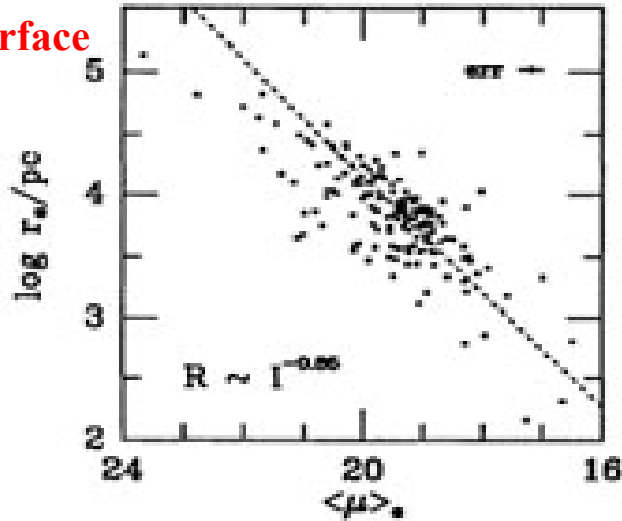
Space of relations in 3D; we find a thin surface in the space.

Faber-Jackson and Kormendy relations (and other 2D relations) are simply projections of this plane on the 2D surface. Their dispersion are simply a reflection of the non-flat shape of this plane seen in 3D.

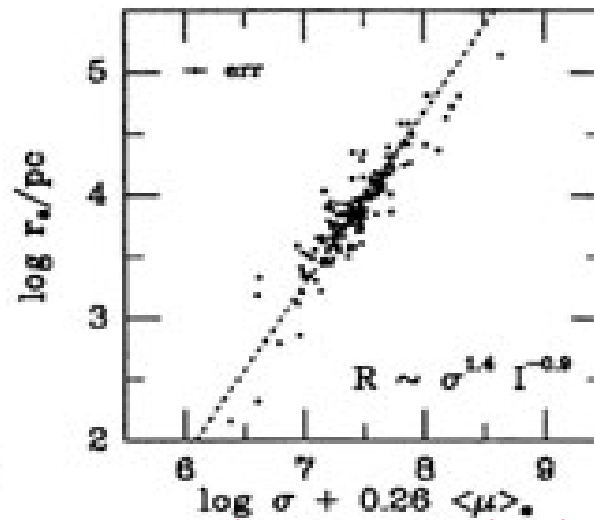
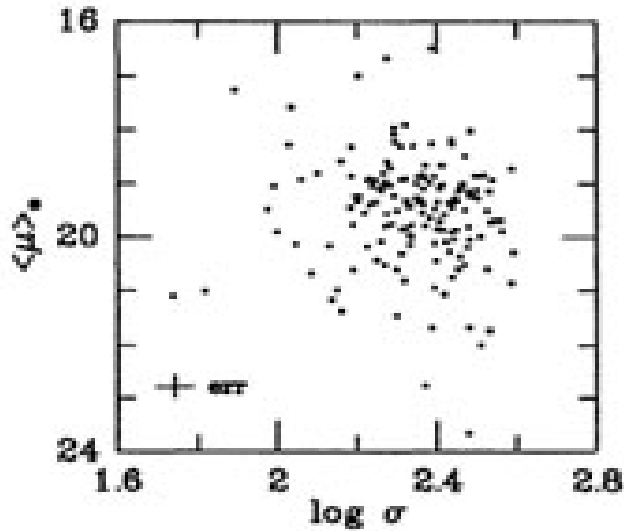
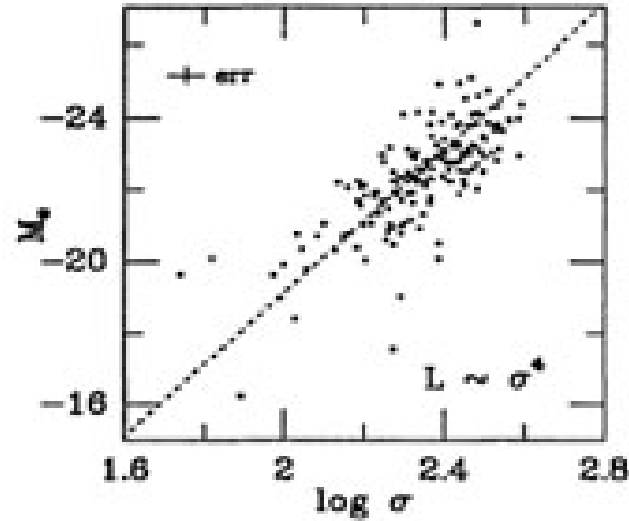


The fundamental plane relation

Radius vs. surface brightness



Faber-Jackson (luminosity vs. velocity dispersion)



Surface brightness vs. velocity dispersion: fundamental plane seen almost from above

Radius vs. a combination of surface brightness and velocity: fundamental plane seen edge-on.

The fundamental plane relation

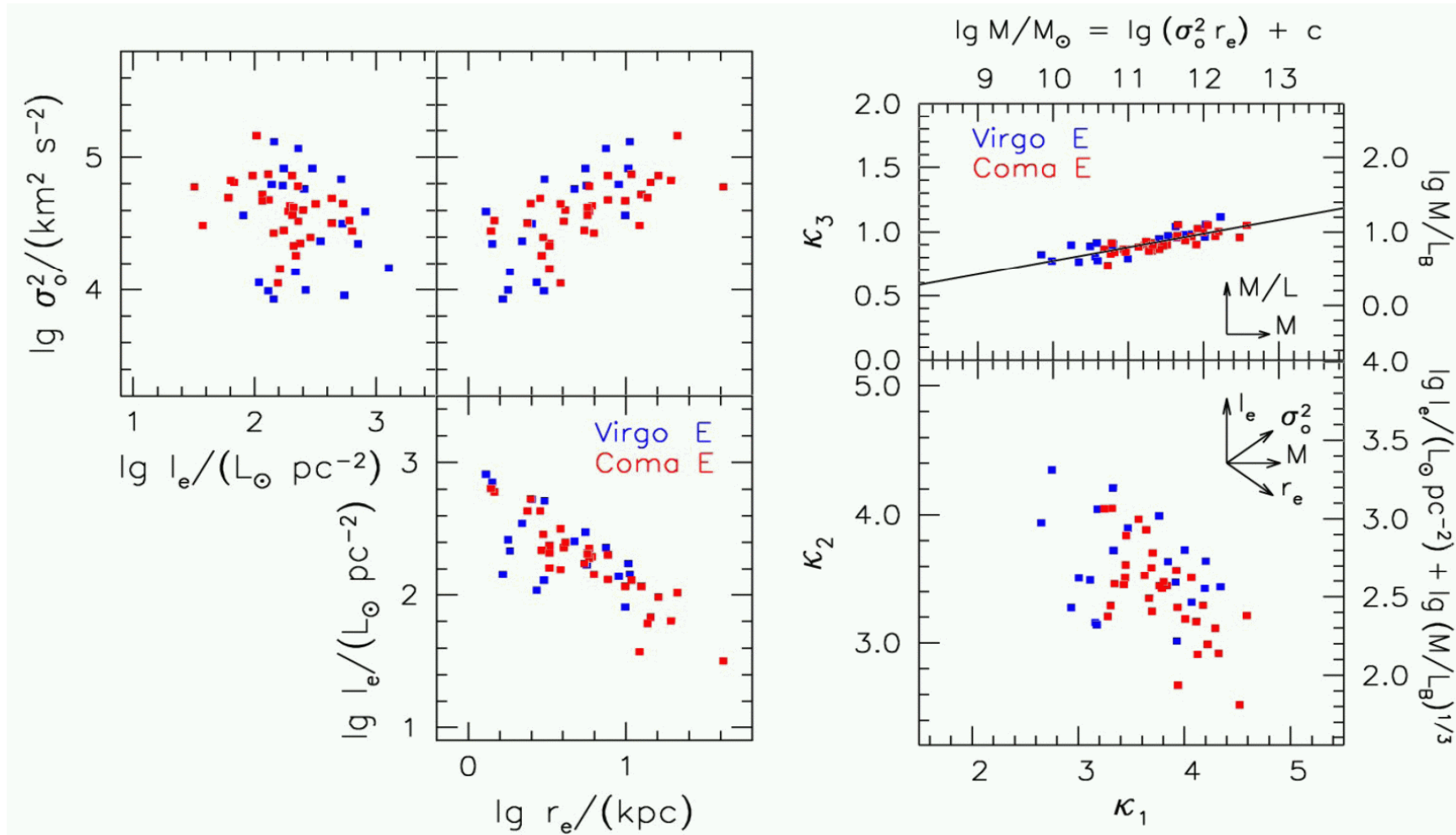
There are also numerous additional or alternative parameters introduced, e.g., Dressler parameter D_n (a radius inside of which the total surface brightness reaches a certain value ($20.75 B \text{ mag arcsec}^{-2}$)).

Among others, the fundamental plane can conveniently be visualized in the κ -parameter space, using the parameters (Bender, Burstein & Faber 1992, 1993, 1994):

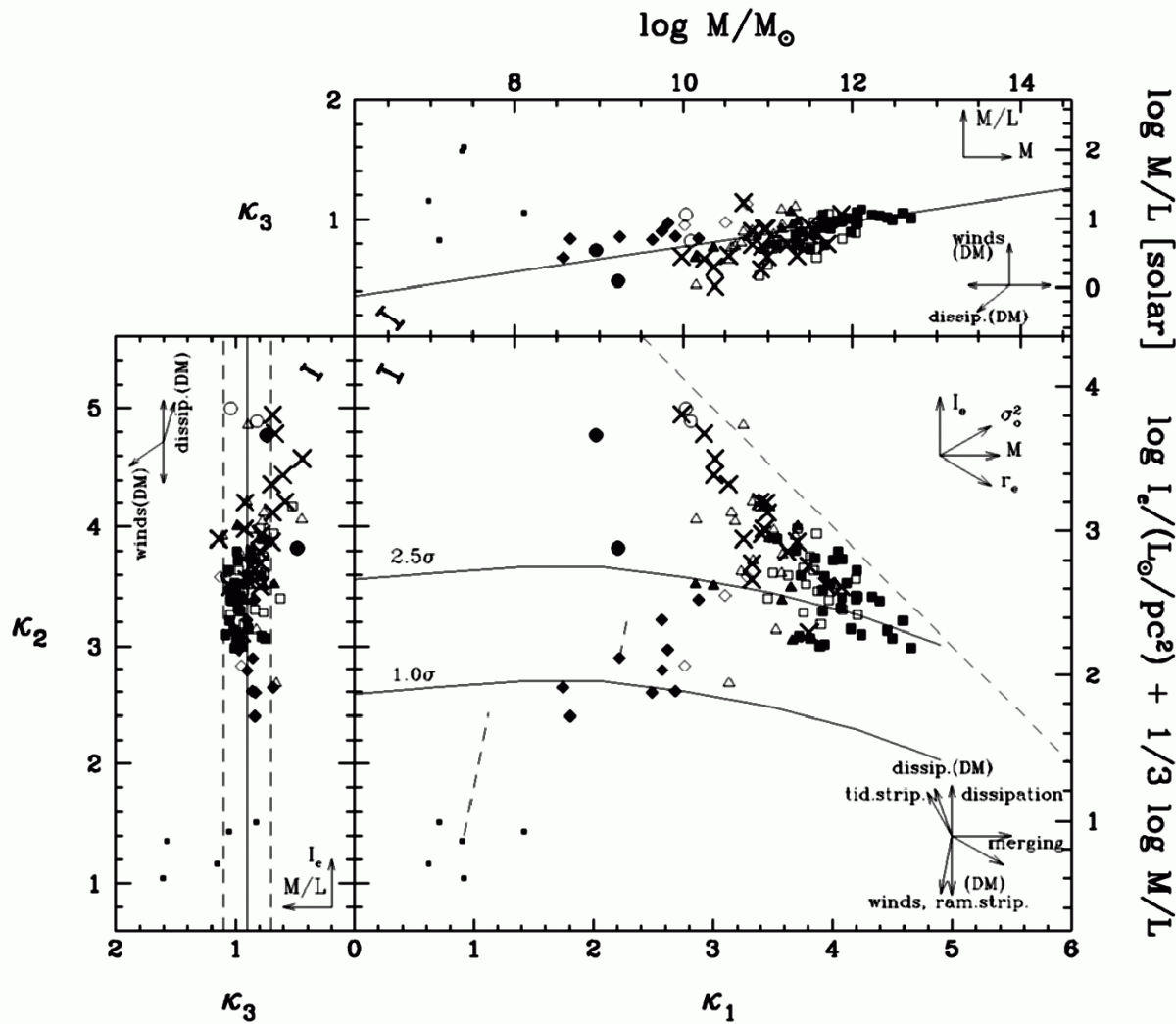
$$\kappa_1 = \frac{\log(\sigma^2 r_e)}{\sqrt{2}} \propto \log M, \quad \kappa_2 = \frac{\log(\sigma^2 \Sigma_e^2 / r_e)}{\sqrt{6}} \propto \log \Sigma_e \left(\frac{M}{L} \right)^{1/3}, \quad \kappa_3 = \frac{\log(\sigma^2 / \Sigma_e / r_e)}{\sqrt{3}} \propto \log \left(\frac{M}{L} \right)$$

These new coordinates can be found systematically by a statistical method like the principal component analysis (PCA).

The fundamental plane relation: κ -space



The fundamental plane relation: κ -space



E: squares
S0: crosses
dE: diamonds
dSph: small squares
compact E: circles

(Bender, Burstein, & Faber 1992, 1993, and 1994)

The fundamental plane relation

Even though the kinematics of ellipticals can appear to be highly complicated in detail, **the objects must in fact be rather similar with respect to their global structure and their stellar M/L .**

No sufficient theoretical explanation yet for the existence of fundamental plane (ellipticals as a result of mergers of disc galaxies?).

2. Spiral Galaxy

2.1 Structure of spiral galaxies

2.2 Rotation curves of spiral galaxies

2.3 Scaling relations for spiral galaxies

2.1 Structure of spiral galaxies

Structure of spirals and lenticulars

We fit luminosities of a disc and spheroidal element (bulge) **separately**.

1. Spheroidal element (bulge) can be described similarly to an elliptical galaxy, i.e., de Vaucouleurs' $r^{1/4}$ -law.

$$I(r) = I_e \cdot 10^{-3.3307 \left(\left(r/r_e \right)^{1/4} - 1 \right)} \quad (1)$$

Integrated luminosity is given by integrating eq.(1),

$$L_{tot} = 7.215 \cdot \pi I_e \cdot r_e^2 \quad (2)$$

Structure of spirals and lenticulars

2. A disk can be almost always described by an exponential fit:

$$I(R) = I_0 e^{-\frac{R}{R_0}} \quad (3)$$

where

r_0 : disk scale length (for the Milky Way, $r_0 = 3$ kpc)

I_0 : the central surface brightness.

***N.B.* the disk scale length is different from disk scale height.**

Luminosity is given by integrating eq.(3),

$$L_{tot} = 2\pi I_0 R_0^2 \quad (4)$$

Structure of spirals and lenticulars: Sérsic profile

To describe these profiles, we can use a generalization of the de Vaucouleurs' formula, which works both for ellipticals and spirals:

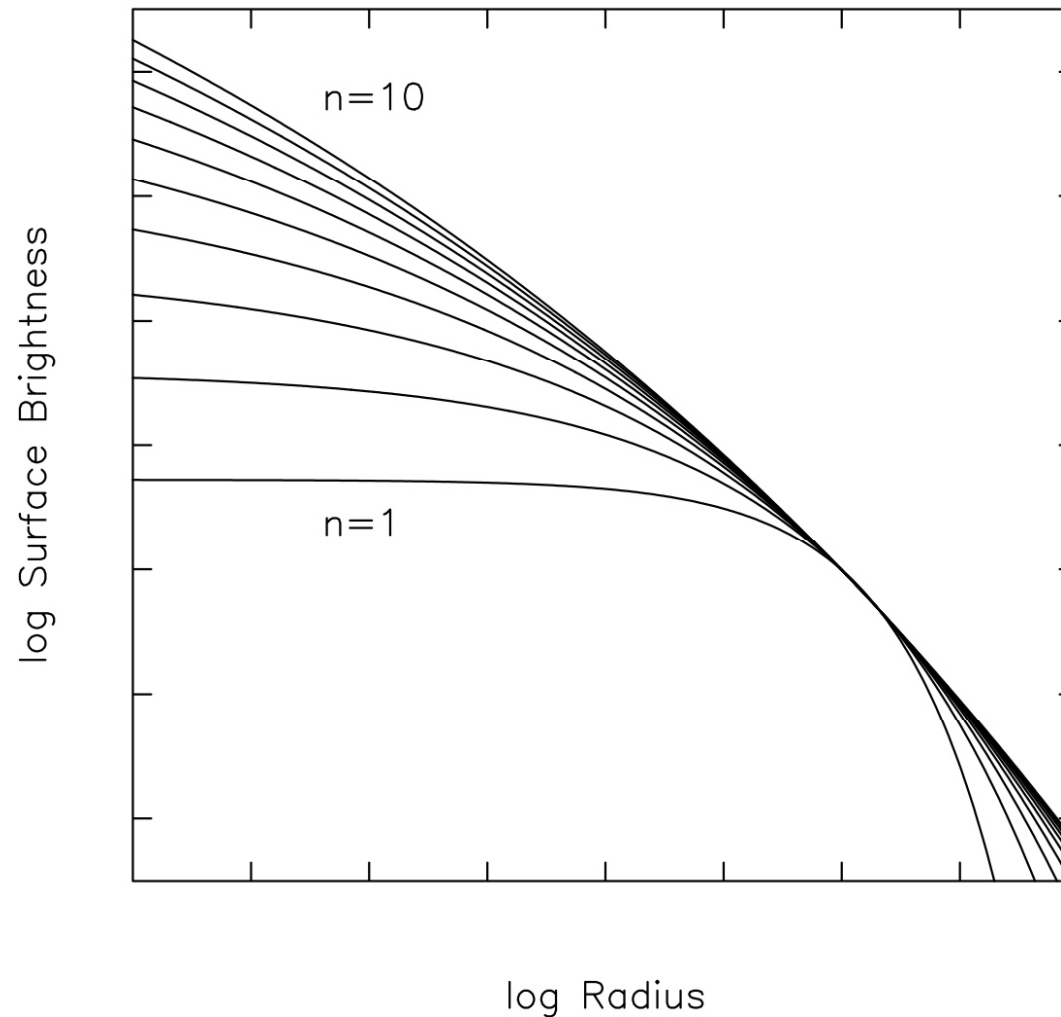
$$I(r) = I(r_e) \exp\{-b_n [(r/r_e)^{1/n} - 1]\} \quad (5)$$

where n : Sérsic index. This profile is called “Sérsic profile”, named after the inventor (Sérsic 1963).

$n = 4$: de Vaucouleurs' profile,

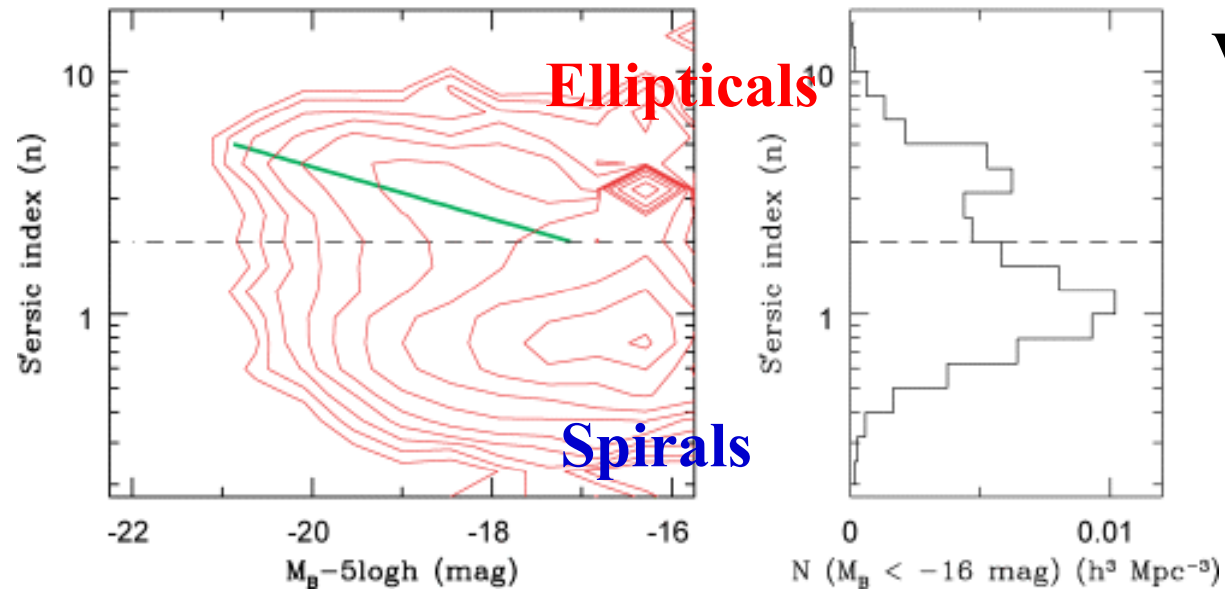
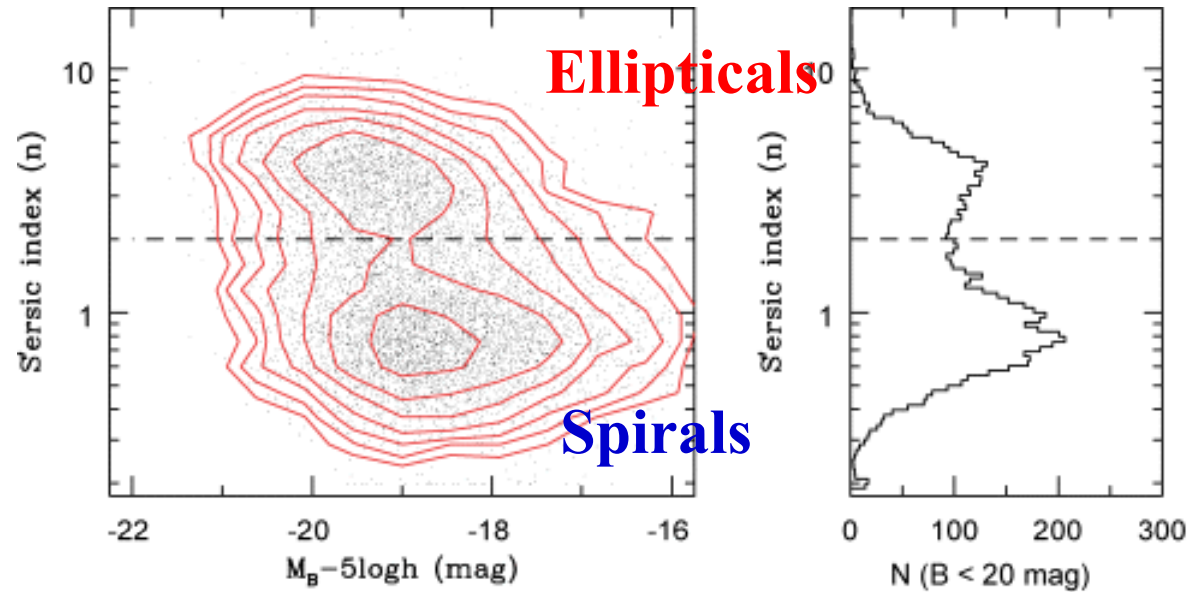
$n = 1$: exponential profile

Structure of spirals and lenticulars: Sérsic profile



***N.B.* this is a log-log plot and an exponential profile is NOT a straight line.**

Sérsic index distribution as a function of luminosity



Raw data

Volume-corrected

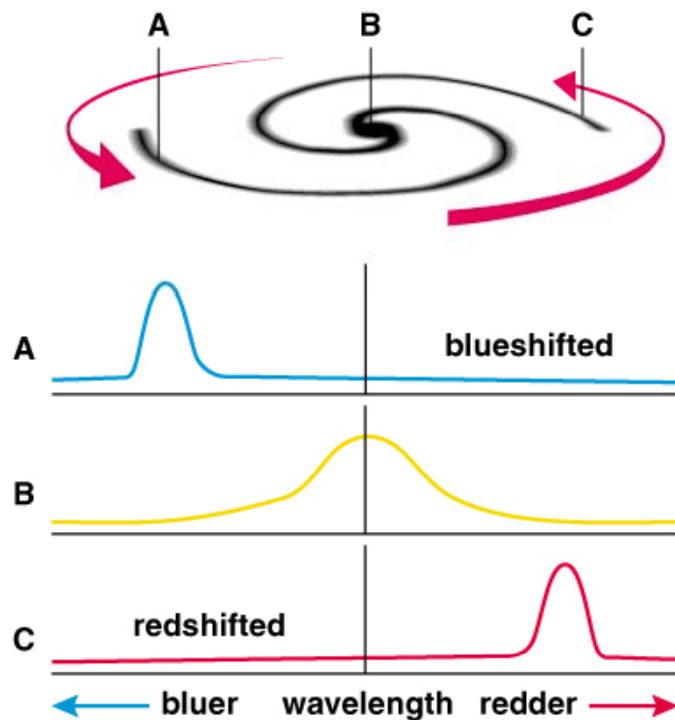
Driver et al. (2006)

2.2 Rotation curve of spiral galaxies

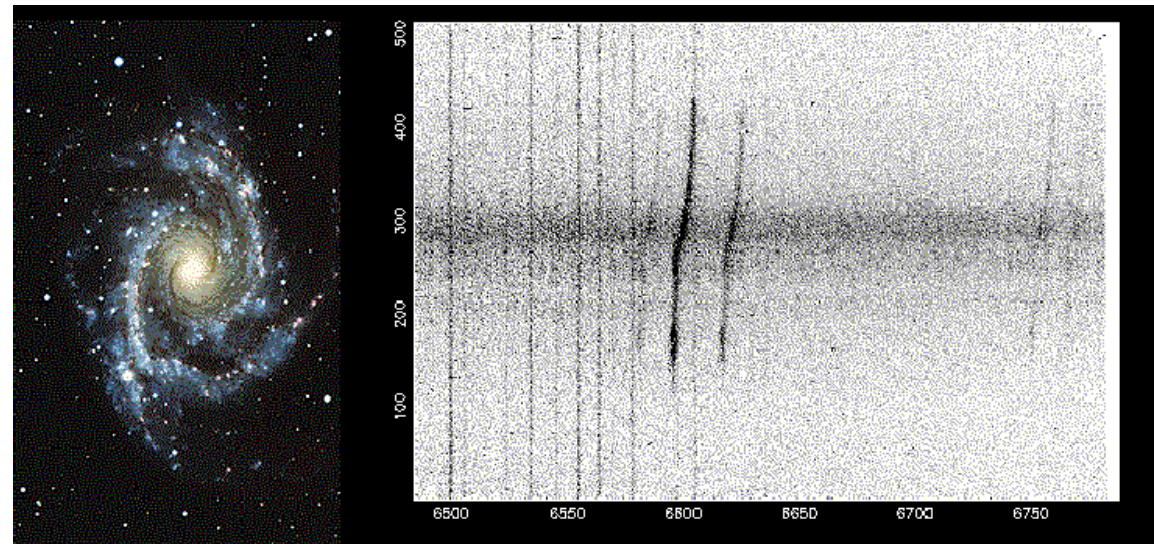
Dynamics of spiral galaxies: observation

Rotation curve: dependence of the rotation velocity around the galaxy center (more generally – any body in any system), $v_{\text{rot}}(r)$, on its distance from the center r .

This is measured by spectroscopic observation of emission lines.

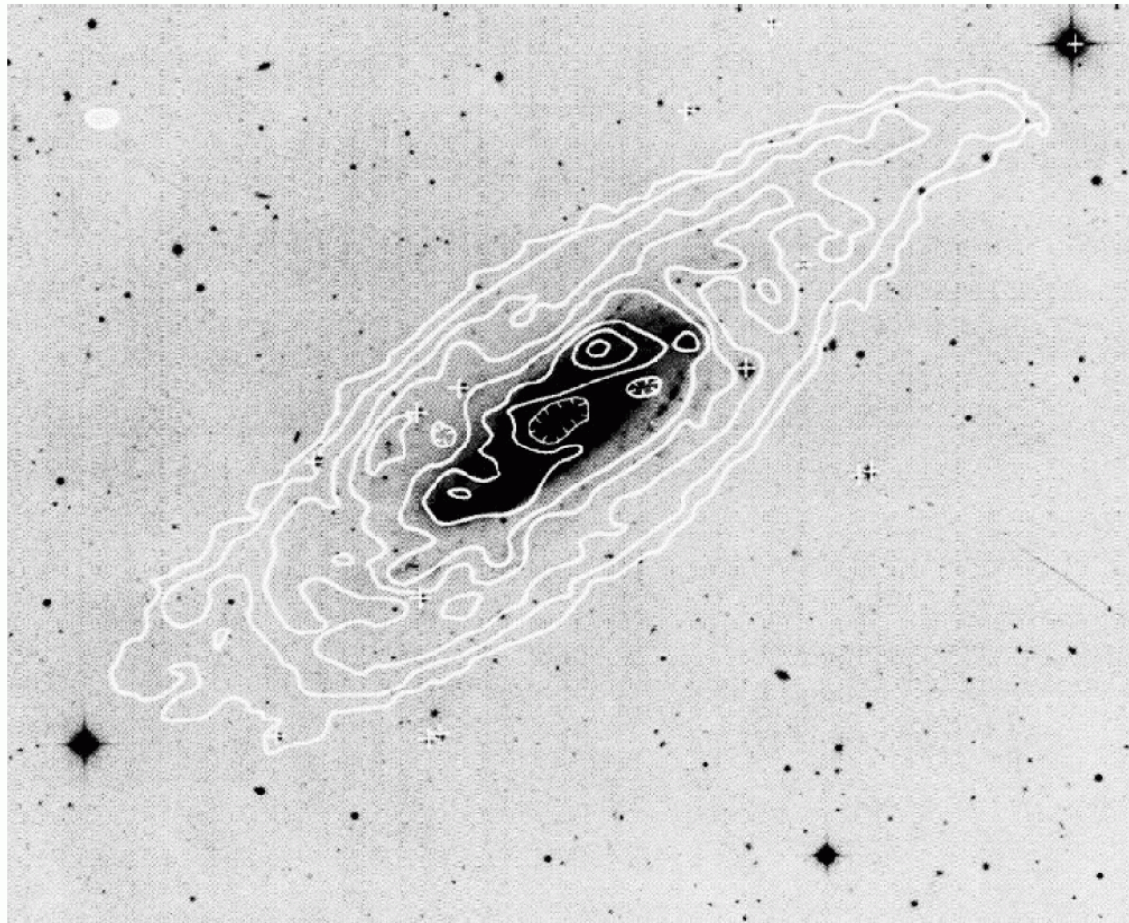


Copyright © Addison Wesley.



Dynamics of spiral galaxies: observation

At optical wavelengths, only the innermost part of galaxy disk can be observed: so radio observation of hydrogen 21cm line is often used.



Dynamics of spiral galaxies: expected rotation curves

Assuming (for simplicity) spherically symmetric structure of a galaxy, the virial theorem can be written as:

$$GM(< R)/R^2 = v_c^2(R)/R \quad (19)$$

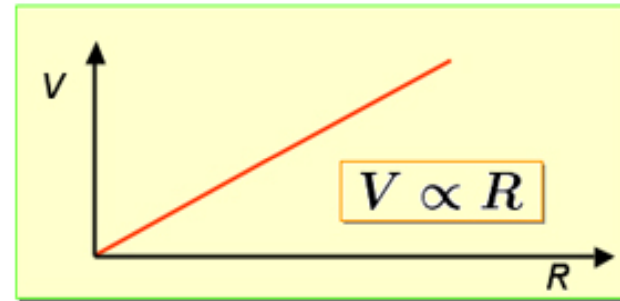
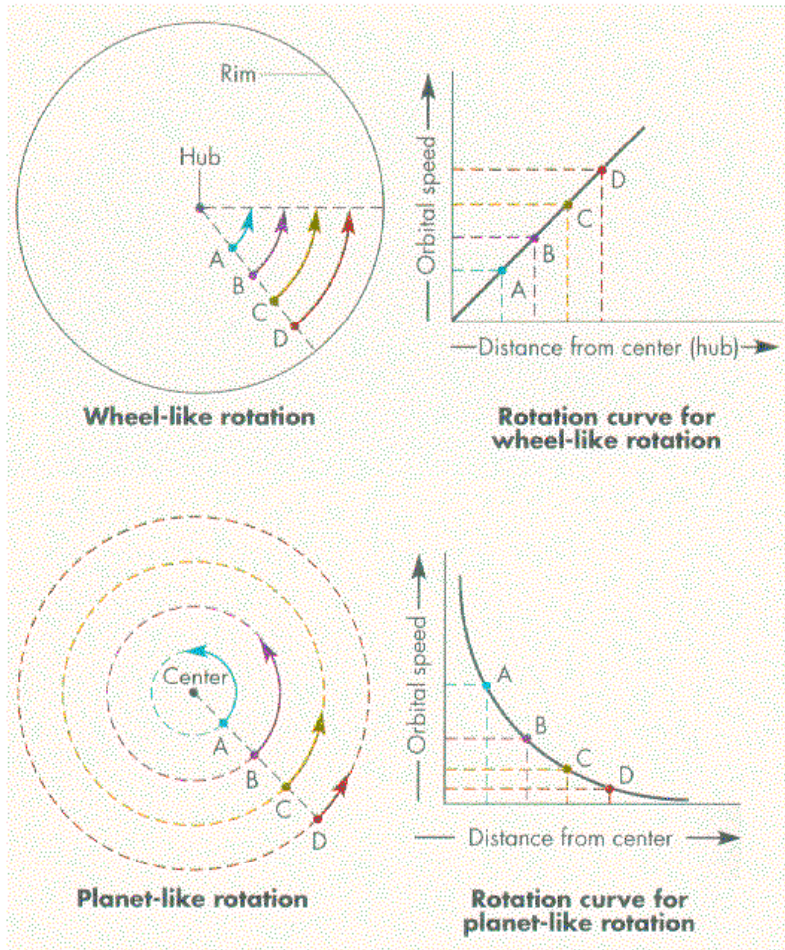
which means

$$M(< R) = v_{\text{rot}}^2(R) R/G \quad (20)$$

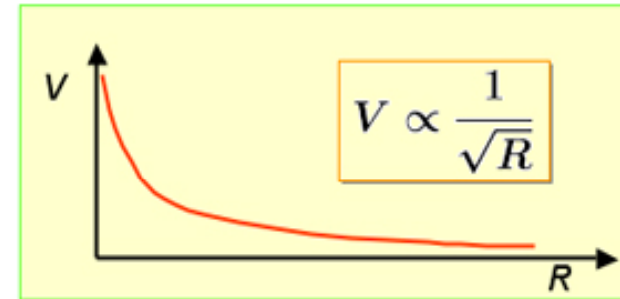
This allows us to compute mass of galaxies, M .

Dynamics of spiral galaxies: expected rotation curves

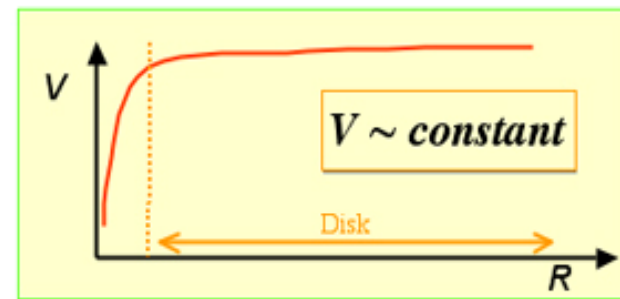
Appearance of a rotation curve depends on the mass distribution of a galaxy $M(< r)$.



Solid Body Rotation

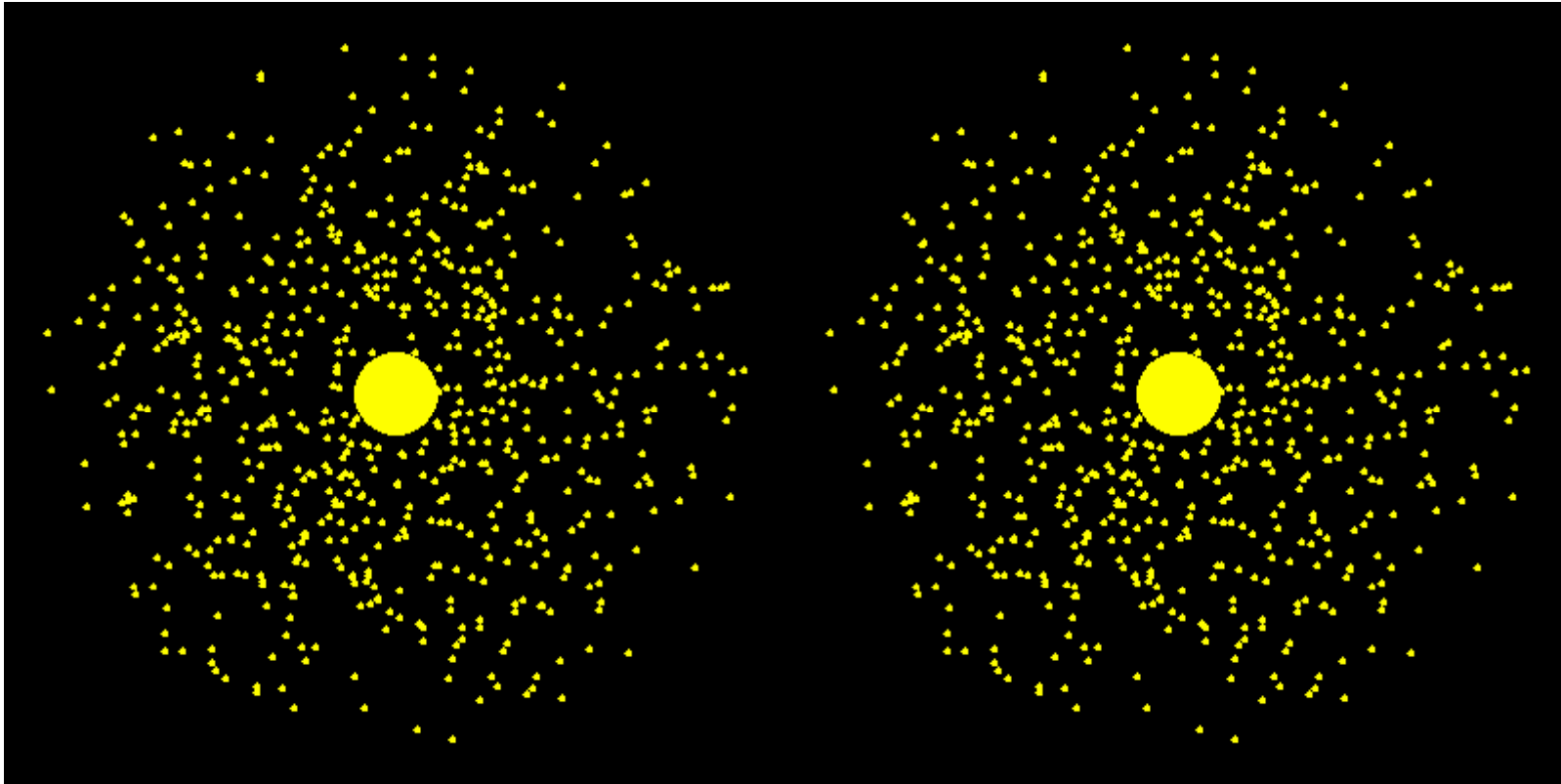


Keplerian Rotation



?

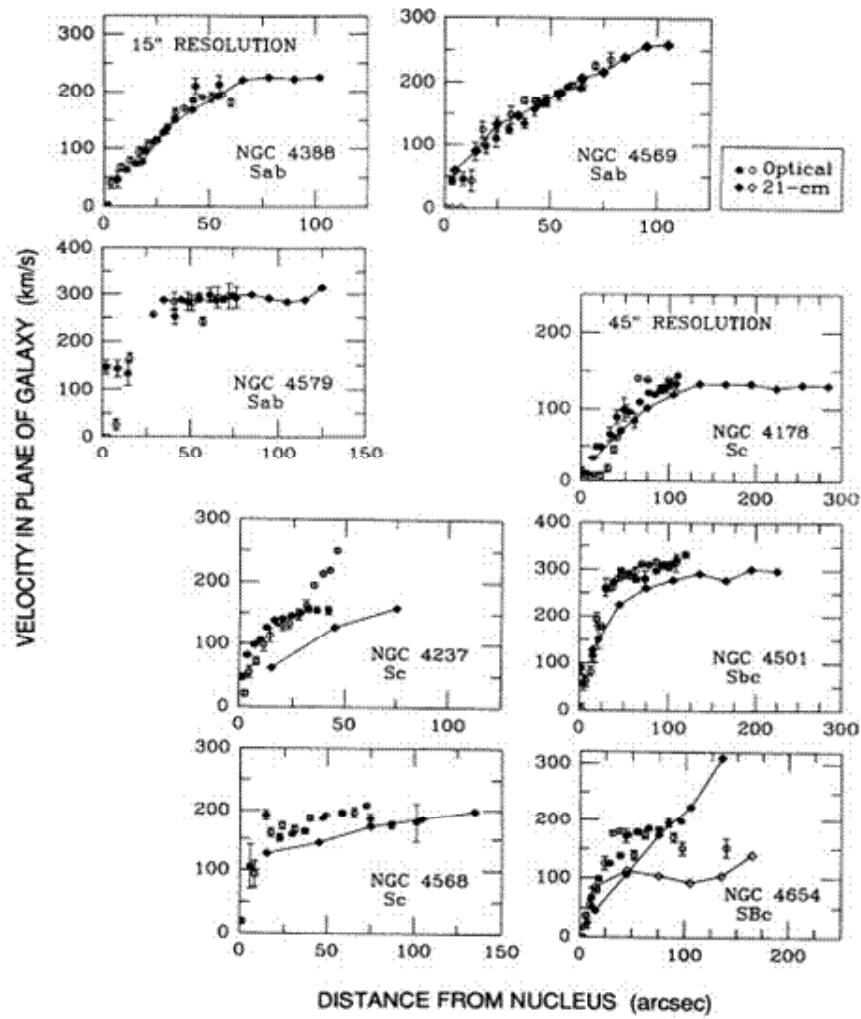
Schematic description of rotation of a disk galaxy



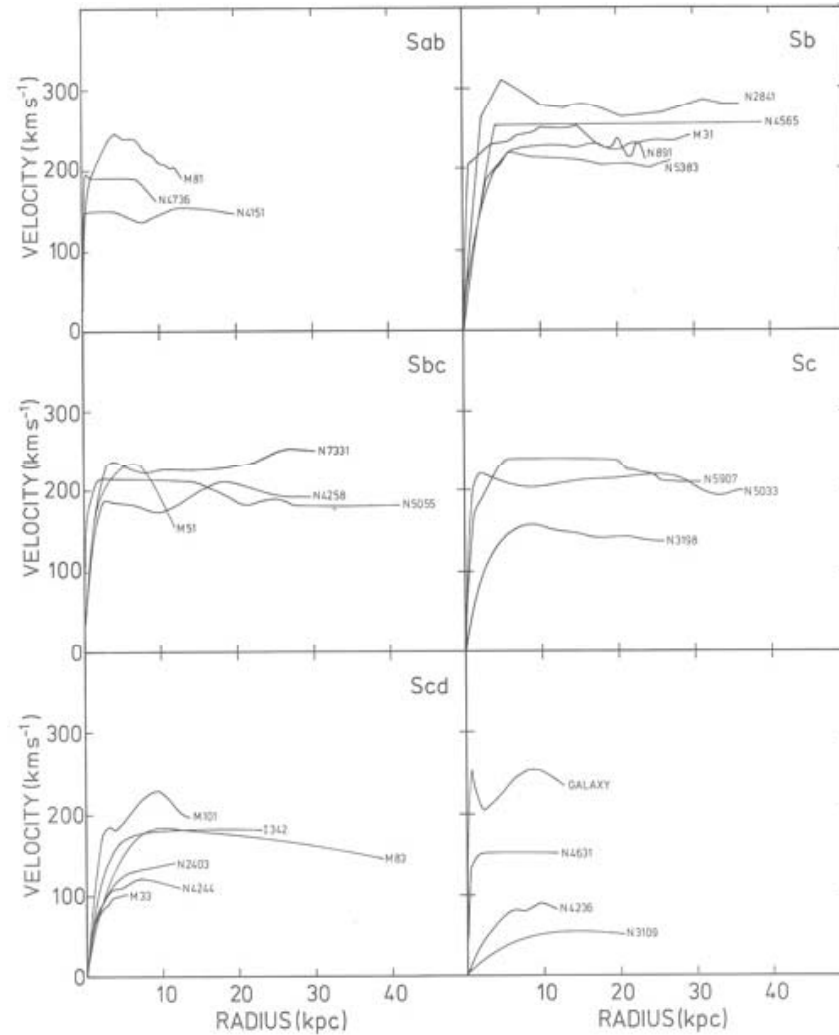
Keplerian disk

Constant velocity

Observed rotation curves of spiral galaxies

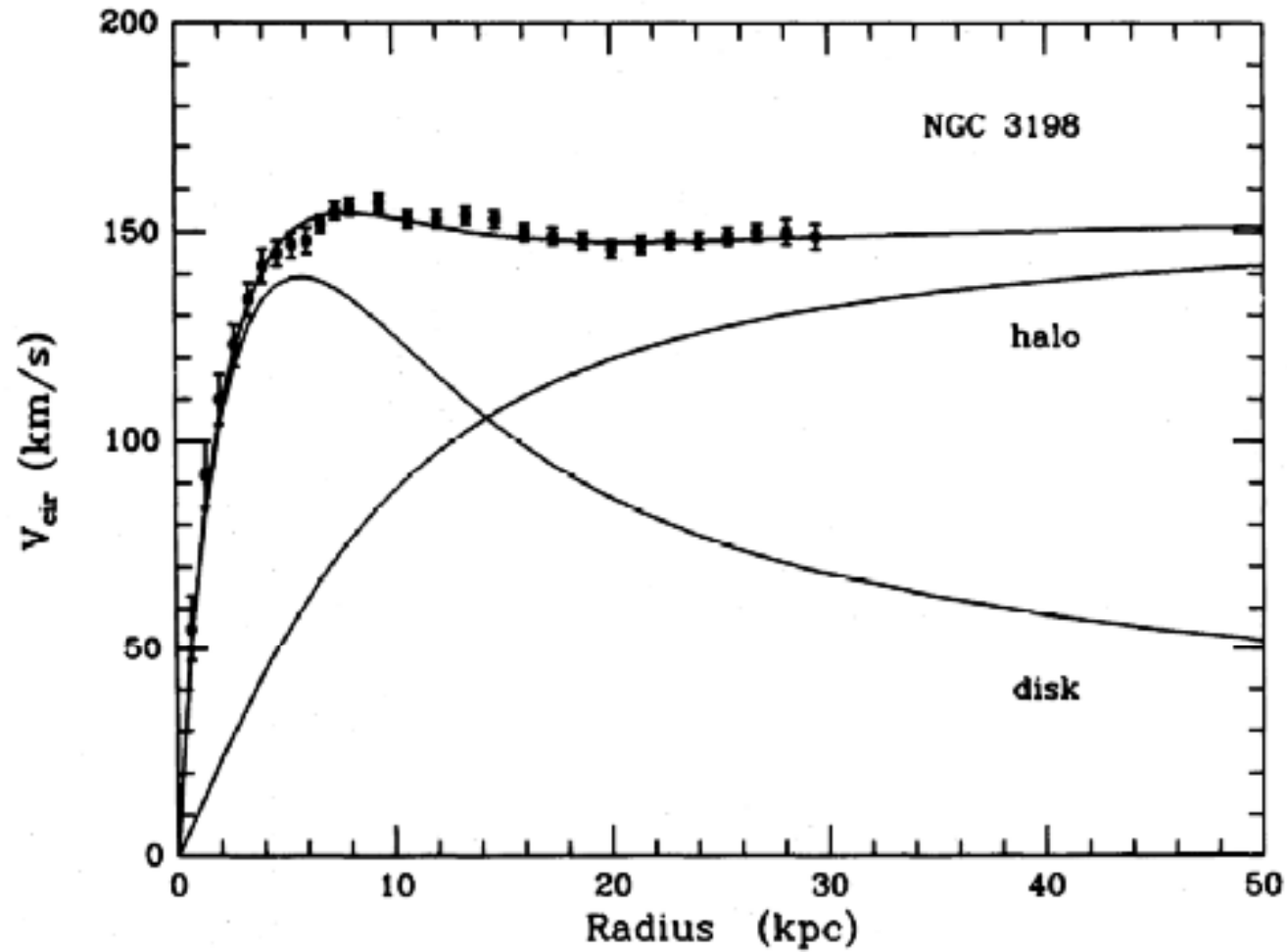


Rubin (1978)



Bosma (1979)

Observed rotation curves of spiral galaxies



van Albada (1985)

Observed rotation curves: implication for dark matter

For most of spiral galaxies, their rotation curves remain flat out to radii much larger than the extent of the optical disk!

From $v(R) \approx \text{constant}$ and eq.(19), it follows

$$M(R) \sim R \quad (21)$$

For the majority of spiral galaxies no decrease in the circular velocity has been measured even beyond radii of 50 kpc to 100 kpc. This implies

$$\frac{M}{L_B} \geq 30 \frac{M_\odot}{L_{B,\odot}} \quad (22)$$

In contrast, only from the observable matter in the galactic disk, we have

$$\frac{M}{L_B} \text{ (stars and gas)} \simeq 5 \frac{M_\odot}{L_{B,\odot}} \quad (23)$$

Dynamically measured mass is at least 5 times more dark matter than $M_* + M_{\text{gas}}$ → strong evidence of dark matter!

2.3 Scaling relations for spiral galaxies

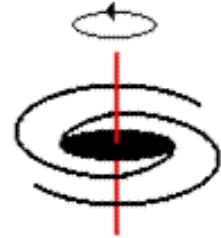
Tully-Fisher relation

Δv : the width of the line of neutral hydrogen H 21cm after correction for inclination. There is a proportional relation between galaxy luminosity at a certain band and Δv :

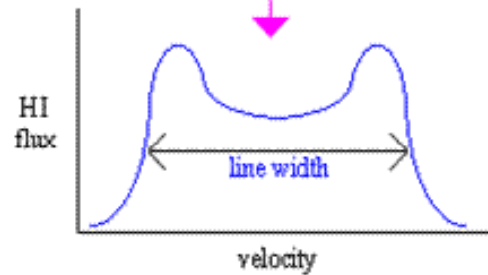
$$L_{\text{band}} \sim (\Delta v)^a \quad (25)$$

1. Öpik (1922) estimated a distance to M31 using the virial theorem **before** it has been proven to be out of the Milky Way.
2. Originally $a = 2.5$ from V-band data (Tully & Fisher 1977).
3. Later more accurate data, $a \sim 3 - 4$ (depending on the observed wavelength).
4. For L_H (1.65 microns) $a=3.2$.

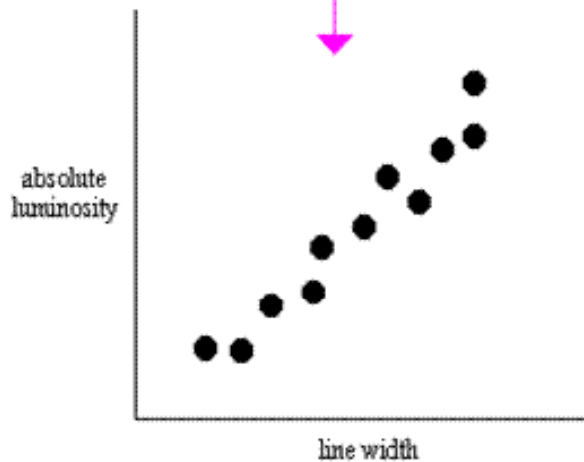
Tully-Fisher relation: schematic description



spiral galaxies rotate, and the rotation speed is proportional to the mass of the galaxy



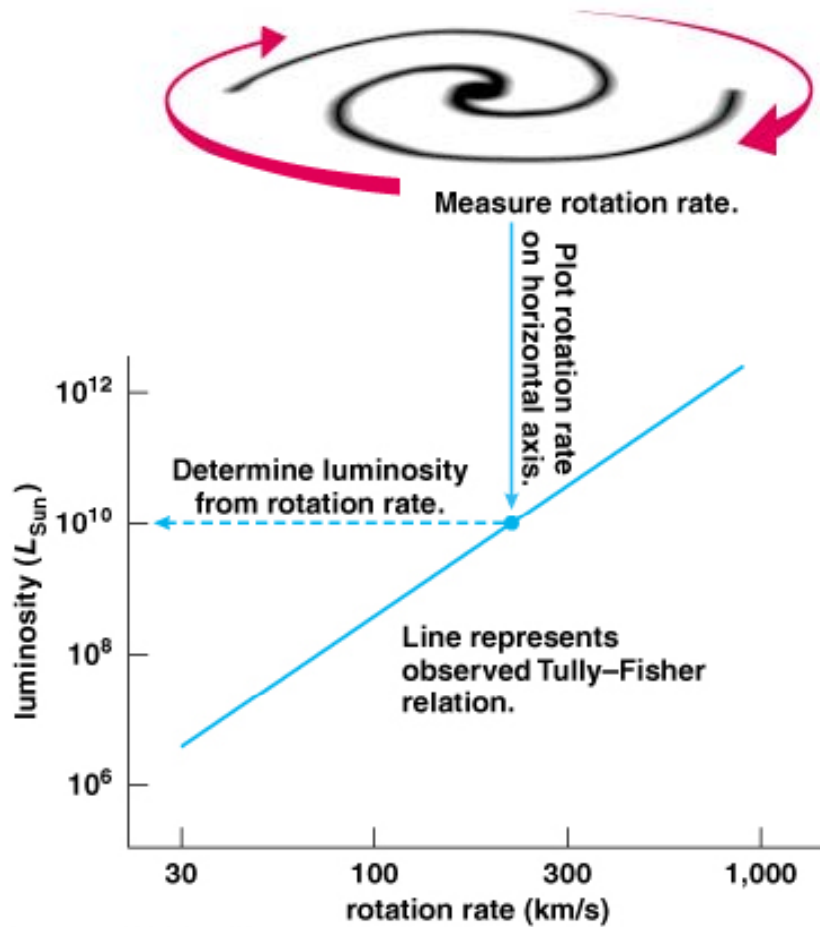
measurements of neutral hydrogen (HI) display a "double-horned" profile, where the width of the line indicates the mass



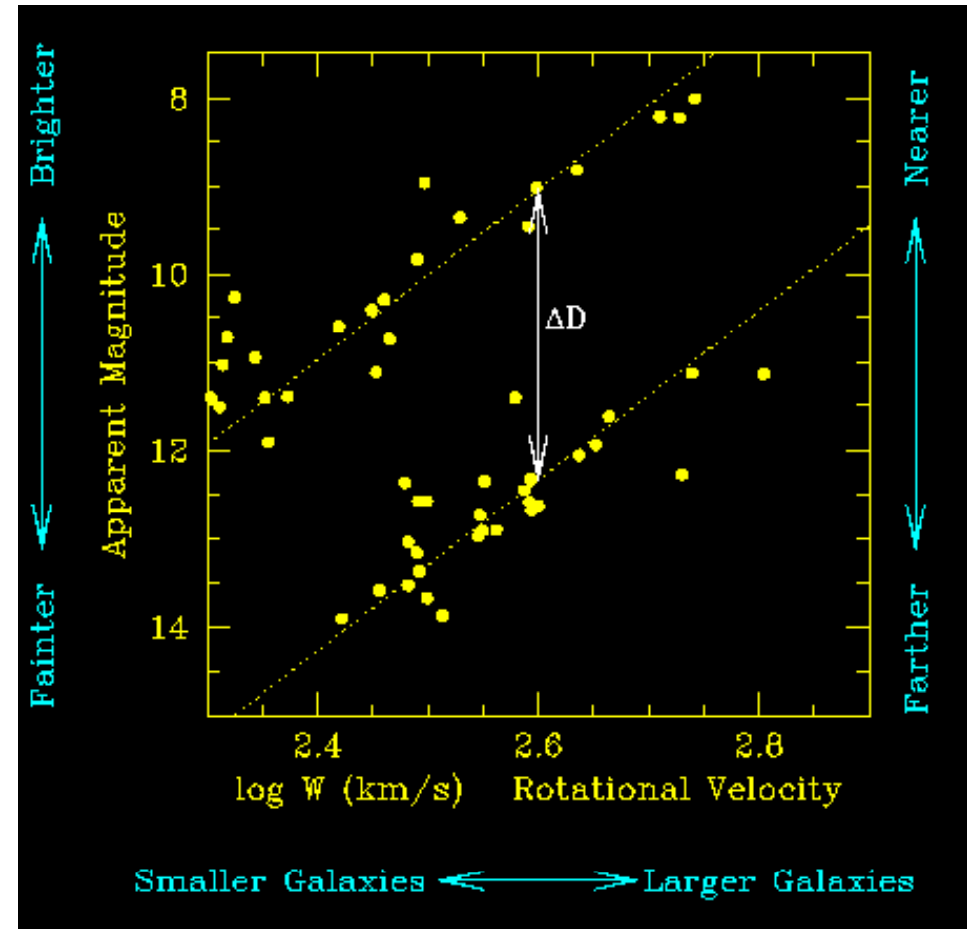
a plot of line width versus absolute luminosity of a galaxy is called the Tully-Fisher relation. When calibrated using galaxies with Cepheid distances, the TF relation is used to determine Hubble's constant.

Tully-Fisher relation as a distance measurement tool

T-F relation at near IR has been proven to be very accurate
→ distance estimation



Copyright © Addison Wesley



Tully-Fisher relation: crude analysis

Assume that the distribution of mass in the disk follows the surface brightness profile

$$I = I_0 \exp(-R/R_0)$$

The total mass in the disc will be then

$$M = \int_0^{\infty} 2\pi R I_0 \exp\left(-\frac{R}{R_0}\right) dR = 2\pi I_0 R_0^2 \quad (26)$$

This means that **a large fraction of mass is concentrated in the disk of the radius $R \sim R_0$.**

Tully-Fisher relation: crude analysis

Assuming that all the mass is concentrated in the disk center and that the gravitational force and centrifugal force balance each other for a given star (or mass element), we have

$$\frac{v_{\max}}{R_0} = 2\pi \frac{I_0 R_0^2}{R_0^2} \quad (27)$$

which yields $v_{\max} \sim (I_0 R_0)^{1/2}$, i.e., $M \sim v_{\max}^3$.

If the surface brightness in the spiral galaxy centers is constant and we assume a constant M/L in the disks, we obtain $L \sim v_{\max}^3$. However, **both of the assumptions are not realistic, as we have seen above.**

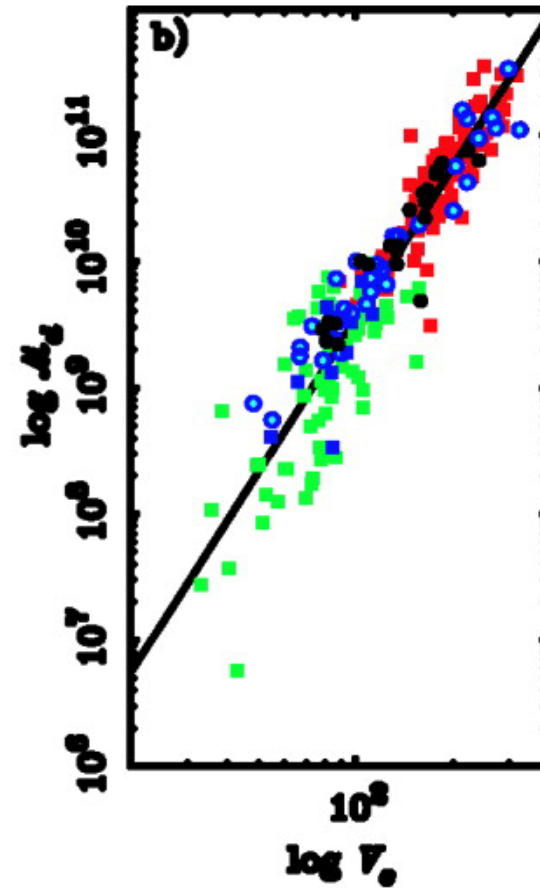
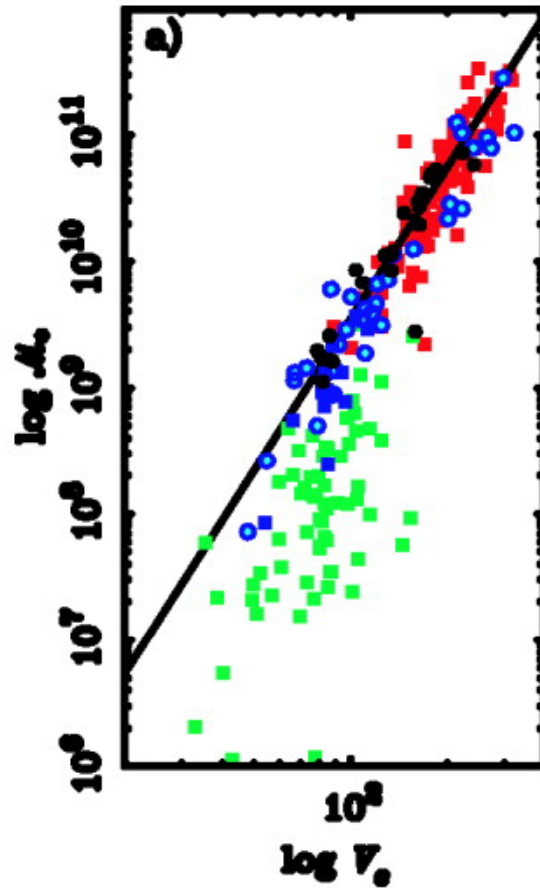
Baryonic Tully-Fisher relation

The classical Tully-Fisher relation depends on the observed wavelength because it uses optical/NIR luminosity, which is strongly dependent on star-formation history or other non-dynamical properties (we see later).

This problem can be overcome by using the baryon mass instead of optical luminosity: baryonic Tully-Fisher relation.

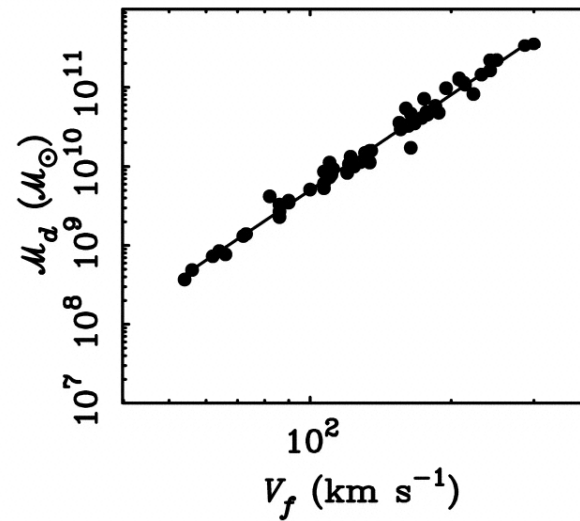
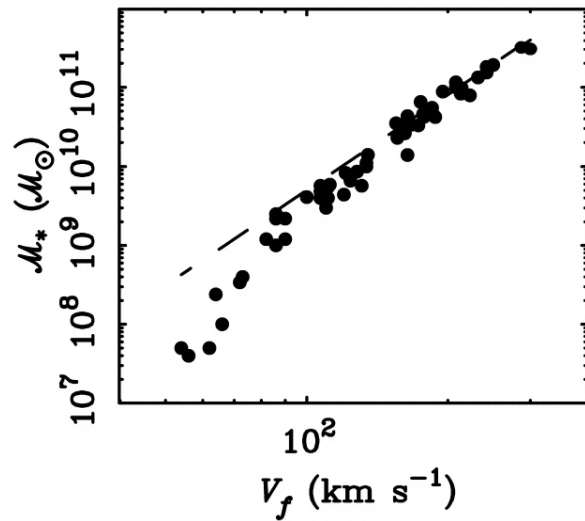
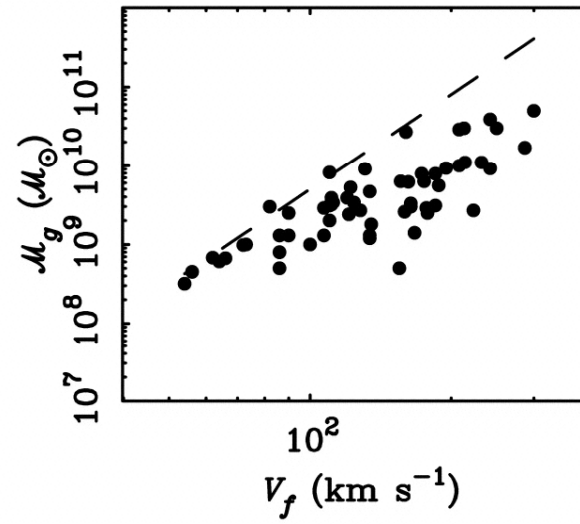
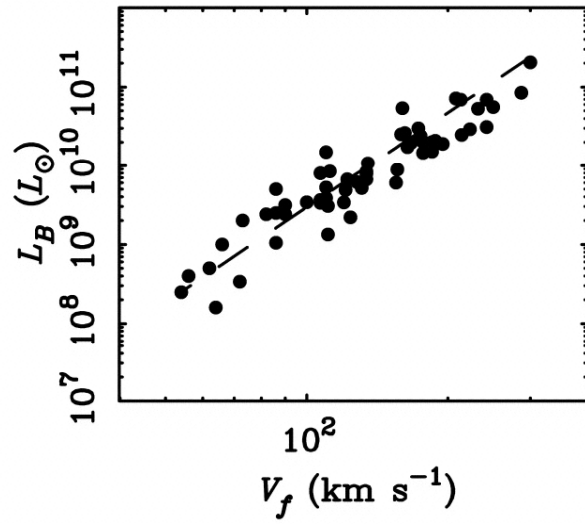
Here it is worth stressing that whichever indicator we use, reproducing Tully-Fisher relation by theoretical model remains a challenge.

Baryonic Tully-Fisher relation

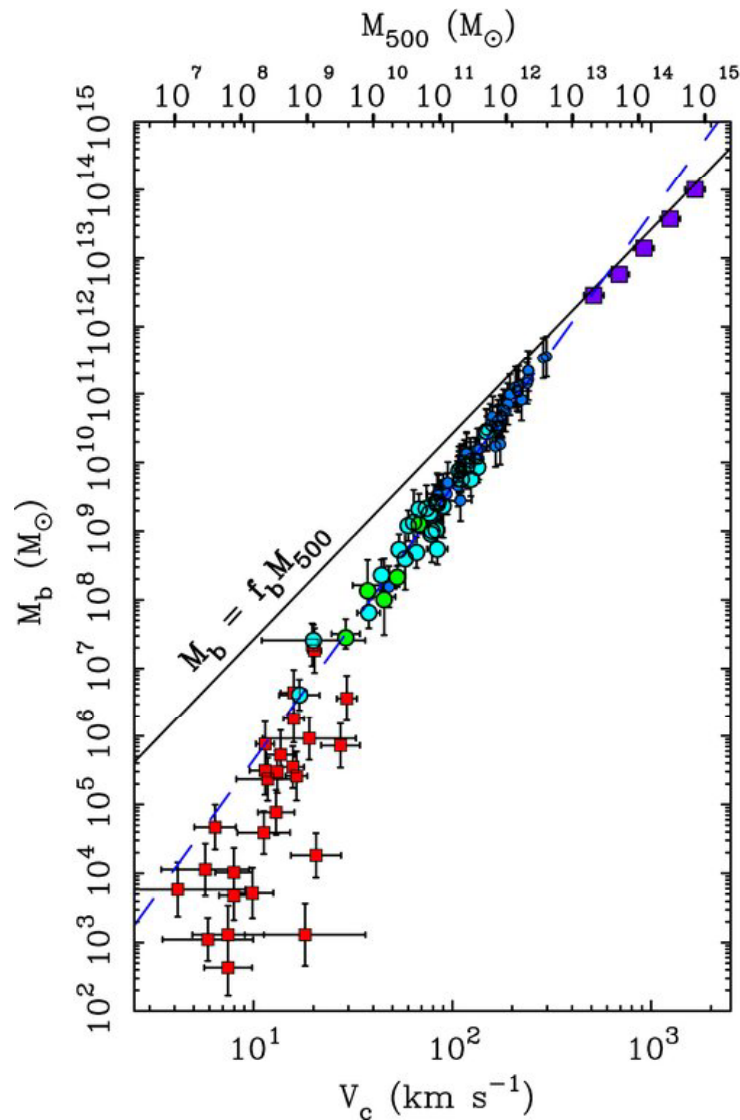


McGaugh et al. (2000)

Baryonic Tully-Fisher relation



The “extended” BTF



(McGaugh et al. 2010)

In the extended BTF, the slope becomes shallower from dwarf spheroidals, normal galaxies, to clusters (clusters: violet symbols, giant galaxies: blue symbols, and dwarf spheroidals: red symbols).

⇒ Feedback?

However, this sample does not include gas-rich dwarf galaxies.

Toward lower HI masses!

Part II: Evolution of Galaxies

3. Luminosity Function of Galaxies

3.1 Definition and basic properties

3.2 Dependence of luminosity functions on various properties

3.3 Evolution of galaxy luminosity function

3.1 Definition and basic properties

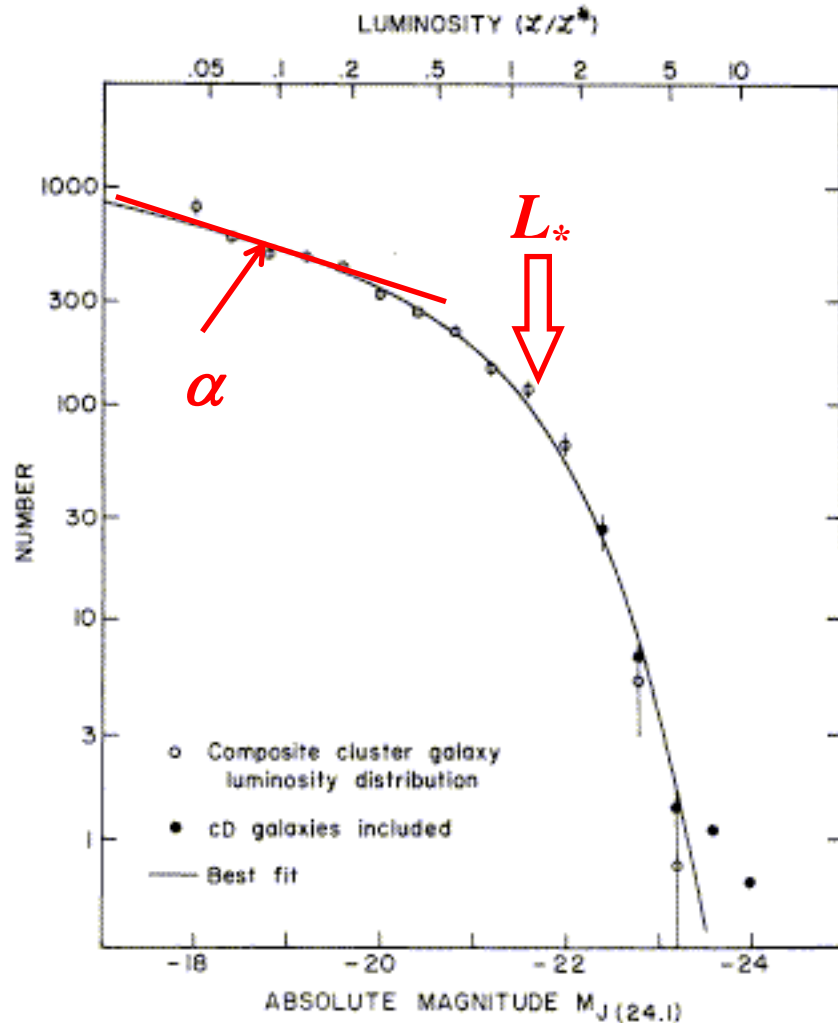
Galaxy luminosity function: definition

Definition: number density of galaxies as a function of luminosity.

More quantitatively, galaxy luminosity function $\phi(L)$ is defined so as to make $\phi(L)dL$ be the number of galaxies with luminosity in an interval $[L, L+dL]$.

N.B. In optical astronomy, absolute magnitude M is always used as an equivalent of luminosity L . In this case, its mathematical functional form is different, but (very confusingly) expressed with the same symbol as $\phi(M)dM$. Also, $\log L$ is very often used, again with the same symbol $\phi(\log L)d \log L$.

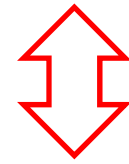
Galaxy luminosity function: Schechter function



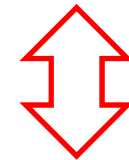
(Schechter 1976)

Phenomenological fitting function to the observed **optical** luminosity function of galaxies, parameterized with α , L_* , and ϕ_* .

$$\phi(L)dL = \phi_* \left(\frac{L}{L_*} \right)^\alpha \exp\left(-\frac{L}{L_*}\right) d\left(\frac{L}{L_*}\right)$$



$$\phi(L)d \log L = (\ln 10) \phi_* \left(\frac{L}{L_*} \right)^{\alpha+1} \exp\left(-\frac{L}{L_*}\right) d \log L$$



$$\begin{aligned} \phi(M)dM &= 0.4(\ln 10) \phi_* 10^{-0.4(\alpha+1)(M-M_*)} \\ &\quad \times \exp\left[-10^{-0.4(M-M_*)}\right] dM. \end{aligned}$$

Schechter-function related physical quantities

Galaxy number density (number per unit comoving volume):

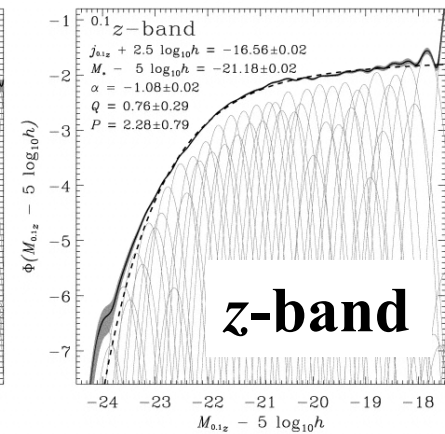
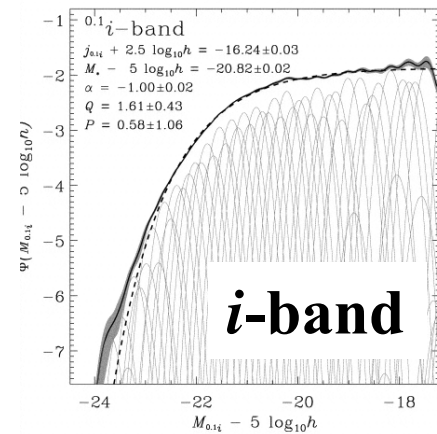
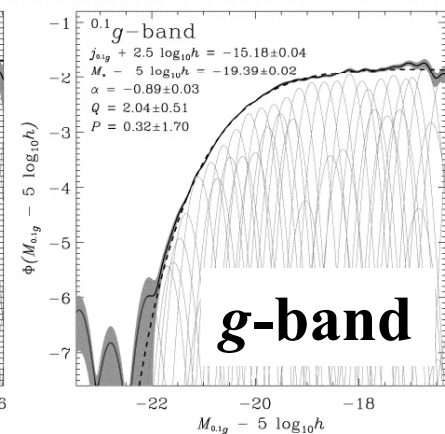
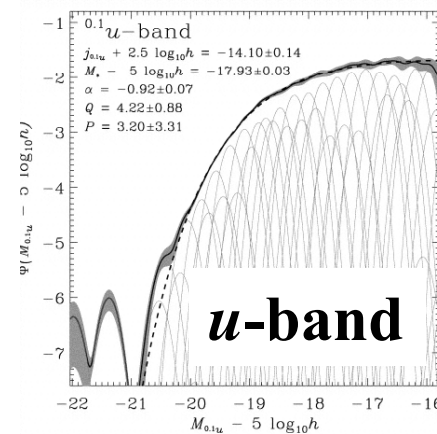
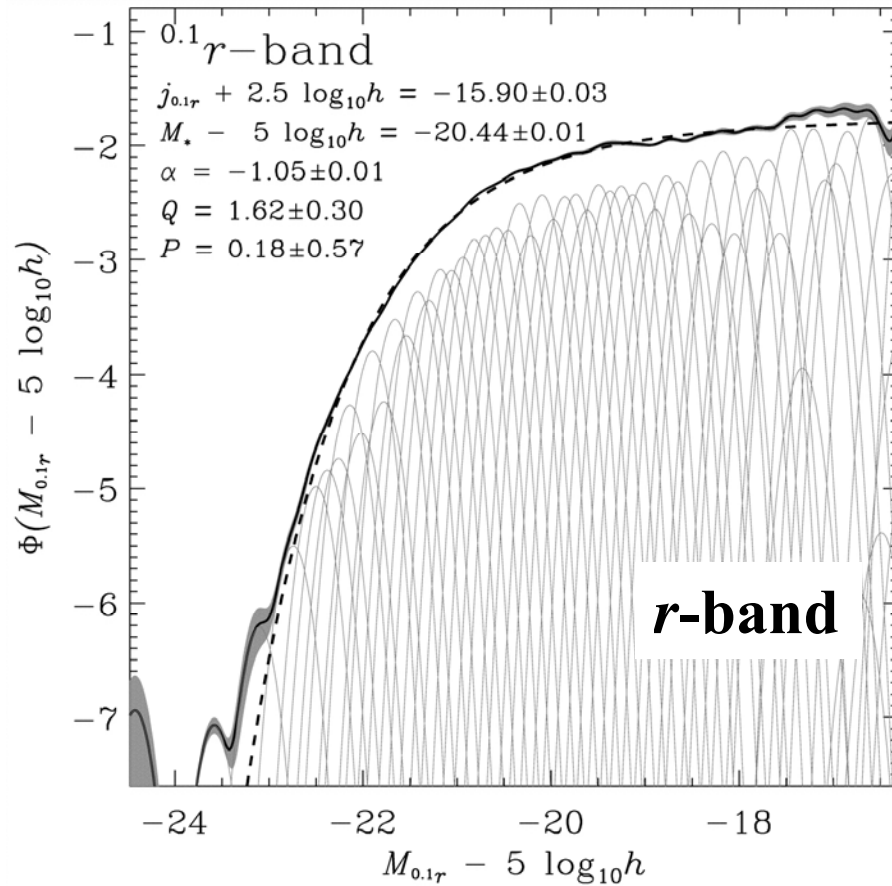
$$N(> L) = \int_L^{\infty} \phi(L') dL' = n_* \Gamma\left(\alpha + 1, \frac{L}{L_*}\right)$$

Galaxy luminosity density (luminosity per unit comoving volume):

$$\rho_L(> L) = \int_L^{\infty} L' \phi(L') dL' = n_* L_* \Gamma\left(\alpha + 2, \frac{L}{L_*}\right)$$

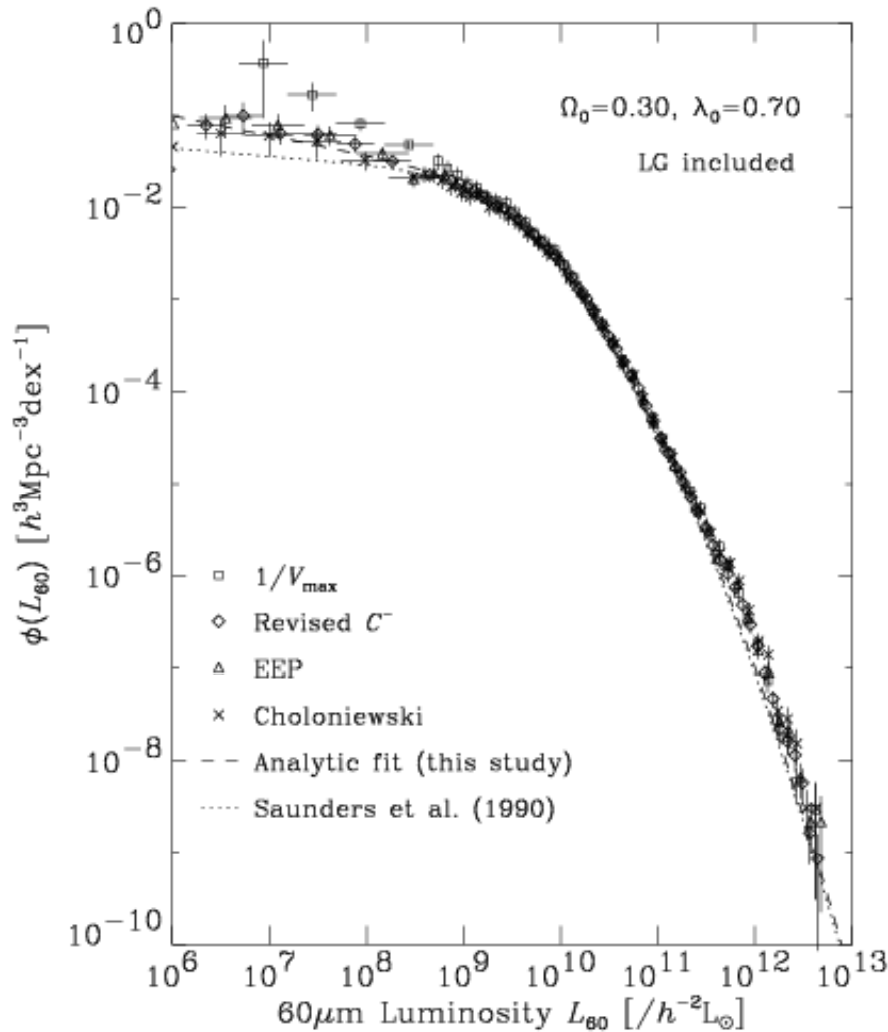
Because of the functional form, the integral properties are described by Gamma function.

Local galaxy luminosity function: SDSS (optical)



Blanton et al. (2003)

Local galaxy luminosity function: IRAS PSCz (far infrared)



Takeuchi et al. (2003)

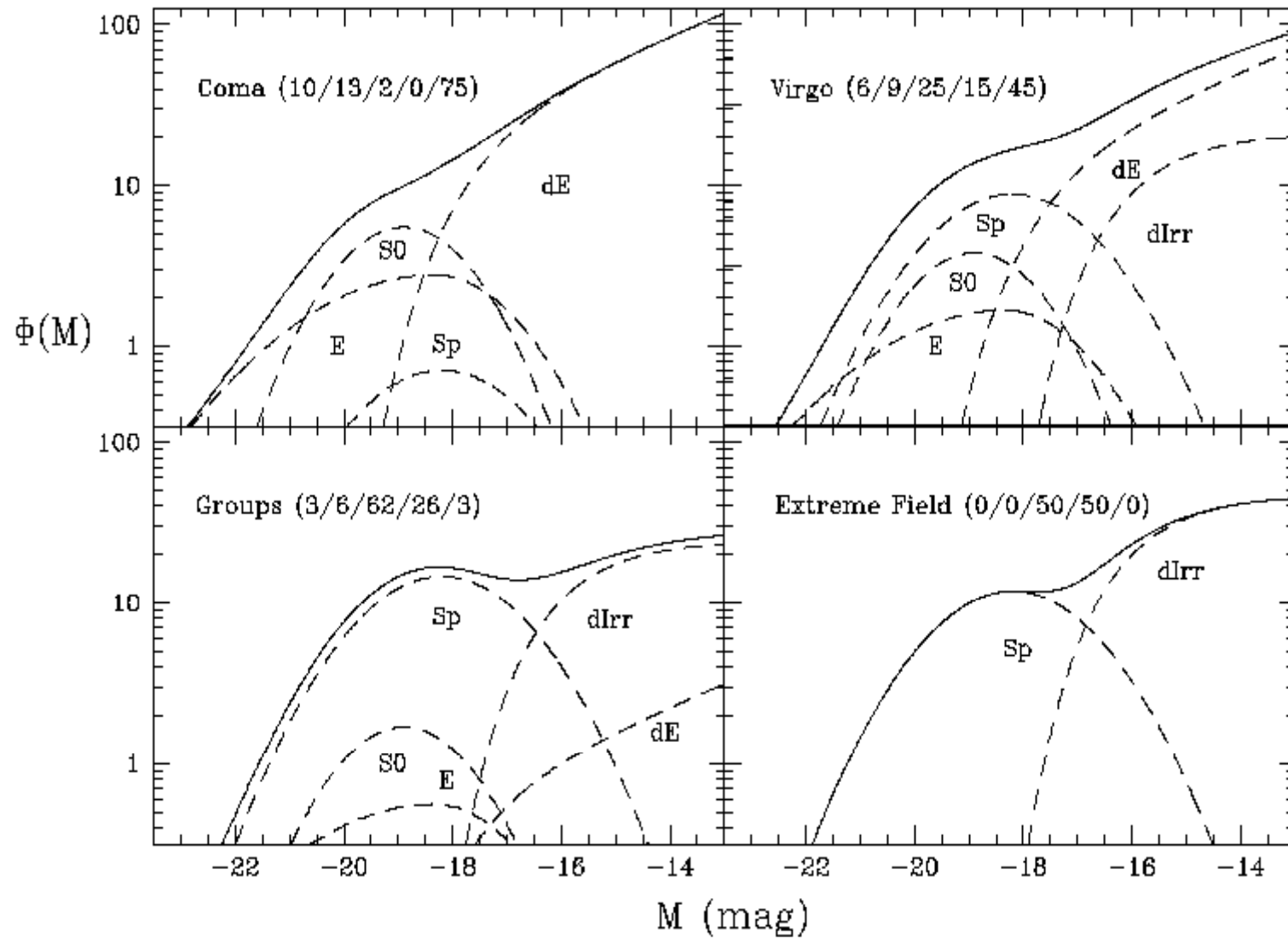
The far-infrared (FIR) galaxy LF is not well described by the Schechter function. Instead, a function with much slower decline at luminous end is used.

$$\phi(L) = \phi_* \left(\frac{L}{L_*} \right)^{\alpha+1} \exp \left[-\frac{1}{2\sigma^2} \log^2 \left(1 + \frac{L}{L_*} \right) \right] \quad (29)$$

This form is one of the most frequently used, proposed by Saunders et al. (1990), parameterized by L_* , ϕ_* , α , and σ .

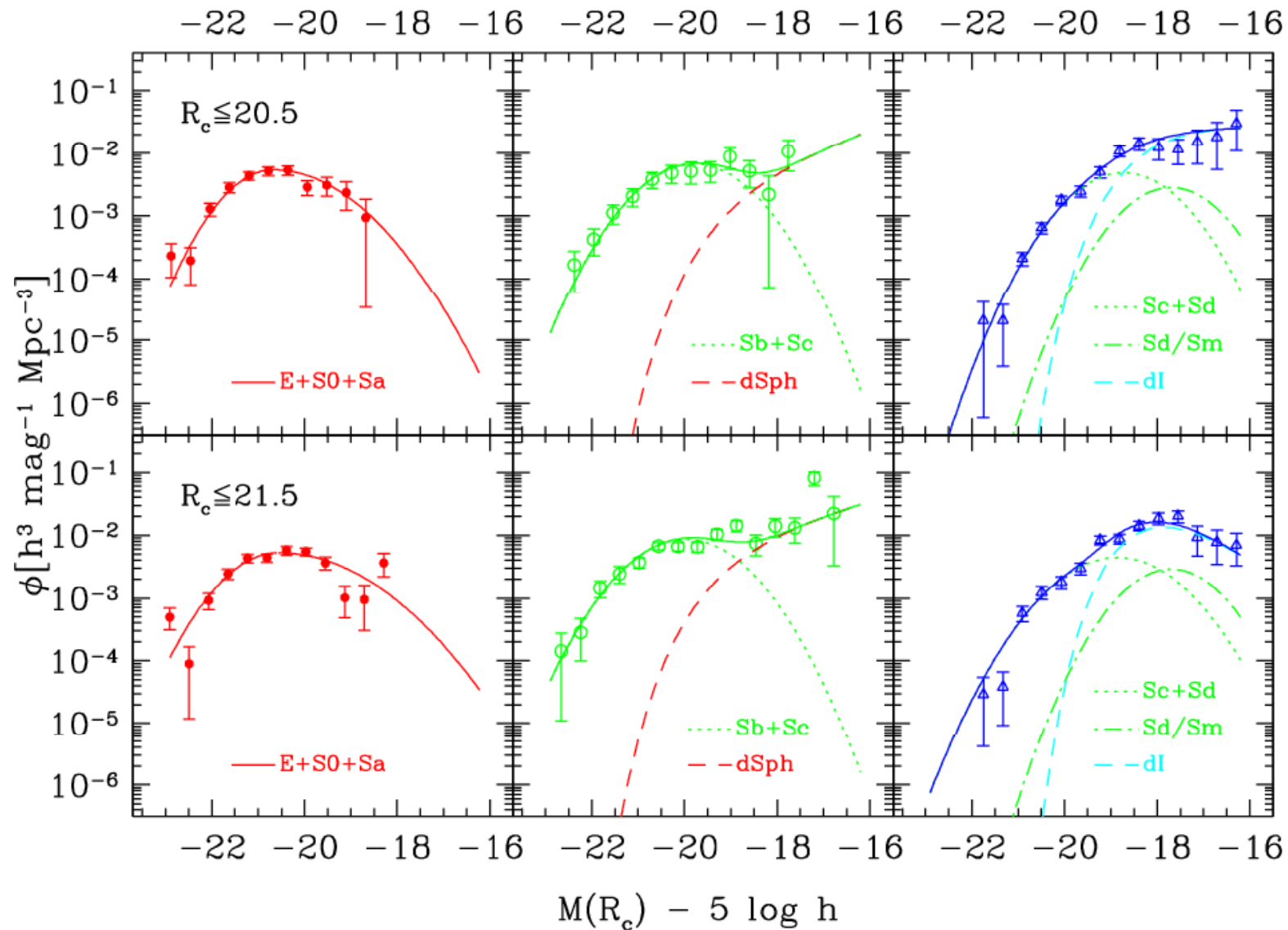
3.2 Dependence of luminosity functions on various properties

Galaxy luminosity function: environmental dependence



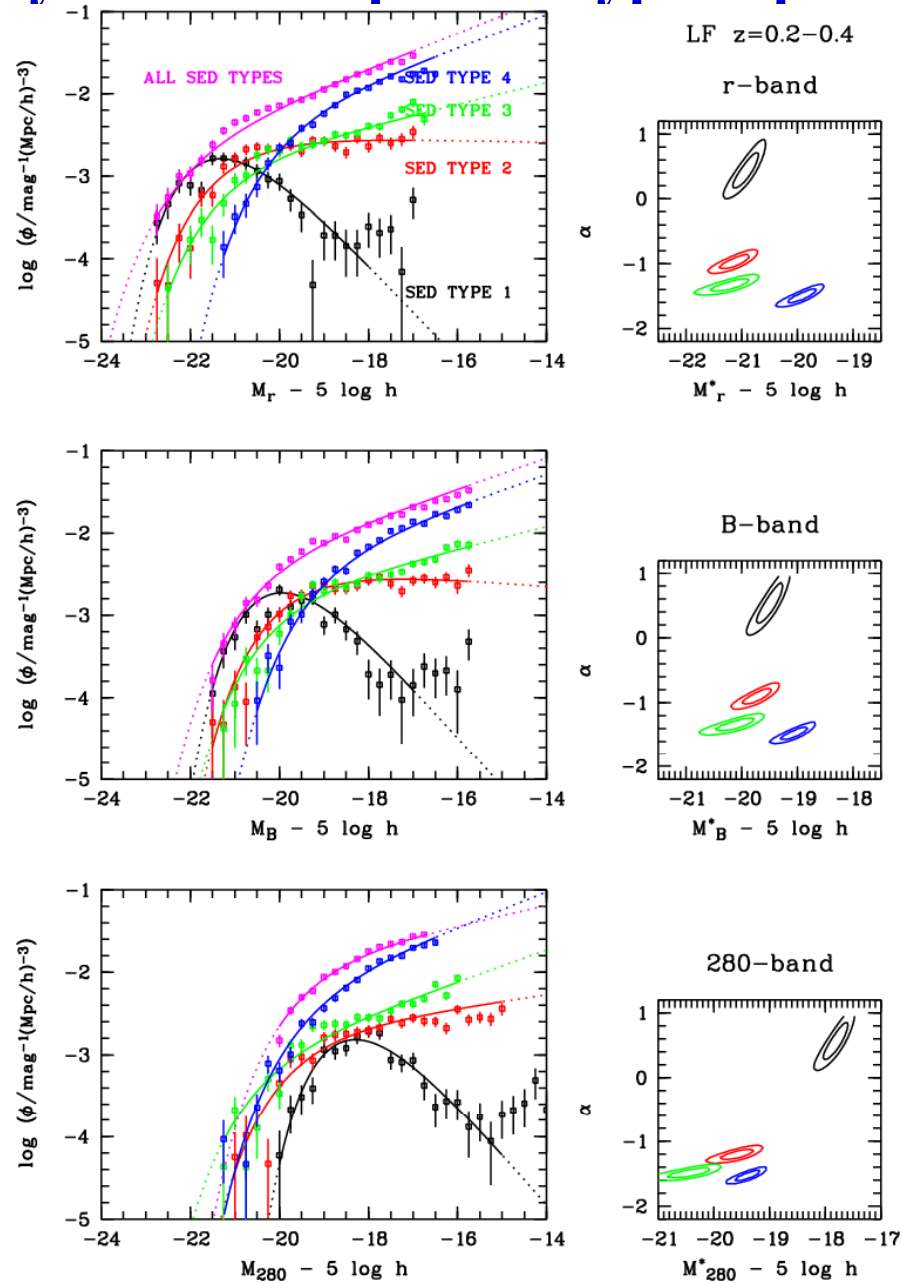
Binggeli et al. (1988)

Galaxy luminosity function: morphological type dependence



de Lapparent et al. (2003)

Galaxy luminosity function: spectral type dependence

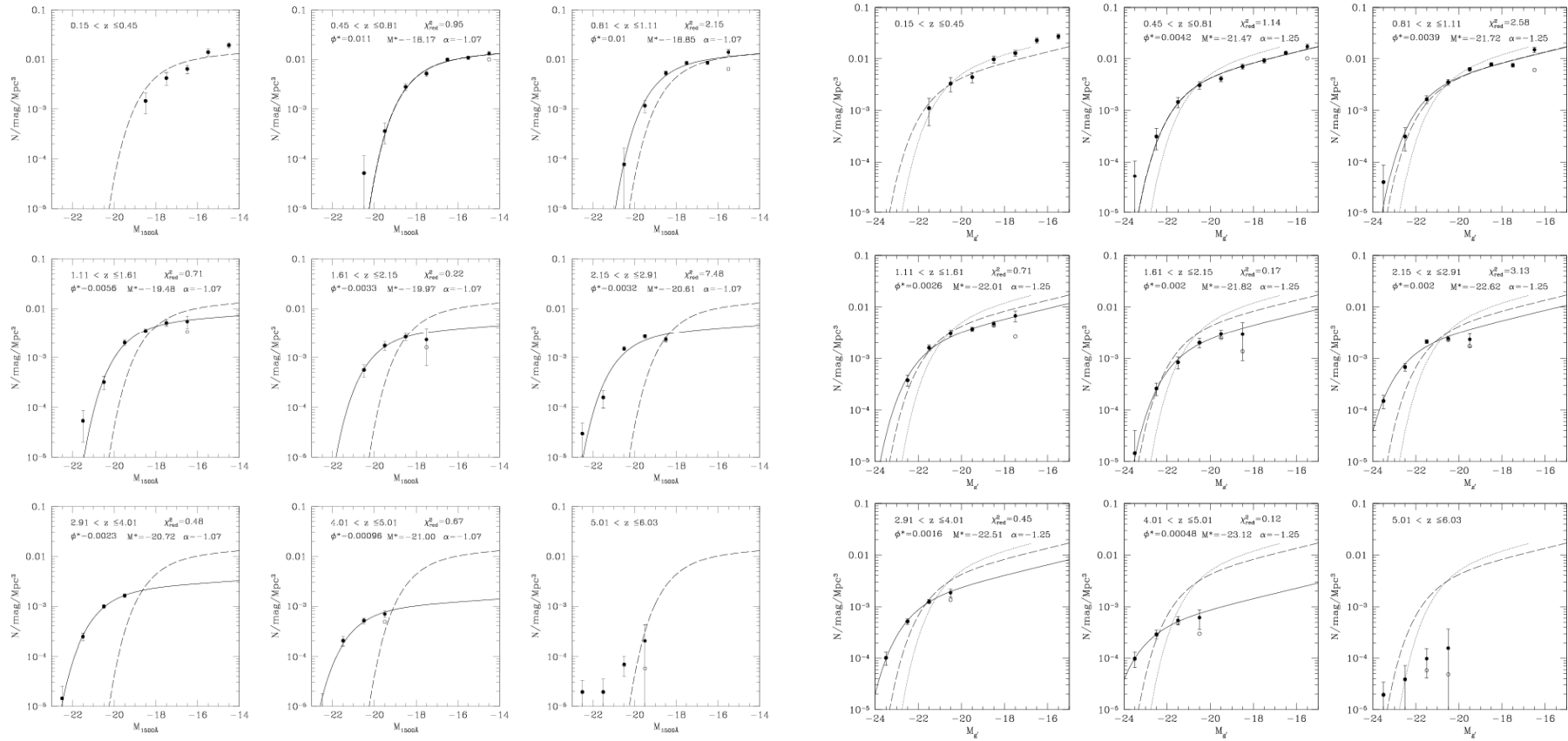


3.3 Evolution of galaxy luminosity function

Galaxy luminosity function: evolution: optical

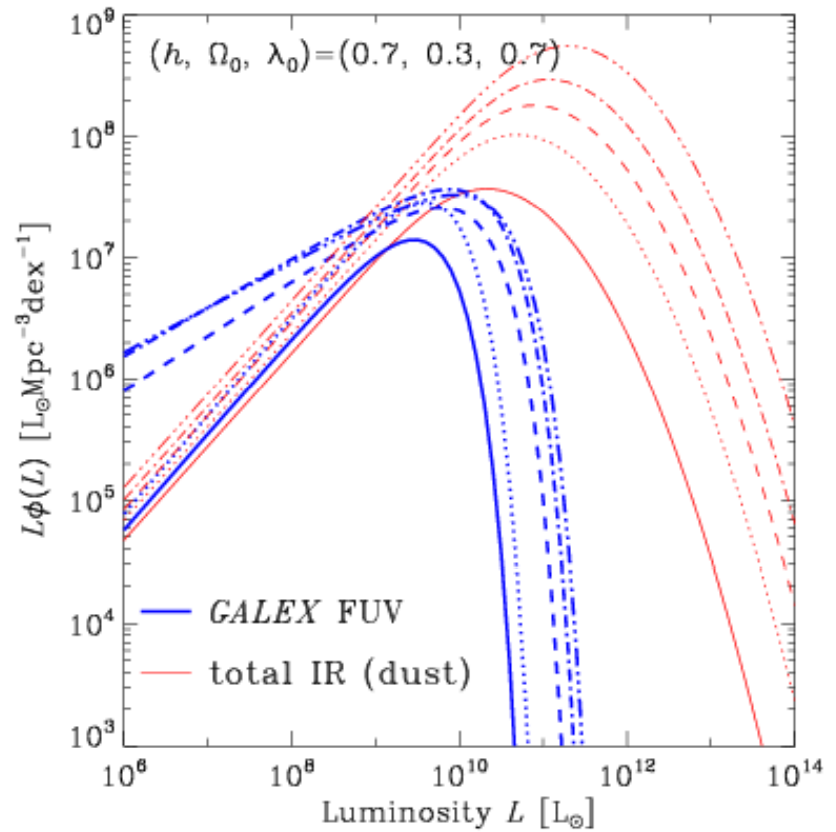
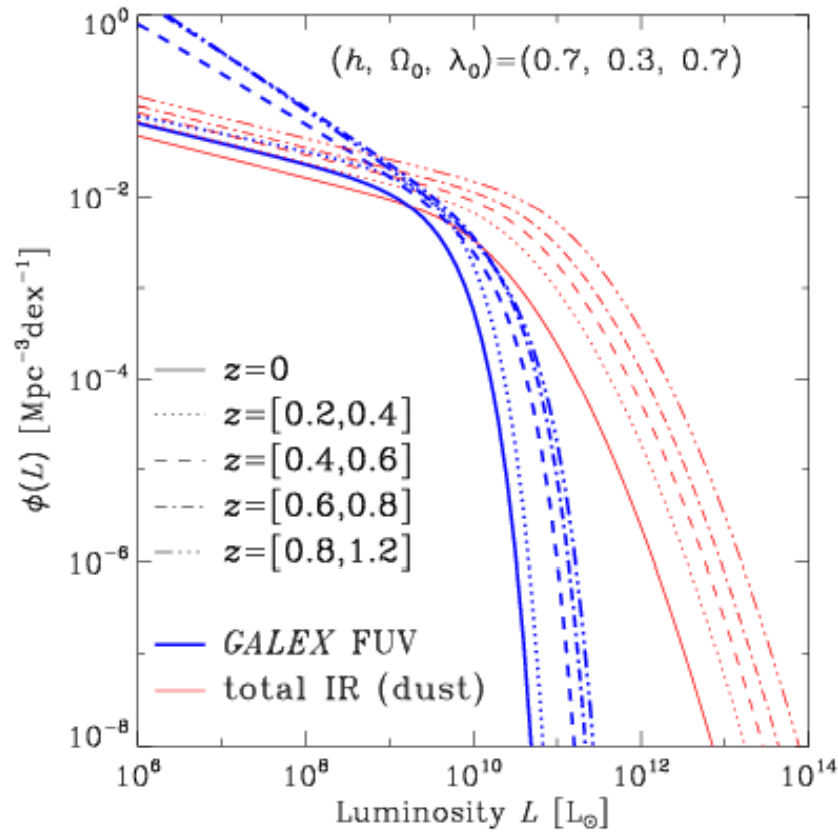
2800Å

g-band



Gabasch et al. (2004)

Galaxy luminosity function: evolution: UV and FIR



Takeuchi et al. (2005)

4. Chemical Evolution of Galaxies

4.1 Stellar evolution

**4.2 Chemical evolution of galaxies: general
framework**

4.3 Evolutionary synthesis model of galaxies

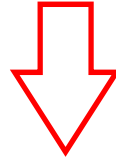
4.4 Star formation history of spiral galaxies

**4.5 Evolution of the total mass, grain size, and
chemical composition of dust**

4.1 Stellar evolution

Stellar evolution: an important ingredient of galaxy evolution

We have seen that **galaxies evolve with time in various senses**. Among others, the most prominent aspect of galaxy evolution is that of stellar population and resulting change of metallicity, appearing in their colors and spectral features (lines, breaks, etc.).



The key factor: stellar evolution

The Life of Stars: basics

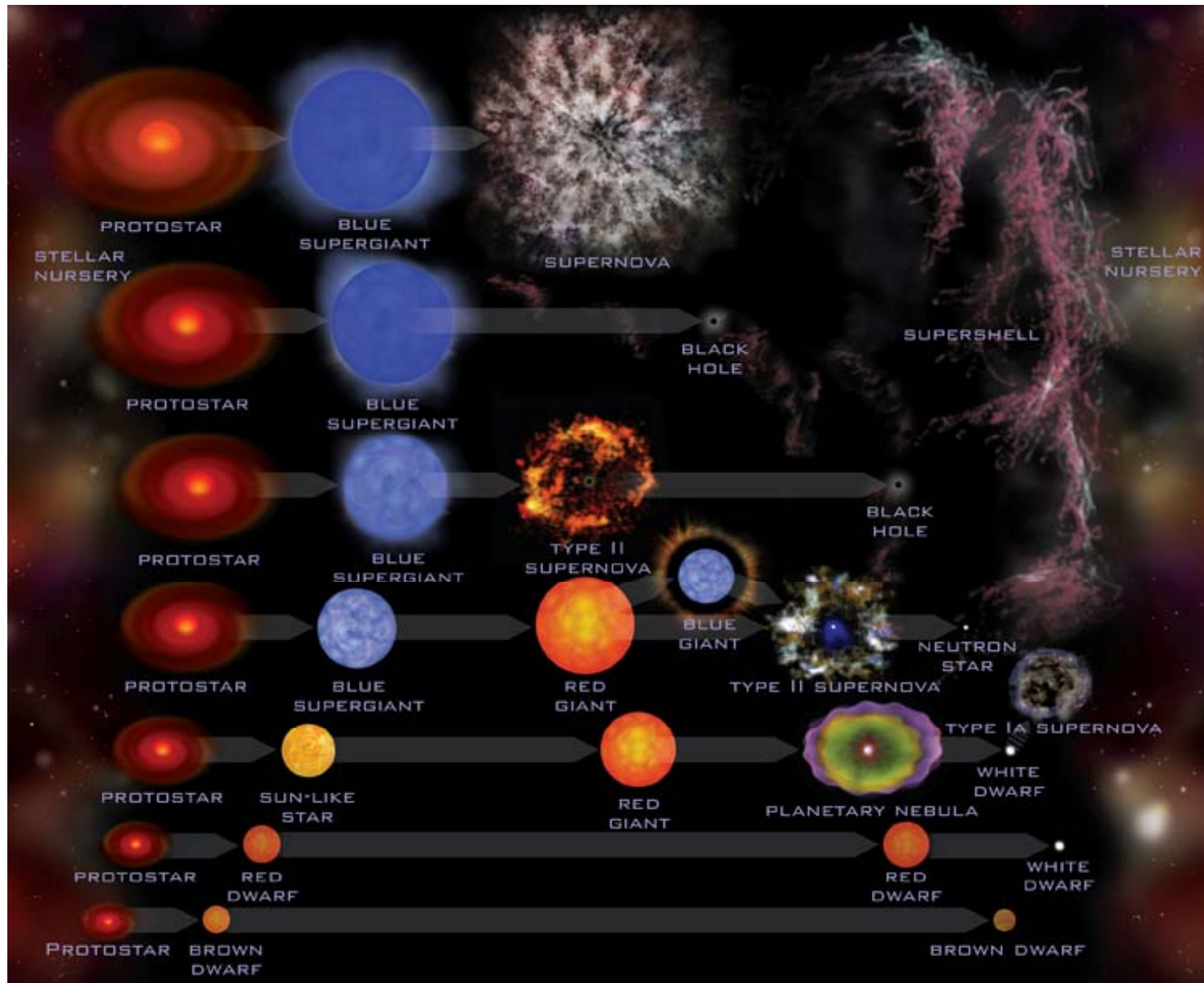
The life of stars is determined by their initial mass.

Light stars live long, end with a moderate ejection of gas and subsequent cooling.



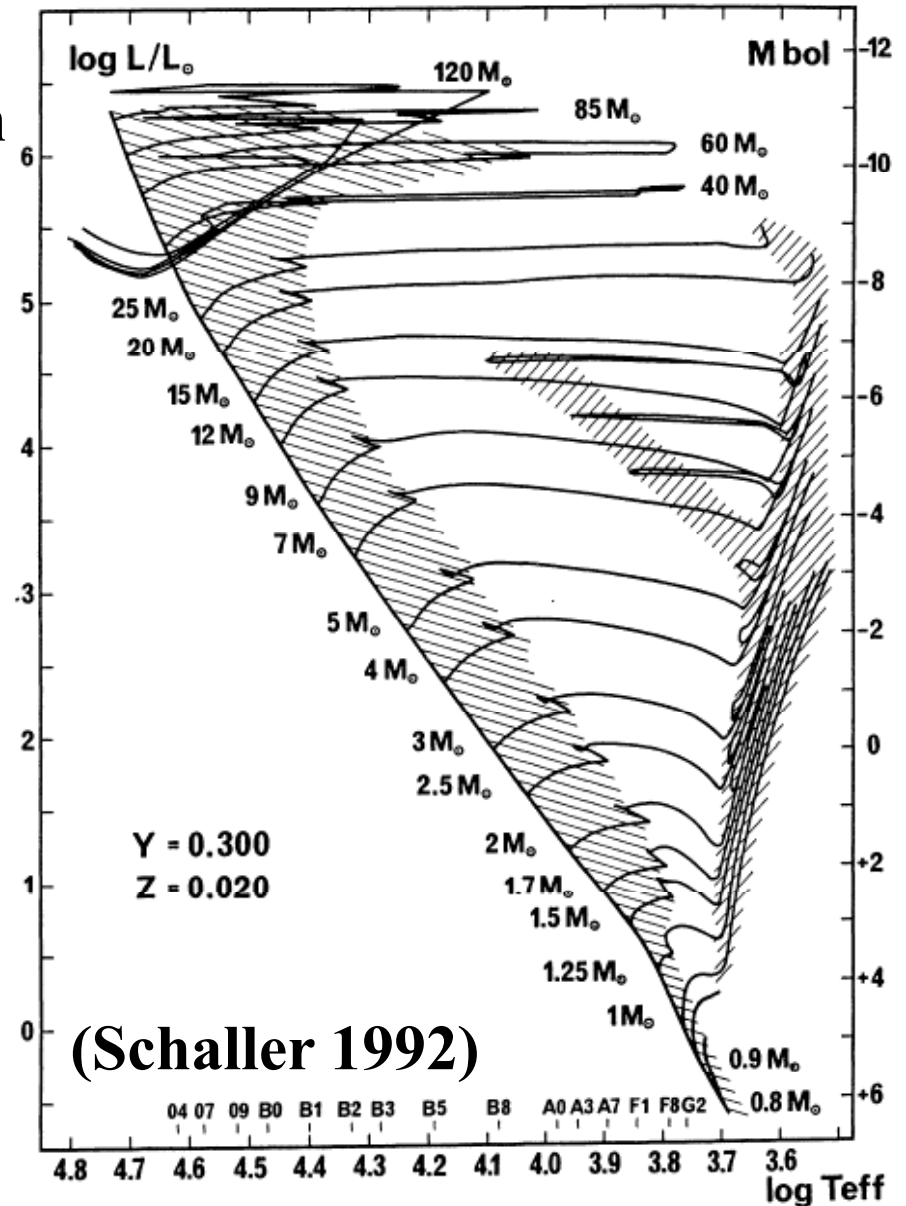
Heavy stars live short, end with violent explosions and mass ejections.

The Life of Stars: basics



Stellar evolution: the Hertzsprung-Russel (HR) diagram

The (theoretical) HR diagram represents a relationship between the effective temperature and luminosity of stars.



Stellar evolution: the Hertzsprung-Russel (HR) diagram

Timescales:

Main sequence lifetimes

1.0 M_{sun} : 9.0×10^9 yr

2.2 M_{sun} : 5.0×10^8 yr

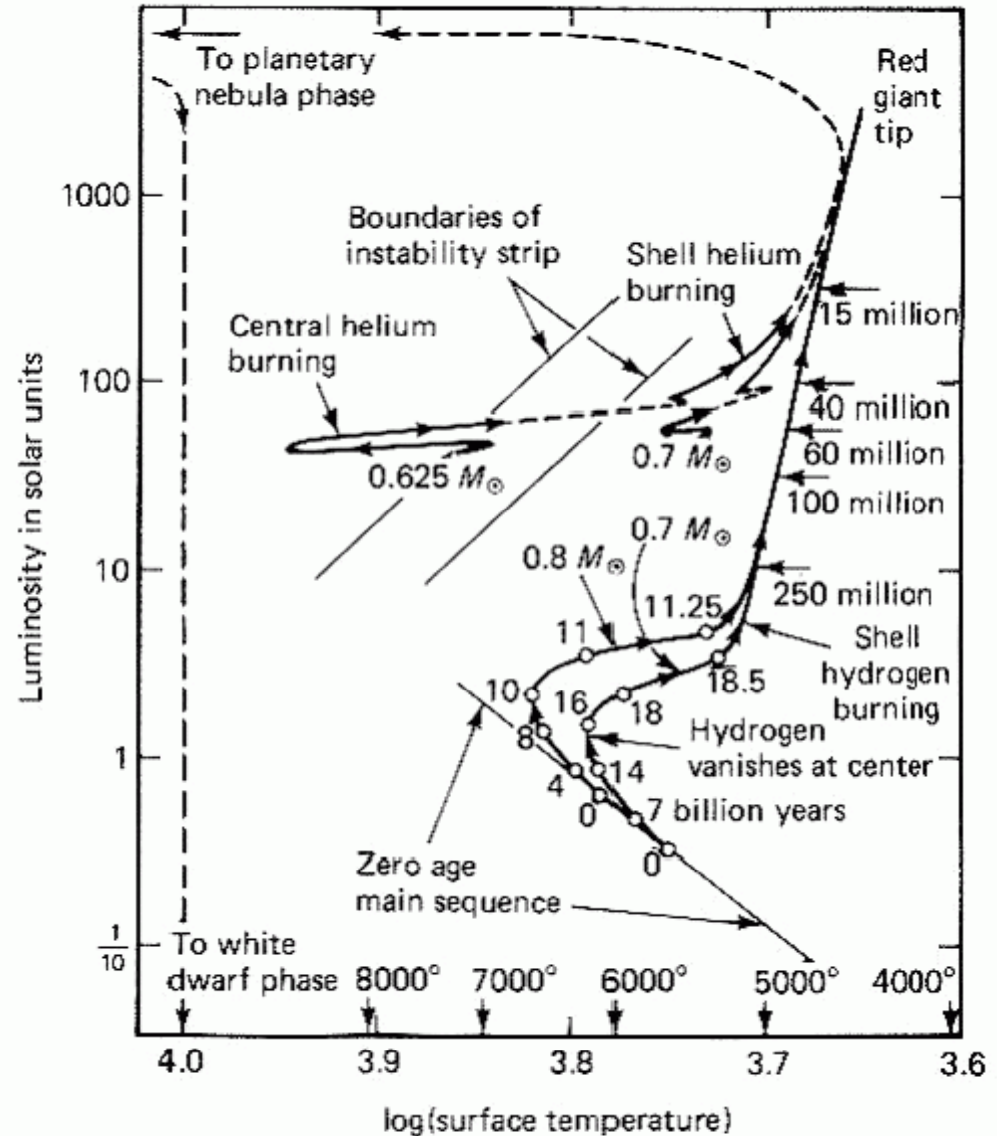
15 M_{sun} : 1.0×10^7 yr

Giant branch lifetimes

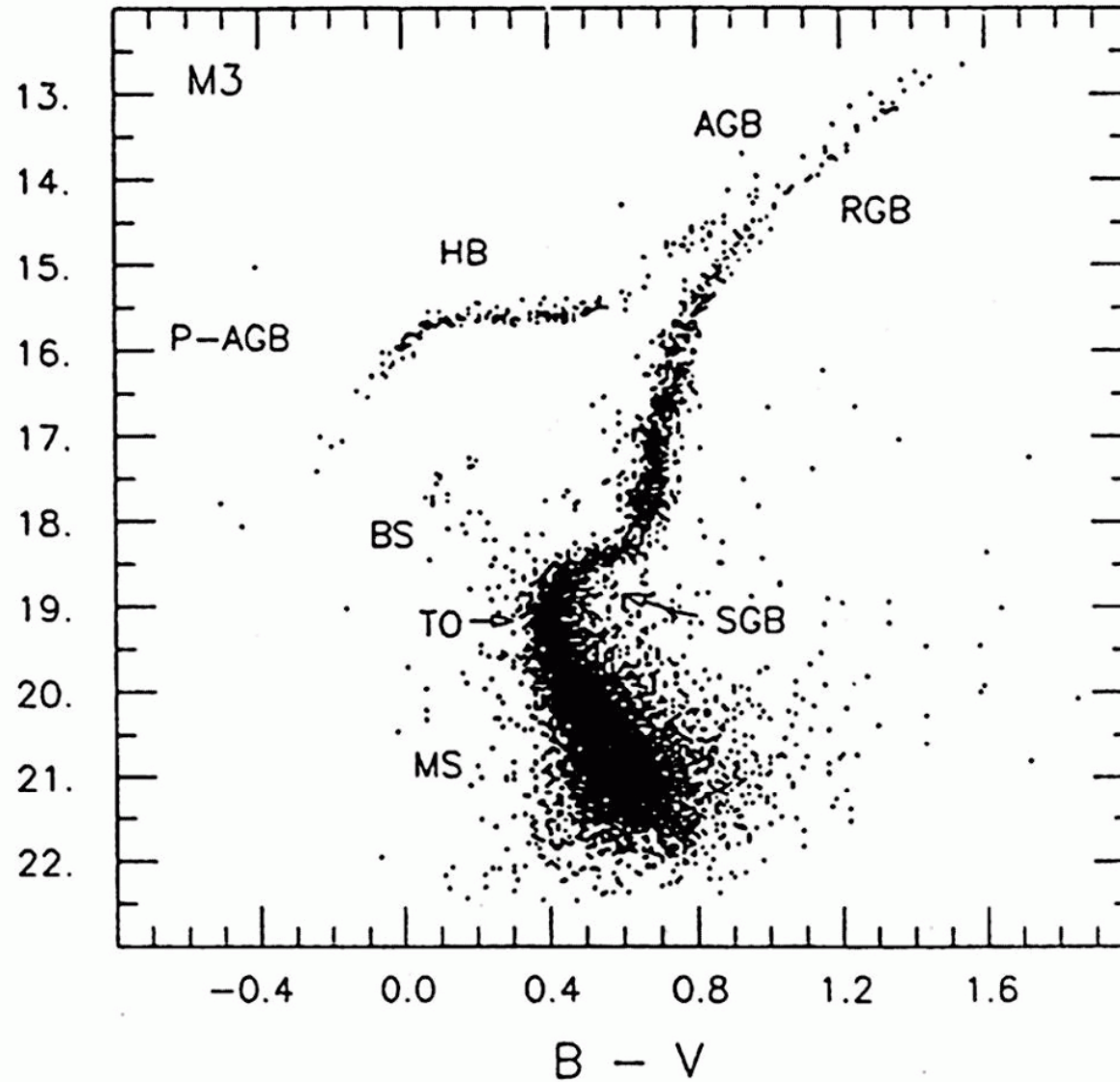
1.0 M_{sun} : 1.0×10^9 yr

2.2 M_{sun} : 2.8×10^7 yr

15 M_{sun} : 1.5×10^6 yr

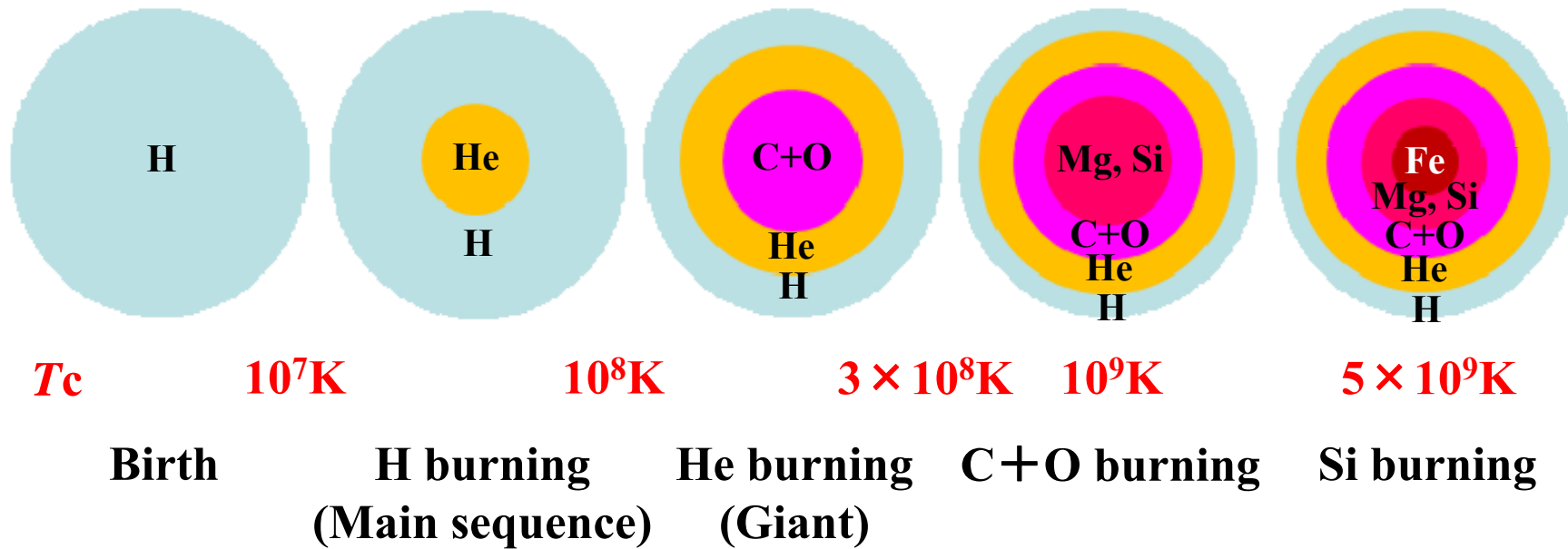


Observed HR diagram



**Messier 3 (M3):
a globular cluster**

Life of stars and their nucleosynthesis

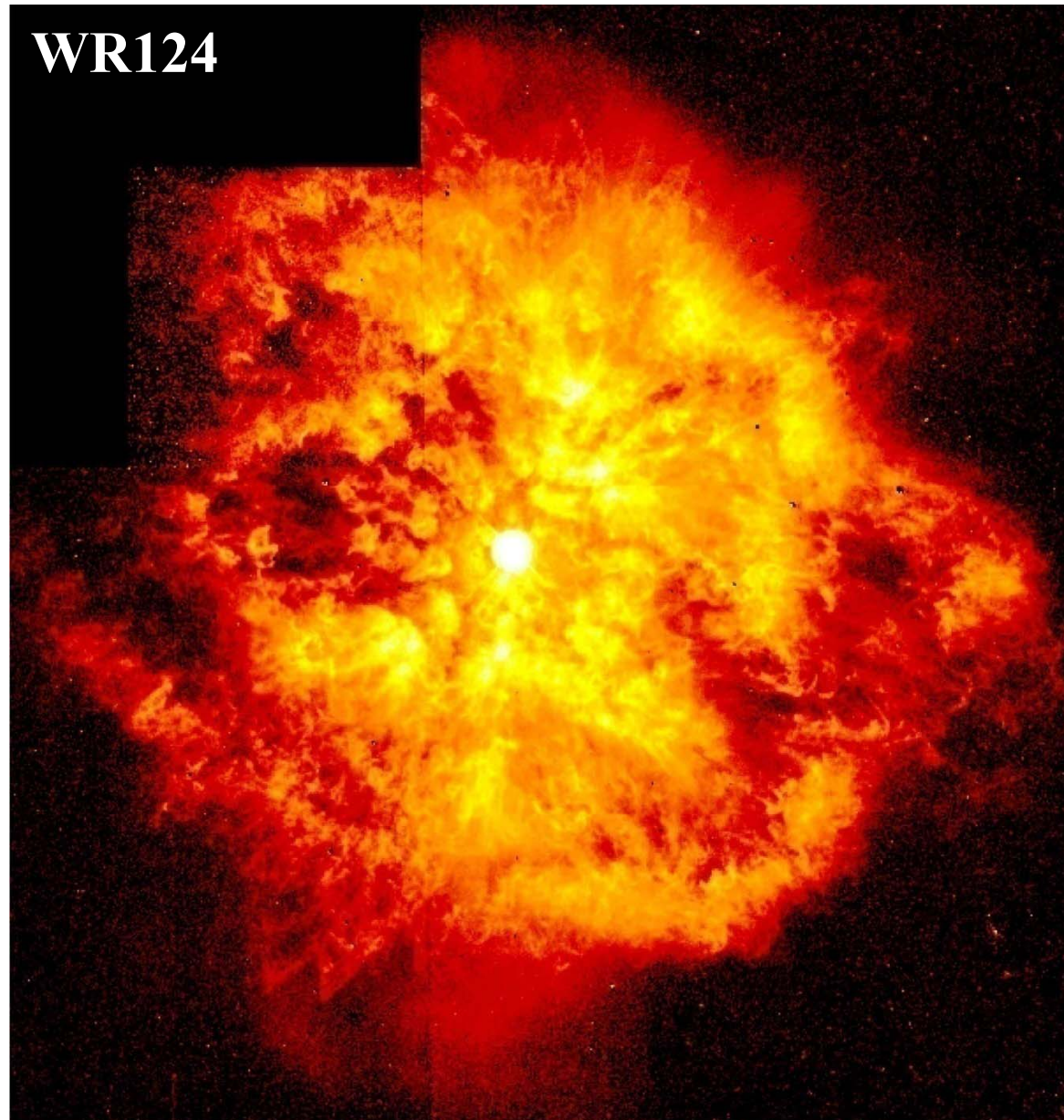


Stars produce heavy elements by the nuclear reaction, and how far the reaction goes depends on the mass of stars.

Lighter than the Sun

Heavier than the Sun

Supply of metals to the interstellar space I: stellar wind



Supply of metals to the interstellar space II: final stage of stars

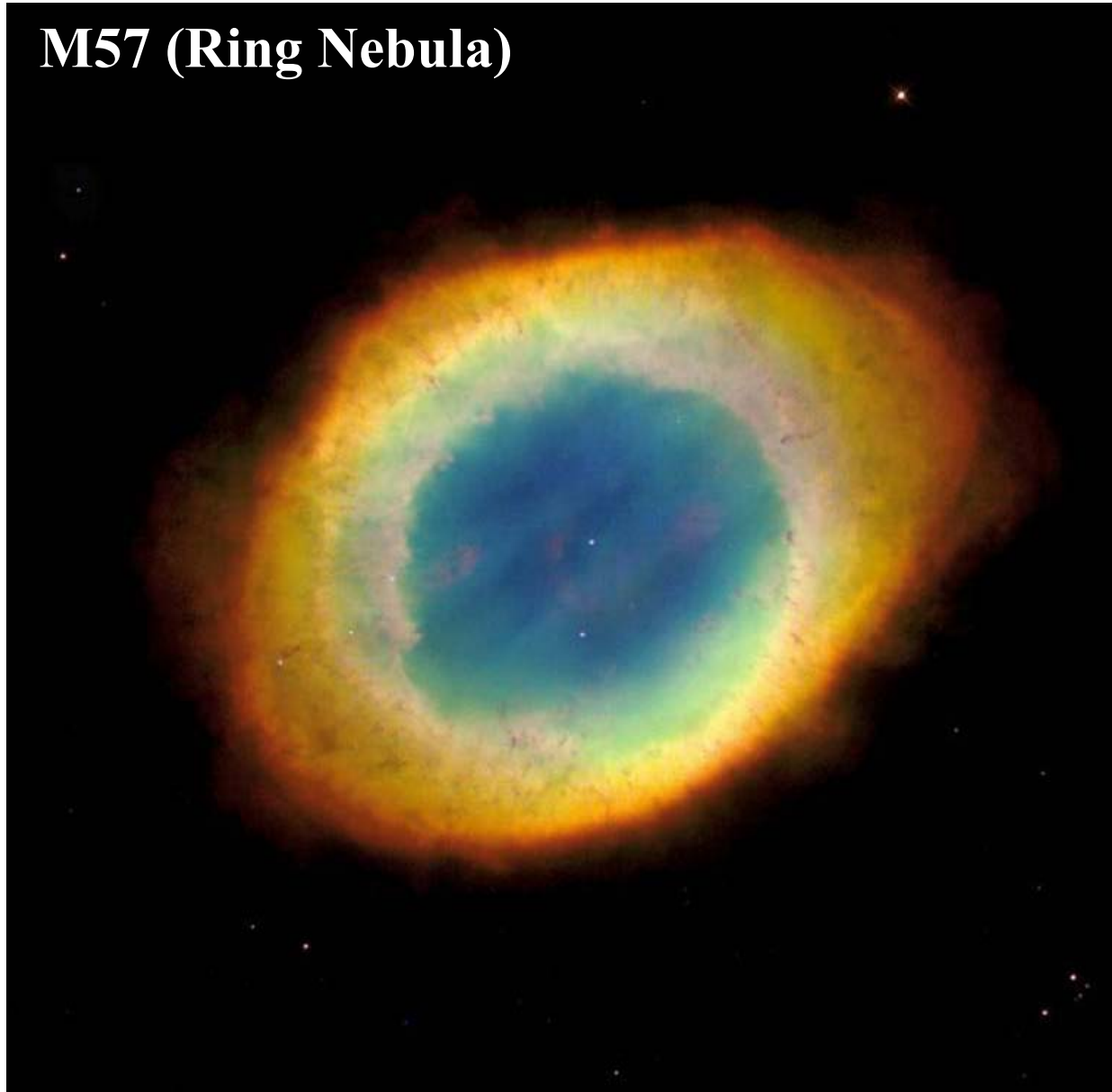
The death of stars with mass $< 8M_{\text{sun}}$: planetary nebulae (PNe)

Stars with similar masses to the Sun run out the hydrogen in the core, change their equilibrium structure and expand, and become cool huge stars (red giant branch stars: RGBs).

After the RGB phase, these stars become unstable and repeat expansion and contraction (**thermal pulse asymptotic giant branch stars: TPAGB**). Because of this pulsation, the outer layer of a star is expelled into the interstellar space and forms a gas nebula, called **planetary nebula (PN)**. The nebulae expand into the space and mix with the interstellar medium (ISM), and provide heavy elements contained in the gas.

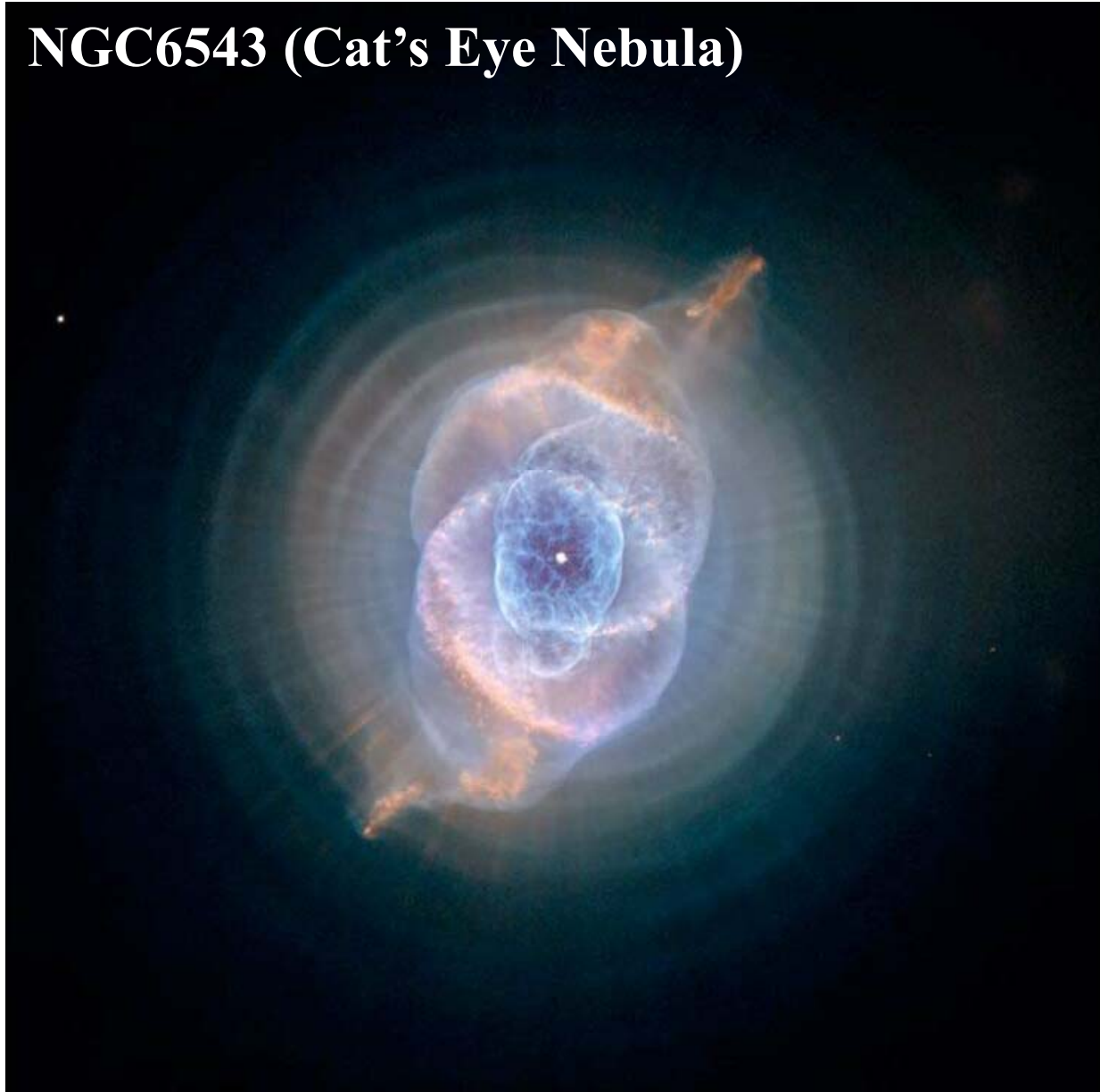
Planetary nebula

M57 (Ring Nebula)



Planetary nebula

NGC6543 (Cat's Eye Nebula)



Supply of metals to the interstellar space II: final stage of stars

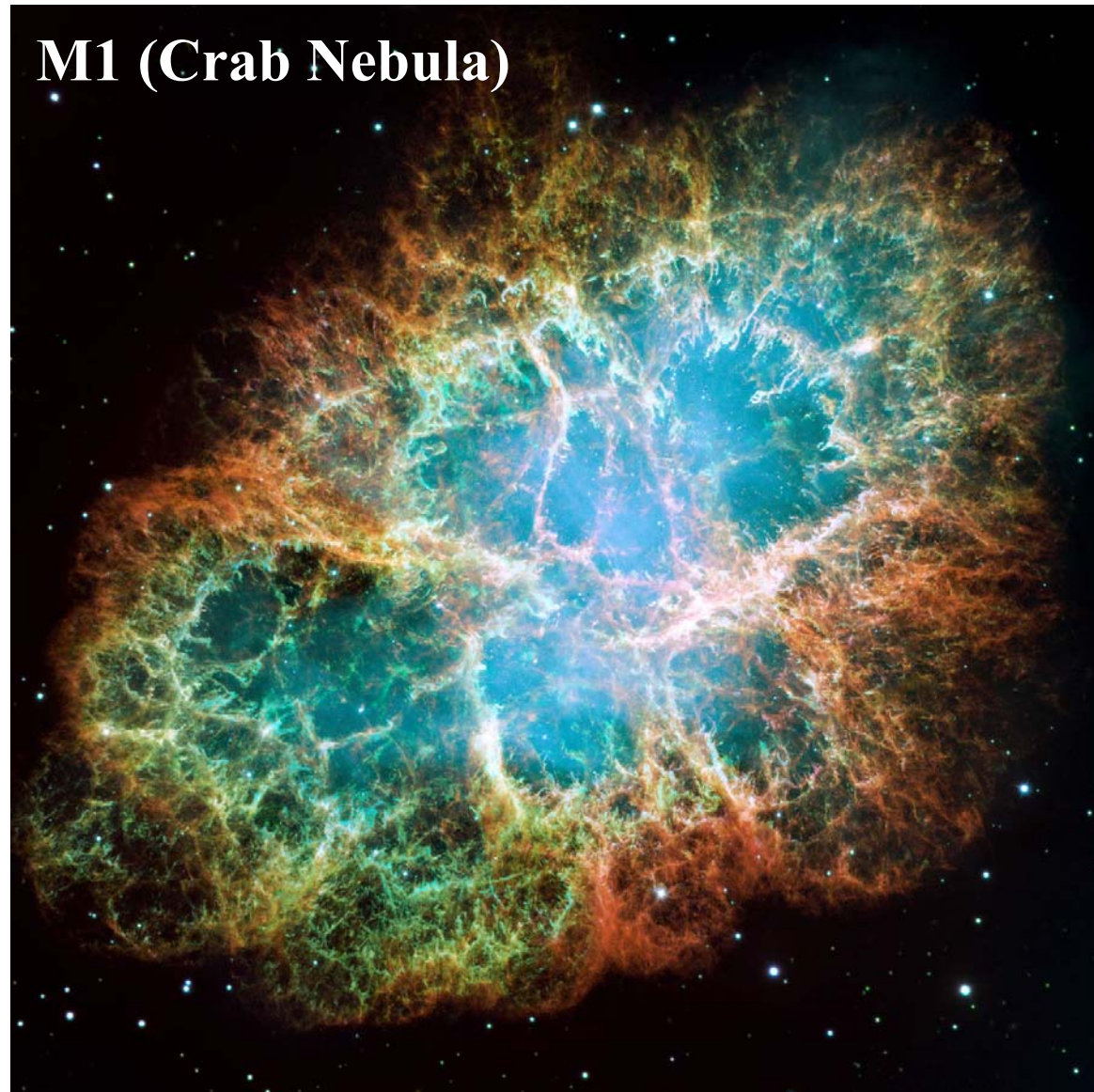
The death of stars with mass $> 8M_{\text{sun}}$: Type II supernovae (SNe II)

Heavy stars repeat expansion and contraction, change their internal structure a few times depending on the mass, and finally start the Si-burning which produces Fe. However, **after this process, they exhaust their energy source because Fe has the highest binding energy per nucleon.** The core loses energy by neutrinos, which leads to its contraction. However, this process leads to even more neutrino loss, and an inverse β -decay related process accelerates the contraction. Then, finally the core contracts with a timescale of 10^{-3} s and produces an outgoing shock, leading a very energetic explosion (**Type II supernova: SN II**). The ejected gas from a star forms a nebula, called a supernova remnant (SNR). This also provides the ISM with heavy elements.

Heavy elements supplied by SN II

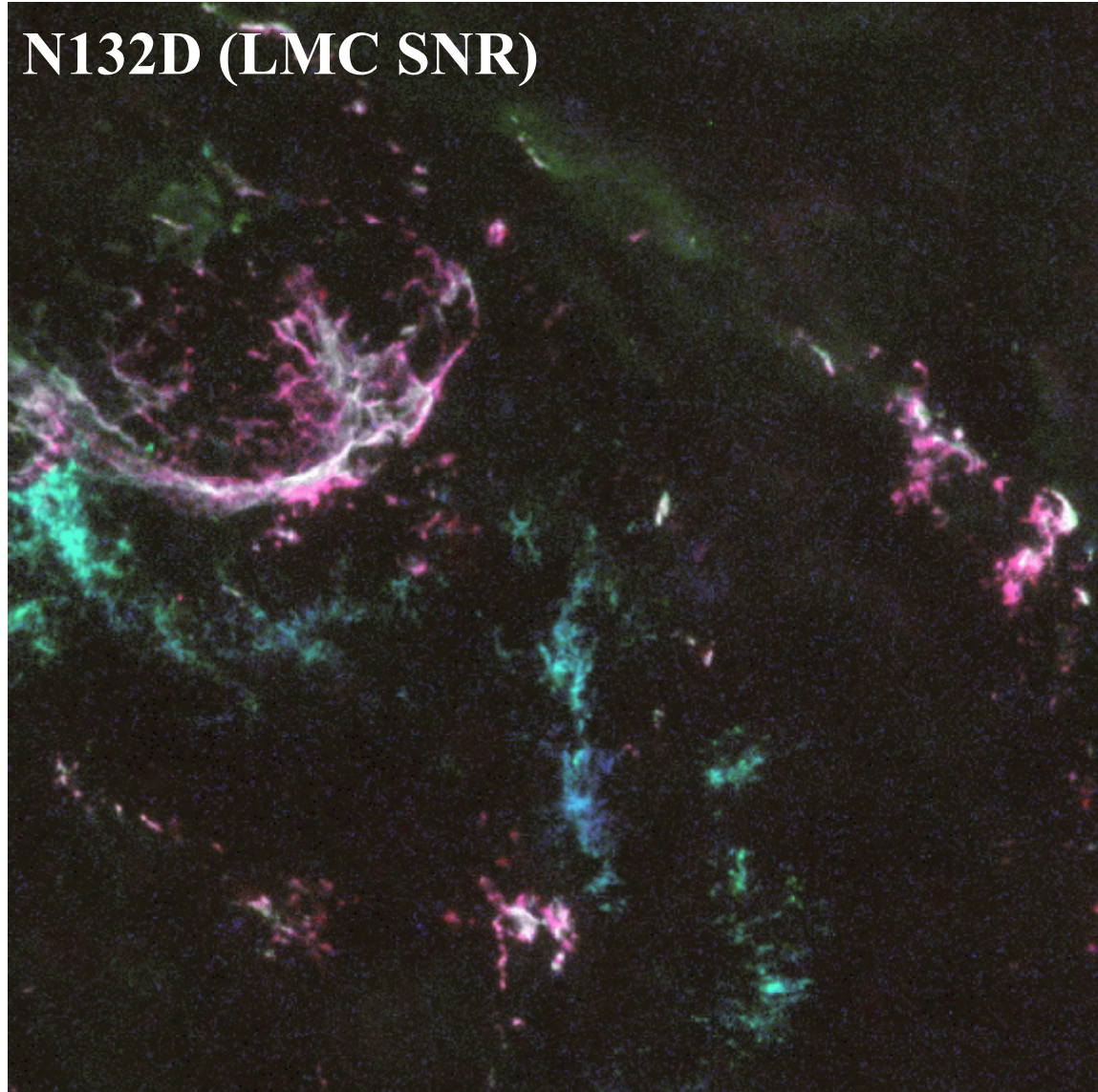
M_{init}	M_{fin}^a	M_{α}^b	M_{CO}^c	He	C	O	Z
120	81	81	59	9.8	0.88	35	42
85	62	62	38	8.1	0.72	23	27
60	47	28	25	6.0	0.70	14	17
40	38	17	14	4.2	0.55	6.8	10
25	25	9	7	3.5	0.40	2.4	4.4
20	19	7	5	2.1	0.30	1.3	2.9
15	15	5	3	1.6	0.20	0.46	1.5
12	12	4	2	1.4	0.10	0.15	0.8
9	9	3	2	1.0	0.06	0.004	0.3
5	5	1	1	0.45			
3	3			0.09			

Supernova II remnant



Supernova II remnant

N132D (LMC SNR)



Blue: [OI]
Green: [OIII]
Red: [SII]

Supply of metals to the interstellar space II: final stage of stars

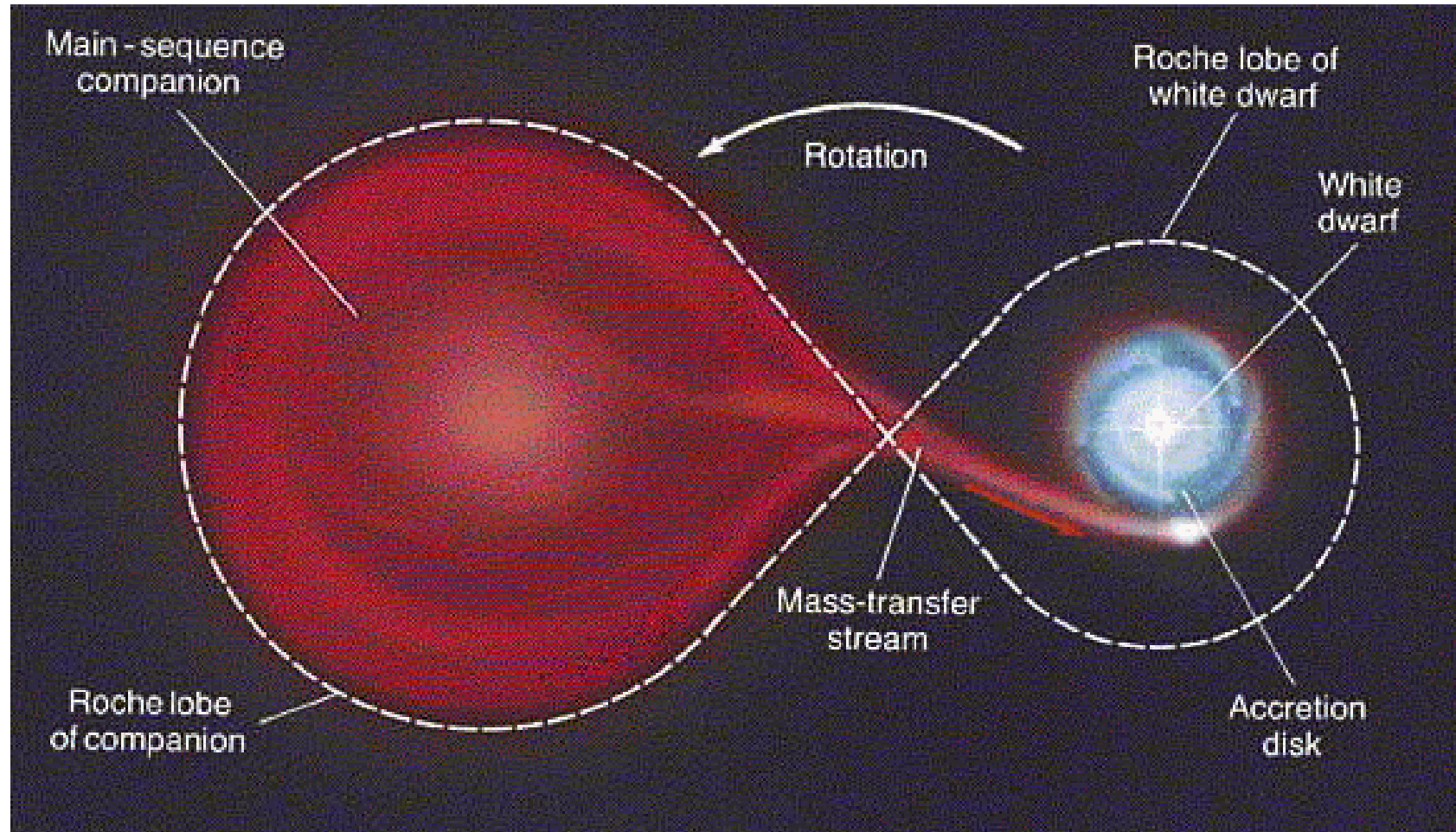
The death of binary stars : Type Ia supernova (SN Ia)

A significant fraction of stars are born as **binaries**.
The last stage of such stars are different from that of single stars because of **mass exchange** between them.

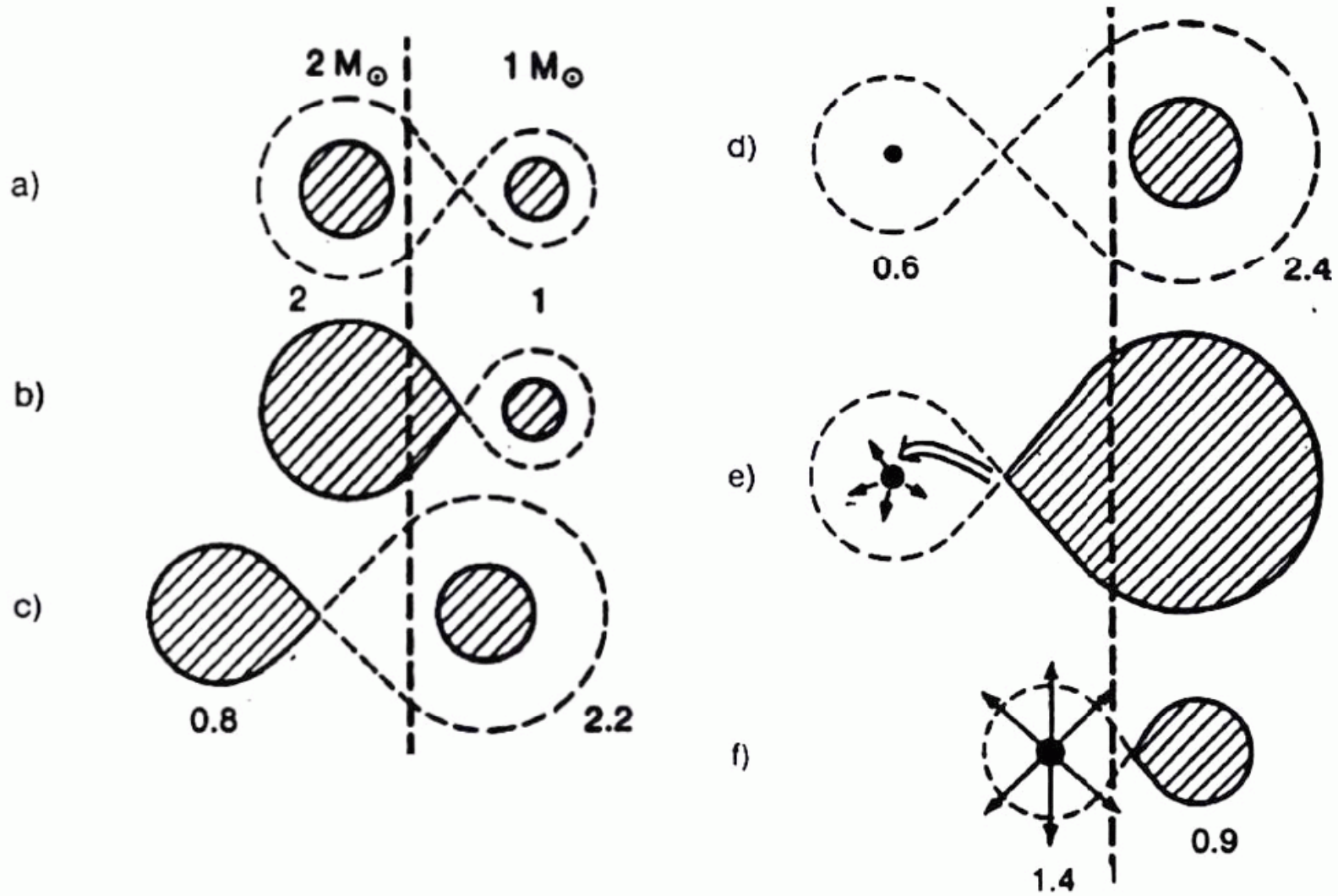
Stars with $M < 8M_{\text{sun}}$ end as white dwarfs (WDs). If they are single, such stars finally have a WD mass below the mass limit above which there is no stable solution (**Chandrasekhar mass $M_{\text{crit}} \approx 0.6M_{\text{sun}}$**).

However, WDs in a binary system can often **accrete gas from a close companion star**. Then, it finally exceeds M_{crit} and collapses, resulting in a runaway fusion reaction: **Type Ia supernova (SN Ia)**. Each SN Ia produces Fe of $0.3\text{-}1.3 M_{\text{sun}}$, i.e., SN Ia is the most important source of iron in a galaxy.

Type Ia supernova: schematic picture of binary mass transfer



Type Ia supernova: binary evolution

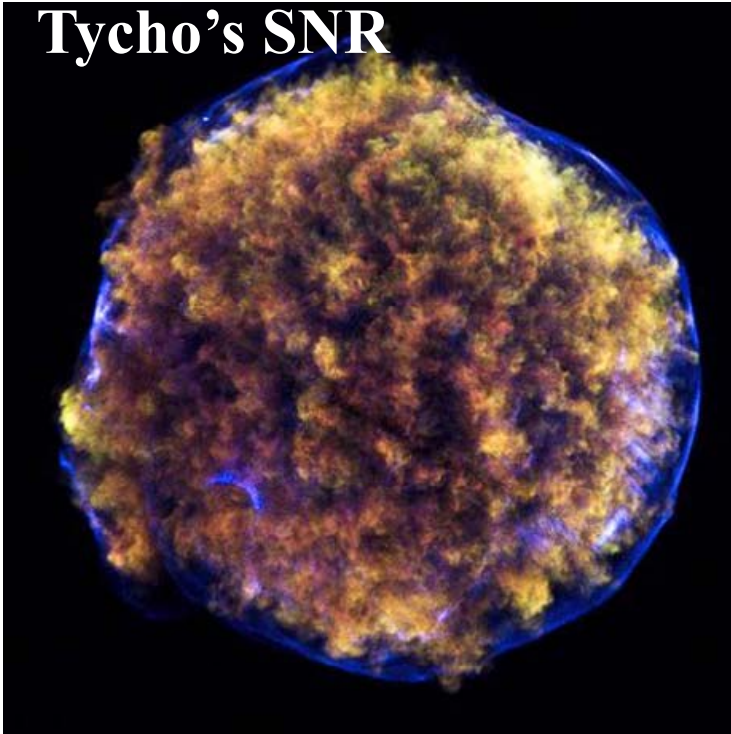


Heavy elements supplied by SN Ia

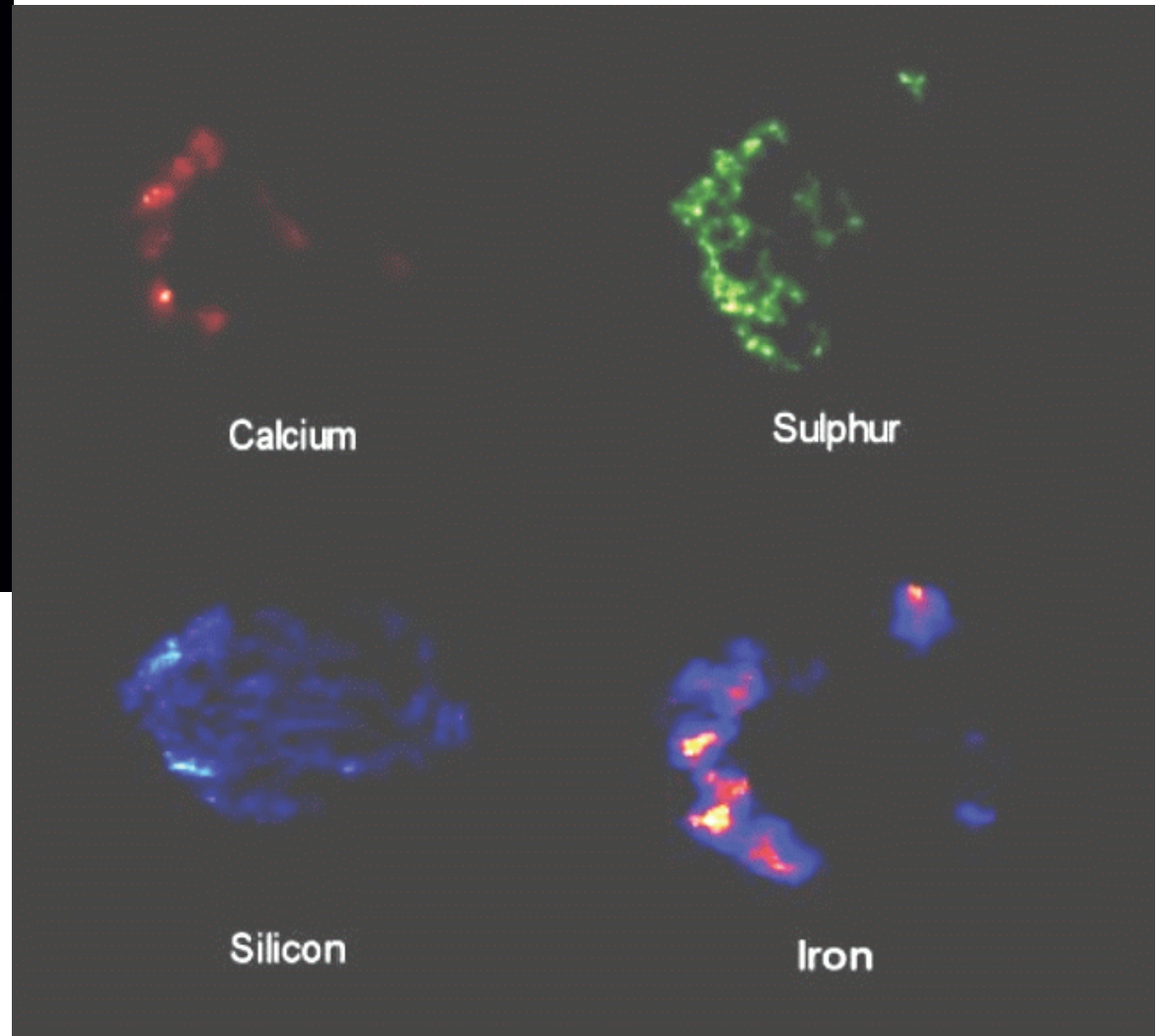
Species	Mass/ M_{\odot}	$[X_i/X_{56}]^a$
^{24}Mg	.09	-1.1
^{28}Si	.16	-0.3
^{32}S	.08	-0.4
^{36}Ar	.02	-0.3
^{40}Ca	.04	0.1
^{54}Fe	.14	0.6
^{56}Fe	.61	0.0
^{58}Ni	.06	0.4
Cr-Ni	.86	

Supernova Ia remnant

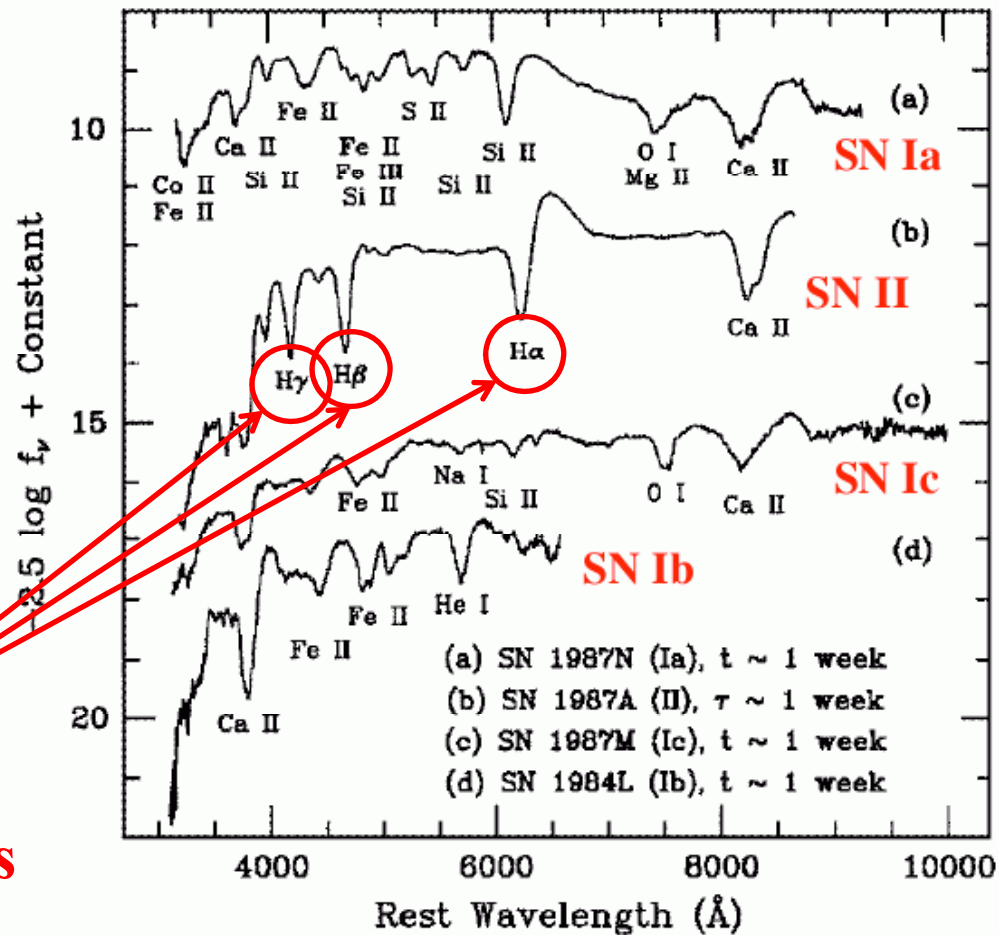
Tycho's SNR



Chandra images



Astronomical classification of supernovae

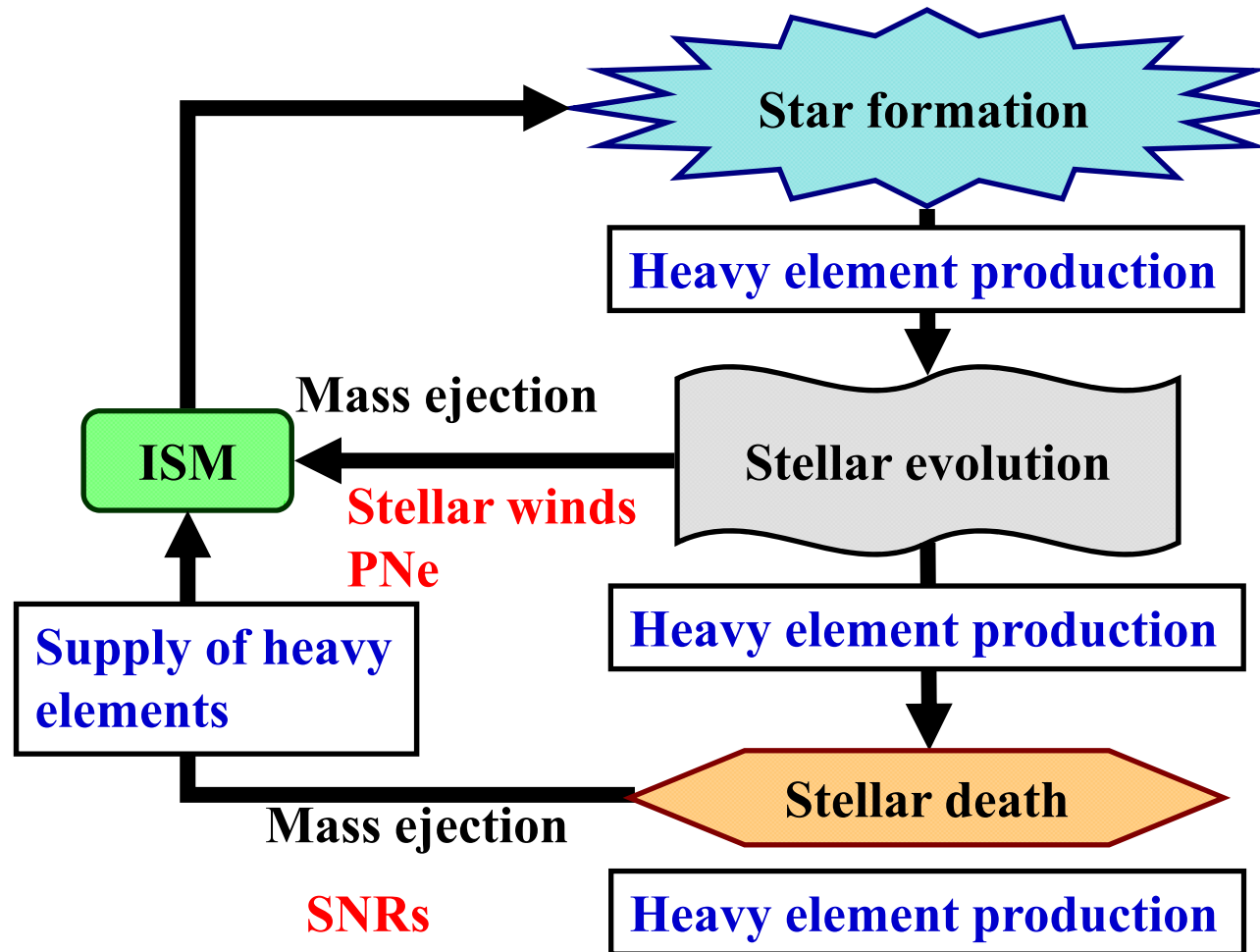


**Hydrogen
absorption lines**

SN Ib, Ic, and II have the same physical origin, while Ia does not. This is disturbing for understanding: it is because the classification was made based on the existence of an H envelope.

4.2 Chemical evolution of galaxies: general framework

Chemical evolution of galaxies



Star formation in galaxies is affected by the amount of heavy elements which galaxies ever produced.

The history of the amount of stars formed in galaxies is called the star formation history (SFH).

Initial mass function (IMF) of stars

A mass distribution function of stars in their birth is referred to as **the initial mass function (IMF)**.

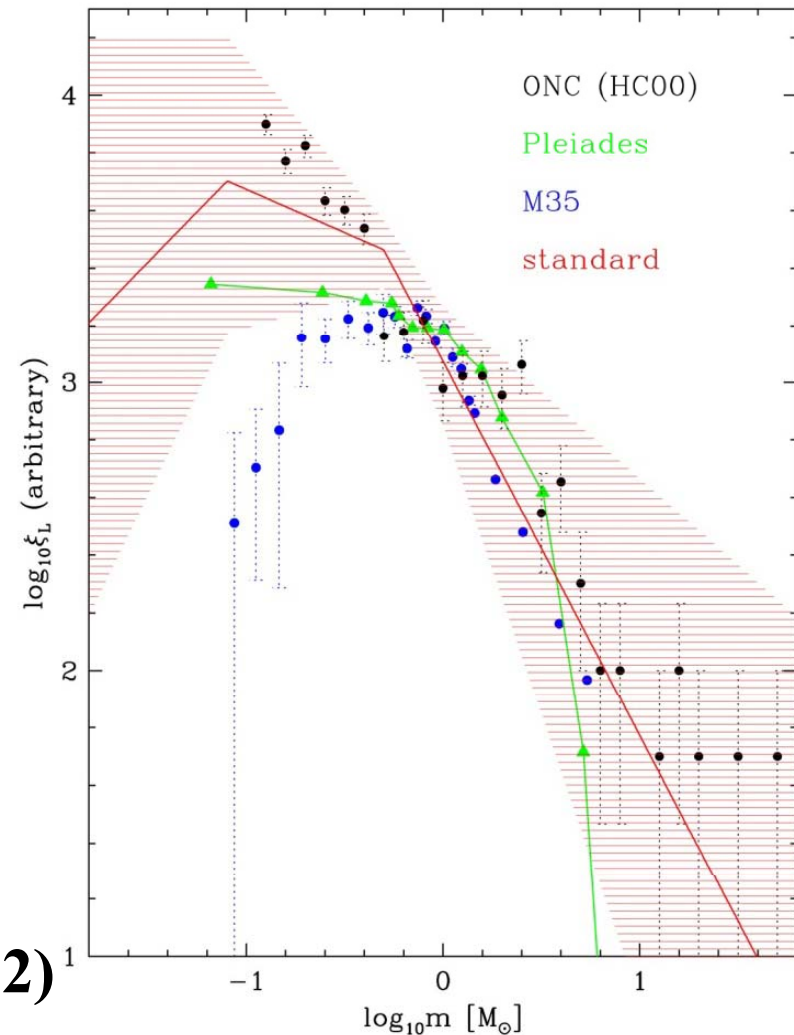
Since the IMF determines the ratio between massive and less massive stars, it plays a crucial role in chemical evolution of galaxies.

IMF normalization:

$$\int m\Phi(m)dm = 1$$

(but often normalized with number.)

(Kroupa 2002)



Chemical evolution model: basic equations

$$M = M_s + M_g$$

$$\frac{dM}{dt} = f - e$$

$$\frac{dM_s}{dt} = \Psi - E$$

$$\frac{dM_g}{dt} = -\Psi + E + f - e$$

M = total mass (**baryon**)

M_s = mass in stars

M_g = mass in gas

f = rate on infalling gas

e = rate on ejected gas

Ψ = star formation rate

E = gas ejection rate of all stars

Chemical evolution model: basic equations

Total gas ejection rate of stars is expressed as

$$E(t) = \int_{m_t}^{\infty} [m - w_m] \Psi_{t-\tau_m(m)} \Phi(m) dm \quad (1)$$

where

m_t : turnoff mass at time t = lowest mass of stars dying at time t

$m - w_m$: ejected mass

$\Psi_{t-\tau_m(m)} \Phi(m)$: birth rate at $t-\tau_m$ = death rate at time t

τ_m : main sequence lifetime for a star with mass m

Remnant mass:
$$\begin{cases} w_m = 0.11m + 0.45M_{\odot} & (m < 6.8M_{\odot}) \\ w_m = 1.5M_{\odot} & (m \geq 6.8M_{\odot}) \end{cases} \quad (2)$$

N.B. Here remnant means not only the final stage of stars but also normal long-lived stars.

Chemical evolution model: basic equations

Evolution of the metal abundance Z is written as

$$\frac{d(ZM_g)}{dt} = -Z\Psi + E_z + Z_f \cdot f - Ze \quad (3)$$

where

E_z : ejection rate of metal(s) from stars (main sequence stars, Wolf-Rayet stars, SNe, etc.)

Z_f : infalling metals per time

ZM_g : mass of metal(s) in the gas.

Chemical evolution model: basic equations

Ejection rate of metals reads

$$E_Z(t) = \int_{m_t}^{\infty} \left[(m - w_m) Z_{t-\tau_m(m)} + mp_{Zm} \right] \Psi_{t-\tau_m(m)} \Phi(m) dm \quad (4)$$

where

$(m - w_m) Z_{t-\tau_m(m)}$: mass of metal(s) which was locked in a star of mass m at time $t - \tau_m(m)$ and is now ejected at time t ,

mp_{Zm} : new metal(s) produced by a star of mass m with originally formed from gas with metallicity Z .

N.B. Ansatz in eqs.(3) and (4): instantaneous mixing of produced metal(s) with the ISM.

Chemical evolution model: basic equations

Returned mass per mass of stars formed is

$$R = \int_{m_1}^{\infty} (m - w_m) \Phi(m) dm \quad (5)$$

This is independent of star formation rate, thus **only valid for a single generation of stars.**

Mass of produced metal(s) per remaining stellar mass (including stellar remnant) is called **yield**. This is expressed as

$$y = \frac{1}{1-R} \int_{m_1}^{\infty} m p_{Zm} \Phi(m) dm \quad (6)$$

Chemical evolution model: instantaneous recycling

As a first order approximation, the instantaneous recycling approximation is often adopted:

- 1. massive stars die immediately after their birth and less massive stars live forever,**
- 2. produced elements are instantaneously mixed with the ISM, is used.**

***N.B.* This is only valid if the SFR is almost constant over a timescale of 10^7 yr for lighter elements like O, C, N, Mg, etc.(SN II origin), and of 10^{8-9} yr for heavier elements like Fe (SN Ia origin).**

Chemical evolution model: instantaneous recycling

If the instantaneous recycling applies, using R and y and **assuming the IMF is constant with time (meaning $R = \text{const.}$)**, we obtain

$$E(t) = R\Psi(t) \quad (7)$$

$$E_z(t) = RZ(t)\Psi(t) + (1-R)y(t)\Psi(t) \quad (8)$$

Inserting eq.(8) into eq.(4), we have

$$\frac{d(ZM_g)}{dt} = -Z\Psi + RZ(t)\Psi(t) + (1-R)y(t)\Psi(t) + Z_f \cdot f - Ze \quad (9)$$

thus

$$\frac{d(ZM_g)}{dt} = (1-R)(-Z + y)\Psi + Z_f \cdot f - Ze \quad (10)$$

Chemical evolution model: instantaneous recycling

As for stellar mass, with eq.(7),

$$\frac{dM_s}{dt} = (1 - R)\Psi(t) \quad (11)$$

and for gas mass,

$$\frac{dM_g}{dt} = -(1 - R)\Psi(t) + f - e \quad (12)$$

Then, we have

$$M_g \frac{dZ}{dt} = (1 - R)y(t)\Psi(t) + (Z_f - Z)f \quad (13)$$

These equations are the framework under the instantaneous recycling.

Chemical evolution model: analytic solution for a simple case

Closed-box model

Assume we have a closed system containing only gas with zero metallicity (not essential) and no stars.

Since $f = e = 0$, $M_g(t = 0) = M$, $M_s(t = 0) = 0$,

$$\frac{dM_s}{dt} = (1 - R)\Psi(t) \quad (14)$$

$$M_g \frac{dZ}{dt} = (1 - R)y(t)\Psi(t) \quad (15)$$

which lead

$$\frac{1}{M_g} \frac{dM_g}{dZ} = -\frac{1}{y} \quad (16)$$

or equivalently

$$\ln M_g \Big|_M^{M_g(t)} = \int_0^{Z(t)} -\frac{dZ}{y} \approx -\frac{Z}{\bar{y}} \quad (17)$$

Chemical evolution model: analytic solution for a simple case

The metallicity of the gas is

$$Z(t) = \bar{y} \ln \frac{M_g(t=0)}{M_g(t)} \quad (18)$$

N.B., $Z(t)$ depends only on $M_g(t)/M$, thus not explicitly on t .

For a simple estimate, we can use

$$\frac{Z}{Z_\odot} \approx \ln \frac{M}{M_g(t)} \quad (19)$$

Chemical evolution model: analytic solution for a simple case

The metallicity of stars can also be obtained as follows.

Under a closed-box assumption, the stars and the gas altogether must contain all elements ever produced. Hence

$$\underbrace{Z_s M_s}_1 + \underbrace{Z M_g}_2 = \underbrace{\int_0^t \int_0^\infty m p_{Zm} \Psi(t') \Phi(m) dm dt'}_3 = \int_1^t (1-R) y \Psi dt \simeq (1-R) \underbrace{\bar{y} \bar{\Psi} t}_4 \quad (20)$$

1: average metallicity of stars (without metals in remnant)

2: metallicity of gas

3: mass of all metals ever produced

4: average values with assumption: $\overline{y\Psi} \simeq \bar{y}\bar{\Psi}$

Chemical evolution model: analytic solution for a simple case

Thus, we have

$$Z_s M_s + Z M_g = (1 - R) \bar{y} \bar{\Psi} t \quad (21)$$

Integrating eq.(11) leads to

$$M_s = (1 - R) \bar{\Psi} t \quad (22)$$

Combining the above, we have

$$Z_s M_s \simeq \bar{y} M_s - Z M_g \quad (23)$$

Finally, we obtain an important result:

$$M_g \ll M_s \Rightarrow Z_s \simeq \bar{y} \quad (24)$$

i.e., the average stellar metallicity cannot exceed the average yield.

4.3 Evolutionary synthesis model of galaxies

Stellar spectra and single (simple) stellar population (SSP)

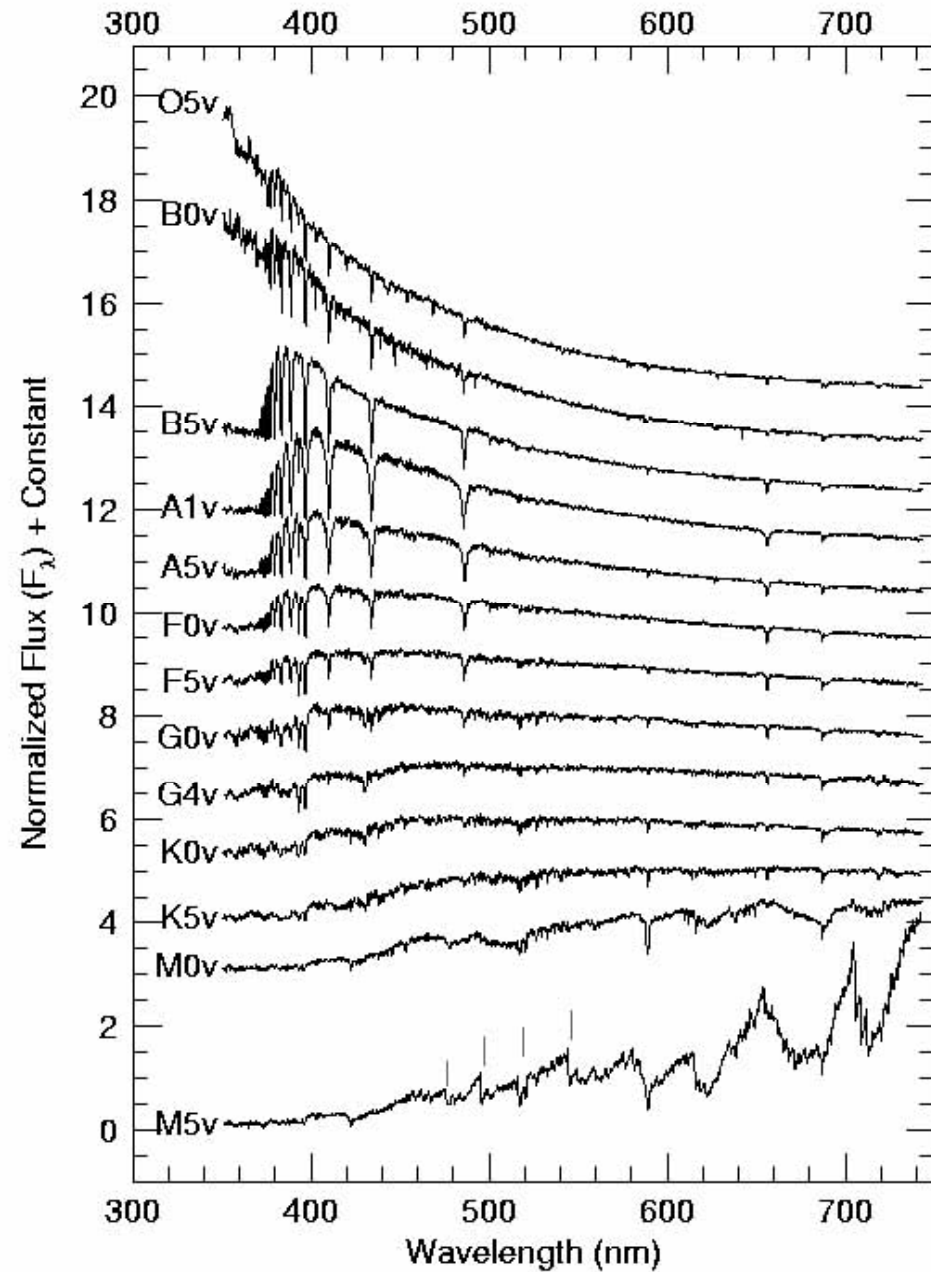
Stars have different spectra depending on their effective temperature (often referred to as **spectral type**) and metallicity.

Suppose a population of stars which were born at the same moment and with a certain IMF and metallicity. **Then, the total spectrum of this population at age t is expressed as a IMF-weighted sum of the spectra of each stellar mass (\Leftrightarrow spectral type) with age t after their birth.**

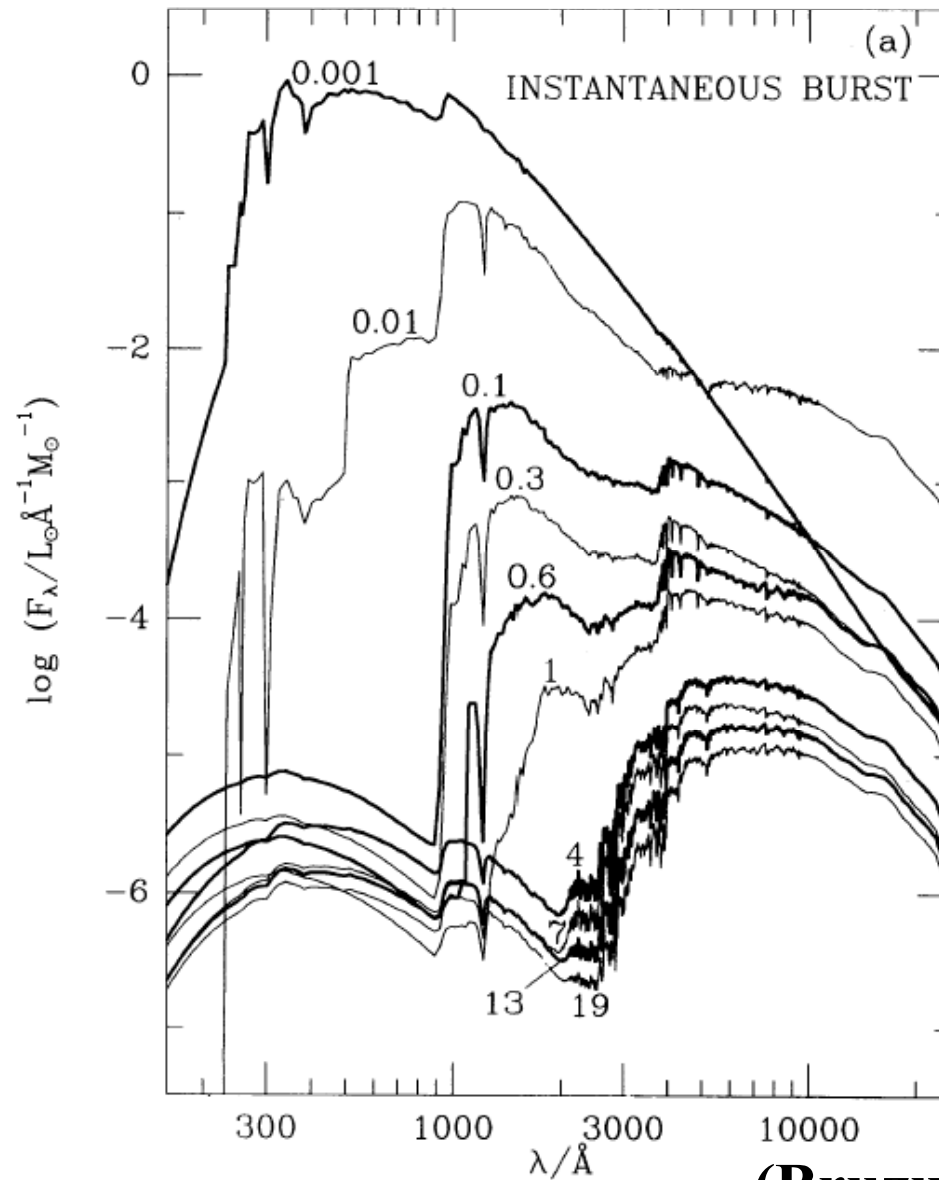
This hypothetical population is called **a single stellar population (SSP)**, and play a fundamental role in theoretical modeling of galaxy spectra. The SSPs vary as a function of age, metallicity, and the adopted IMF.

Stellar spectra

Hotter to cooler from
the top to the bottom.



Single stellar population (SSP)



(Bruzual & Charlot 1993)

Evolutionary synthesis of galaxy spectra

Synthesizing isochrones can convolve with arbitrary star formation history (Green's function):

$$F_{\lambda}(t) = \int_0^t \Psi(t - \tau) f_{\lambda, Z(t-\tau)}(\tau) d\tau \quad (25)$$

$f_{\lambda, Z(t')}(t)$: an SSP of age t and metallicity $Z(t')$

$F_{\lambda}(t)$: the spectrum of a population with arbitrary SFR $\Psi(t)$.

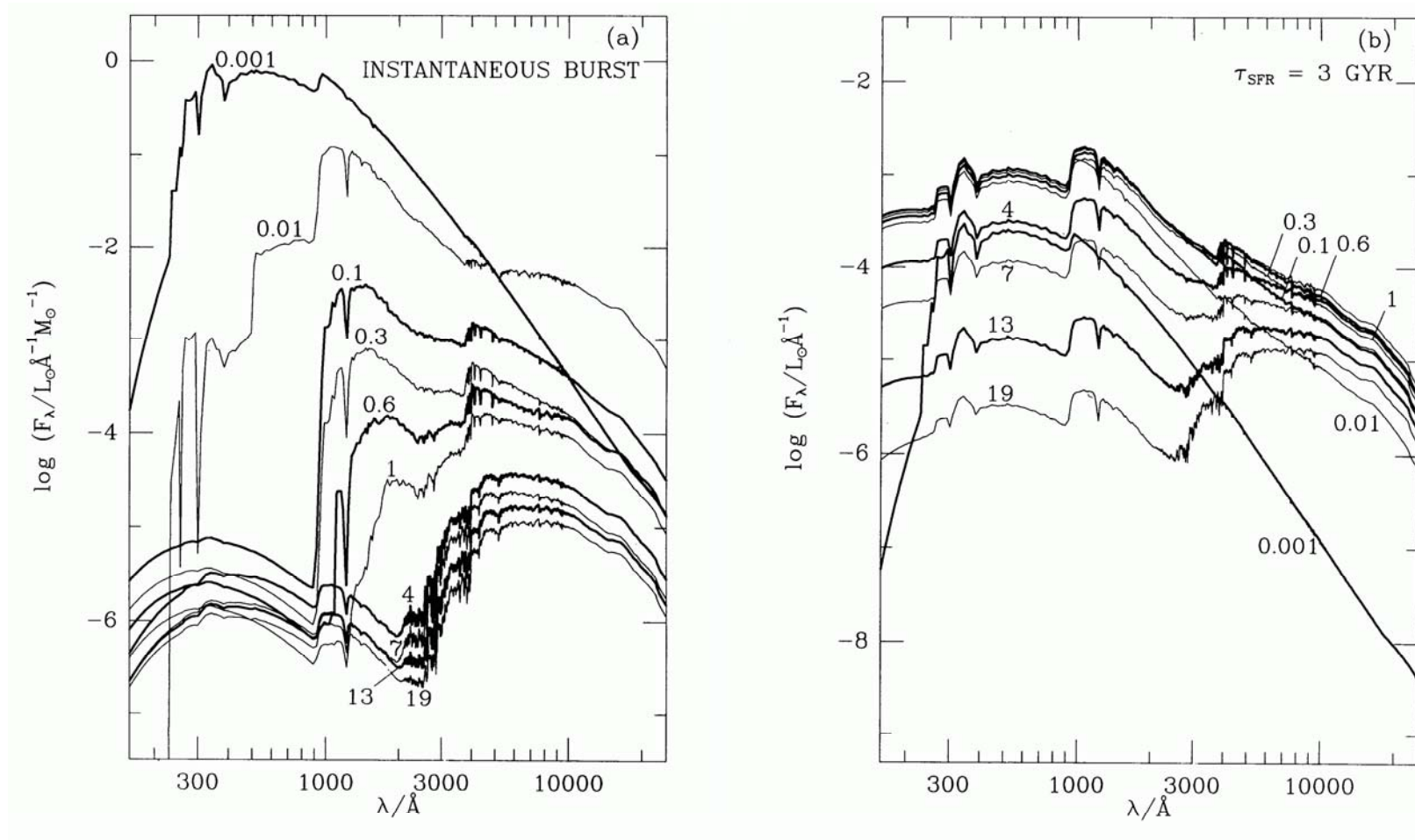
***N.B.* this assumes time-invariant IMF.**

Commonly used is exponentially decaying SFR:

$$\Psi(t) = \tau^{-1} \exp(-t/\tau) \quad (26)$$

Evolutionary synthesis of galaxy spectra

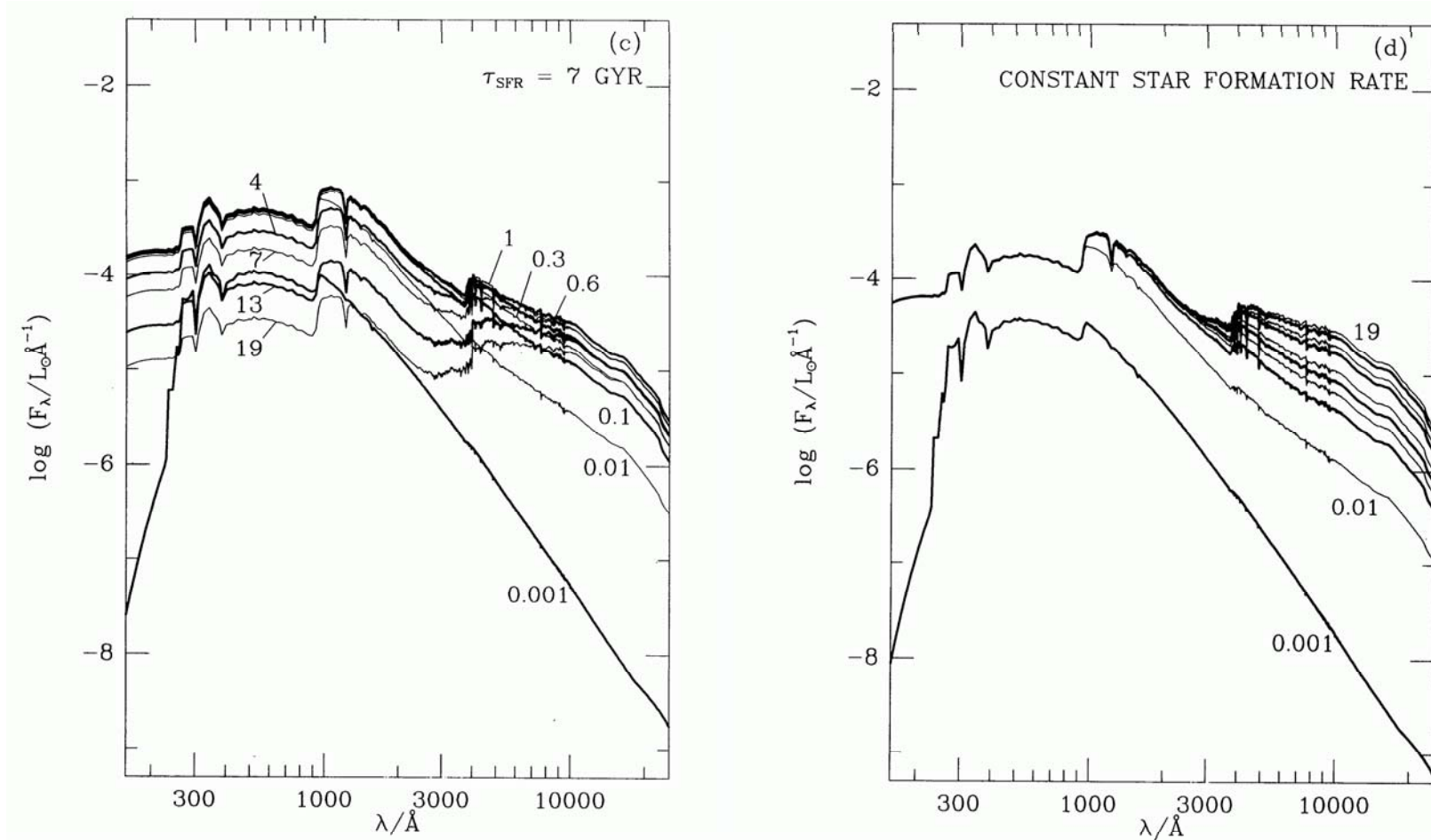
The effect of star formation history



(Bruzual & Charlot 1993)

Evolutionary synthesis of galaxy spectra

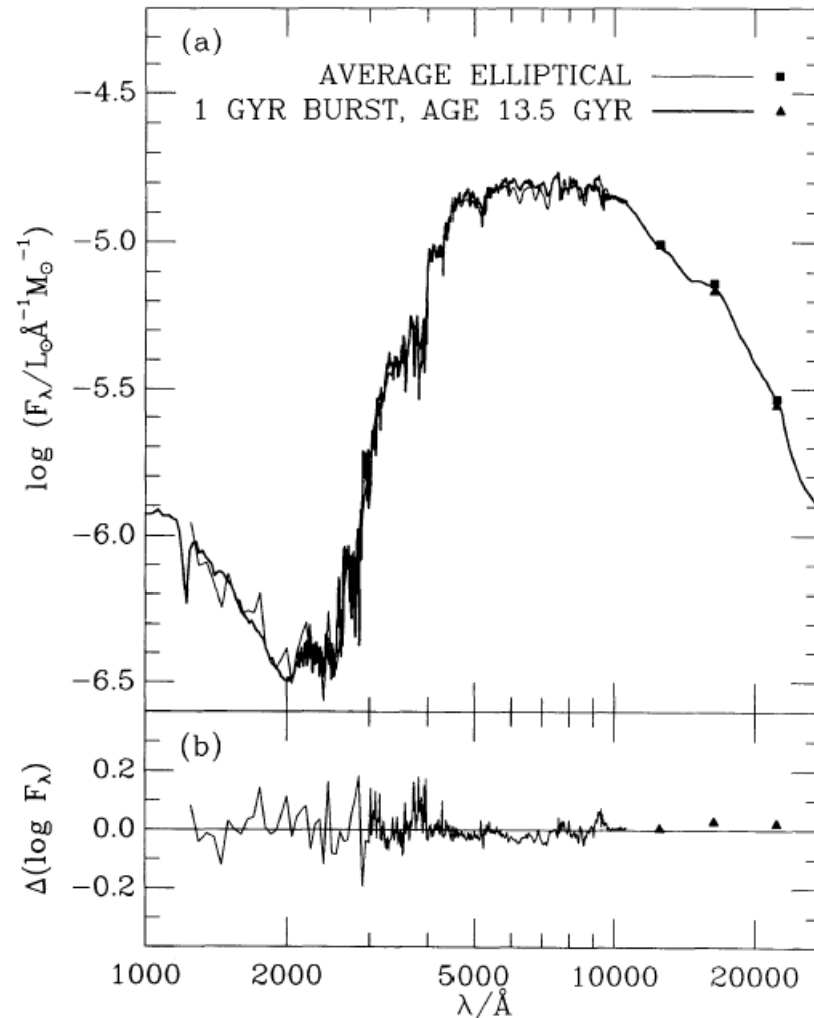
The effect of star formation history



(Bruzual & Charlot 1993)

Evolutionary synthesis of galaxy spectra

Application to ellipticals



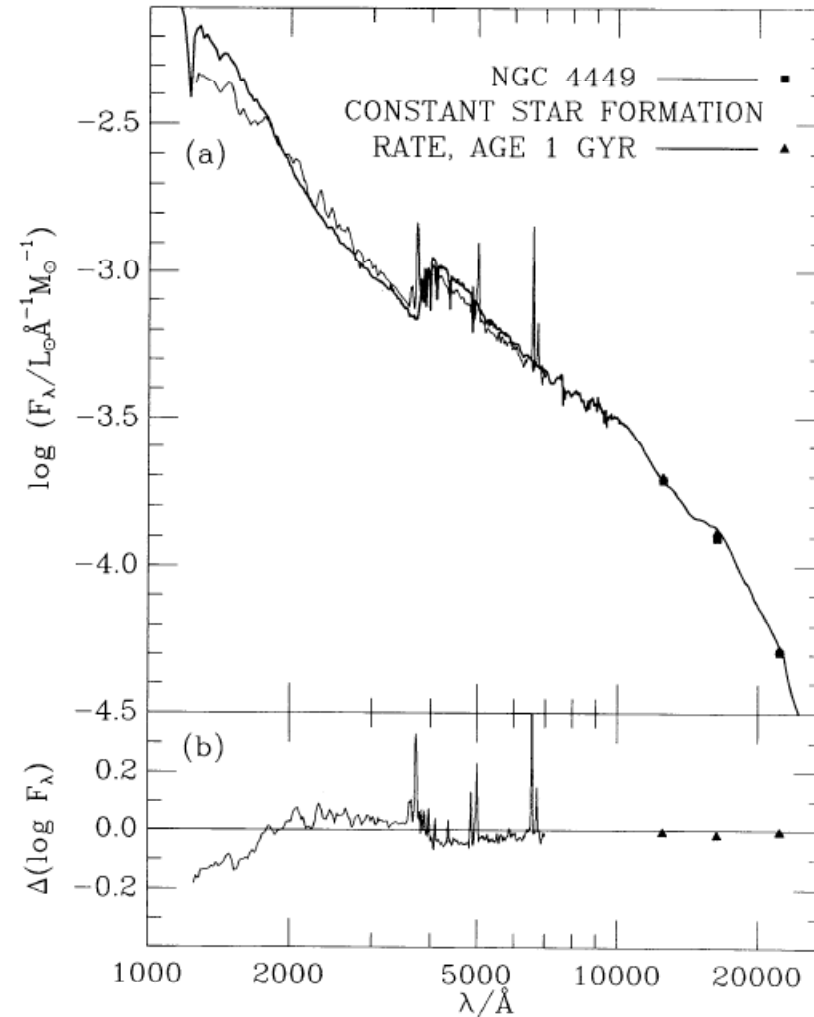
(Bruzual & Charlot 1993)

- **Best-fitting age model and composite elliptical spectrum**
- **Fairly good fit over entire spectral range**
- **Note UV-rising branch, highlighting importance of accurate **AGB modeling****
- **Authors admit that these are large-aperture spectra, so metallicity will be roughly solar**

Evolutionary synthesis of galaxy spectra

Application to irregulars

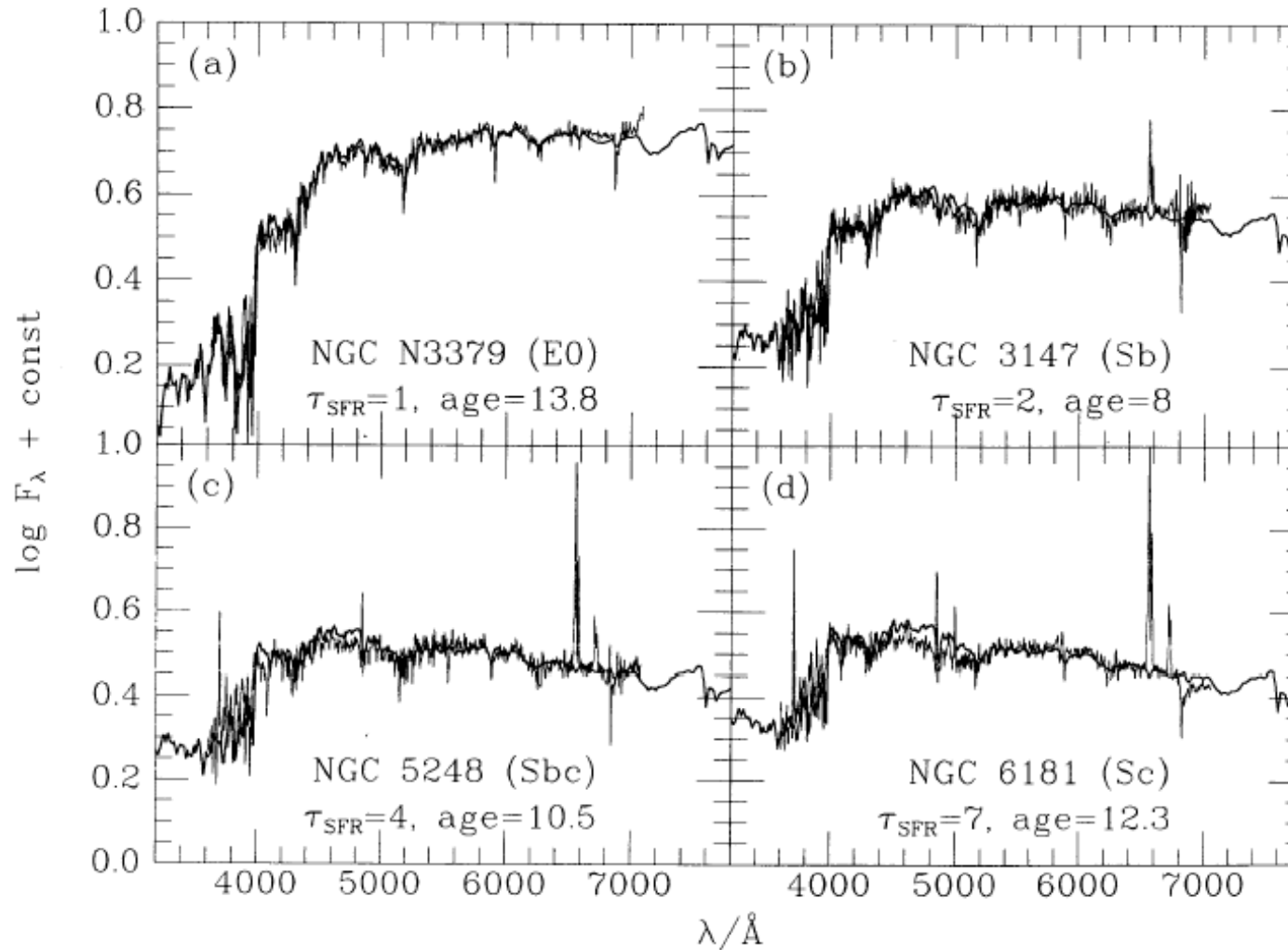
- Note that emission lines will never be fit (BC93 models only include stars)
- Overprediction of flux at blue end, because of **internal extinction due to dust**



(Bruzual & Charlot 1993)

Evolutionary synthesis of galaxy spectra

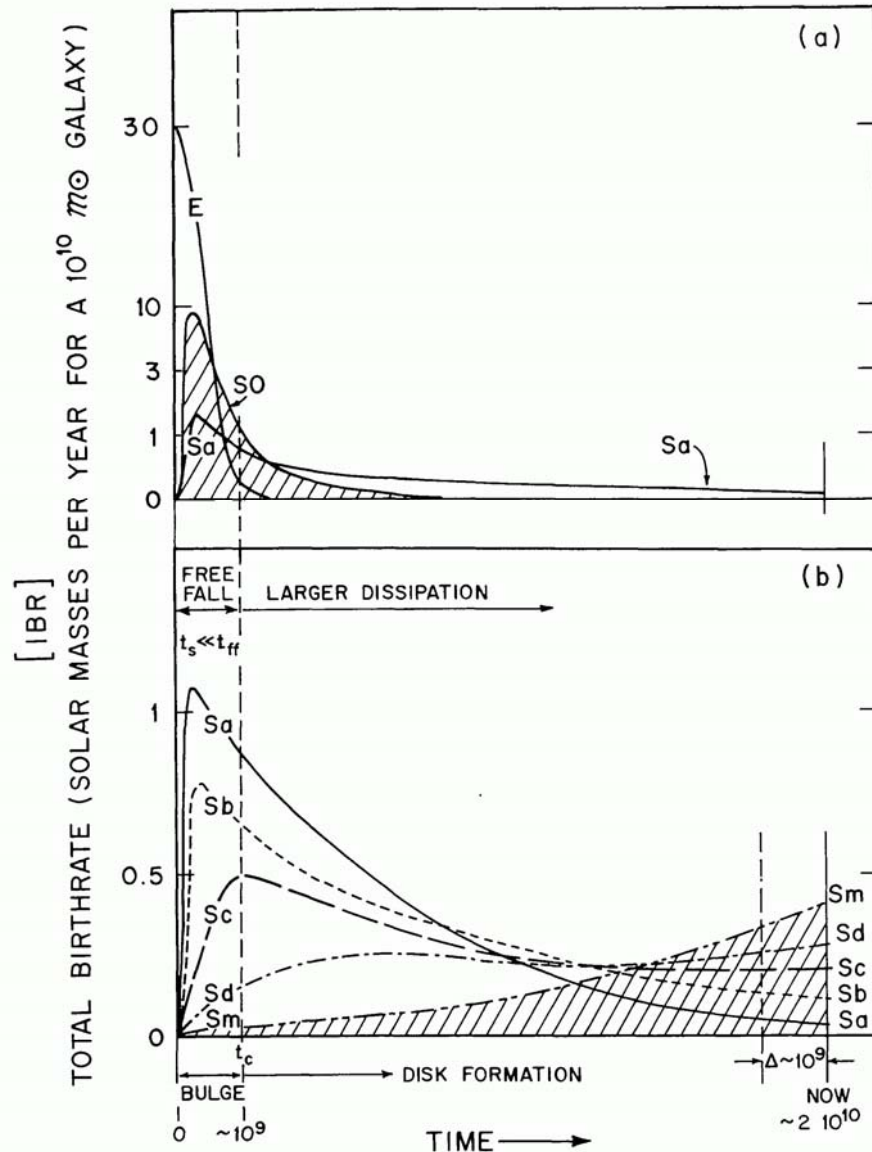
Application to spirals



(Bruzual & Charlot 1993)

4.4 Star formation history of spiral galaxies

Observed star formation histories



Observationally, spiral galaxies have a slowly continuous decaying SFH after a short burst.

From earlier to later types, the timescale of SF becomes longer. This trend also holds including Es and Irrs: **Sandage law.**

(Sandage 1986)

Star formation history in chemical evolution

The star formation history (SFH) plays a central role to control the chemical evolution. Though in the simplest model, the SFH did not appear explicitly, generally we have to put a certain physical model to specify the SFH.

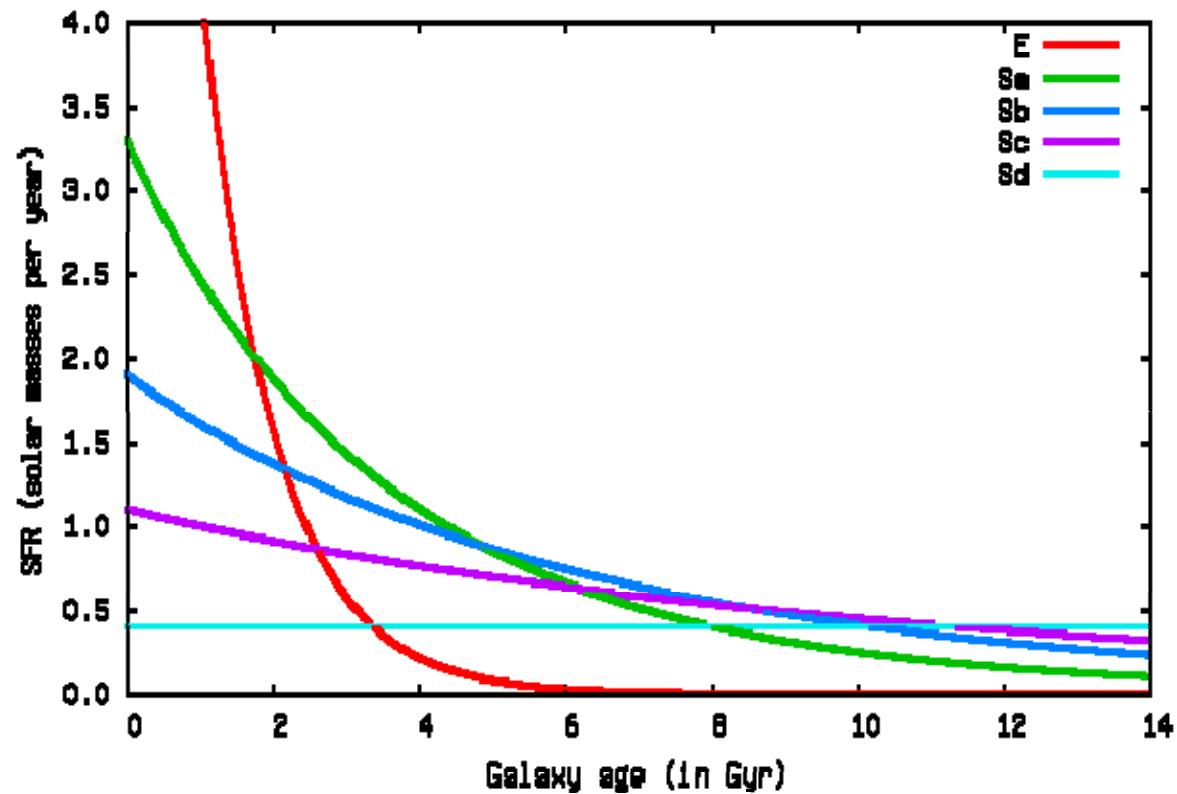
In reality, this part is complicated and still poorly understood, we often adopt the following empirical law, referred to as **the Schmidt law** (Schmidt 1959) or its variant:

$$\text{SFR} \propto \rho^n \quad n = 1 - 2 \quad (27)$$

N.B. In the observational side, it is expressed as a function of surface gas density, and in the chemical evolution modeling, yet a different form is often used.

Application of Schmidt law to chemical evolution

Applying the Schmidt law to the chemical evolution, we can reproduce an exponential-type SFH in a self-consistent manner (not by hand).



<http://model.galev.org/>

4.5 Evolution of the total mass, grain size, and composition of dust (Asano Model)

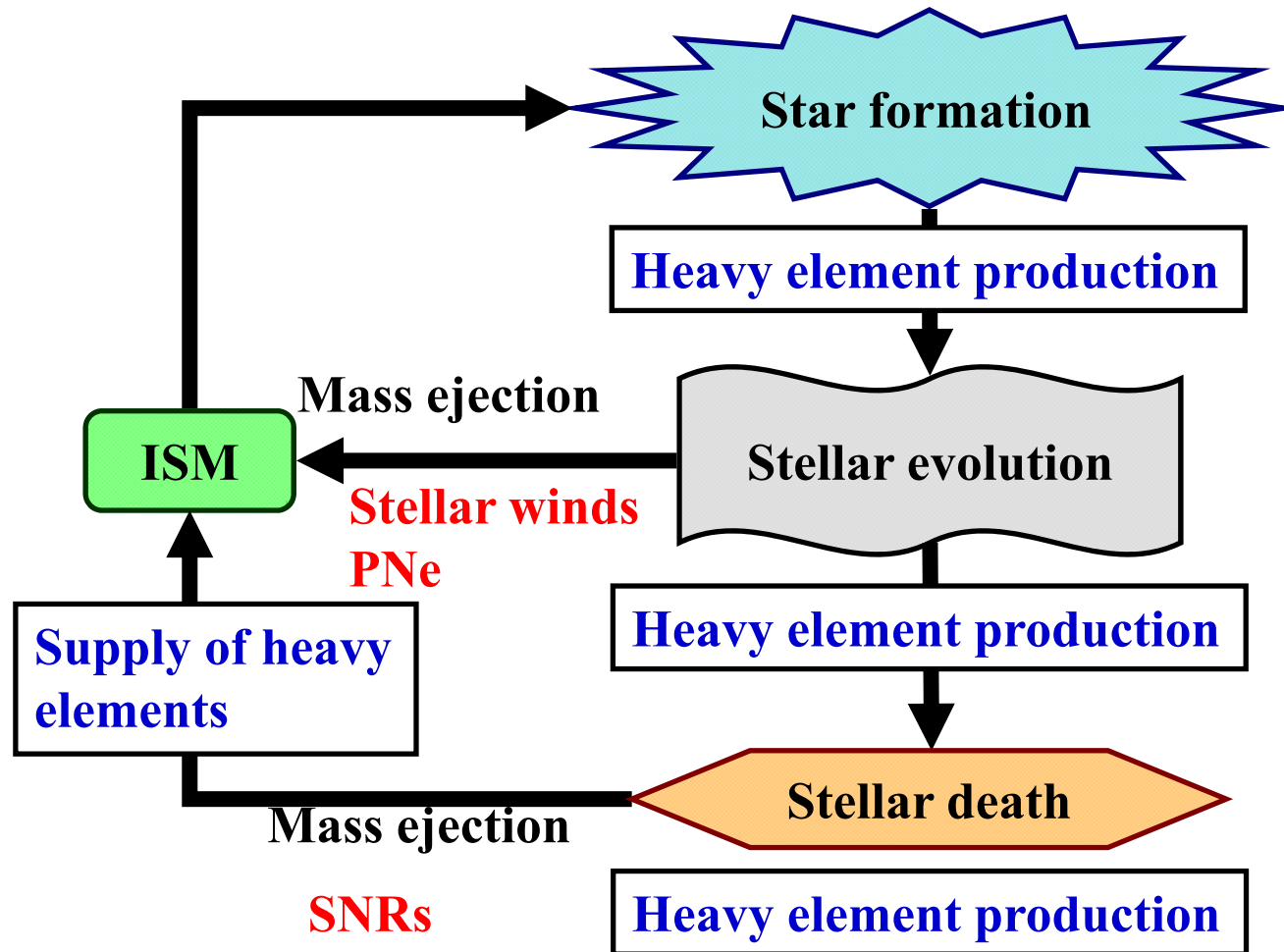
4.5.1 Chemical evolution of galaxies: metal and dust

The produced heavy elements are not always in a gas state: indeed, more than a half of the heavy elements form tiny solid grains, called dust. Dust grains are usually suspended within the ISM in galaxies.

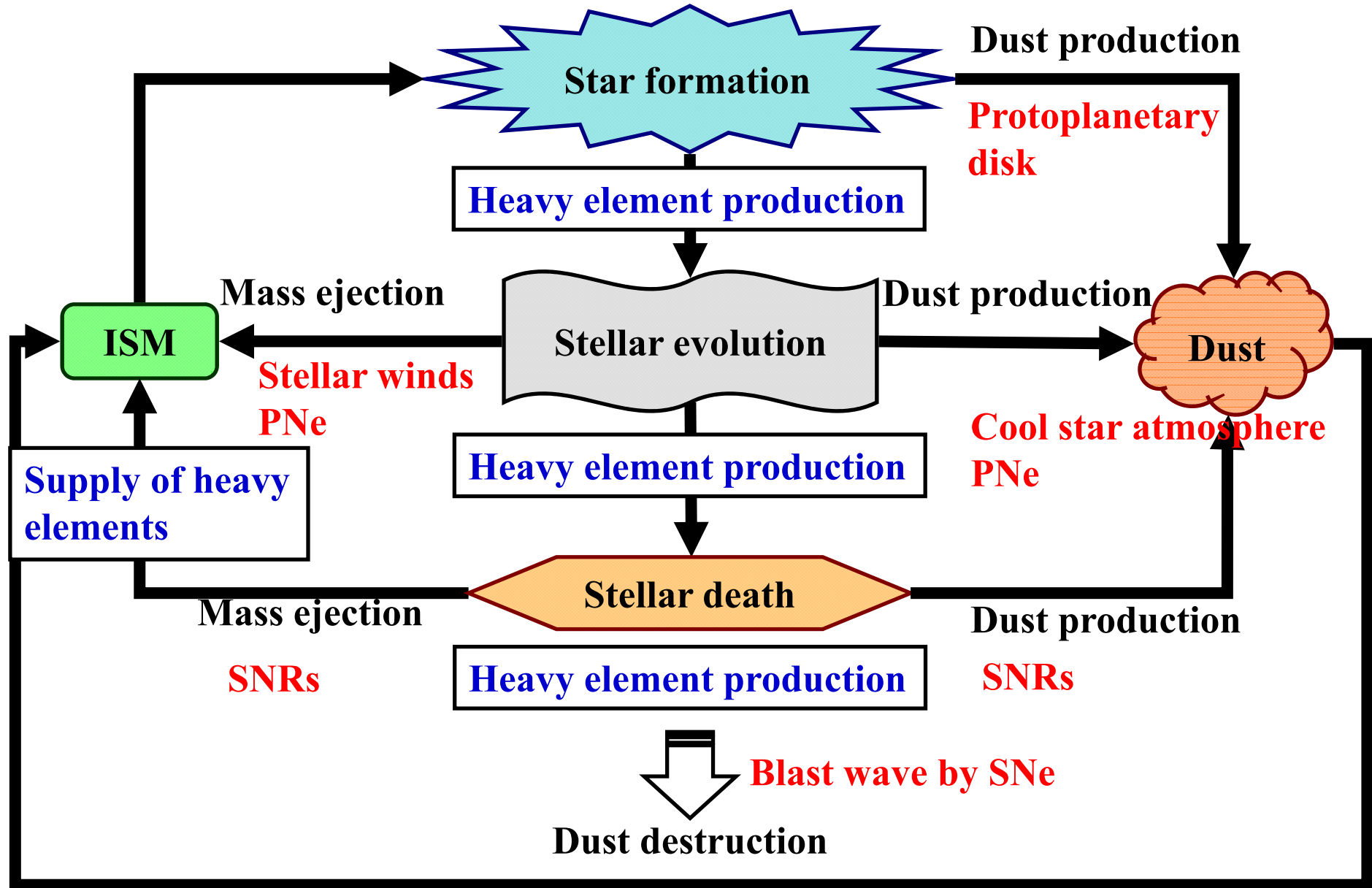
Star formation activity is closely related to heavy element production. This therefore mean that the star formation is also connected to the production of dust.

Hence, intense star formation always accompanies active dust production. On the other hand, dust grains also accelerate the efficiency of star formation. The interplay between the star formation and dust is very complex and nonlinear.

Chemical evolution of galaxies: metal and dust



Chemical evolution of galaxies: metal and dust

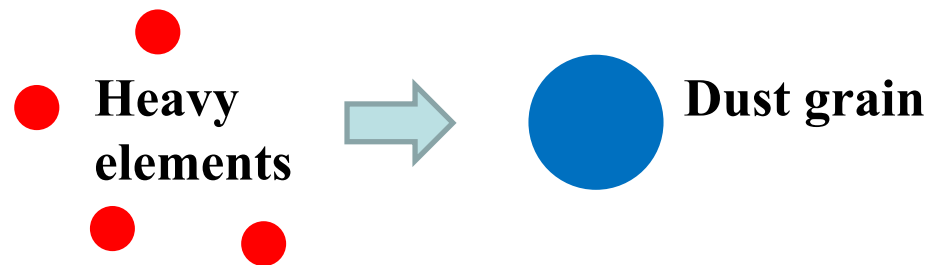


4.5.2 Role of dust in galaxies

What are dust grains?

Dust grains are

- formed by **condensation of heavy elements.**



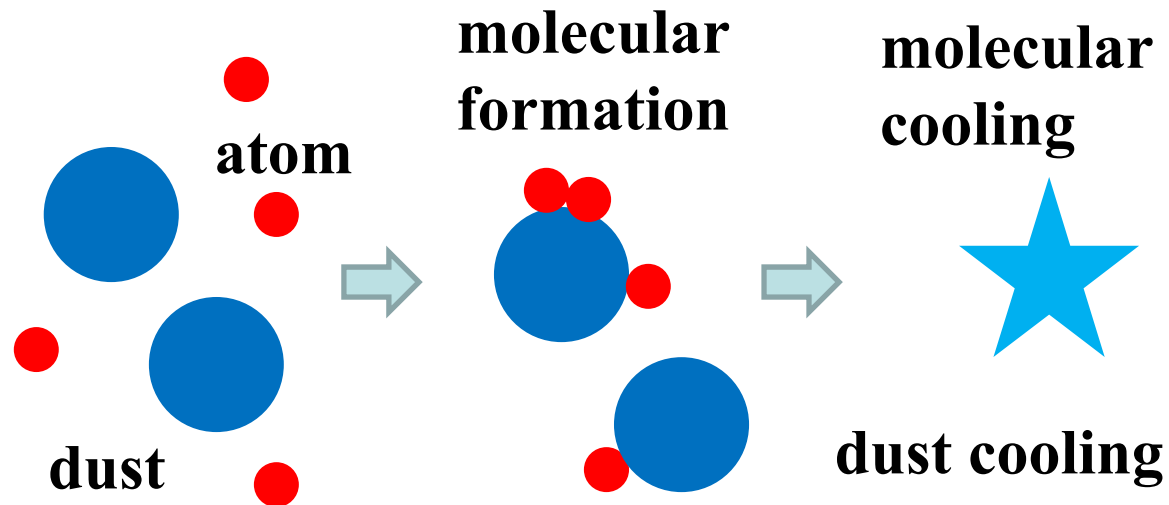
Heavy elements are supplied **only by stars.**

- tightly connected to **galaxy evolution**

There are many important physical quantities affected by dust.

Role of dust for the first star formation

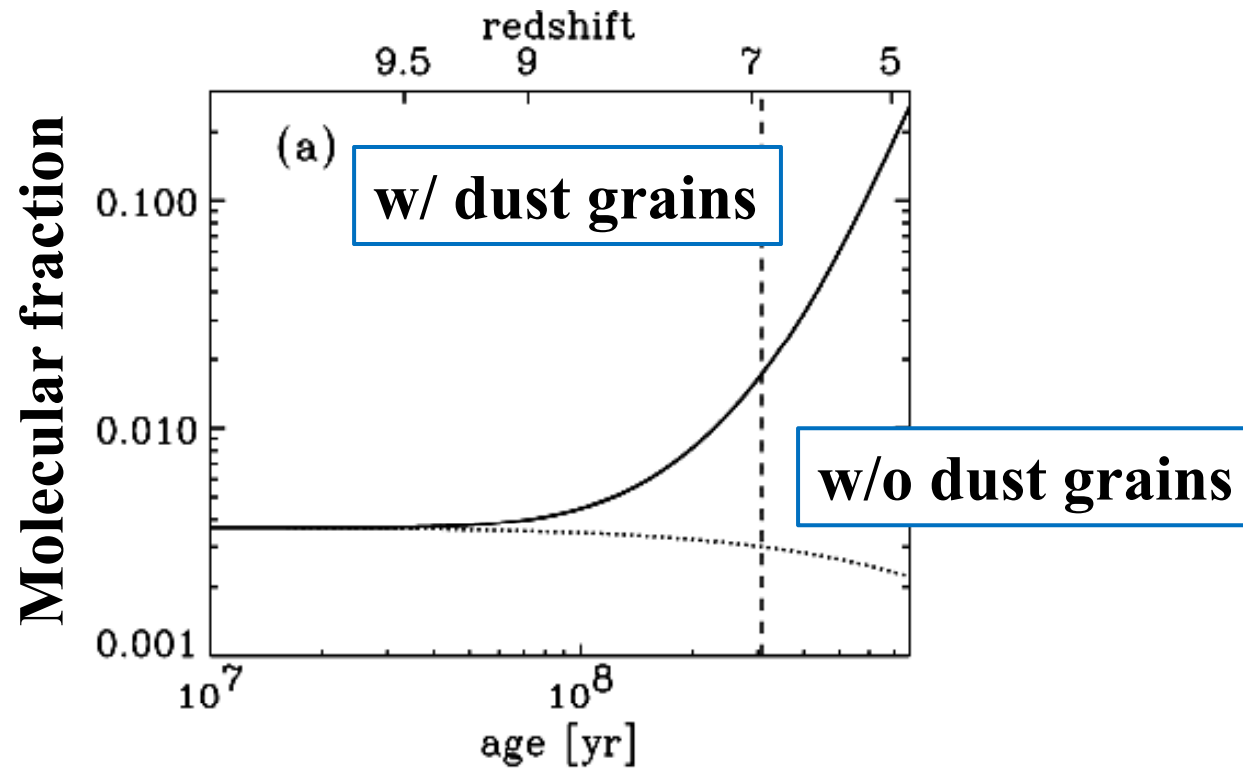
Surface of dust grains



These processes depend strongly on the amount and size distribution of dust grains.

Role of dust for the first star formation

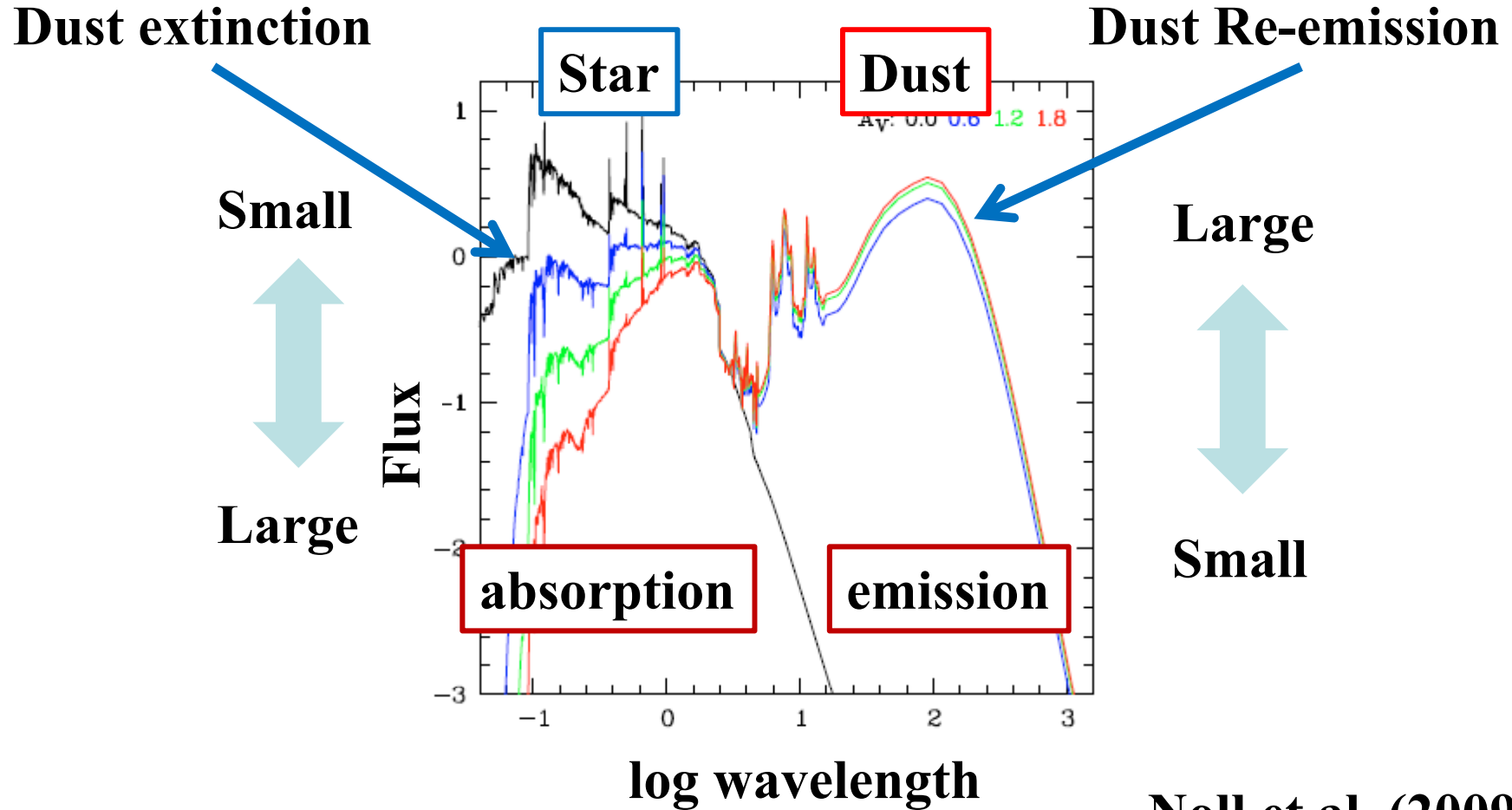
Surface of dust grains



Hirashita & Ferrara (2002)

Dust grains drive the star formation.

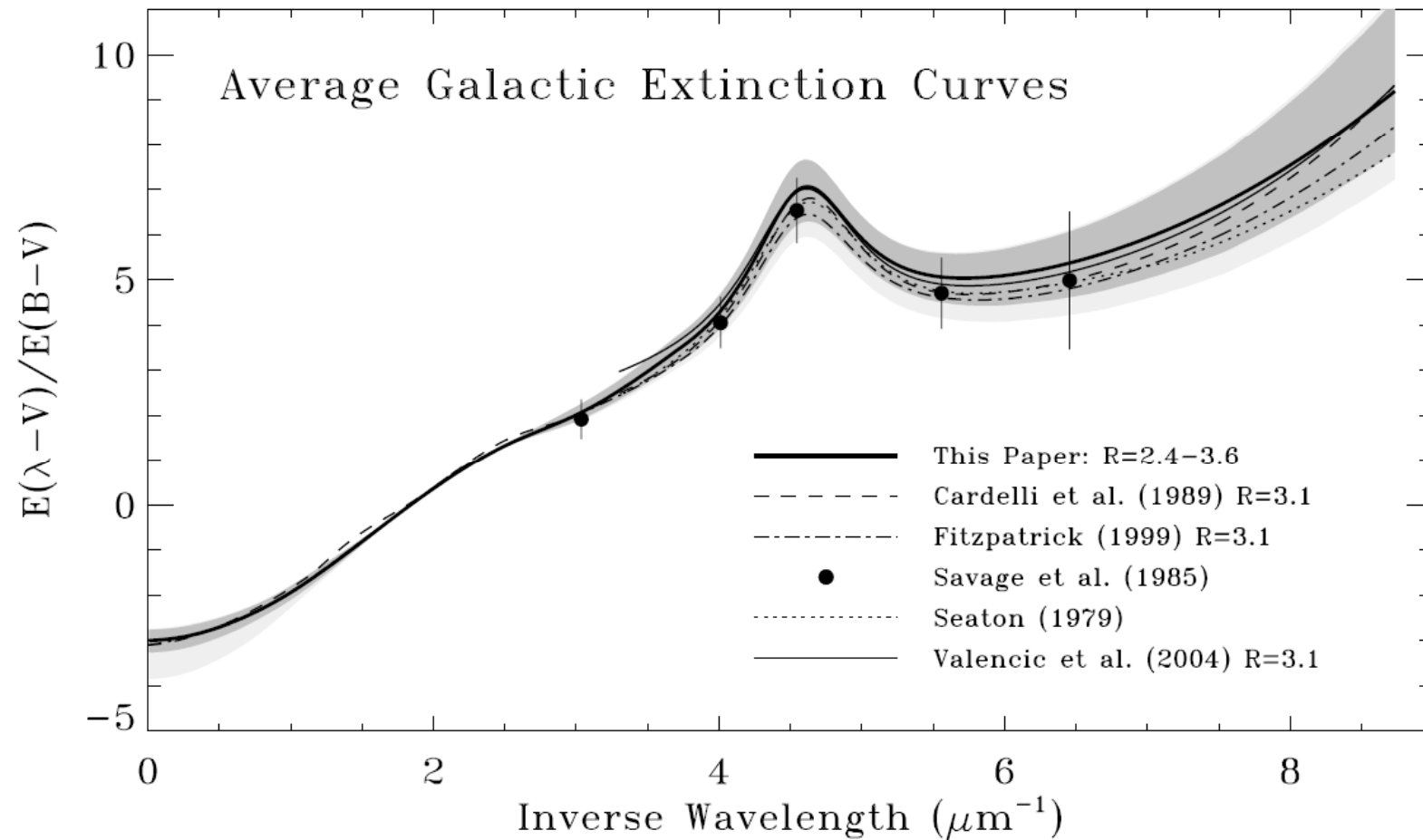
Spectral energy distribution (SED)



Noll et al. (2009)

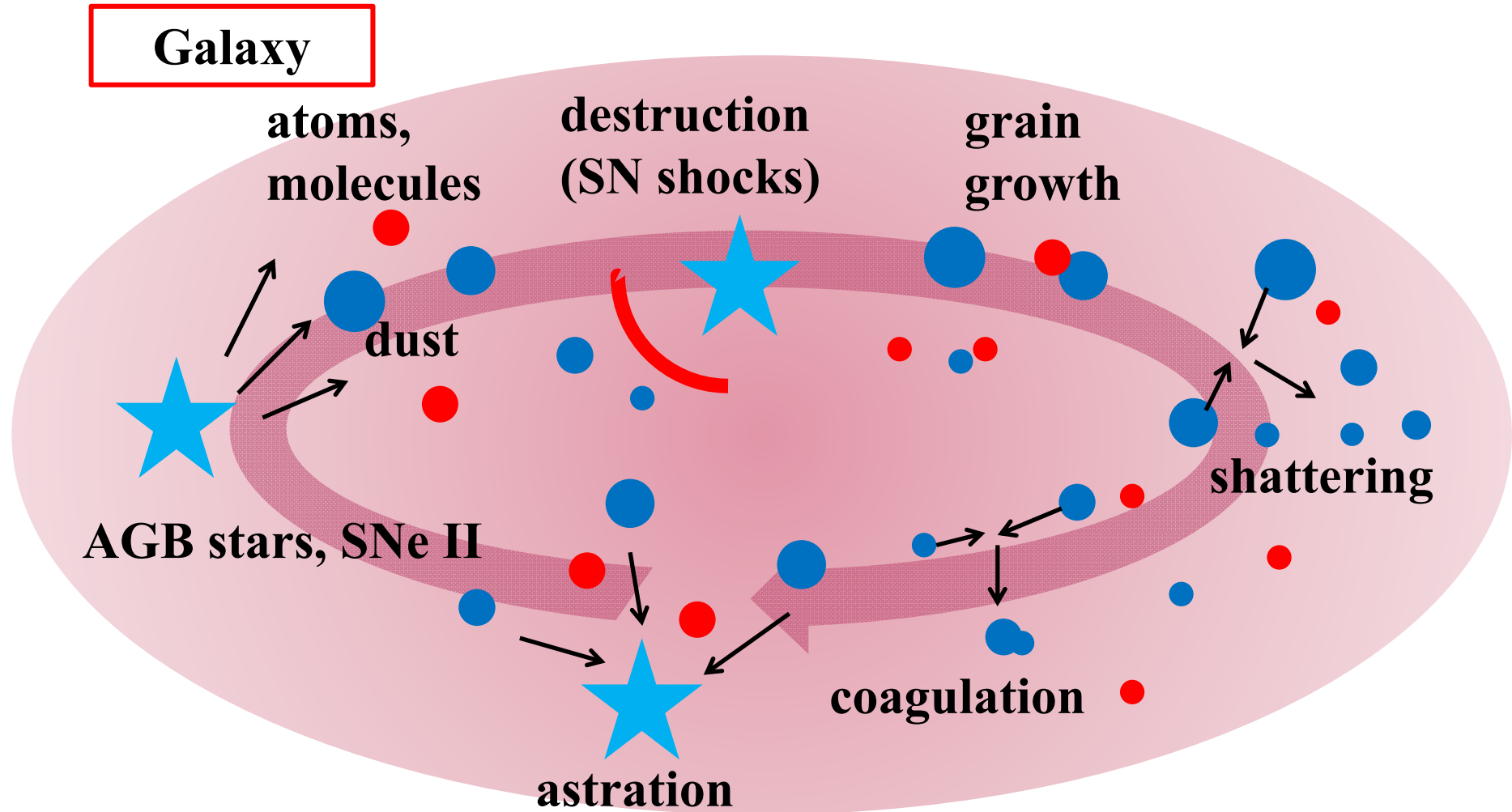
Extinction curve

Wavelength dependence of extinction by dust



Fitzpatrick & Massa (2007)

4.5.3 Dust and matter circulation in a galaxy



Dust supply

AGB stars

Log-normal distribution
Large size grains are produced

Winters et al. (1997)

Yasuda & Kozasa (2012)

Dust mass data

Zhukovska et al. (2008)

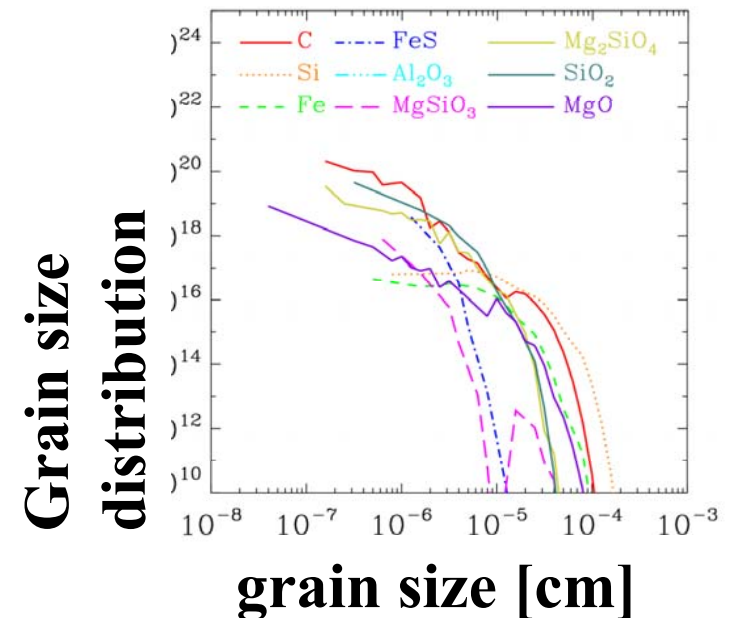
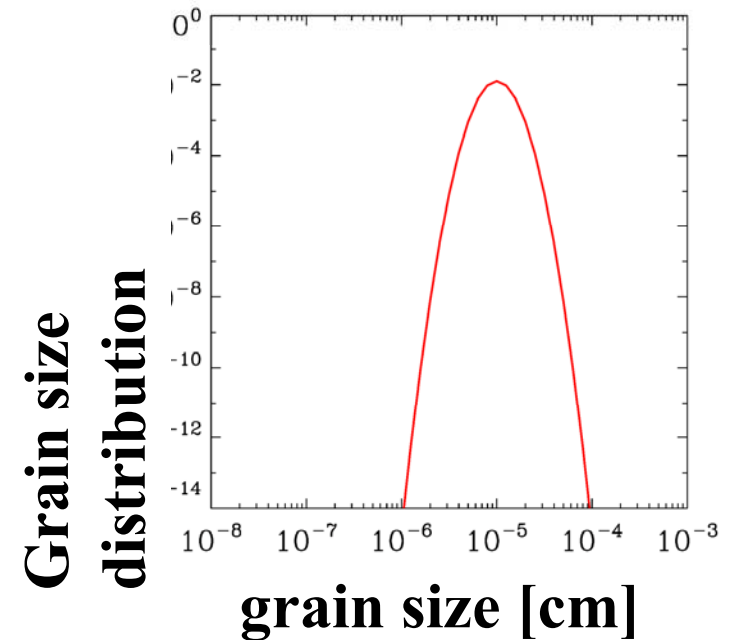
Type II Supernovae (SNe II)

Broken power-law
Biased to large grains

Nozawa et al. (2007)

Dust mass data

Nozawa et al. (2007)

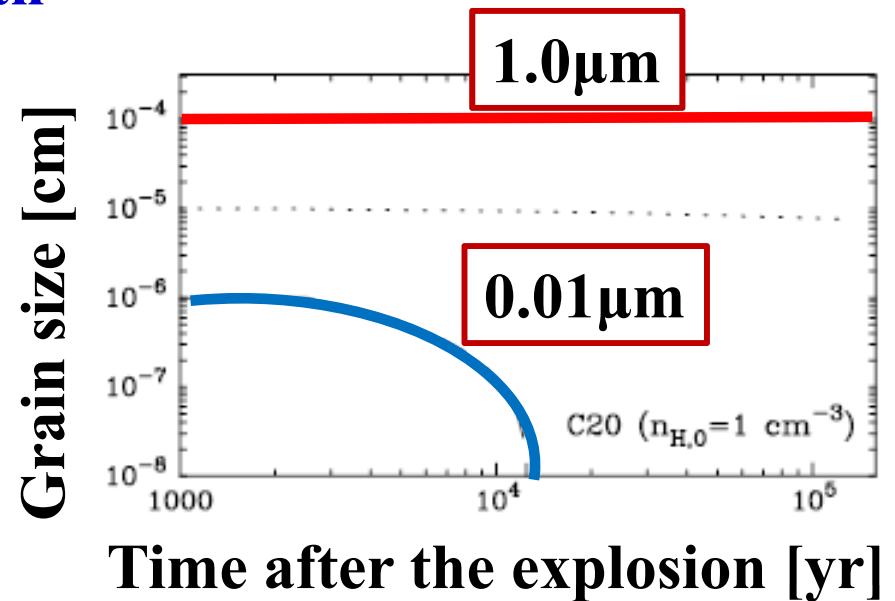


Dust destruction and grain growth

Dust destruction by SN shocks

Smaller grains are mainly destroyed by SN shocks.

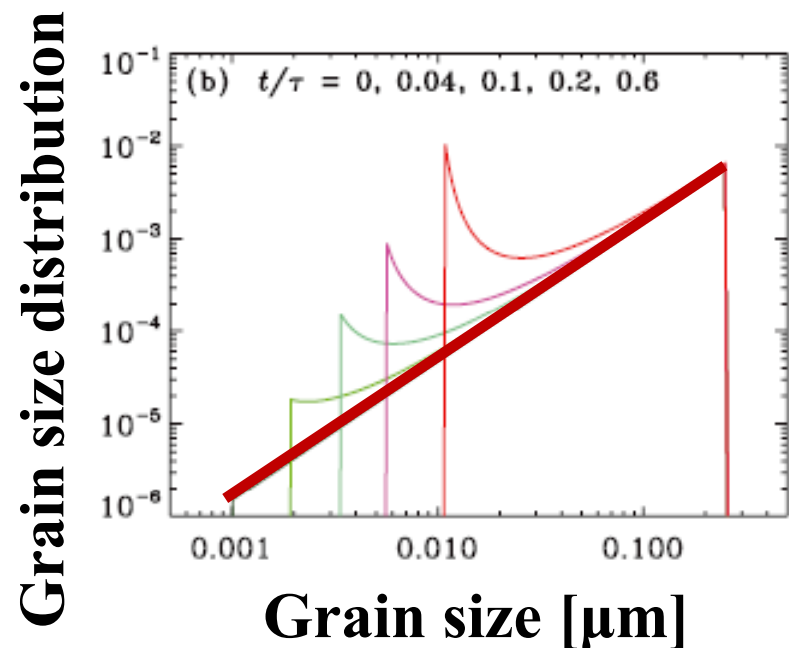
Nozawa et al. (2006)



Grain growth (metal accretion onto grains)

Smaller grains grow to larger grains.

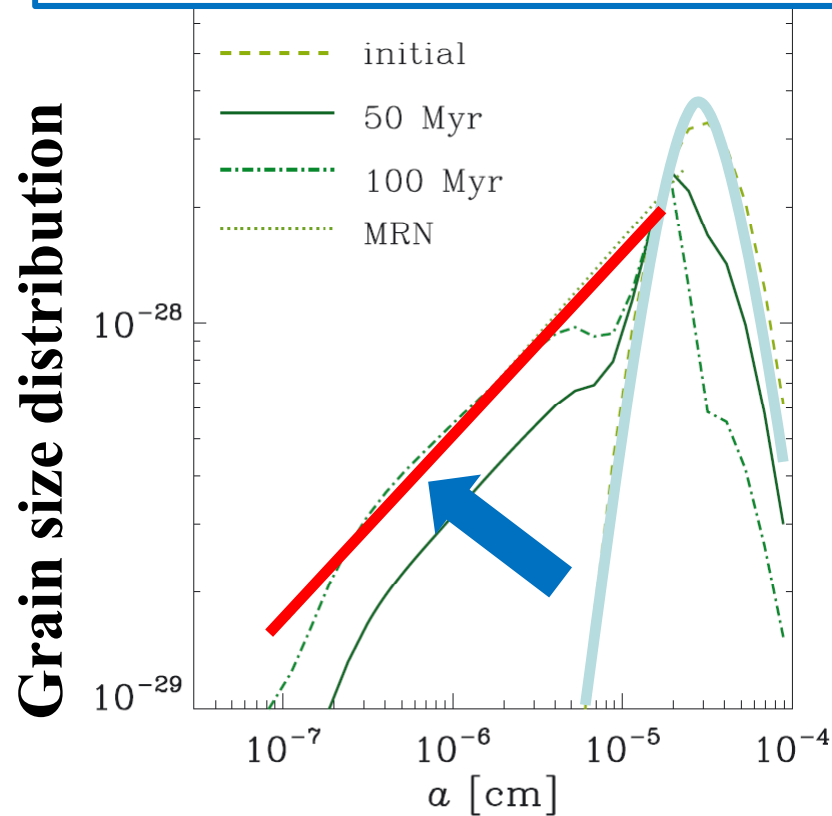
Hirashita & Kuo (2011)



Shattering and coagulation (driven by ISM turbulence)

Shattering

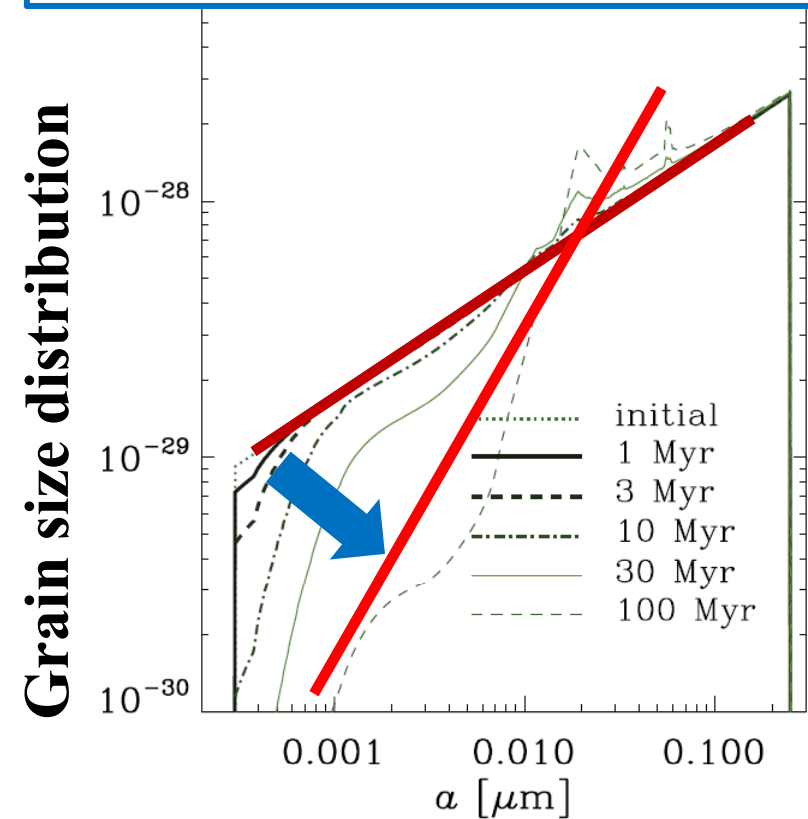
Smaller grains are produced by larger grains



Hirashita (2010)

Coagulation

Larger grains are produced by smaller grains



Hirashita (2012)

4.5.4 Evolution of the Total Dust Amount

Evolution of the total stellar mass, M_* , ISM mass, M_{ISM} , metal mass, M_Z , dust mass, M_d in a galaxy

$$\frac{dM_*(t)}{dt} = \text{SFR}(t) - R(t),$$

$$\frac{dM_{\text{ISM}}(t)}{dt} = -\text{SFR}(t) + R(t),$$

$$\frac{dM_Z(t)}{dt} = -Z(t)\text{SFR}(t) + R_Z(t) + Y_Z(t),$$

$$\frac{dM_d(t)}{dt} = -\mathcal{D}(t)\text{SFR}(t) + Y_d(t) - \frac{M_d}{\tau_{\text{SN}}} + \eta \frac{M_d(1 - \delta)}{\tau_{\text{acc}}}$$

$$Z(t) \equiv M_Z/M_{\text{ISM}}$$

$$\delta \equiv M_d/M_Z$$

$$\mathcal{D} \equiv M_d/M_{\text{ISM}}$$

$$\text{SFR}(t) = \frac{M_{\text{ISM}}(t)}{\tau_{\text{SF}}}$$

4.5.4 Evolution of the Total Dust Amount

Evolution of the total stellar mass, M_* , ISM mass, M_{ISM} , metal mass, M_Z , dust mass, M_d in a galaxy

$$\frac{dM_*(t)}{dt} = \text{SFR}(t) - R(t),$$

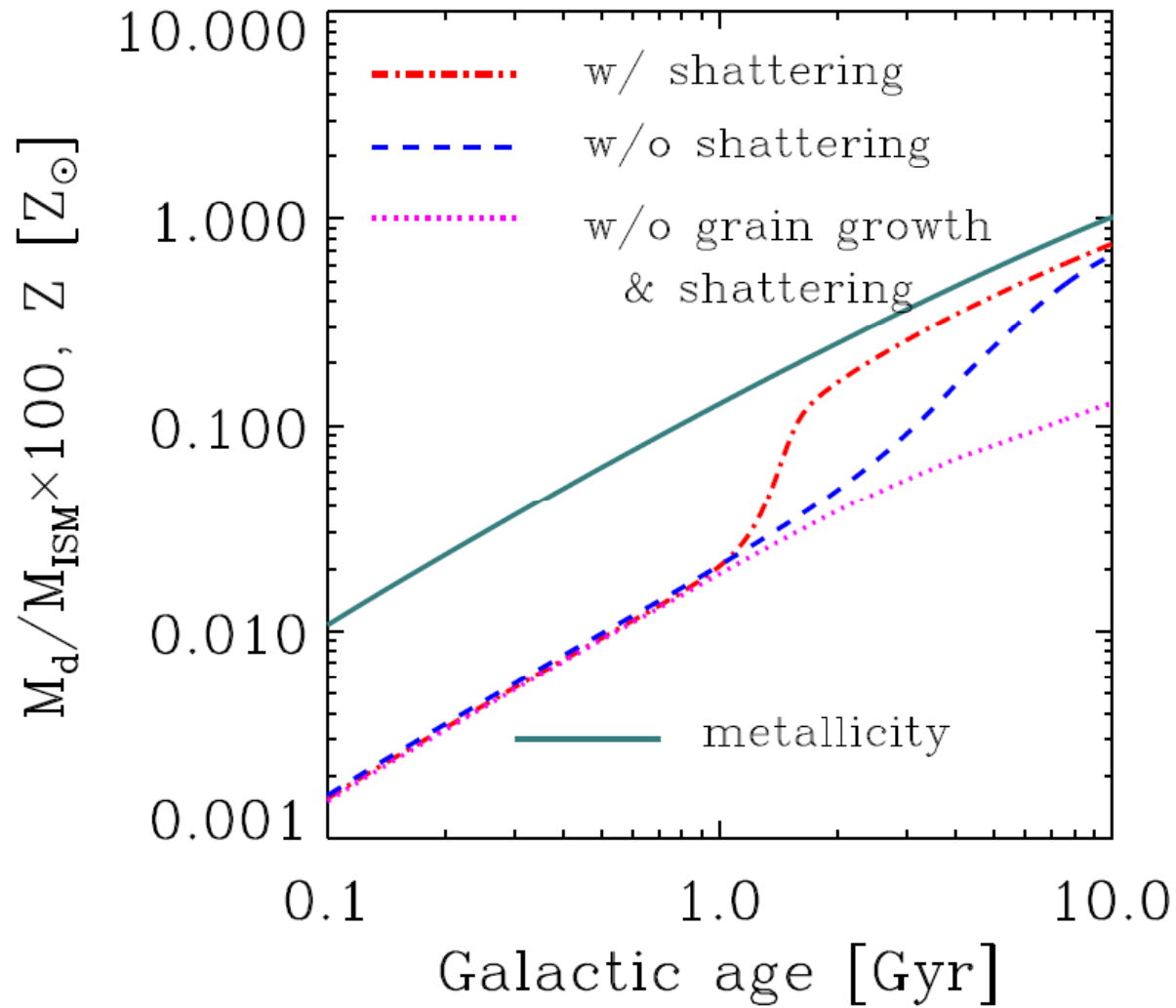
$$\frac{dM_{\text{ISM}}(t)}{dt} = -\text{SFR}(t) + R(t),$$

$$\frac{dM_Z(t)}{dt} = -Z(t)\text{SFR}(t) + R_Z(t) + Y_Z(t),$$

$$\frac{dM_d(t)}{dt} = -\mathcal{D}(t)\text{SFR}(t) + Y_d(t) - \frac{M_d}{\tau_{\text{SN}}} + \eta \frac{M_d(1 - \delta)}{\tau_{\text{acc}}}$$

- **Injection/ejection** from stars
- **Destruction** by **SN shocks**
- **Grain growth** in the ISM

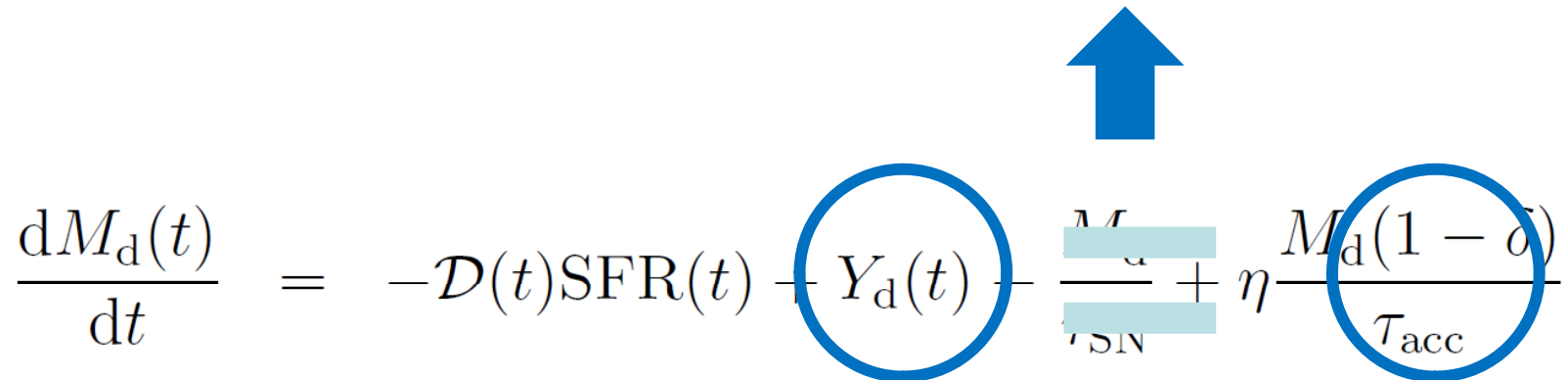
Dust-to-gas mass ratio



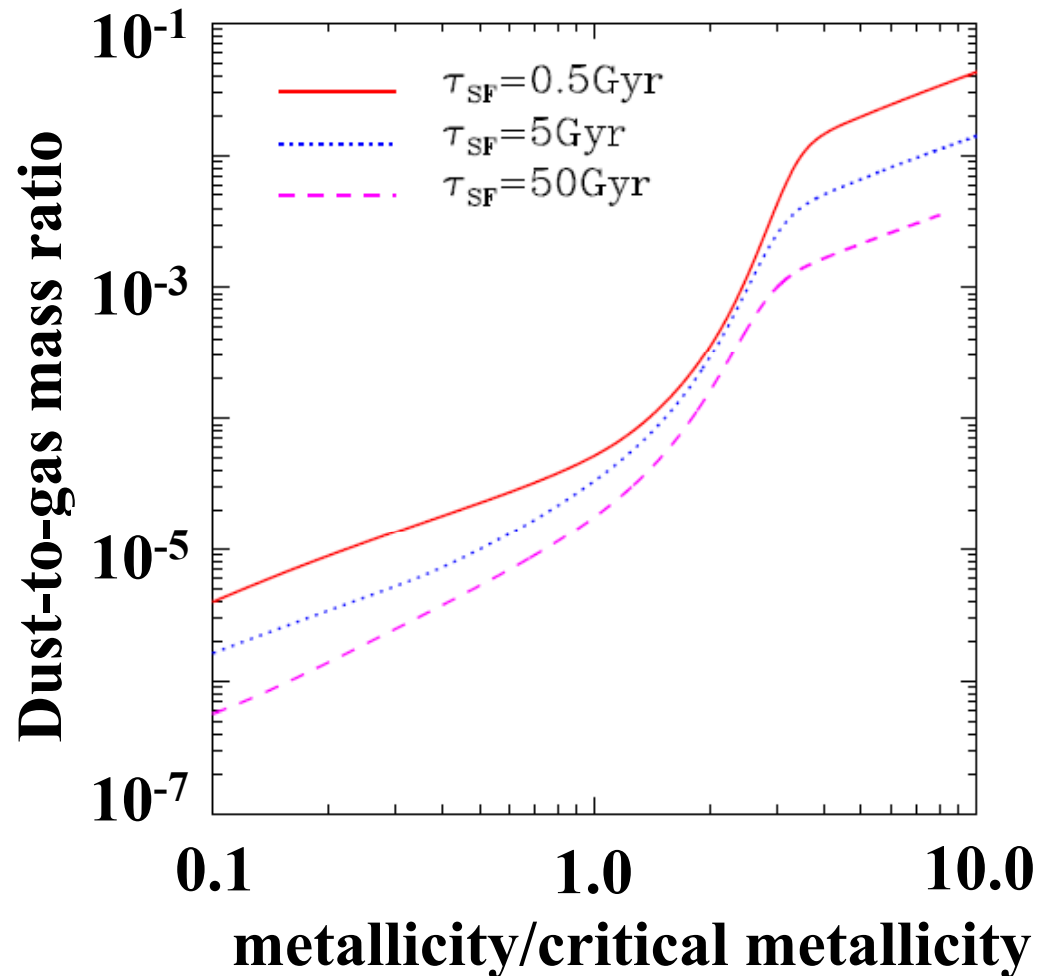
Nozawa et al. (2015)

Critical metallicity for grain growth

$$Z = \left[\frac{D}{\eta\delta(1-\delta)} \right]^{\frac{1}{2}} \left(\frac{\tau_{\text{acc},0}}{\tau_{\text{SF}}} \right)^{\frac{1}{2}}$$

$$\frac{dM_d(t)}{dt} = -\mathcal{D}(t)\text{SFR}(t) - Y_d(t) - \frac{M_d}{\tau_{\text{SN}}} + \eta \frac{M_d(1-\delta)}{\tau_{\text{acc}}}$$


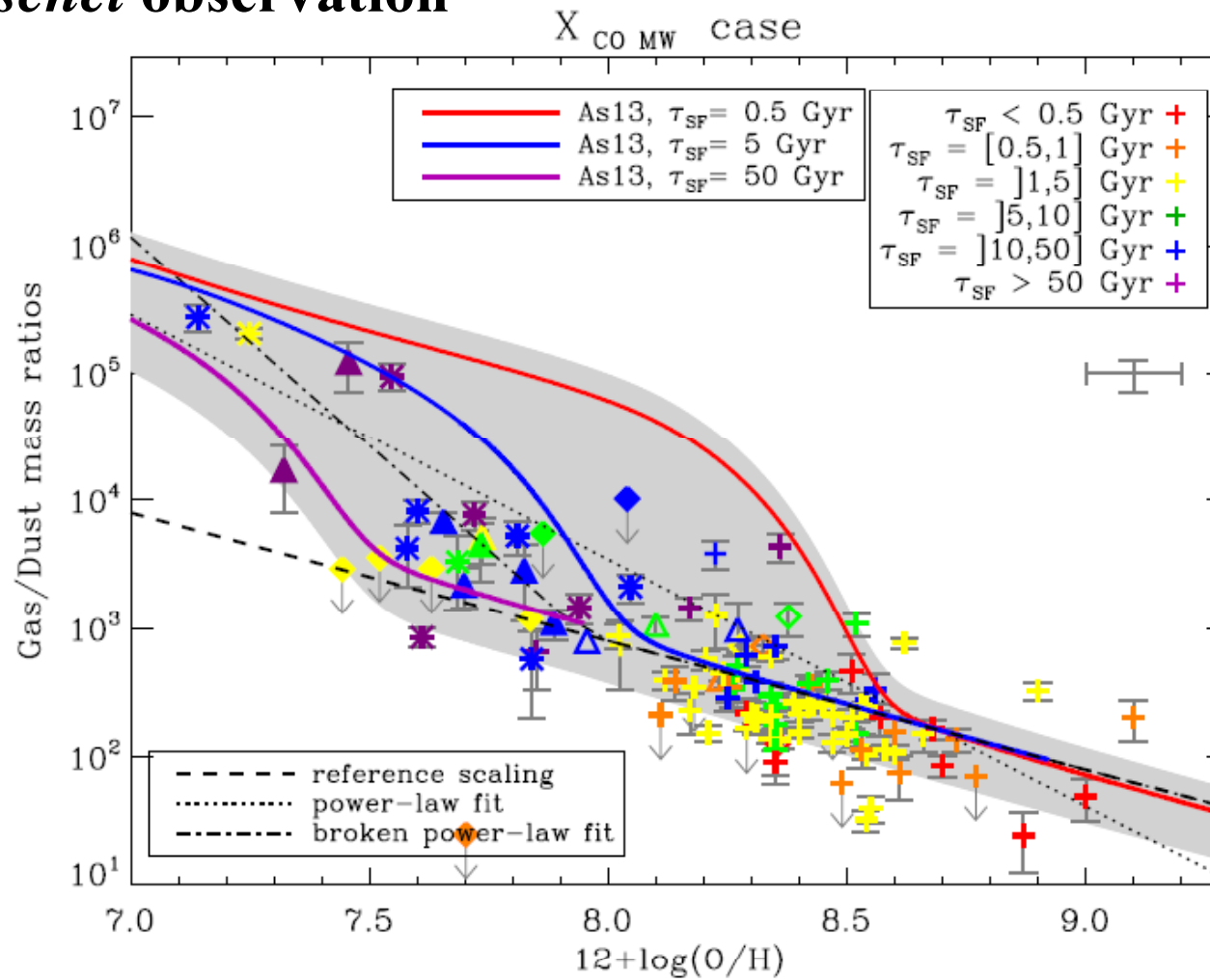
Critical metallicity for grain growth



Evolutionary tracks of the dust-to-gas mass ratio are unified by using Z/Z_{crit} . Metallicity tuned out to be fundamental for dust evolution (Asano et al. 2013a).

Application to the observed data

Herschel observation



Rémy-Ruyer et al. (2014)

4.5.5 Evolution of Dust Grain Size Distribution

Asano et al. (2013b)

- **Closed-box model**

(total baryon mass is a constant)

- **Two-phase ISM (WNM and CNM)**
- **Schmidt law : $\text{SFR}(t) = M_{\text{ISM}}(t)/\tau_{\text{SF}}$**

- **Dust formation by SNe II and AGB stars**
- **Dust reduction through the astration**
- **Dust destruction by SN shocks in the ISM**
- **Grain growth in the CNM**
- **Grain-grain collisions (shattering and coagulation)
in the ISM (mass-preserving processes)**

4.5.5 Evolution of Dust Grain Size Distribution

Asano et al. (2013b)

- **Closed-box model**
(total baryon mass is a constant)
- **Two-phase ISM (WNM and CNM)**
- **Schmidt law : $SFR(t) = M_{ISM}(t)/\tau_{SF}$**

This determines the SFH!

⇒ To be improved.

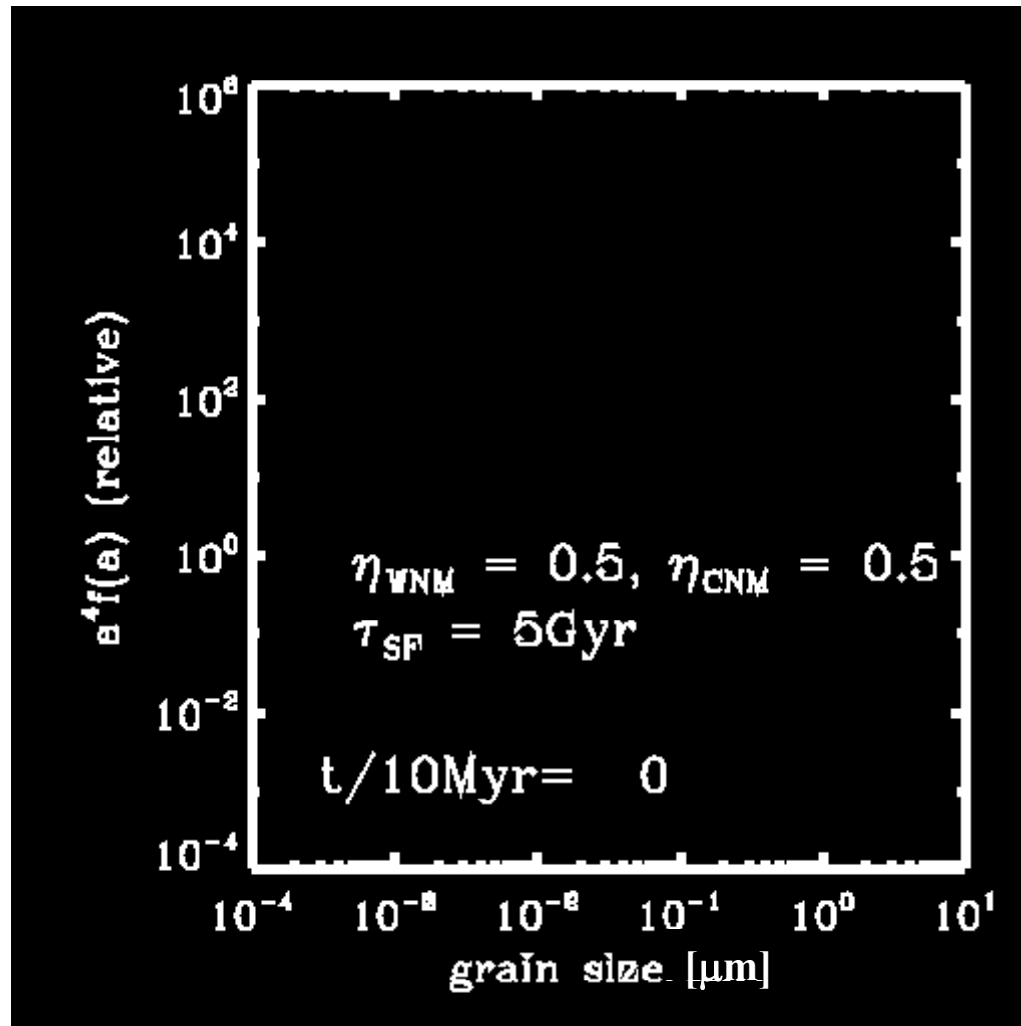
- **Dust formation by SNe II and AGB stars**
- **Dust reduction through the astration**
- **Dust destruction by SN shocks in the ISM**
- **Grain growth in the CNM**
- **Grain-grain collisions (shattering and coagulation) in the ISM (mass-preserving processes)**

Formulation of the grain-size dependent evolution of dust mass

$M_d(a, t) = m(a)f(a, t)da$: dust mass with a grain radius $[a, a+da]$ at a galactic age t

$$\begin{aligned}
 \frac{dM_d(a, t)}{dt} = & -\frac{M_d(a, t)}{M_{\text{ISM}}(t)} \text{SFR}(t) + Y_d(a, t) && \text{Stellar effects} \\
 & -\frac{M_{\text{swept}}}{M_{\text{ISM}}(t)} \gamma_{\text{SN}}(t) \left[M_d(a, t) - m(a) \int_0^\infty \xi(a, a') f(a', t) da \right] && \text{Destruction by SN shocks} \\
 & + \eta_{\text{CNM}} \left[dm \frac{\partial [m(a) f_m(m, t)]}{\partial t} \right] && \text{Grain growth} \\
 & + \eta_{\text{WNM}} \left[\frac{dM_d(a, t)}{dt} \right]_{\text{shat,WNM}} + \eta_{\text{CNM}} \left[\frac{dM_d(a, t)}{dt} \right]_{\text{shat,CNM}} && \text{Shattering} \\
 & + \eta_{\text{WNM}} \left[\frac{dM_d(a, t)}{dt} \right]_{\text{coag,WNM}} + \eta_{\text{CNM}} \left[\frac{dM_d(a, t)}{dt} \right]_{\text{coag,CNM}} && \text{Coagulation}
 \end{aligned}$$

Evolution of the grain size distribution



4.5.6 Evolution of Extinction Curve

Extinction = absorption + scattering by dust grains

Extinction in unit of magnitude at a wavelength: A_λ

$$A_\lambda = 1.086 \sum_j \tau_{j,\lambda}$$

$$\tau_{\lambda, j} = \int_0^\infty \pi a^2 Q_{\text{ext}, j}(\lambda, a) C f_j(a) da$$

λ : wavelength
 a : radius of a grain
 j : grain species

Optical constant:

graphite and astronomical silicate

($\text{Mg}_1 \text{Fe}_{0.9} \text{SiO}_4$)

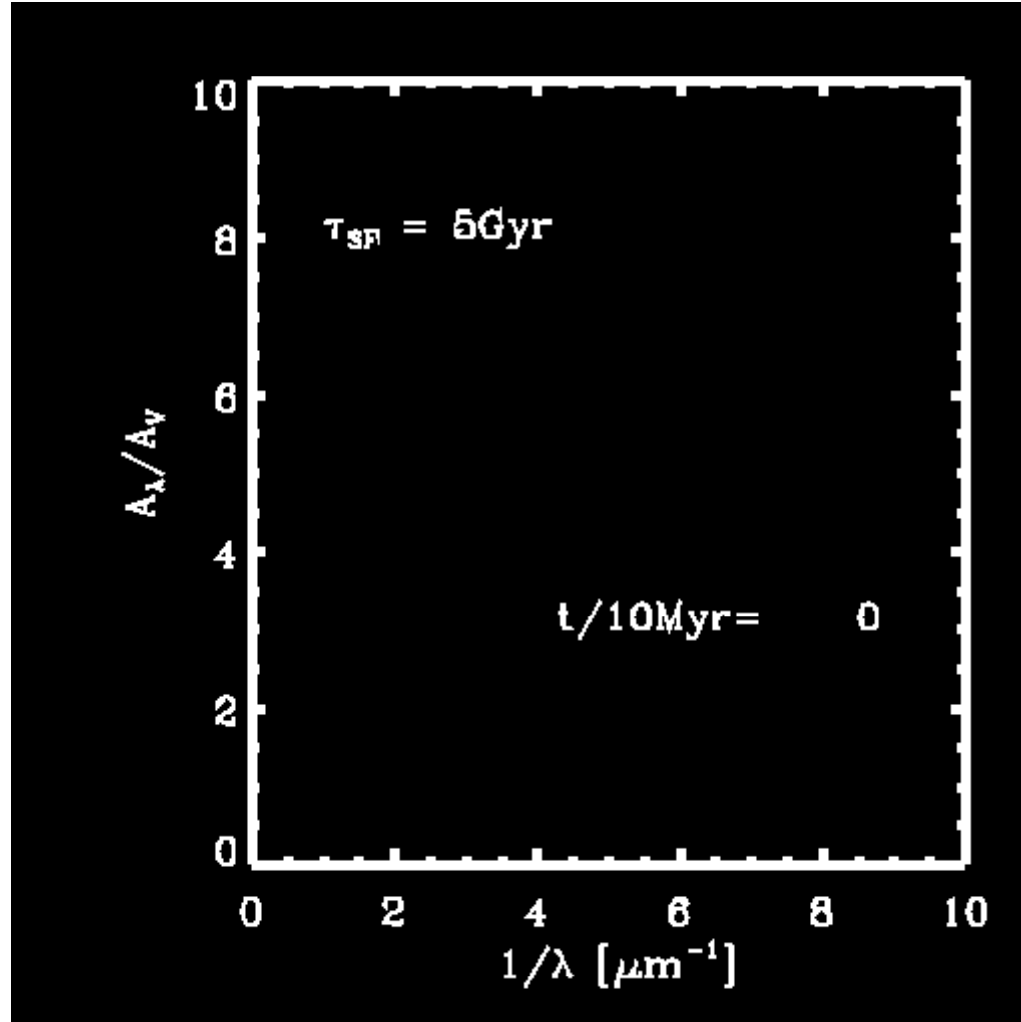
Draine & Lee (1984)

Grain size distribution:

Evolution model of grain size distribution

Asano et al. (2013b)

Evolution of the extinction curve in galaxies



Part III: Formation of Structures and Galaxies

5. Structure Formation I

5.1 Structure formation: fundamentals

5.2 Linear theory

5.2 Structure formation: fundamentals

From structure formation to galaxy formation

Input of the Harrison-Zel'dovich spectrum

Deformation of the power-law form

Initial fluctuation

Gravitational instability

Growth of inhomogeneity (dark matter)

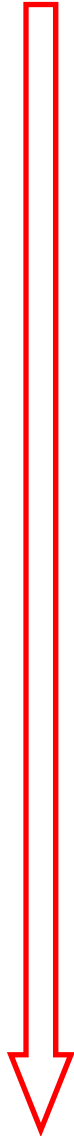
Linear growth: large-scale structure

Nonlinear growth: clusters, galaxies

Dark halo formation

Physics of baryons

Star formation and galaxy formation



Characterization of fluctuation

Density fluctuation: $\delta \equiv \frac{\rho(\mathbf{x}) - \bar{\rho}}{\bar{\rho}}$ (14)

Dispersion: $\sigma^2 \equiv \langle \delta^2 \rangle$ (15)

Fourier component: $\delta_k \equiv |\delta_k| e^{i\phi_k} = \int \delta(\mathbf{x}) e^{i\mathbf{k}\cdot\mathbf{x}} d^3x$ (16)

Power spectrum: $P(k) \equiv \langle |\delta_k|^2 \rangle$ (17)

Higher-order power spectra (bispectrum \Leftrightarrow 3-point correlation function; trispectrum \Leftrightarrow 4-point correlation function) are also defined.

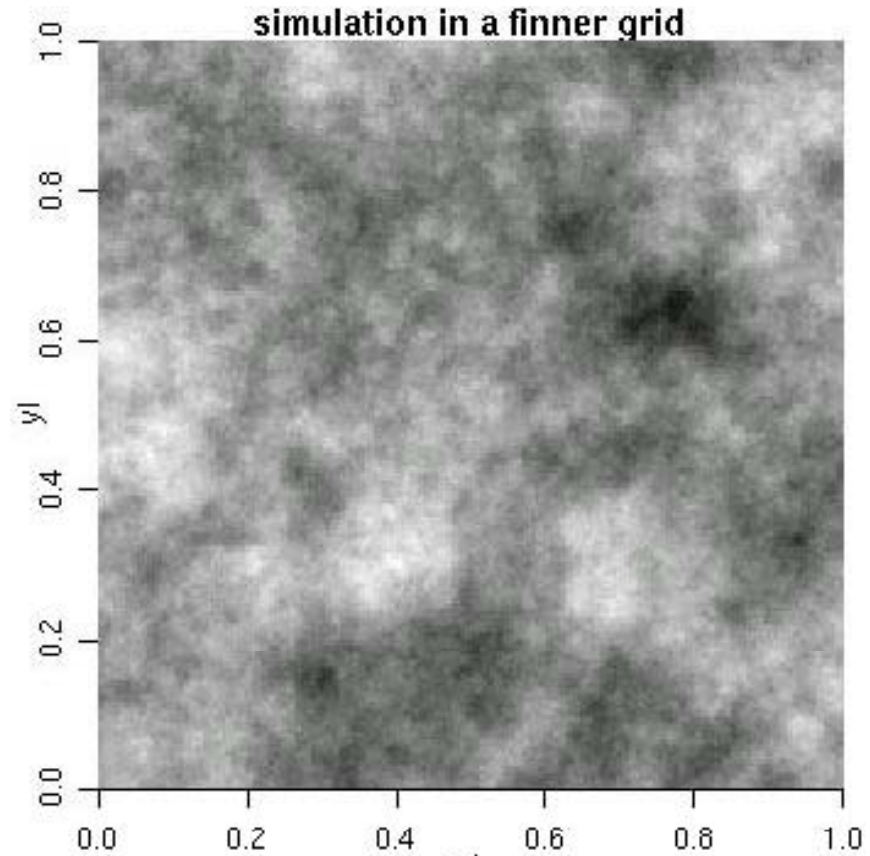
In general, a set of infinite number of moments (or their Fourier counterparts) are needed to specify the properties of a stochastic field.

Gaussian random field

Gaussian random field is a stochastic field whose distribution is described by Gaussian and its Fourier phases have no correlation.

$$f(\delta)d\delta = \frac{1}{\sqrt{2\pi\sigma^2}} e^{-\frac{\delta^2}{2\sigma^2}} d\delta \quad (18)$$

$$\langle \phi_k \phi_{k'} \rangle \propto \delta_D(k - k')$$

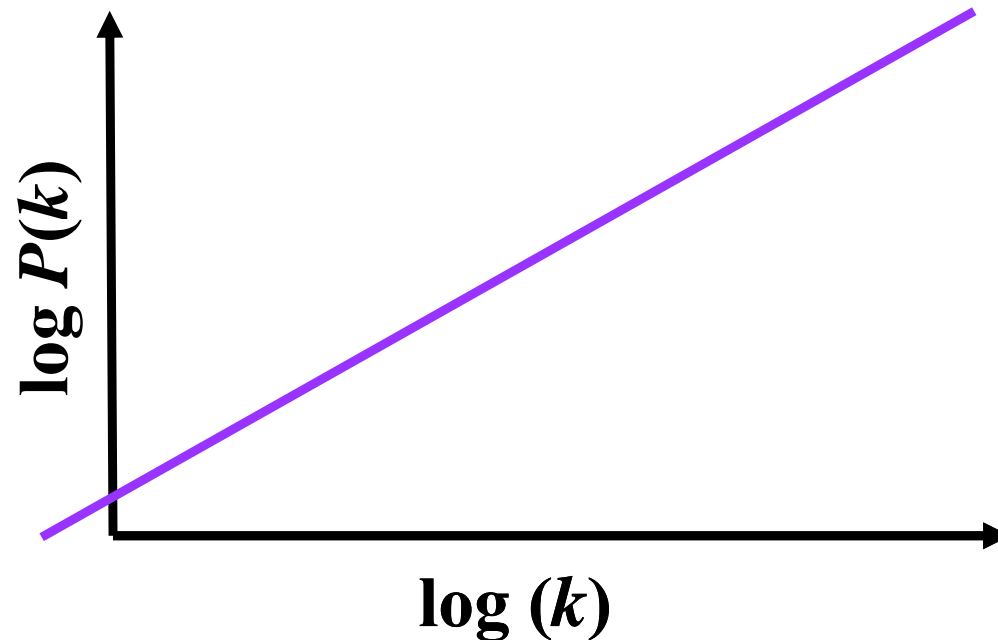


All the stochastic properties of a field is uniquely characterized by the power spectrum $P(k)$ for Gaussian random fields.

Observationally, density fluctuation in the Universe can be regarded as (almost) Gaussian.

Initial fluctuation: Harrison-Zel'dovich spectrum

A power-law form $P(k) \propto k^n$ for the initial power spectrum has been propounded from heuristic requirements to the structure formation in the Universe. **The case with $n=1$ is especially called Harrison-Zel'dovich spectrum** (Harrison 1970; Zel'dovich 1972).



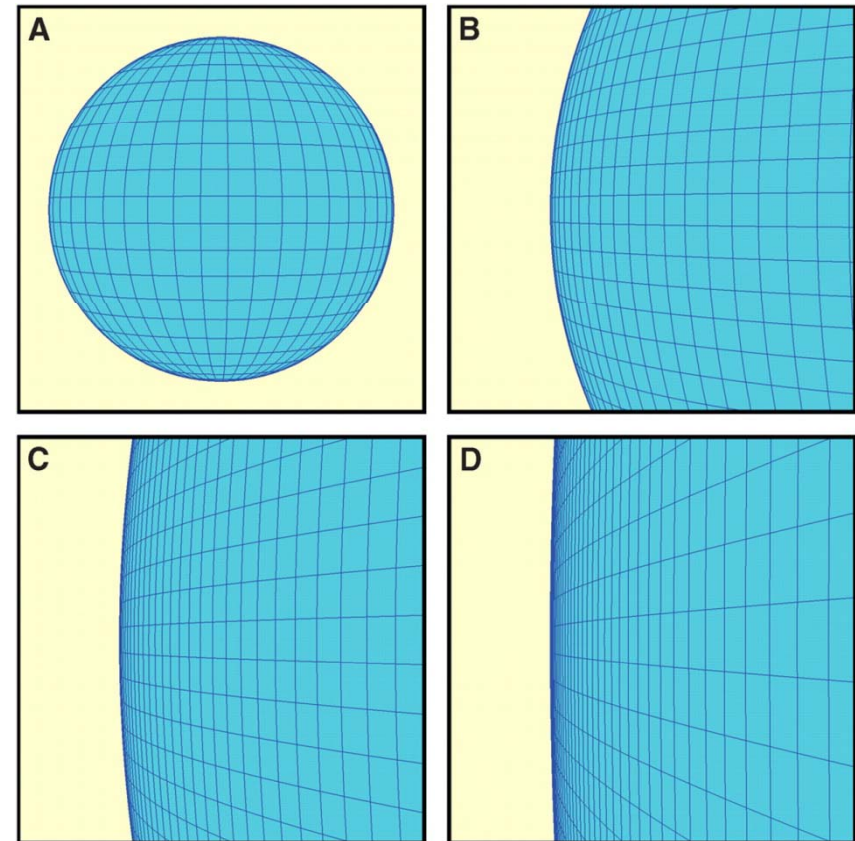
Inflation

Inflation: exponential expansion of the Universe before the Big Bang fireball

It has appeared on the scene of cosmology as a theory to solve the flatness and horizon problem, as well as to provide initial fluctuation of the cosmic structure (Guth 1981; Sato 1981).

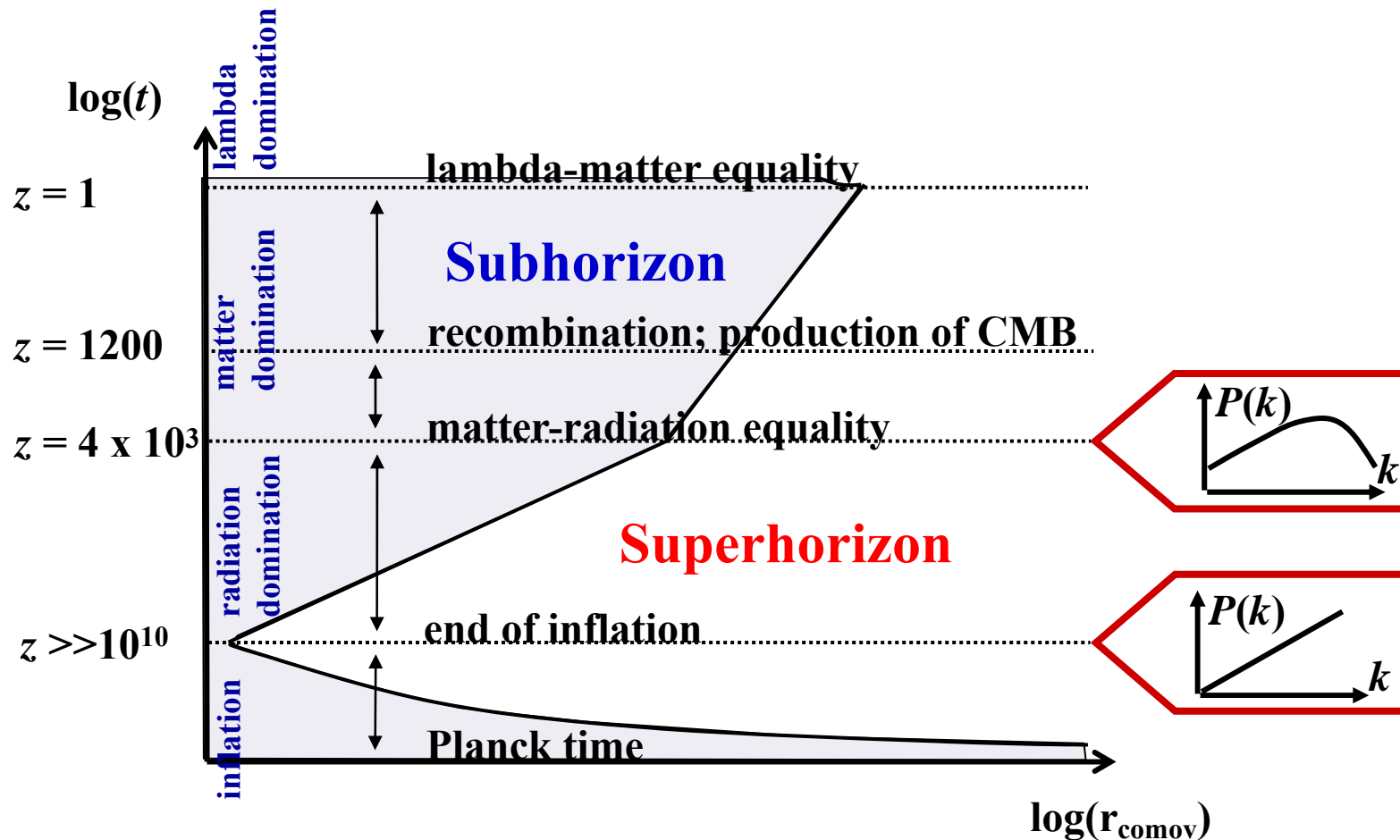
Inflation produces a (nearly) Gaussian fluctuation with a power spectrum of $P(k) \propto k$.

N.B. Not exact in a modern framework.



(Guth & Kaiser 2005)

Deformation of the Harrison-Zel'dovich spectrum



Growth rate of a density perturbation depends on the epoch (i.e. what component dominates global expansion dynamics at that time), and whether a perturbation is super- or subhorizon.

Deformation of the initial spectrum

Radiation dominant epoch: when the initial power spectrum enters the horizon ($L_H = ct$)(the horizon expands to the scale of fluctuation), fluctuations can grow little because photons sweep out all the fluctuations of dark matter (Mészáros effect; stagspansion).

Since fluctuations larger than the horizon can grow, the power spectrum bents at the horizon scale of the epoch and deviates from a single power-law. The scale of the bent is

$$k_H(t_{\text{eq}}) = a(t_{\text{eq}})H(t_{\text{eq}}) = 0.102\Omega_m h [\text{Mpc}]^{-1} \quad (18)$$

Caution to the superhorizon-scale fluctuation

***N.B.* Fluctuations larger than the horizon should be treated fully relativistically**, but because of the large degree of freedom of coordinate transformation in general relativity, the form of fluctuation cannot be determined uniquely: for example, we can always take a coordinate system in which fluctuations vanish completely.

It is popular now to use the **gauge-invariant formulation** (Bardeen 1980; Kodama & Sasaki 1984).

Transfer function

A power spectrum at a certain time t can be described as **the initial power spectrum \times deformation**. This deformation part is called **the transfer function**.

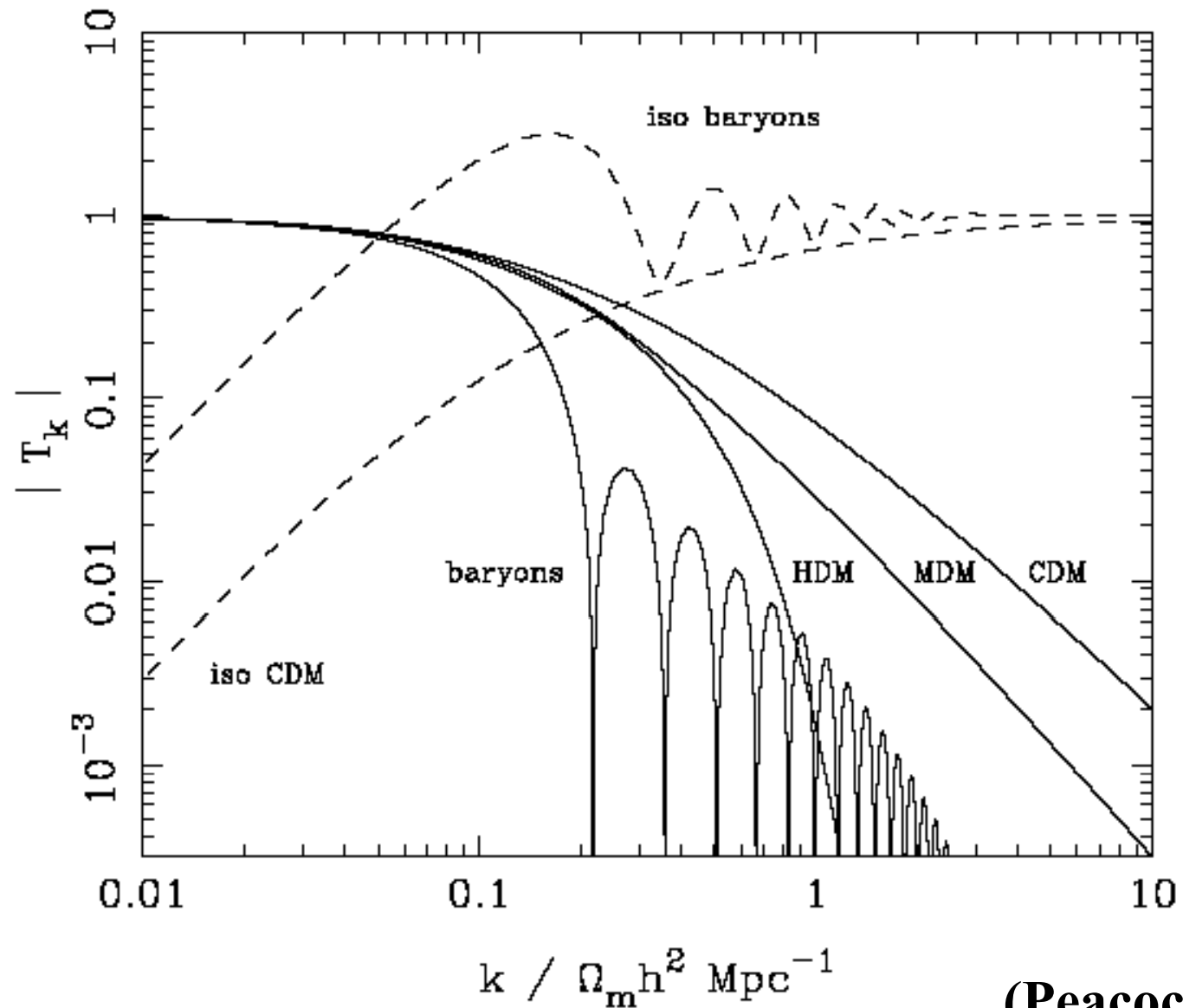
In the case of CDM, since only the stagspansion is the cause of the deformation, then we can write as

$$T(k) \propto \begin{cases} 1 & k \ll k_H(t_{\text{eq}}) \\ k^{-2} & k \gg k_H(t_{\text{eq}}) \end{cases} \quad (19)$$

Hence, the power spectrum is expressed as

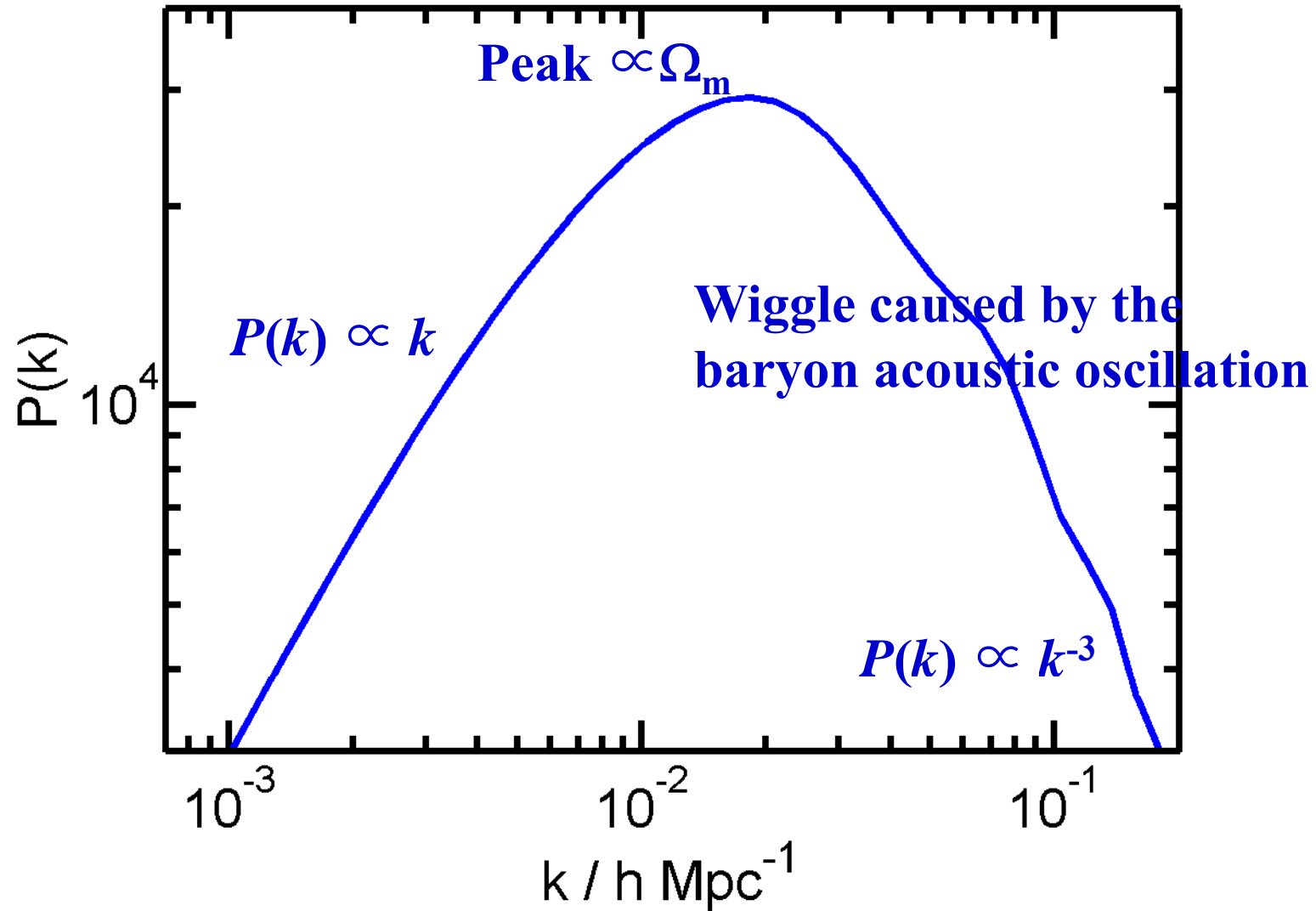
$$P(k) \propto kT^2(k) \propto \begin{cases} k & k \ll k_H(t_{\text{eq}}) \\ k^{-3} & k \gg k_H(t_{\text{eq}}) \end{cases} \quad (20)$$

Transfer functions for various kind of matter

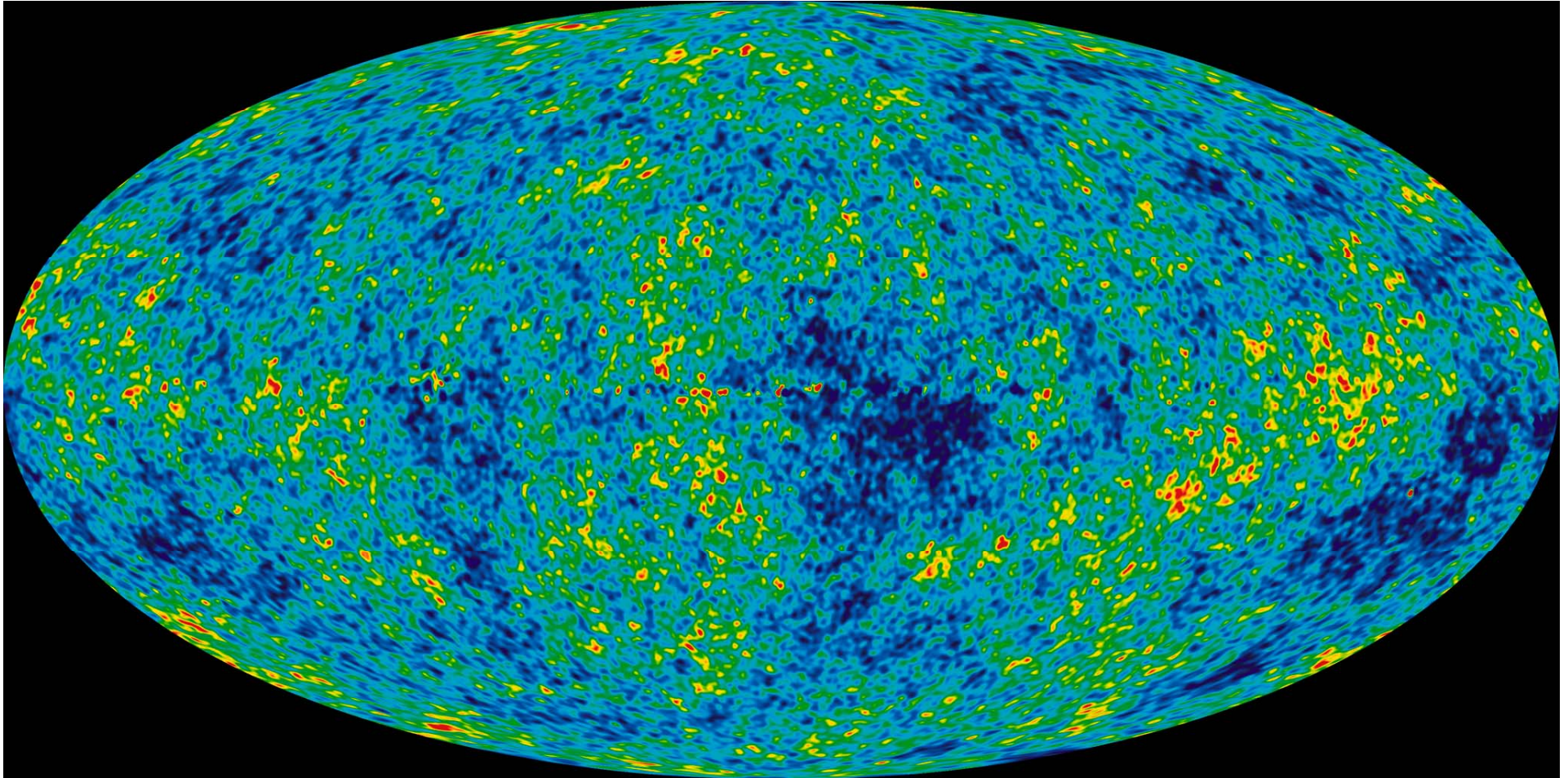


(Peacock 1993)

Typical power spectrum with CDM and baryon



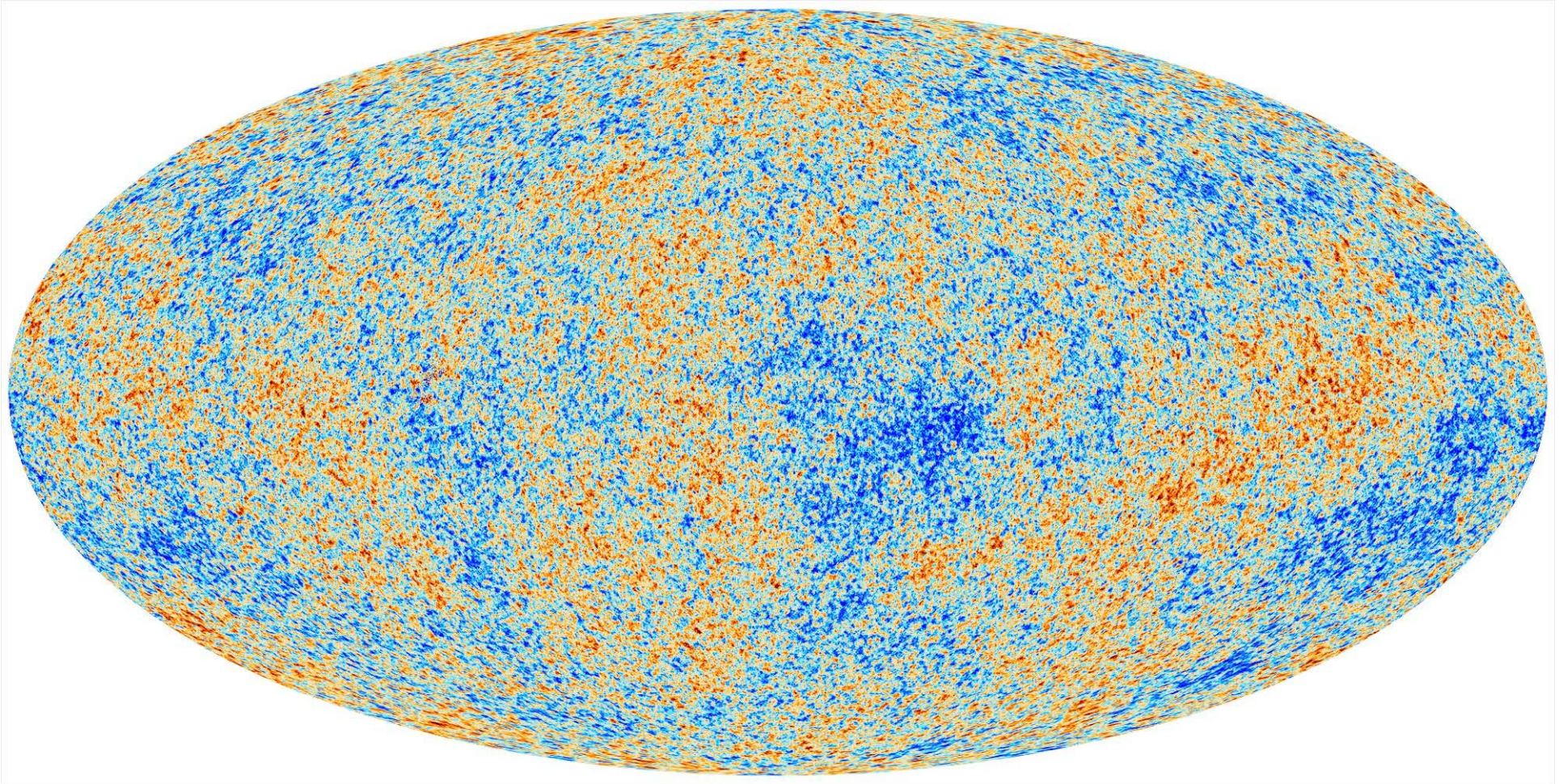
The cosmic microwave background radiation (CMB)



WMAP 5 year data

http://map.gsfc.nasa.gov/m_mm.html

The cosmic microwave background radiation (CMB)



***Planck* first data**

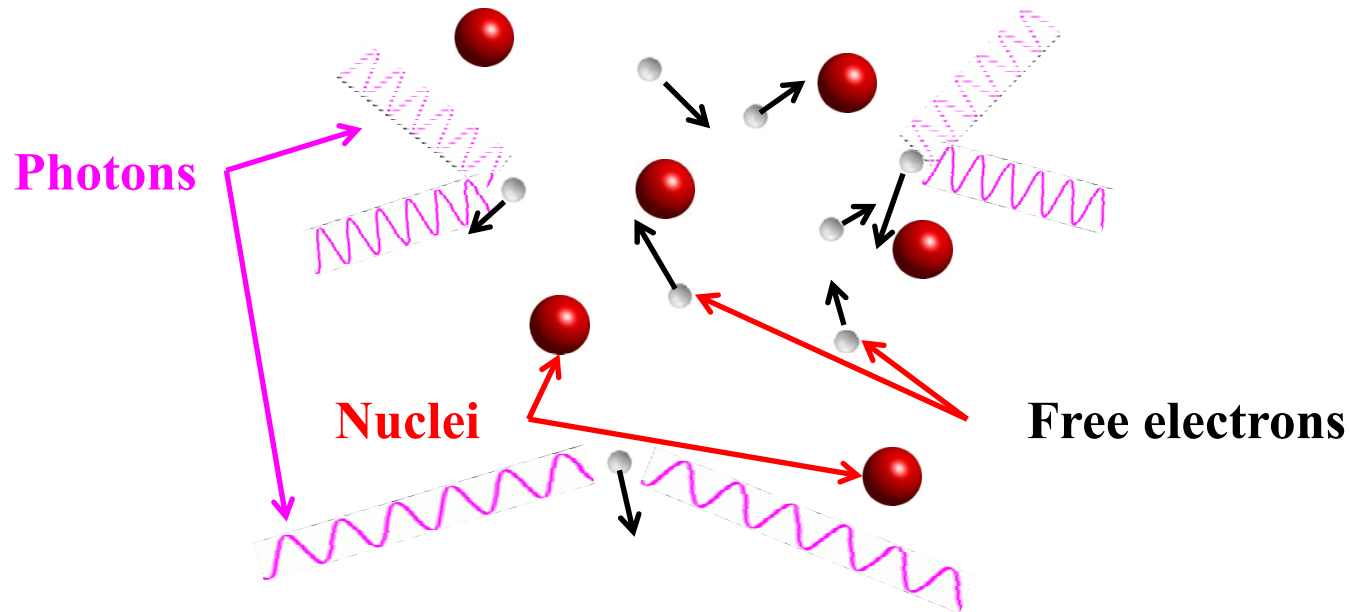
<http://www.rssd.esa.int/index.php?project=Planck>

The cosmic microwave background radiation (CMB)

- $T = 2.725 \pm 0.002$ K.
- **The most perfect blackbody in the Universe.**
- Rayleigh-Jeans tail at the cm regime, and the peak locates around 2 mm.
- Fluctuation $\delta T/T \sim 10^{-5}$.
- **This fluctuation is the line-of-sight integrated initial fluctuations which, in principle, contain the full information of the initial power spectrum when the structures have started to grow (if the fluctuations are adiabatic).**
- However, because of numerous physical processes, the power spectrum is somewhat deformed especially at higher k (small scale) regime.

Recombination

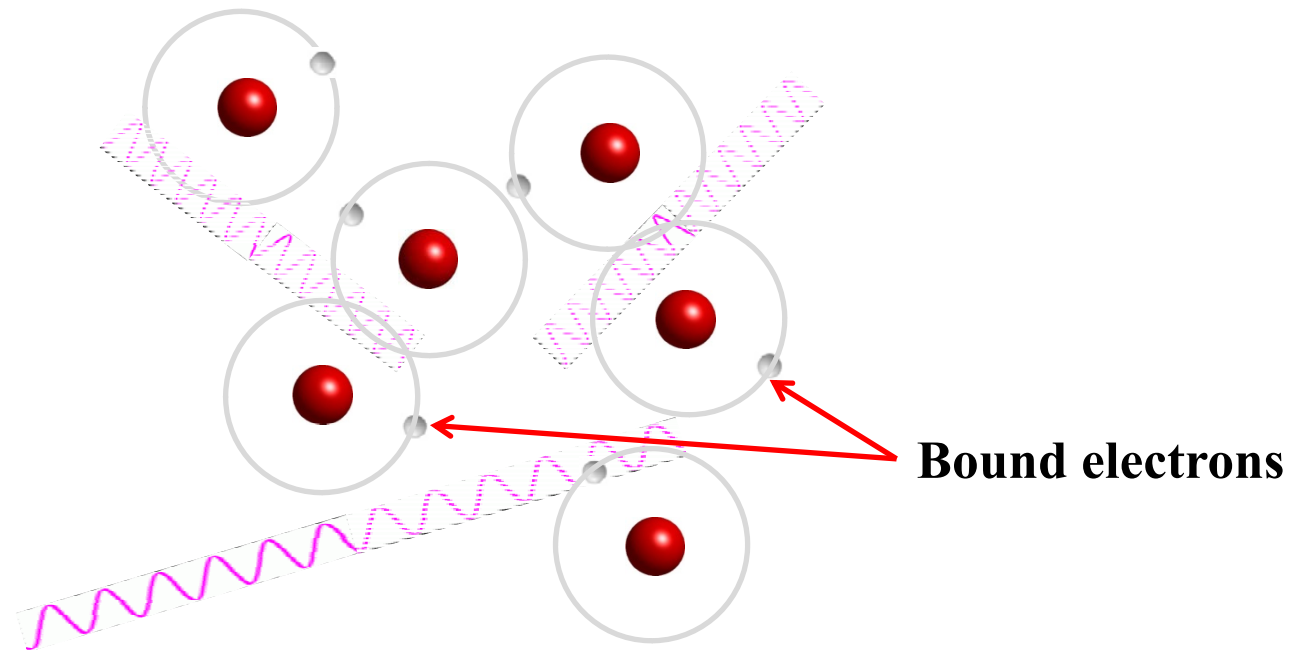
The Big-Bang fireball: plasma



Photons cannot penetrate plasma because of the Thomson scattering by free electrons.

Recombination

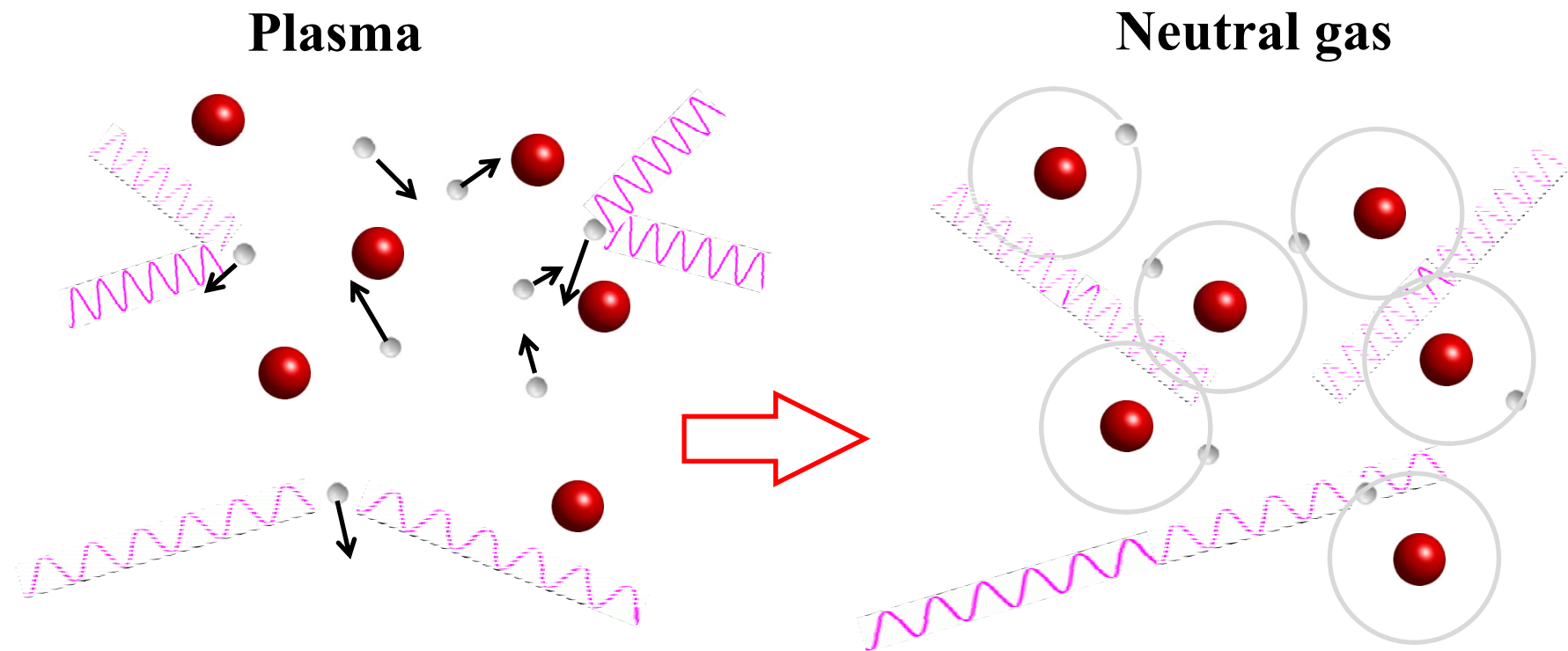
380 Myr after the birth of the Universe, **matter turns from plasma into atoms.**



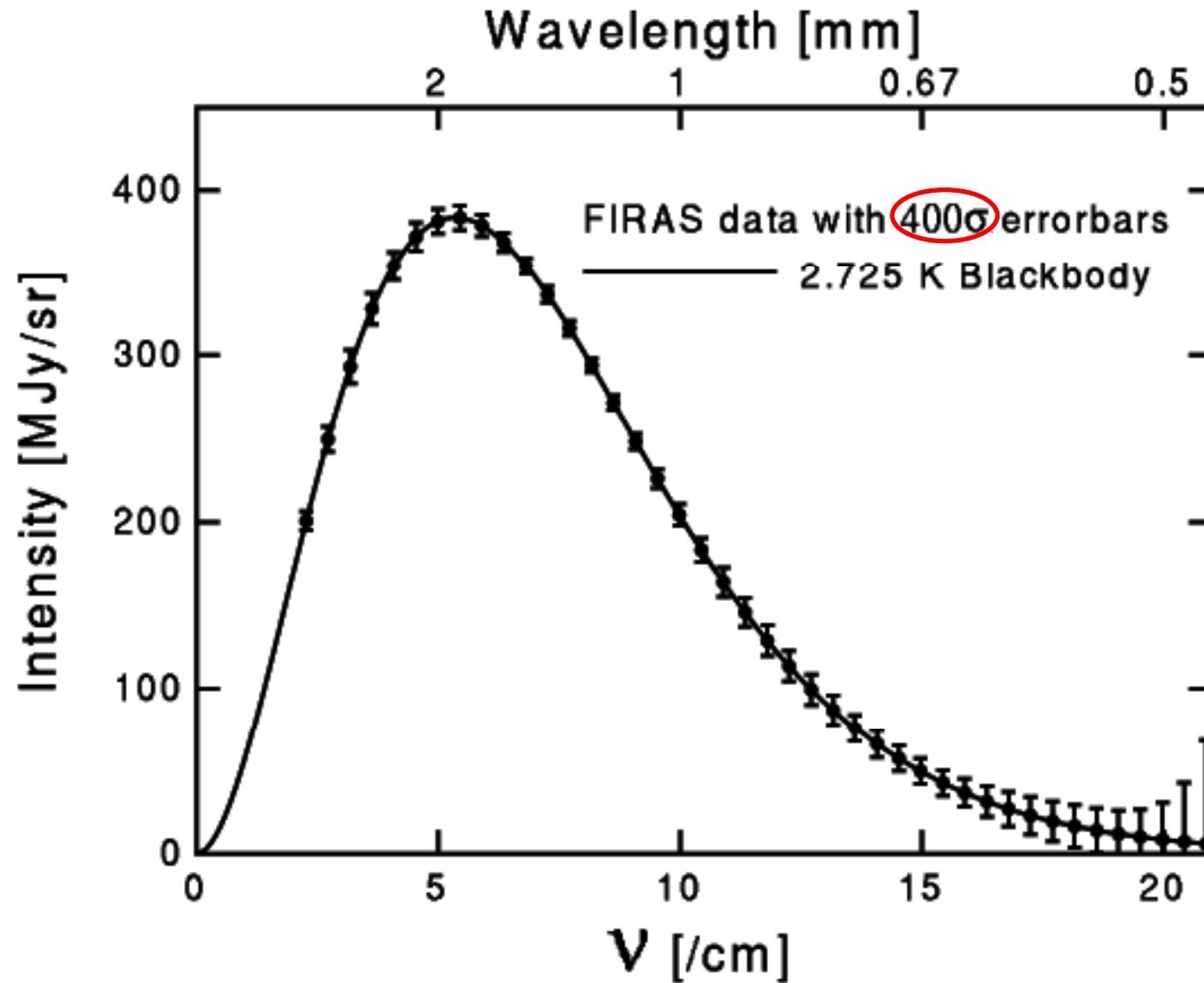
Neutral atoms do not scatter light and photons can go straight in the Universe.

The last scattering surface

When the matter turns neutral (neutralization), the Universe becomes transparent against photons. The photons scattered in the last moment of plasma era (the last scattering surface: LSS) are observed as the CMB.



Energy spectrum of the CMB



CMB power spectrum: spherical harmonics

The CMB fluctuations are usually expressed in terms of spherical harmonics:

$$\frac{\delta T}{T}(\theta, \phi) = \sum_{\ell=0}^{\infty} \sum_{-l}^{+l} a_{\ell m} Y_{\ell m}(\theta, \phi) \quad (21)$$

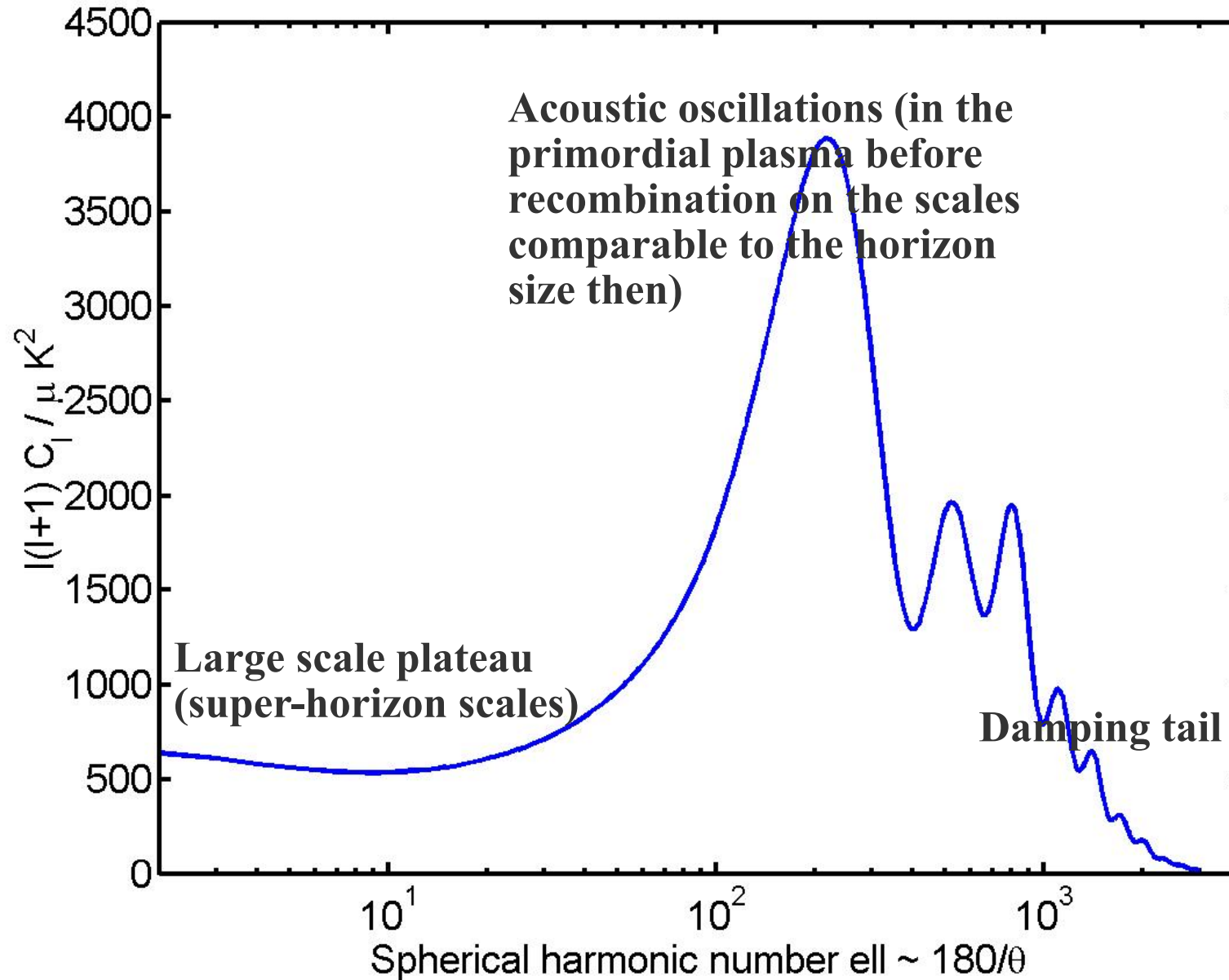
with the angular power spectrum being then defined as follows:

$$C_{\ell} = \frac{1}{2\ell + 1} \sum_m a_{\ell m} a_{\ell m}^* = \langle |a_{\ell m}|^2 \rangle \quad (22)$$

To have an intuitive idea about ℓ , it is useful to write

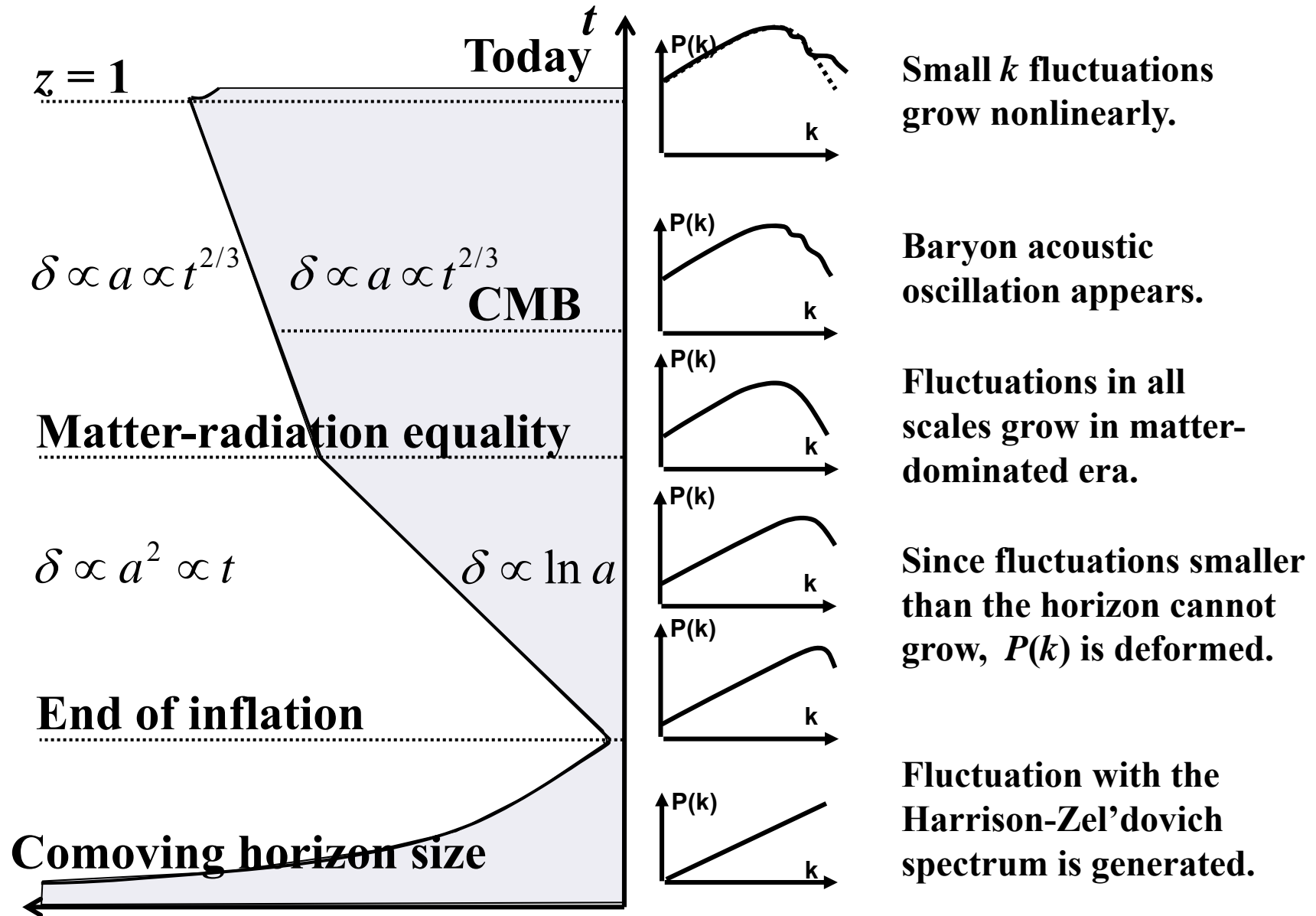
$$\ell \approx \frac{180}{\theta [\text{deg}]} \quad (23)$$

CMB power spectrum: origins of fluctuations

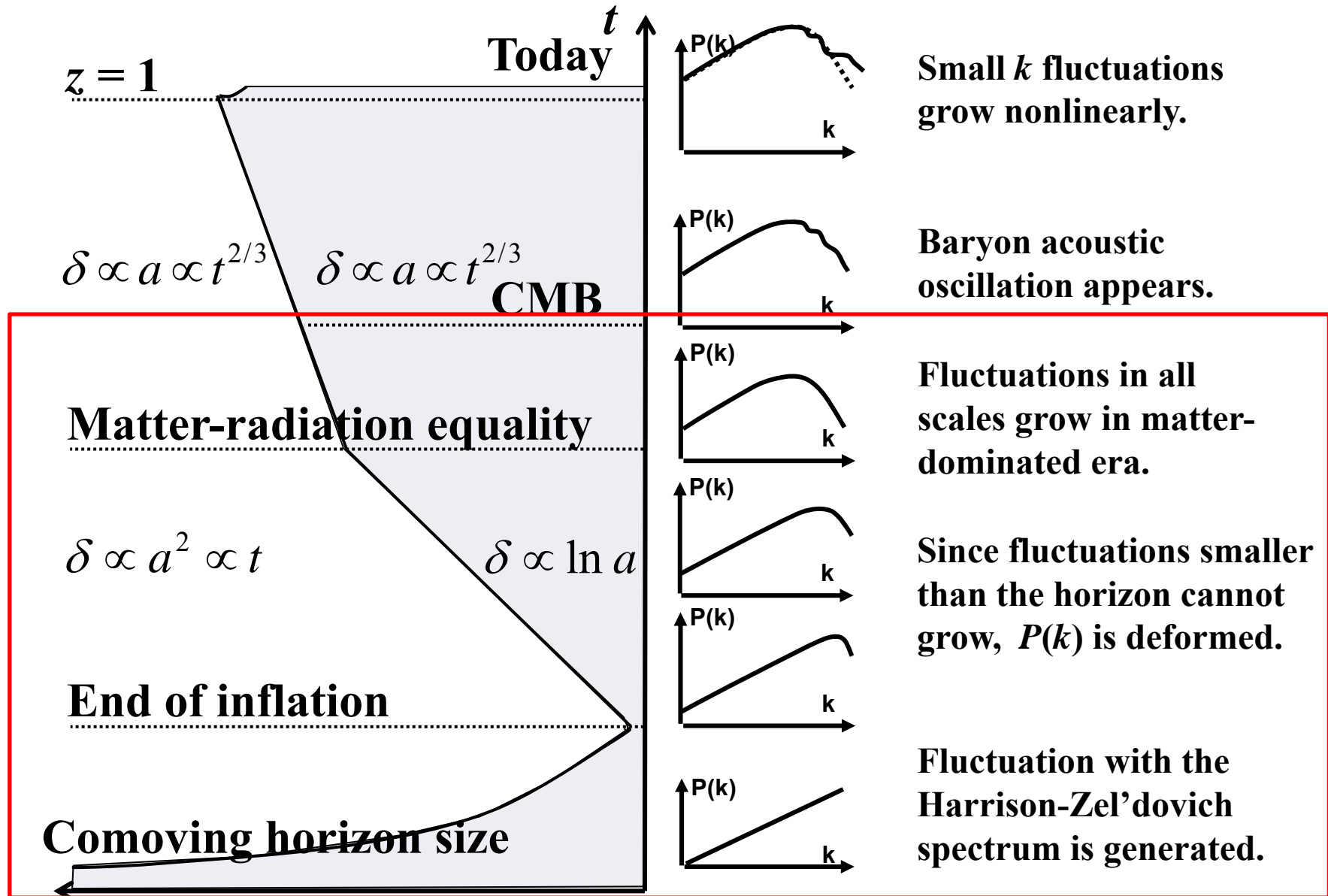


5.3 Linear theory

Schematic view of the evolution of the CDM power spectrum



Linear regime



Linear theory: Jeans mass of the cosmic structures

We first adopt **the Newtonian fluid approximation**, which is valid for slowly moving matter in a range much smaller than the horizon. Under this assumption, we have

$$\frac{\partial \rho}{\partial t} + \nabla \cdot (\rho \vec{v}) = 0 \quad (27)$$

$$\frac{\partial \vec{v}}{\partial t} + (\vec{v} \cdot \nabla) \vec{v} = -\frac{\nabla p}{\rho} - \nabla \phi \quad (28)$$

$$\nabla^2 \phi = 4\pi G \rho \quad (29)$$

Equations (1) – (3) are written in **physical** coordinates.

Linear theory: Jeans mass of the cosmic structures

We introduce **comoving coordinates** so that we treat structure formation in the expanding universe.

$$\vec{r} = a(t)\vec{x} \quad (30)$$

$$\begin{aligned} \vec{v} &= \frac{d\vec{r}}{dt} = \dot{\vec{r}} = \dot{a}\vec{x} + a\dot{\vec{x}} = H(t)a\vec{x} + a\dot{\vec{x}} \\ &\equiv H\vec{r} + \vec{u} \end{aligned} \quad (31)$$

Here \vec{u} is a peculiar velocity.

Further, we obtain for the differential operators:

$$\left(\frac{\partial}{\partial t}\right)_r = \left(\frac{\partial}{\partial t}\right)_x - \frac{\dot{a}}{a}\vec{x} \cdot \nabla_x \quad (32)$$

$$\nabla_r = \frac{1}{a}\nabla_x \quad (33)$$

Hereafter, we drop the subscript x .

Linear theory: Jeans mass of the cosmic structures

By changing the coordinates from physical to comoving, we have the continuity equation [eq. (27)]

$$\frac{\partial \rho}{\partial t} + 3H\rho + \frac{1}{a} \nabla \cdot (\rho \vec{u}) = 0 \quad (34)$$

and Euler equation [eq. (28)]

$$\frac{\partial \vec{u}}{\partial t} + H\vec{u} + \frac{1}{a} (\vec{u} \cdot \nabla) \vec{u} = -\frac{1}{a\rho} \nabla p - \frac{1}{a} \nabla \phi - \ddot{a}\vec{x} \quad (35)$$

By defining a new potential

$$\Phi \equiv \phi + \frac{a\ddot{a}\vec{x}}{2} \quad (36)$$

we have

$$\frac{\partial \vec{u}}{\partial t} + H\vec{u} + \frac{1}{a} (\vec{u} \cdot \nabla) \vec{u} = -\frac{1}{a\rho} \nabla p - \frac{1}{a} \nabla \Phi \quad (37)$$

Derivation of eq. (34)

$$\begin{aligned}
 & \frac{\partial \rho}{\partial t} - \frac{\dot{a}}{a} \vec{x} \cdot \nabla \rho + \frac{1}{a} \nabla \cdot (\rho \vec{v}) \\
 &= \frac{\partial \rho}{\partial t} - \frac{\dot{a}}{a} \vec{x} \cdot \nabla \rho + \frac{1}{a} \nabla \rho \cdot \vec{v} + \frac{1}{a} \rho \nabla \cdot \vec{v} \\
 &= \frac{\partial \rho}{\partial t} - \frac{\dot{a}}{a} \vec{x} \cdot \nabla \rho + \frac{1}{a} \nabla \rho \cdot (\dot{a} \vec{x} + a \dot{\vec{x}}) + \frac{1}{a} \rho \nabla \cdot (\dot{a} \vec{x} + a \dot{\vec{x}}) \\
 &= \frac{\partial \rho}{\partial t} - \frac{\dot{a}}{a} \vec{x} \cdot \nabla \rho + \frac{\dot{a}}{a} \vec{x} \cdot \nabla \rho + \dot{\vec{x}} \cdot \nabla \rho + \frac{\dot{a}}{a} \rho \nabla \cdot \vec{x} + \rho \nabla \cdot \dot{\vec{x}} \\
 &= \frac{\partial \rho}{\partial t} + \dot{\vec{x}} \cdot \nabla \rho + \underbrace{\left(\frac{\dot{a}}{a} \right)}_H \underbrace{\rho \nabla \cdot \vec{x}}_3 + \rho \nabla \cdot \dot{\vec{x}} \\
 &= \frac{\partial \rho}{\partial t} + 3H\rho + \nabla \cdot (\rho \dot{\vec{x}}) \\
 &= \frac{\partial \rho}{\partial t} + 3H\rho + \frac{1}{a} \nabla \cdot (\rho \vec{u})
 \end{aligned}$$

Derivation of eq. (35)

$$\begin{aligned}
 \frac{\partial \vec{v}}{\partial t} - \frac{\dot{a}}{a} (\vec{x} \cdot \nabla) \vec{v} + \frac{1}{a} (\vec{v} \cdot \nabla) \vec{v} &= -\frac{1}{a\rho} \nabla p - \frac{1}{a} \nabla \phi \\
 &= \frac{\partial}{\partial t} (\dot{a}\vec{x} + a\dot{\vec{x}}) - \frac{\dot{a}}{a} (\vec{x} \cdot \nabla) (\dot{a}\vec{x} + a\dot{\vec{x}}) + \frac{1}{a} [(\dot{a}\vec{x} + a\dot{\vec{x}}) \cdot \nabla] (\dot{a}\vec{x} + a\dot{\vec{x}}) \\
 &= \frac{\partial}{\partial t} (\dot{a}\vec{x}) + \frac{\partial}{\partial t} (a\dot{\vec{x}}) - \frac{\dot{a}}{a} (\vec{x} \cdot \nabla) (\dot{a}\vec{x} + a\dot{\vec{x}}) + \frac{\dot{a}}{a} (\vec{x} \cdot \nabla) (\dot{a}\vec{x} + a\dot{\vec{x}}) + (\dot{\vec{x}} \cdot \nabla) (\dot{a}\vec{x} + a\dot{\vec{x}}) \\
 &= \frac{\partial}{\partial t} (\dot{a}\vec{x}) + \frac{\partial \vec{u}}{\partial t} + (\dot{\vec{x}} \cdot \nabla) (\dot{a}\vec{x} + \vec{u}) \\
 &= \dot{\ddot{a}\vec{x}} + \frac{\partial \vec{u}}{\partial t} + \left(\frac{\vec{u}}{a} \cdot \nabla \right) (\dot{a}\vec{x} + \vec{u}) \\
 &= \ddot{a}\vec{x} + \frac{\partial \vec{u}}{\partial t} + H(\vec{u} \cdot \nabla) \vec{x} + \frac{1}{a} (\vec{u} \cdot \nabla) \vec{u} \\
 &= \ddot{a}\vec{x} + \frac{\partial \vec{u}}{\partial t} + H\vec{u} + \frac{1}{a} (\vec{u} \cdot \nabla) \vec{u}
 \end{aligned}$$

Since this is not d/dt , it does not make terms with $\dot{\vec{x}}$.

Linear theory: Jeans mass of the cosmic structures

The Poisson equation [eq. (29)] leads

$$\nabla^2 \phi = 4\pi G a^2 \rho \quad (38)$$

From the Friedmann equation [eq. (5)], we have

$$3a\ddot{a} = (\nabla \cdot \vec{x})a\ddot{a} = \left(\nabla^2 \frac{x^2}{2} \right) a\ddot{a} = -4\pi G \bar{\rho} \quad (39)$$

Then, we obtain

$$\nabla^2 \Phi = 4\pi G a^2 (\rho - \bar{\rho}) \quad (40)$$

The solution of this equation is

$$\Phi = -G a^2 \int d^3 x' \frac{\rho - \bar{\rho}}{|\vec{x}' - \vec{x}|} \quad (41)$$

Linear theory: Jeans mass of the cosmic structures

Consider a small fluctuation from the background universe:

$$\begin{aligned}\rho_b &= \bar{\rho}(t) \\ \vec{u} &= \vec{0}, \nabla\Phi = \vec{0}, \nabla p = \vec{0}\end{aligned}\tag{42}$$

We introduce fluctuations from the homogeneous background as

$$\delta(\vec{x}, t) = \frac{\rho(\vec{x}, t) - \bar{\rho}(t)}{\bar{\rho}(t)},\tag{13}$$

$$\delta p(\vec{x}, t) \equiv p(\vec{x}, t) - \bar{p}(t)\tag{43}$$

Thus, from eq. (40) we have

$$\nabla^2\Phi = 4\pi G a^2 \bar{\rho} \delta\tag{44}$$

Linear theory: Jeans mass of the cosmic structures

The continuity equation [eq. (34)] leads

$$\frac{\partial}{\partial t} [\bar{\rho}(1 + \delta)] + 3H\bar{\rho}(1 + \delta) + \frac{\bar{\rho}}{a} \nabla \cdot [(1 + \delta)\vec{u}] = 0 \quad (45)$$

Here we should note that

$$\frac{\partial \bar{\rho}}{\partial t} + 3H\bar{\rho} = 0 \quad \left(\because \frac{\partial}{\partial t} [a^3 \bar{\rho}(t)] = 0 \right) \quad (46)$$

From eqs. (45) and (46)

$$\begin{aligned} & \frac{\partial(\bar{\rho}\delta)}{\partial t} + 3H\bar{\rho}\delta + \frac{\bar{\rho}}{a} \nabla \cdot [(1 + \delta)\vec{u}] \\ &= \left(\frac{\partial \bar{\rho}}{\partial t} + 3H\bar{\rho} \right) \delta + \bar{\rho} \frac{\partial \delta}{\partial t} + \frac{\bar{\rho}}{a} \nabla \cdot [(1 + \delta)\vec{u}] = 0 \end{aligned} \quad (47)$$

Linear theory: Jeans mass of the cosmic structures

Thus, the continuity equation [eq. (34)] becomes

$$\frac{\partial \delta}{\partial t} + \frac{1}{a} \nabla \cdot [(1 + \delta) \vec{u}] = 0 \quad (48)$$

and the Euler equation [eq. (36)]

$$\frac{\partial \vec{u}}{\partial t} + H \vec{u} + \frac{1}{a} (\vec{u} \cdot \nabla) \vec{u} = - \frac{\nabla(\delta p)}{a \bar{\rho} (1 + \delta)} - \frac{1}{a} \nabla \Phi \quad (49)$$

Equations (44), (48), and (49) are the startpoint to derive the solutions which describe the linear growth of fluctuations.

Linear theory: Jeans mass of the cosmic structures

Here, we neglect terms including multiplications of δ , δp , and \vec{u} since they are small (**linearization**).

Then the continuity equation [eq. (34)] and the Euler equation now read

$$\frac{\partial \delta}{\partial t} + \frac{1}{a} \nabla \cdot \vec{u} = 0 \quad (50)$$

$$\frac{\partial \vec{u}}{\partial t} + H\vec{u} + \frac{1}{a} \nabla \Phi + \frac{\nabla(\delta p)}{a\bar{\rho}} = 0 \quad (51)$$

Then, manipulating eqs. (50) and (51) gives

$$\frac{\partial}{\partial t} [\text{eq. (50)}] = \frac{\partial^2 \delta}{\partial t^2} + \frac{1}{a} \left(\nabla \cdot \frac{\partial \vec{u}}{\partial t} \right) - \frac{\dot{a}}{a} \nabla \cdot \vec{u} = 0 \quad (52)$$

$$\nabla \cdot [\text{eq. (51)}] = \nabla \cdot \frac{\partial \vec{u}}{\partial t} + H \nabla \cdot \vec{u} + \frac{1}{a} \nabla^2 \Phi + \frac{1}{a\bar{\rho}} \nabla^2 (\delta p) = 0 \quad (53)$$

Linear theory: Jeans mass of the cosmic structures

Performing an algebra eq. (52) – eq. (51)/ a gives

$$\begin{aligned} & \frac{\partial^2 \delta}{\partial t^2} + 2 \frac{\dot{a}}{a^2} (\nabla \cdot \vec{u}) - 4\pi G \bar{\rho} \delta - \frac{\nabla^2(\delta p)}{a^2 \bar{\rho}} \\ & = \frac{\partial^2 \delta}{\partial t^2} + 2H \frac{\partial \delta}{\partial t} - \left[4\pi G \bar{\rho} \delta + \frac{\nabla^2(\delta p)}{a^2 \bar{\rho}} \right] = 0 \end{aligned} \quad (54)$$

Consider the sound velocity of the fluid

$$c_s = \sqrt{\left. \frac{\partial p}{\partial \rho} \right|_S} \quad (55)$$

Here S is the entropy. Suppose that the entropy fluctuation is small, we have

$$\delta p = c_s \bar{\rho} \delta \quad (56)$$

Linear theory: Jeans mass of the cosmic structures

Since the basic equations are linear, we can deal with **Fourier components for each k** . Consider

$$\delta(\vec{x}) = \sum_k \delta_k e^{i\vec{k}\cdot\vec{x}} \quad (57)$$

Then,

$$\begin{aligned} & \frac{\partial^2 \delta_k}{\partial t^2} + 2H \frac{\partial \delta_k}{\partial t} - \left[4\pi G \bar{\rho} \delta_k - \frac{c_s^2 \bar{\rho} k^2 \delta_k}{a^2 \bar{\rho}} \right] \\ &= \frac{\partial^2 \delta_k}{\partial t^2} + 2H \frac{\partial \delta_k}{\partial t} - \left[4\pi G \bar{\rho} - \frac{c_s^2 k^2}{a^2} \right] \delta_k = 0 \end{aligned} \quad (58)$$

Linear theory: Jeans mass of the cosmic structures

The third term in \square controls the evolution of fluctuation.

1. $\square < 0$

Fluctuations oscillate and decay. This happens when c_s is large. This also happens when k is large (small scale) because the fluctuation does not contain enough mass to contract gravitationally.

2. $\square > 0$

Fluctuations grow.

Linear theory: Jeans mass of the cosmic structures

Here we define k_J so that

$$\frac{c_s^2 k_J^2}{a^2} = 4\pi G \bar{\rho} \quad (59)$$

then we can also define **the Jeans length λ_J** :

$$\lambda_J = \frac{2\pi a}{k_J} = c_s \sqrt{\frac{\pi}{G \bar{\rho}}} \quad (60)$$

Fluctuation smaller than λ_J decay, while ones larger than λ_J can grow by gravitational instability.

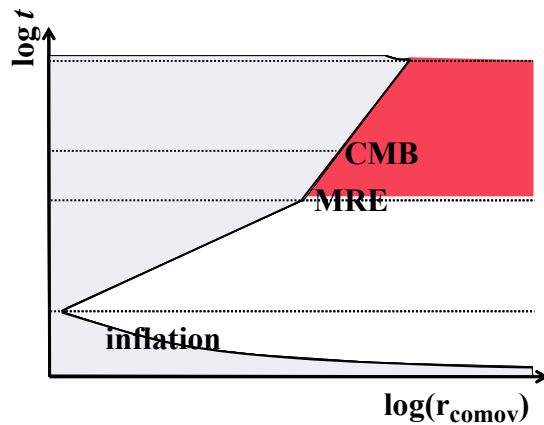
$$M_J = \frac{4\pi}{3} \bar{\rho} \left(\frac{\lambda_J}{2} \right)^3 \quad (61)$$

is referred to **as the Jeans mass.**

Linear theory: superhorizon-scale (DM or baryons)

Fully relativistic treatment is required. Here we do not go deeper into the discussion.

MD



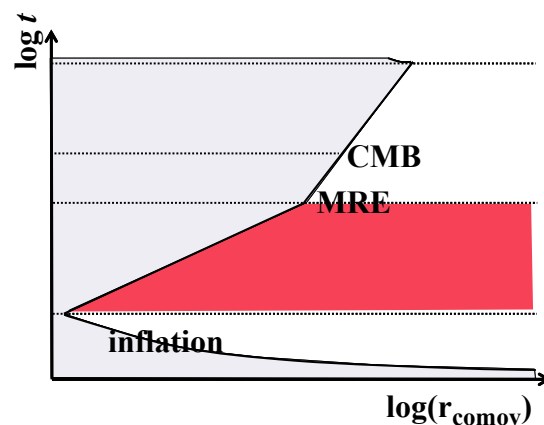
The mean density evolves as

$$\bar{\rho} \propto a^{-3}$$

hence fluctuations grow as

$$\delta_k \propto a$$

RD



The mean density evolves as

$$\bar{\rho} \propto a^{-4}$$

hence fluctuations grow as

$$\delta_k \propto a^2$$

Linear theory: growth of fluctuations for DM I

The evolution of the Universe is governed by the energy density through eqs. (4) and (5). In the early Universe, radiation dominates the energy density (**radiation-dominated: RD**), while later matter dominates (**matter-dominated: MD**).

Consider the evolution of fluctuations of DM. DM is thought to be **pressureless**. Then, eq. (54) or (58) becomes (since they are linear, real or Fourier space treatment does not differ)

$$\frac{\partial^2 \delta}{\partial t^2} + 2H \frac{\partial \delta}{\partial t} - 4\pi G \bar{\rho} \delta = 0 \quad (62)$$

In the Einstein-de Sitter universe, $a \propto t^{2/3}$. Then,

$$\frac{\partial^2 \delta}{\partial t^2} + \frac{4}{3t} \frac{\partial \delta}{\partial t} - \frac{2}{3t^2} \delta = 0 \quad (63)$$

Linear theory: growth of fluctuations for DM I

Assume a solution with the form

$$\delta = A_+(x)D_+(t) + A_-(x)D_-(t) \quad (64)$$

Then, eq. (63) is solved with a general solution

$$\delta = A_+(x)t^{2/3} + A_-(x)t^{-1} \quad (65)$$

The second term is **a decaying mode** and can be neglected at larger t . Then,

$$\delta = A_+(x)t^{2/3} \propto a \quad (66)$$

Defining the growth factor $D(t)$, eq. (66) is also expressed as

$$D(t) \propto a(t) \propto t^{2/3} \quad (67)$$

Linear theory: growth of fluctuations for DM II (stagspansion)

As outlined above, during the RD era, the DM fluctuations are suppressed within the horizon size (**stagspansion**).

$$\frac{\partial^2 \delta_M}{\partial t^2} + 2H \frac{\partial \delta_M}{\partial t} - 4\pi G \bar{\rho} \delta_M = 0 \quad (68)$$

$$H^2 = \frac{8\pi G}{3} (\bar{\rho}_M + \bar{\rho}_R) \quad (69)$$

Here subscript M and R denotes matter and radiation. We also define

$$\zeta \equiv \frac{\bar{\rho}_M}{\bar{\rho}_R} = \frac{a}{a_{\text{eq}}} \quad (70)$$

(a_{eq} : scale factor at the matter-radiation equality). Then we have

$$\frac{\partial^2 \delta_M}{\partial \zeta^2} + \frac{2+3\zeta}{2\zeta(1+\zeta)} \frac{\partial \delta_M}{\partial \zeta} - \frac{3\delta_M}{2\zeta(1+\zeta)} = 0 \quad (71)$$

Linear theory: growth of fluctuations for DM II (stagspansion)

By assuming

$$\frac{d^2 \delta_M}{d\zeta^2} = 0 \quad (72)$$

we find a solution of the form

$$\delta_M \propto 1 + \frac{3}{2} \zeta \quad (73)$$

MD: $\zeta \gg 1$

$$\delta_M \propto a \quad (74)$$

RD: $\zeta \ll 1$

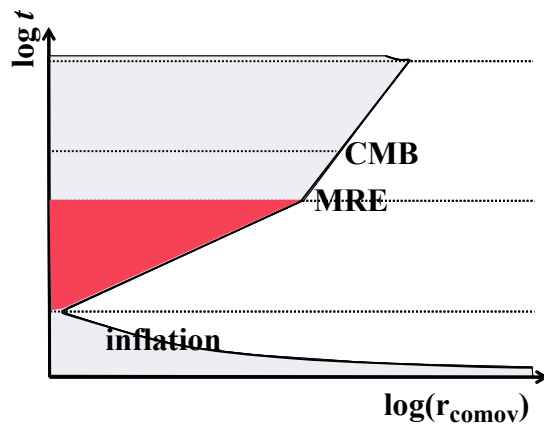
$$\delta_M \propto \text{constant} \quad (75)$$

(more precisely, $\delta_M \propto \ln a$).

Thus, we could see quantitatively the effect of stagspansion.

Linear theory: subhorizon-scale (DM, radiation-dominated)

Jeans analysis can be applied. Dark matter is pressureless, but during the period in which DM particles couple with photons, radiation pressure works as the effective pressure of DM. Then subhorizon-size fluctuations cannot grow.



The mean density evolves as

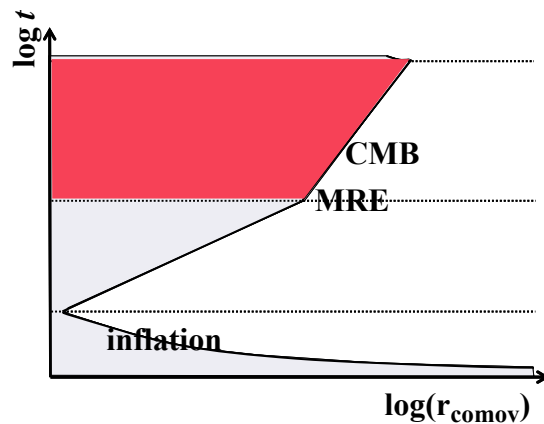
$$\bar{\rho} \propto a^{-4}$$

Fluctuations grow as

$$\delta_k \propto \ln a$$

Linear theory: subhorizon-scale (DM, matter-dominated)

Dark matter becomes decoupled from radiation, and subhorizon-size fluctuations start to grow. At early epoch, the Universe can be approximated as Einstein-de Sitter.



The mean density evolves as

$$\bar{\rho} \propto a^{-3}, \quad a \propto t^{2/3}$$

The Jeans equation has a general solution:

$$\delta_k = At^{2/3} + Bt^{-1}$$

Growing mode

Decaying mode

Since the decaying mode becomes negligible along with the evolution, we have

$$\delta_k \propto a$$

Linear theory: growth of fluctuations for baryons

For baryon fluctuations, gravitational potentials are made by DM:

$$\frac{\partial^2 \delta_B}{\partial t^2} + 2H \frac{\partial \delta_B}{\partial t} - 4\pi G \bar{\rho}_M \delta_M = 0 \quad (76)$$

where subscript **B** denotes baryons. If we define $\eta \equiv \frac{a}{a_{\text{rec}}}$,

$$\delta_M \propto \eta \quad (77)$$

Then we have

$$\eta^{1/2} \frac{d}{d\eta} \left(\eta^{3/2} \frac{d\delta_B}{d\eta} \right) = \frac{3}{2} \delta_M \quad (78)$$

The solution is

$$\delta_B = \left(1 - \frac{1}{\eta} \right) \delta_M \quad (79)$$

Linear theory: growth of fluctuations for baryons

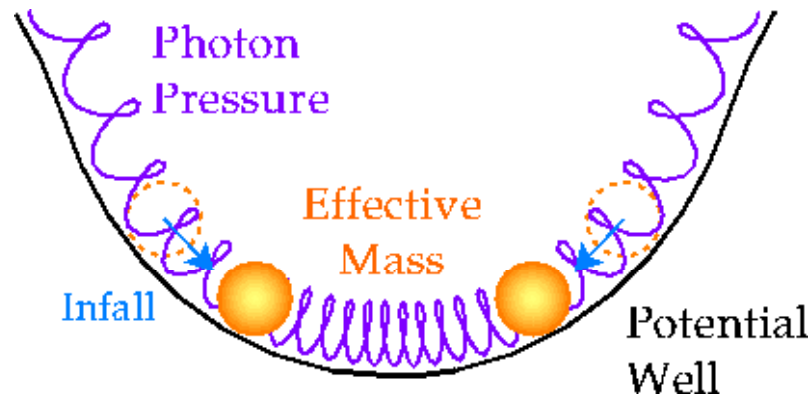
This solution means that

$$\begin{aligned} a \approx a_{\text{dec}} &\Leftrightarrow \eta = 1 & : & \delta_{\text{B}} \approx 0 \\ a \gg a_{\text{dec}} &\Leftrightarrow \eta \gg 1 & : & \delta_{\text{B}} \approx \delta_{\text{M}} \end{aligned} \tag{80}$$

This means that just after the decoupling, there is no fluctuation in baryons, but later ($\eta \gg 1$), they have the same fluctuation as DM. This is called **catch-up**.

Linear theory: baryon acoustic oscillation

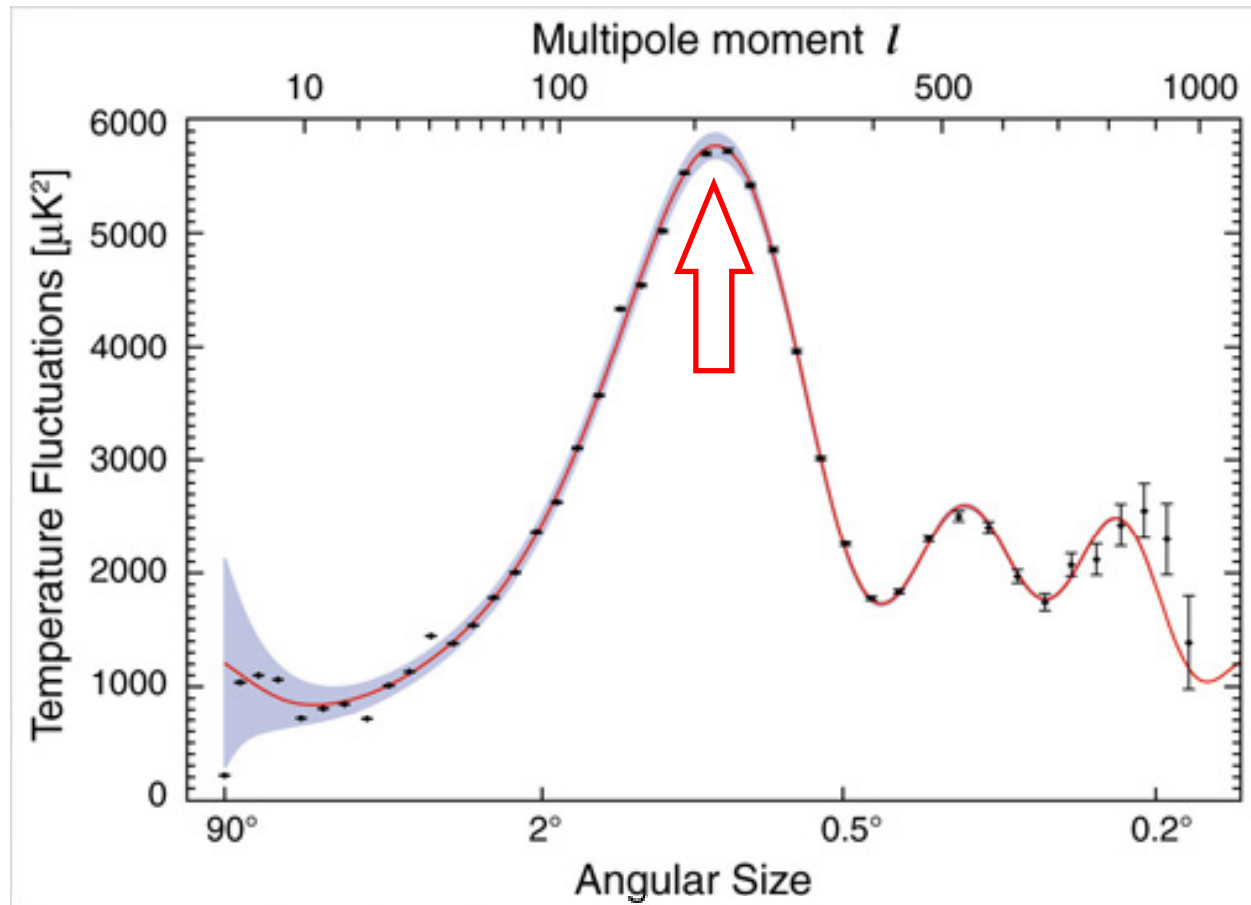
Before decoupling, radiation pressure from the photons resists the gravitational compression of the baryon fluid into potential wells and sets up **acoustic oscillations** in the fluid



Springs represent photon pressure and balls represent the effective mass of the fluid.

The shorter the wavelength of the potential fluctuation, the faster the fluid oscillates such that at last scattering the phase of the oscillation reached scales with the wavelength. Since compressed regions (maxima) represent hot regions and expanding regions (minima) cold regions, there will be a harmonic series of peaks in wavelength associated with the acoustic oscillations.

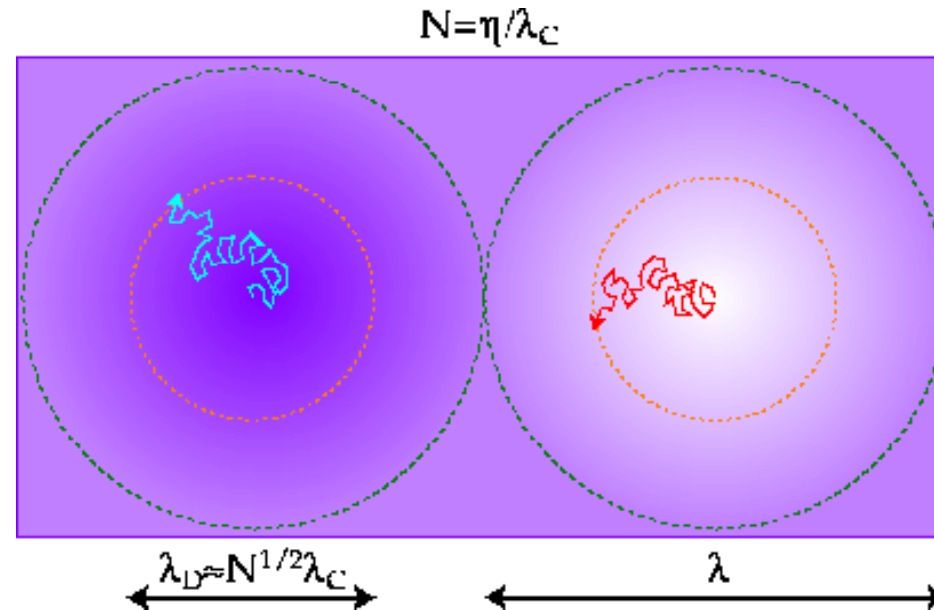
Linear theory: baryon acoustic oscillation



The strongest and the most important structures in the CMB spectrum result from the acoustic oscillation.

Linear theory: Silk damping (diffusion damping)

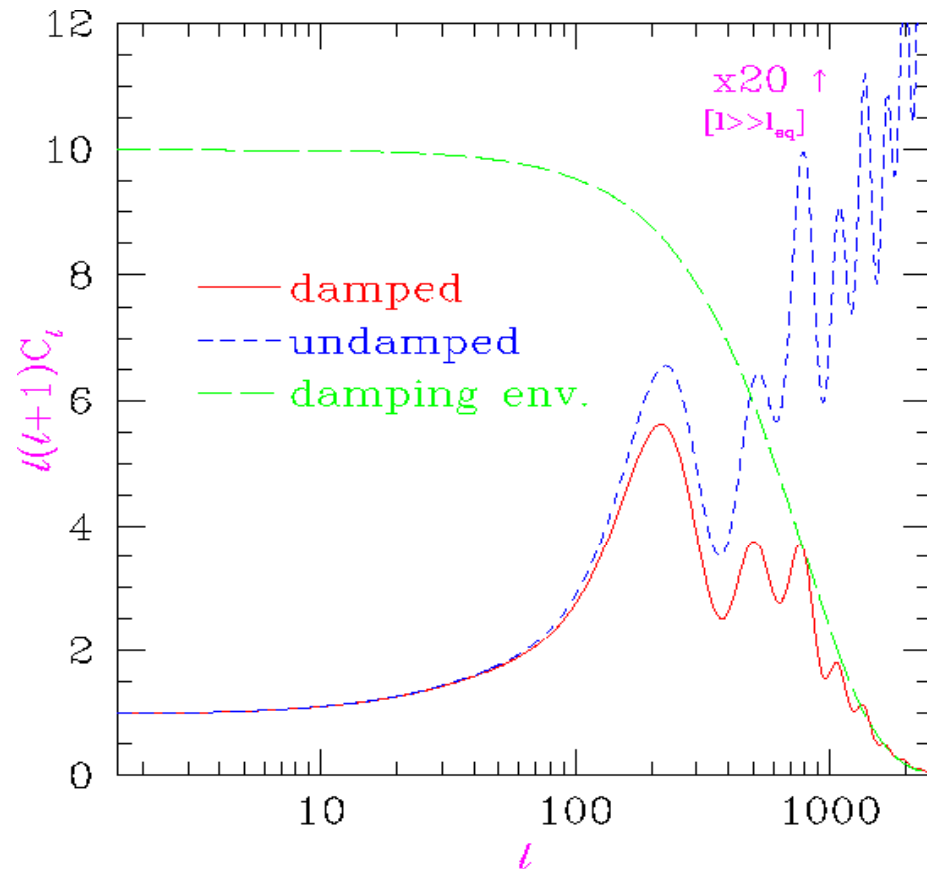
In reality, the coupling between baryons (electrons) and photons is imperfect since the photons possess a mean free path to **Compton scattering**.



As the photons random walk through the baryons, hot and cold regions are mixed. Fluctuations damp nearly exponentially as the diffusion length overtakes the wavelength. This is called **Silk damping**.

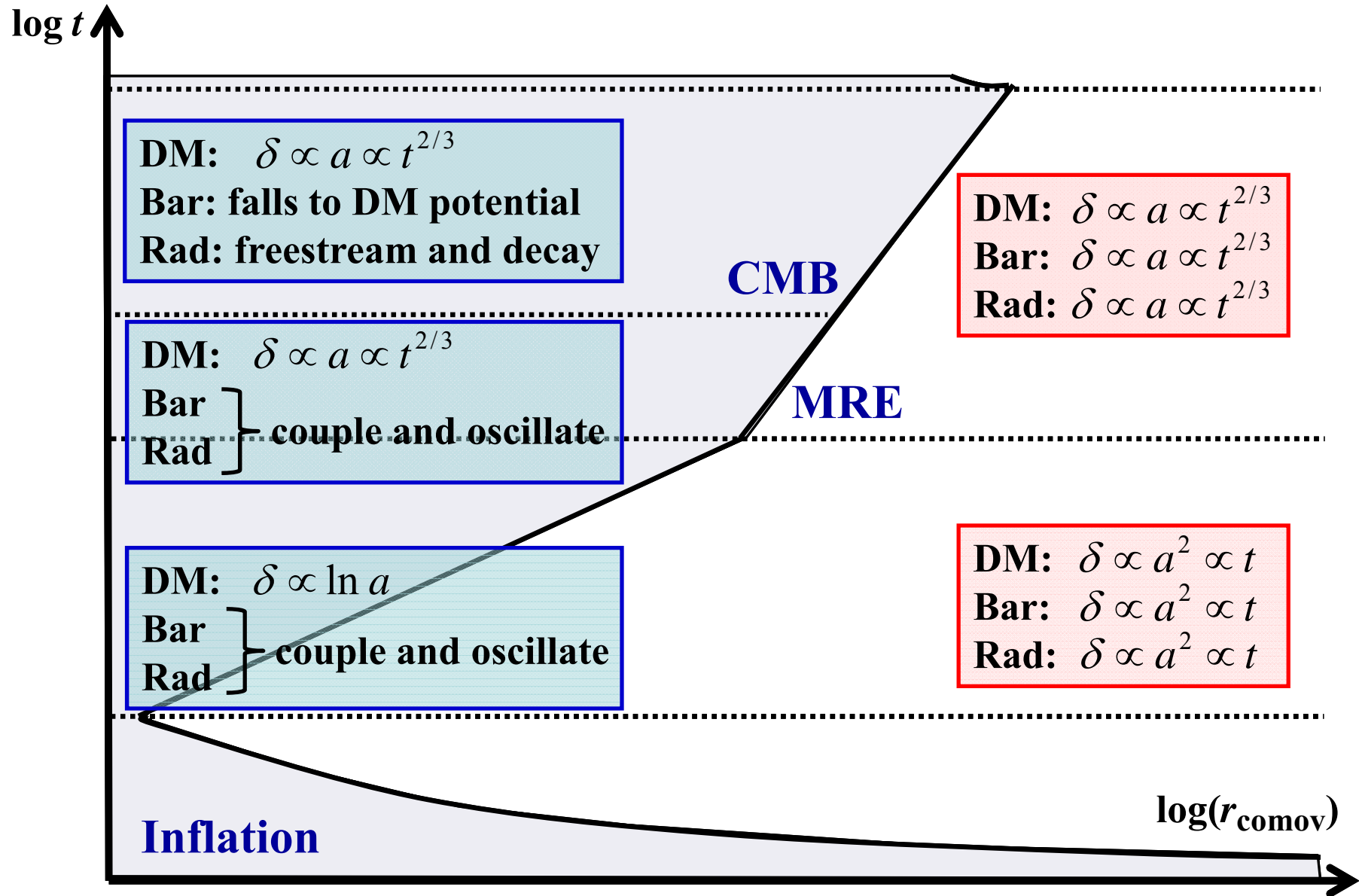
Linear theory: Silk damping (diffusion damping)

At last scattering, the ionization fraction decreases due to recombination, thus increasing the mean free path of the photons. The effective diffusion scale becomes the thickness of the last scattering surface providing a cut off in the anisotropy spectrum.

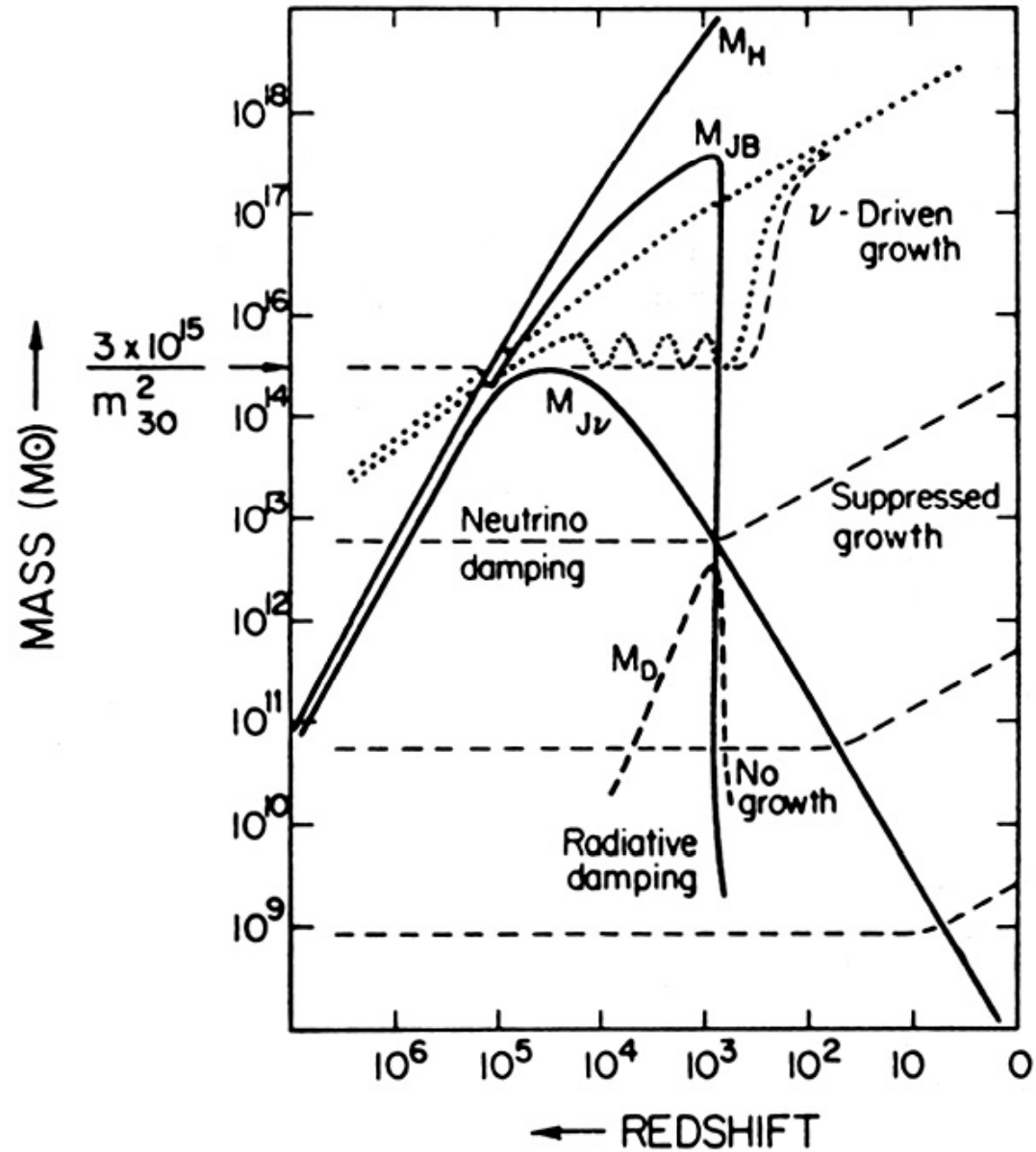


Hu & White (1997)

Linear theory: summary of the growth of baryon perturbations



Linear theory: schematic summary of fluctuation growth



6. Structure Formation II

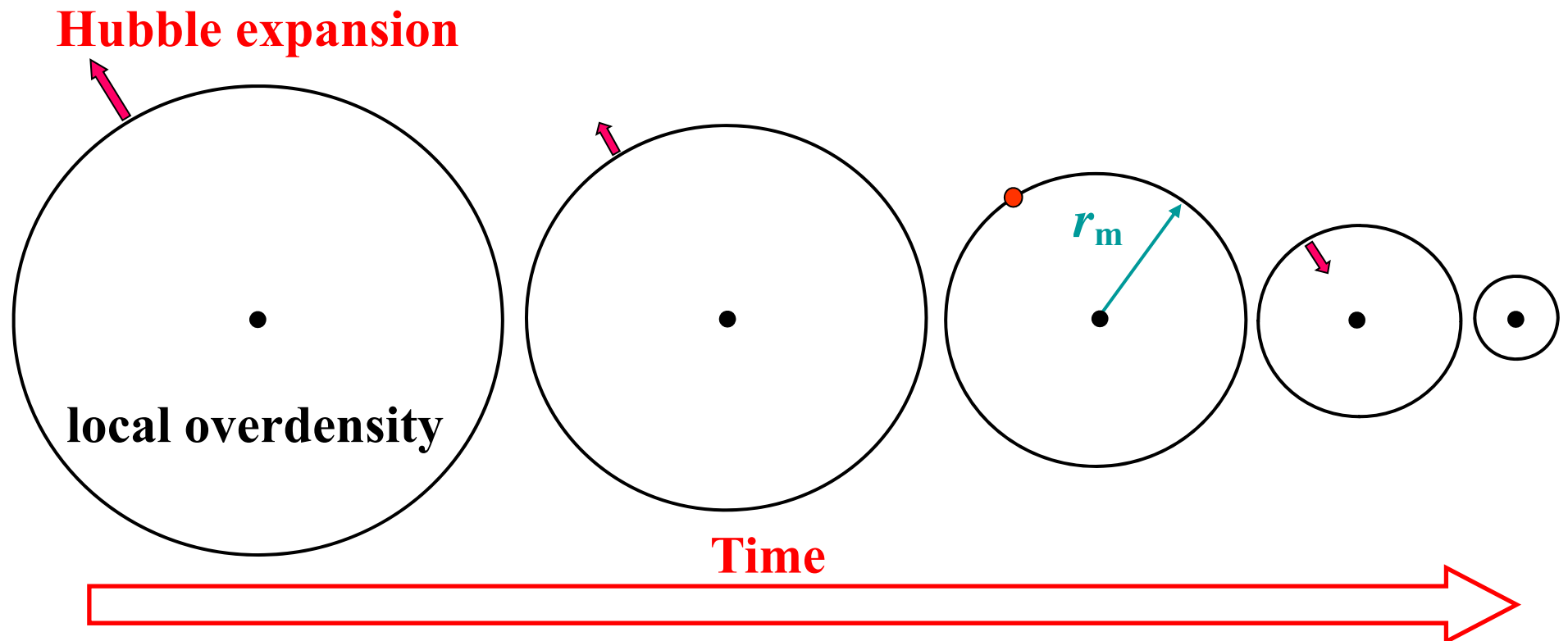
6.1 Nonlinear theory: Press-Schechter formalism

6.2 Bias

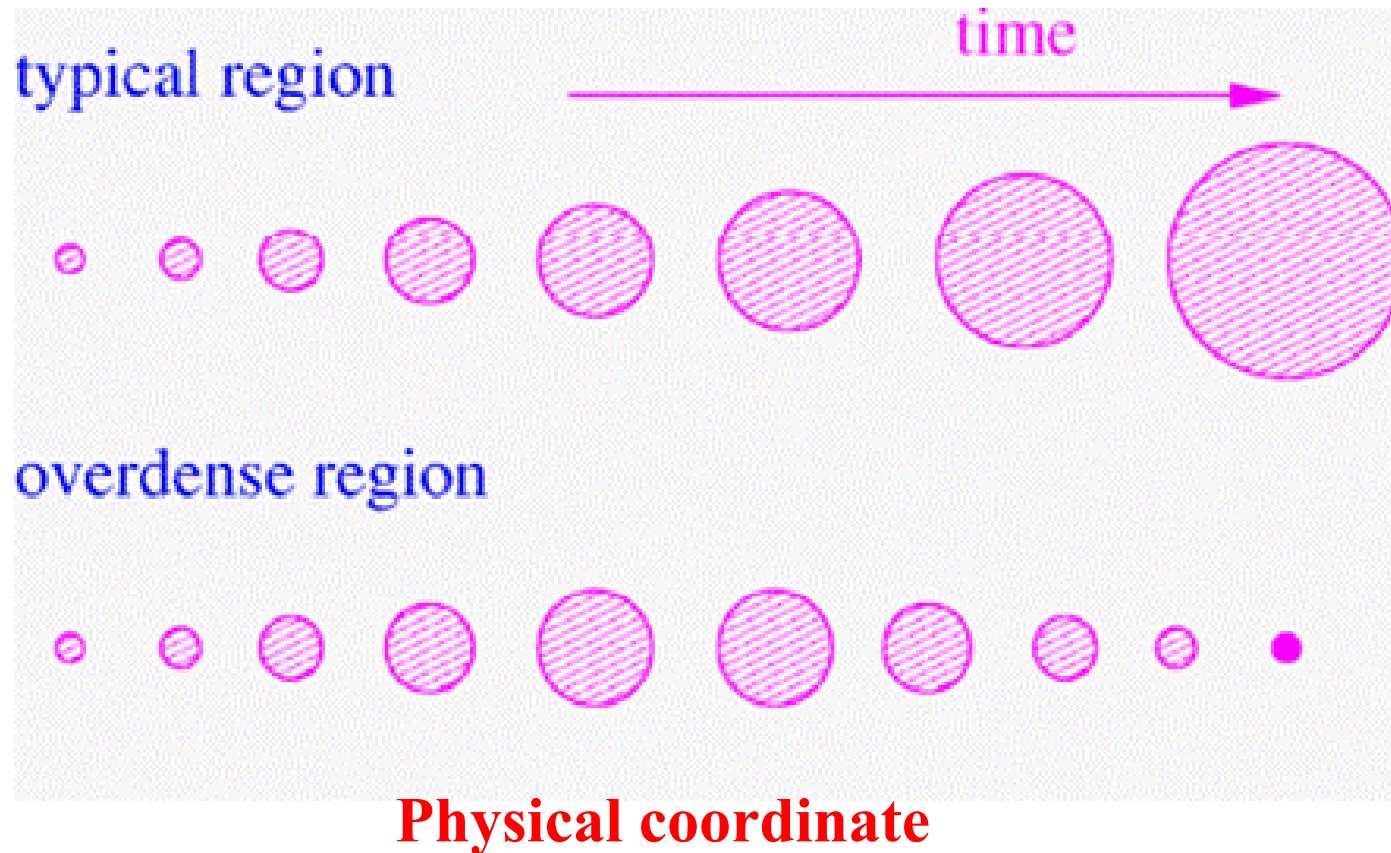
6.1 Nonlinear theory: Press-Schechter formalism

Spherical collapse model: concept

In **comoving** coordinates a sphere, centered on a local overdensity shrinks in time; Hubble expansion is getting retarded by the overdensity. At some point, the sphere's expansion stops (turn-around), and the sphere starts to collapse.

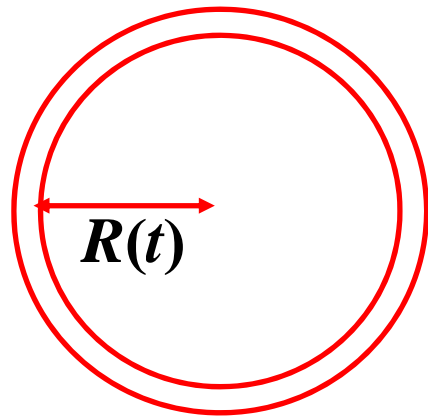


Spherical collapse model: concept



Spherical collapse model

Consider the evolution of a spherical overdensity region as a simple model of the nonlinear evolution of fluctuation. (Tomita 1969; Gunn & Gott 1972).

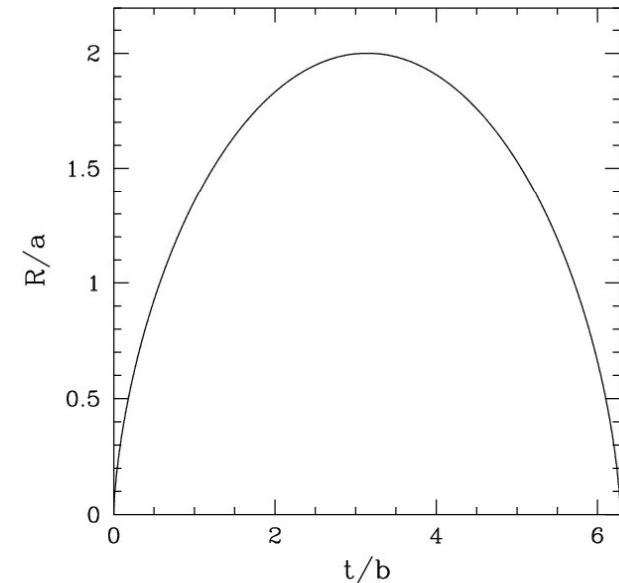


$$\frac{d^2R}{dt^2} = -\frac{GM}{R^2} \quad \Rightarrow \quad \left(\frac{dR}{dt}\right)^2 = \frac{2GM}{R} + 2E$$

“Energy” $E < 0$: bounded

$$\begin{cases} R = C^2(1 - \cos\theta) \\ t = \frac{C^3}{\sqrt{GM}}(\theta - \sin\theta) \end{cases}$$

C : integration constant, corresponding to the size of the shell. This curve is called “cycloid”.

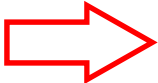


N.B. “Energy” $E > 0$: unbounded. Corresponding to voids.

Spherical collapse model

Densities of overdense and average regions are

$$\rho = M \left(\frac{4\pi R^3}{3} \right)^{-1} \quad \bar{\rho} = \frac{1}{6\pi G t^2}$$

 $\delta(t) = \frac{9GMt^2}{2R^3} - 1 = \frac{9}{2} \frac{(\theta - \sin\theta)^2}{(1 - \cos\theta)^3}$

$\theta = \pi$: expansion \Rightarrow contraction (turn-around)

$$R_{\text{turn}} = 2C^2 \quad t_{\text{turn}} = \frac{\pi C^3}{\sqrt{GM}}$$

$\theta = 2\pi$: collapse ($R = 0$)

$$t_{\text{coll}} = \frac{2\pi C^3}{\sqrt{GM}}$$


Spherical collapse model

In reality, $R = 0$ is not established, but the overdense region becomes **an object with R_{vir}** , via some mechanism like the violent relaxation. Suppose a mass M , then from the conservation of energy, we have

$$\frac{GM^2}{R_{\text{turn}}} = \frac{1}{2} \frac{GM^2}{R_{\text{coll}}}$$

hence

$$R_{\text{coll}} = \frac{R_{\text{turn}}}{2}$$

 $\delta_{\text{vir}} = \frac{M}{\left(\frac{4\pi R_{\text{vir}}^2}{3}\right) \bar{\rho}(t_{\text{coll}})} - 1 = 18\pi^2 - 1 \approx 177 \quad (1)$

Spherical collapse model

Correspondence with a linear regime

At early phase, the growth is the same as the linear growth. Expanding with θ , we have

$$\begin{cases} \delta = \frac{3}{20}\theta^2 + O(\theta^4) \\ t = \frac{C^3}{6\sqrt{GM}}\theta^3 + O(\theta^5) \end{cases} \quad \Rightarrow \quad \delta \propto t^{\frac{2}{3}}$$

Let it δ_L ,

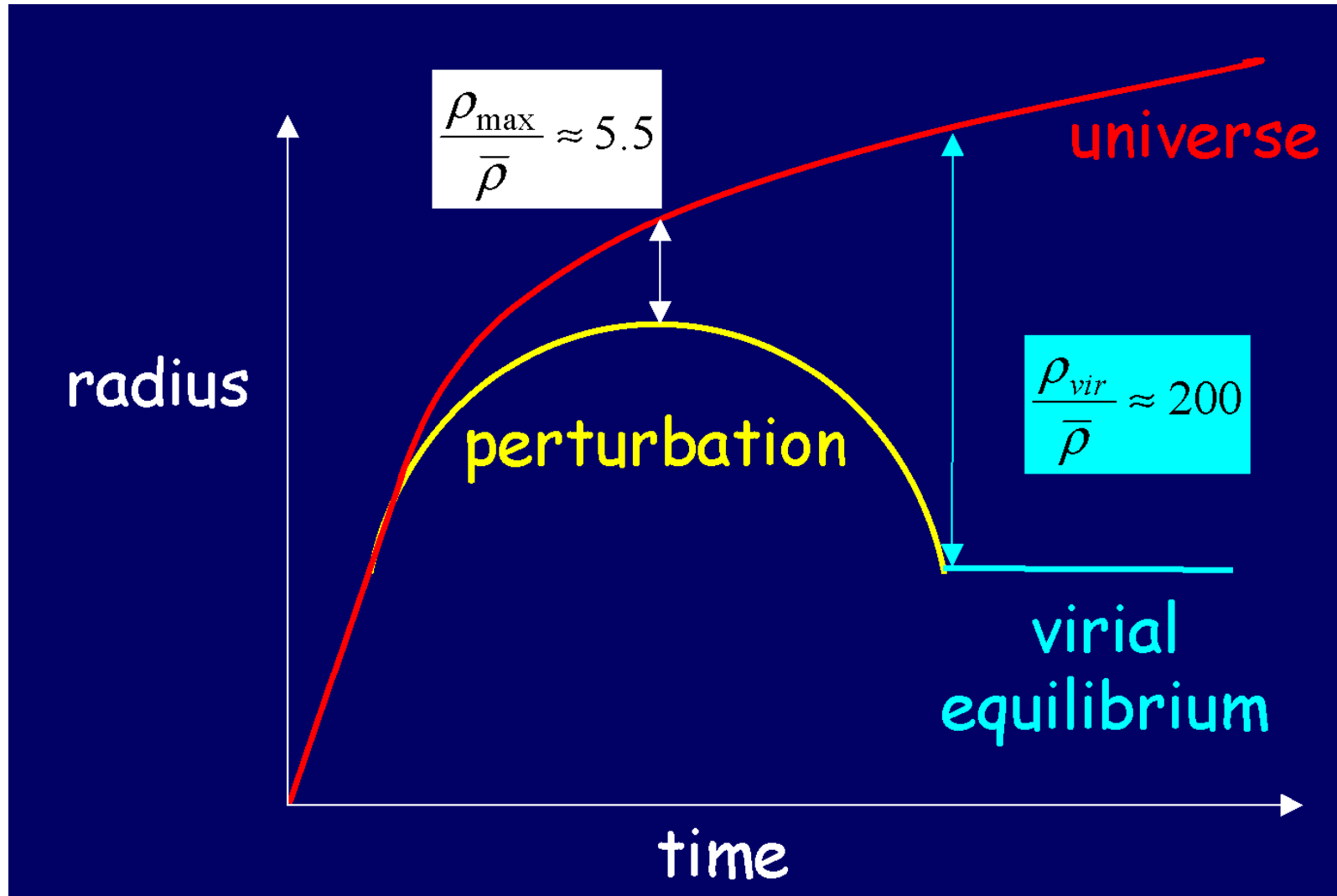
$$\delta_L = \frac{3}{20} \left(\frac{6\sqrt{GM}}{C^3} t \right)^{\frac{2}{3}}$$

Since both the nonlinear δ of spherical collapse and linear δ_L are monotonic functions of t , we can estimate the value of δ from δ_L if we have a relation between δ and δ_L .

$$\delta_L(t_{\text{coll}}) = \frac{3(12\pi)^{\frac{2}{3}}}{20} \simeq 1.69 \quad (2)$$

Thus, we regard a region with $\delta = 1.69$ as a collapsed object.

Spherical collapse model



Spherical collapse model

Above discussion was based on the Einstein-de Sitter Universe. In the case of the flat Λ -dominated Universe, δ_L becomes as follows (Nakamura & Suto 1997).

$$\Omega_{\text{vir}} \equiv \Omega(t_{\text{vir}}) \quad \chi \equiv \frac{\Omega_{\Lambda} H_0^2 R_{\text{turn}}}{GM} \quad w_{\text{vir}} \equiv \frac{1}{\Omega_{\text{vir}}} - 1$$
$$\delta_{\text{coll}} = \left(\frac{R_{\text{turn}}}{R_{\text{vir}}} \right)^3 \frac{2w_{\text{vir}}}{\chi} - 1 \simeq 18\pi^2 (1 + 0.04093 w_{\text{vir}}^{0.9052}) - 1$$
$$\delta_L = \frac{3}{5} F \left(\frac{1}{3}; 1; \frac{11}{6}; -w_{\text{vir}} \right) \left(\frac{2w_{\text{vir}}}{\chi} \right)^{\frac{1}{3}} \left(1 + \frac{\chi}{2} \right) - 1$$
$$= \frac{3(12\pi)^{\frac{2}{3}}}{20} (1 + 0.0123 \log \Omega_{\text{vir}}) \quad (F: \text{hypergeometric function})$$

Press-Schechter (PS) formalism

Press & Schechter (1974)

Linear growth solution of density fluctuation + extrapolation to the nonlinear regime through a spherical collapse model \Rightarrow **An analytic model of halo formation**

Let the number density of objects whose mass is between M and $M+dM$ be $n(M)dM$. Then, this $n(M)$ is called the mass function. PS formalism gives an analytic solution of $n(M)$.

$$M = \frac{4\pi R^3}{3} \bar{\rho}$$

The smoothed (averaged) overdensity in a sphere whose radius R corresponding to the mass M is called a fluctuation δ_M of mass scale M .

Press-Schechter (PS) formalism

Original fluctuation δ : Gaussian

\Rightarrow Smoothed fluctuation δ_M : Gaussian

$$P(\delta_M)d\delta_M = \frac{1}{\sqrt{2\pi\sigma(M)^2}} e^{-\frac{\delta_M^2}{2\sigma(M)^2}} d\delta_M \quad (3)$$

$(\sigma(M))^2$: variance of dM

At a certain point, if the linear δ_M exceeds the threshold value δ_c , a collapsed object with mass M is formed. We set $\delta_c = \delta_{\text{coll}} = 1.69$ as the spherical collapse model.

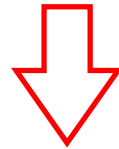
***N.B.* Recently, a number of theoretical studies adopt more complicated form for δ_c , reflecting more realistic physical conditions.**

Press-Schechter (PS) formalism

The spatial fraction of the regions with $\delta > \delta_c$ is

$$\begin{aligned} P(> \delta_c)(M) &= \int_{\delta_c}^{\infty} P(\delta_M) d\delta_M = \frac{1}{\sqrt{2\pi\sigma(M)^2}} \int_{\delta_c}^{\infty} e^{-\frac{\delta_M^2}{2\sigma(M)^2}} d\delta_M \\ &= \frac{1}{\sqrt{2\pi}} \int_{\frac{\delta_c}{\sigma(M)}}^{\infty} e^{-\frac{x}{2}} dx \end{aligned} \quad (4)$$

The amount of matter involved in an object with mass $> M$ per unit volume is $\bar{\rho}P(> \delta_c)(M)$



$$\begin{aligned} \bar{\rho}P(> \delta_c)(M + dM) - \bar{\rho}P(> \delta_c)(M) &= \bar{\rho} \frac{dP(> \delta_c)}{dM} dM \\ &= n(M)M dM \end{aligned} \quad (5)$$

Press-Schechter (PS) formalism

The discussion above ignored the possibility that a once collapsed object would be involved in a larger object (cloud-in-cloud problem).

And the region with $\delta < 0$ will never be involved in any collapsed object (i.e., $P(> \delta_c) \rightarrow 1/2$ as $\sigma(M) \rightarrow \infty$). **Then, simply we multiply a factor 2 to avoid the problem.**

$$\Rightarrow n(M)M dM = 2\bar{\rho} \left| \frac{dP(> \delta_c)}{dM} \right|_M dM \quad (6)$$

Hence

$$n(M) = \sqrt{\frac{2}{\pi}} \frac{\bar{\rho}}{M^2} \left| \frac{d \ln \sigma(M)}{d \ln M} \right| \frac{\delta_c}{\sigma(M)} e^{-\frac{\delta_c^2}{2\sigma(M)^2}} \quad (7)$$

When $\sigma(M) \propto M^{-\alpha} \Leftrightarrow P(k) \propto k^n$, $\alpha = \frac{n+3}{6}$

$$n(M) = \frac{2\alpha}{\sqrt{\pi}} \frac{\bar{\rho}}{M_*^2} \left(\frac{M}{M_*} \right)^{\alpha-2} e^{-\left(\frac{M}{M_*} \right)^{2\alpha}} \quad (8)$$

Press-Schechter (PS) formalism

The Schechter function, often used as an approximation form of galaxy luminosity function was originally inspired from the PS mass function.

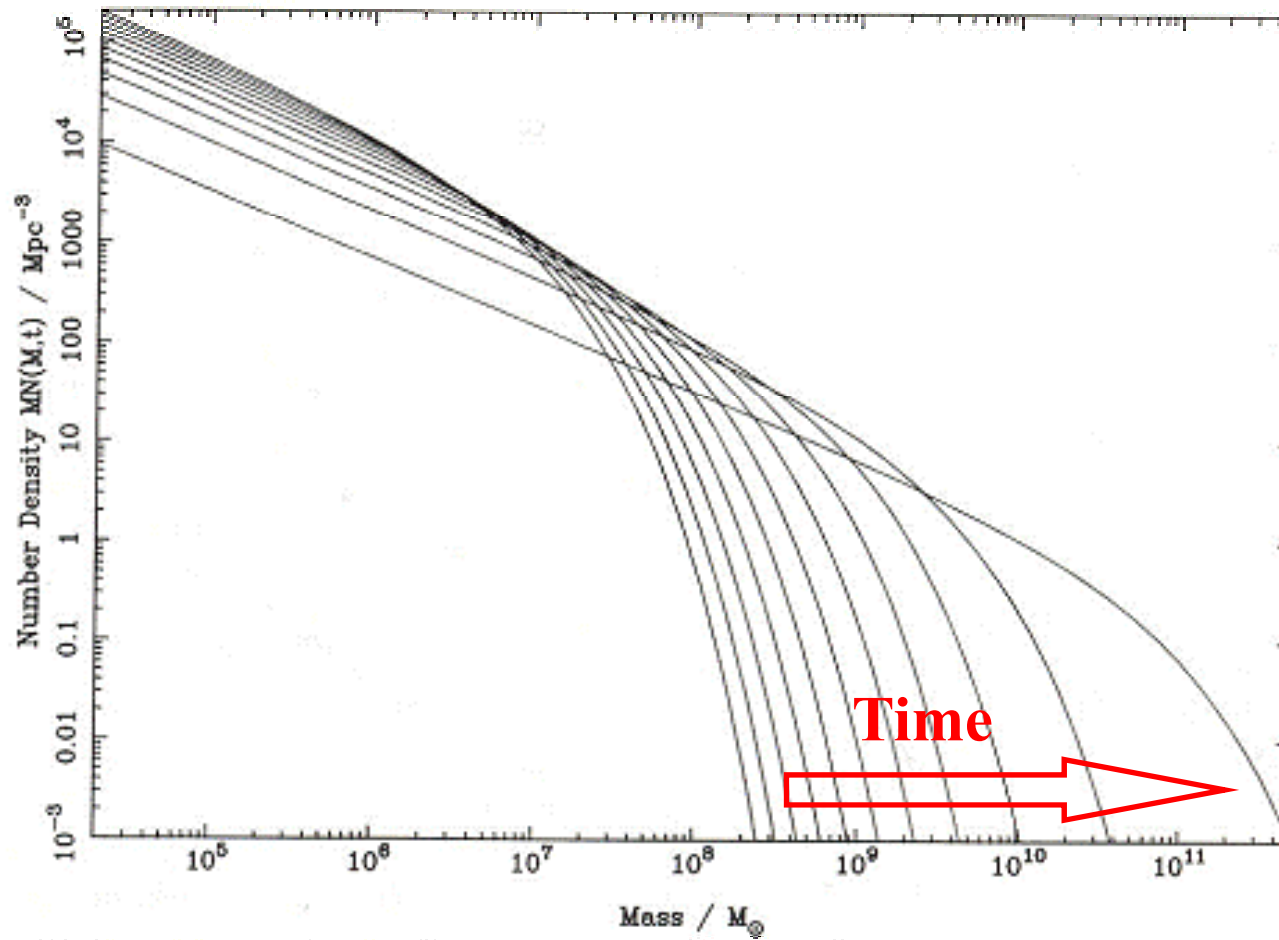
However, the original formulation by Press & Schechter contains many insufficient assumption as a mature theoretical framework.



The current main stream of the mass function formulation is to derive the PS mass function by modeling the merging of galaxy halos (extended PS formalism: e.g., Lacey & Cole 1993).

Since this framework itself gives a formula which better fits the N -body simulation results, purely theoretical attempts to aim at better understanding of the physics of halo formation is in progress(e.g., Nagashima 2001).

Press-Schechter mass function with cosmic time

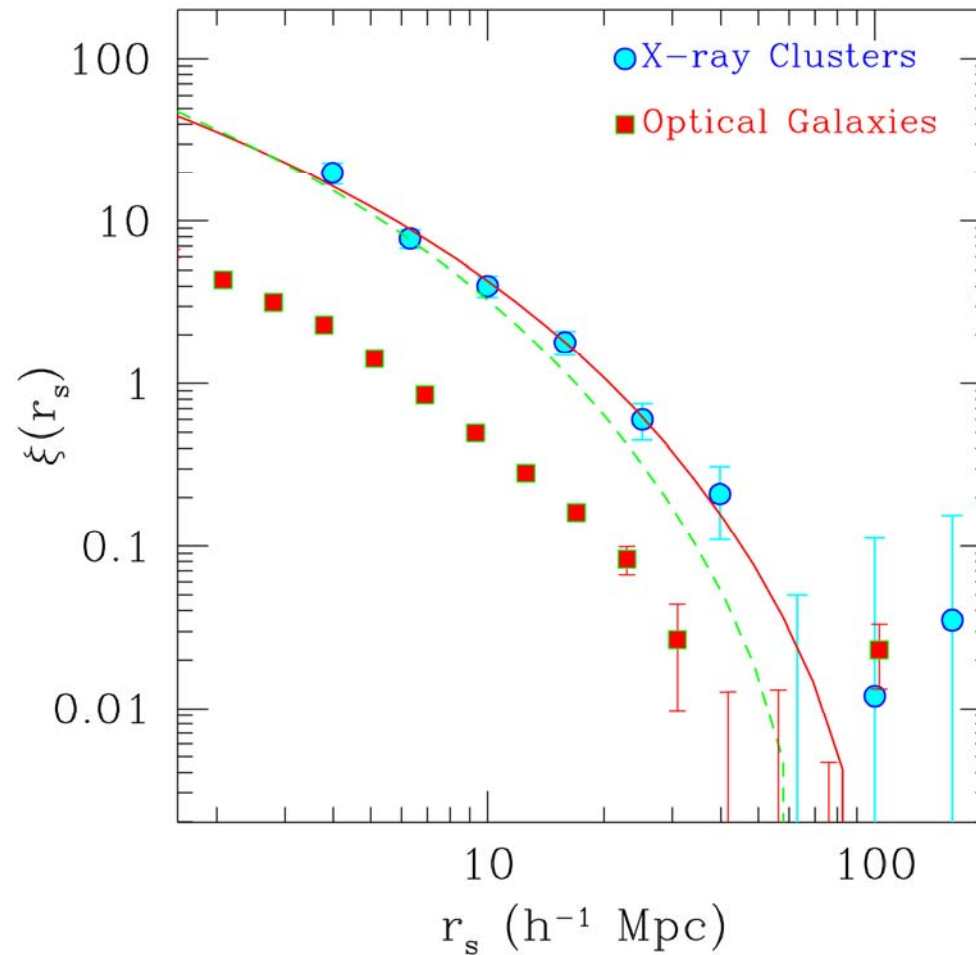


(Longair 2007)

6.2 Bias

Basic concept of bias: why is it needed?

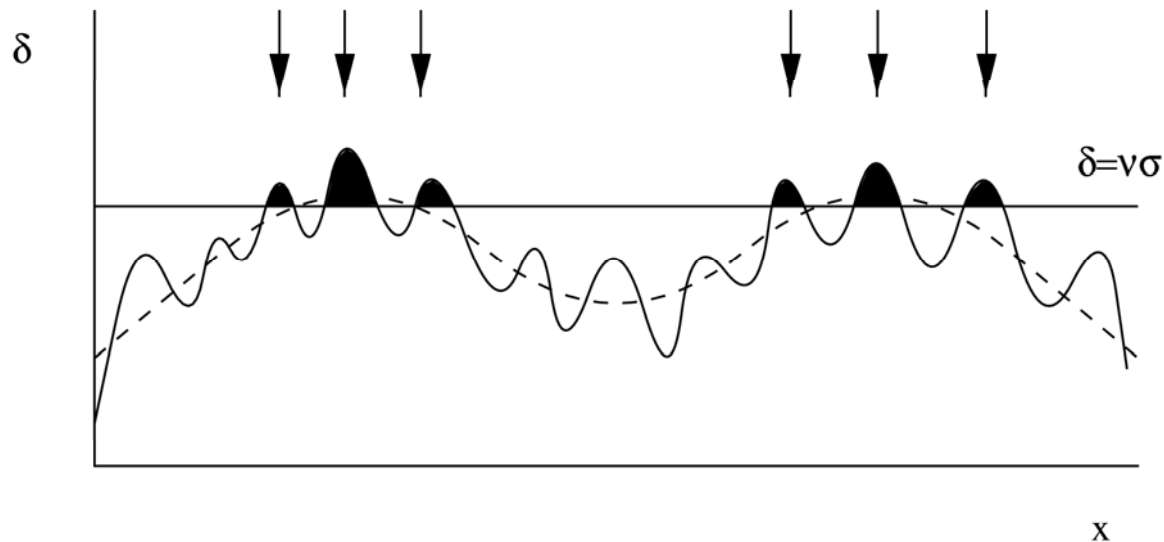
Observational fact: clusters of galaxies are more strongly clustered than galaxies.



(Borgani & Guzzo 2001)

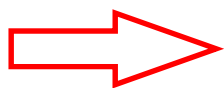
Peak model and halo bias

Basic assumption: when fluctuations smoothed with a certain scale R , δ_R , exceed a threshold δ_c , they start to grow nonlinearly and form objects (dark halos).



(Peacock 1999)

Fluctuations which are on a larger spatial scale fluctuation (dashed line) are easier to exceed the threshold.



The distribution of dark halos is more localized than the dark matter: halo bias

Peak model and halo bias

Consider a density fluctuation field:

$\delta(\vec{x})$: density fluctuation field with a zero mean and dispersion σ^2 .

$\xi(r)$: correlation function of the density field δ .

$\xi_{>v}(r)$: correlation function of density peaks which lie above a threshold $v\sigma$.

$\xi_{>v}(r)$ is defined as a fractional probability that $\delta_2 \equiv \delta(x_2) > v\sigma$ given that $\delta(x_1) > v\sigma$, where $r \equiv |\vec{r}_1 - \vec{r}_2|$.

Peak model and halo bias

If δ is a **Gaussian random field**, the probability P_1 such that $\delta > v\sigma$ at x_1 is expressed as

$$P_1 = \int_{v\sigma}^{\infty} P(y)dy \equiv \int_{v\sigma}^{\infty} \frac{1}{\sqrt{2\pi\sigma^2}} e^{-\frac{y^2}{2\sigma^2}} dy \quad (9)$$

Then the probability that both δ_1 and δ_2 lie above the threshold $v\sigma$, P_2 , is

$$\begin{aligned} P_2 &= \int_{v\sigma}^{\infty} \int_{v\sigma}^{\infty} P(y_1, y_2) dy_1 dy_2 \\ &\equiv \int_{v\sigma}^{\infty} \int_{v\sigma}^{\infty} \frac{1}{2\pi [\xi(0)^2 - \xi(r)^2]^{1/2}} \exp \left\{ -\frac{1}{2[\xi(0)^2 - \xi(r)^2]} (y_1, y_2) \begin{pmatrix} \xi(0) & \xi(r) \\ -\xi(r) & \xi(0) \end{pmatrix} \begin{pmatrix} y_1 \\ y_2 \end{pmatrix} \right\} \\ &= \int_{v\sigma}^{\infty} \int_{v\sigma}^{\infty} \frac{1}{2\pi [\xi(0)^2 - \xi(r)^2]^{1/2}} \exp \left\{ -\frac{\xi(0)y_1^2 + \xi(0)y_2^2 - 2\xi(r)y_1y_2}{2[\xi(0)^2 - \xi(r)^2]} \right\} dy_1 dy_2 \quad (10) \end{aligned}$$

Peak model and halo bias

Using P_1 and P_2 , the correlation of the high-peak regions is defined as

$$1 + \xi_{>\nu}(r) = \frac{P_2}{P_1^2} \quad (11)$$

To calculate this quantity, we should perform some arithmetic: define $y = \sigma\eta$, $dy = \sigma d\eta$, then we have

$$\int_{\nu\sigma}^{\infty} \frac{1}{\sqrt{2\pi\sigma^2}} e^{-\frac{y^2}{2\sigma^2}} dy = \int_{\nu}^{\infty} \frac{1}{\sqrt{2\pi}} e^{-\frac{\eta^2}{2}} d\eta = \frac{1}{\sqrt{\pi}} \operatorname{erfc}\left(\frac{\nu}{\sqrt{2}}\right) \quad (12)$$

Peak model and halo bias

And since $\xi(0) = \sigma^2$, $y_1 = \sigma\eta_1$, and $y_2 = \sigma\eta_2$, we obtain

$$\begin{aligned}
 P_2 &= \frac{1}{2\pi \left[1 - \frac{\xi(r)^2}{\xi(0)^2}\right]^{1/2}} \int_{\nu}^{\infty} \int_{\nu}^{\infty} \exp \left\{ -\frac{\left[\eta_1 - \frac{\xi(r)}{\xi(0)}\eta_2\right]^2}{2 \left[1 - \frac{\xi(r)^2}{\xi(0)^2}\right]} \right\} e^{-\frac{\eta_2^2}{2}} d\eta_1 d\eta_2 \\
 &= \frac{1}{\sqrt{2\pi}} \int_{\nu}^{\infty} \operatorname{erfc} \left(\frac{\nu - \frac{\xi(r)}{\xi(0)}}{2 \left[1 - \frac{\xi(r)^2}{\xi(0)^2}\right]^{1/2}} \right) d\eta
 \end{aligned} \tag{13}$$

Peak model and halo bias

By using eqs. (12) and (13), we get

$$\frac{P_2}{P_1^2} = \sqrt{2} \frac{\int_{\nu}^{\infty} e^{-\frac{\eta^2}{2}} \operatorname{erfc}\left\{-\frac{\nu - \xi(r)/\xi(0)}{\sqrt{2[1 - \xi(r)/\xi(0)]}}\right\} d\eta}{\left[\operatorname{erfc}\left(\frac{\nu}{\sqrt{2}}\right)\right]^2} \quad (14)$$

Equation (14) is approximated in extreme cases as follows:

$$\xi(r) \ll 1 \quad \xi_{>\nu}^{\xi}(r) \approx \frac{1}{\left(e^{-\frac{\nu^2}{2}} \int_{\nu}^{\infty} e^{-\frac{y^2}{2}} dy\right)^2} \frac{\xi(r)}{\sigma^2} \quad (15)$$

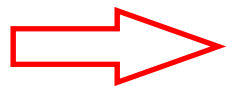
$$\nu \gg 1 \quad \xi_{>\nu}^{\xi}(r) \approx \frac{\nu^2}{\sigma^2} \xi(r) \quad (16)$$

Equation (16) is the high-peak bias formula derived by Kaiser (1984).

Galaxy bias and galaxy formation

From eq. (16), the larger δ_c is, the more strongly the density enhancement localizes, i.e., the fluctuation becomes stronger.

Baryon gas cools and falls onto the halo potential well and contract to form galaxies.



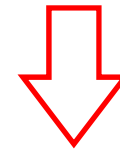
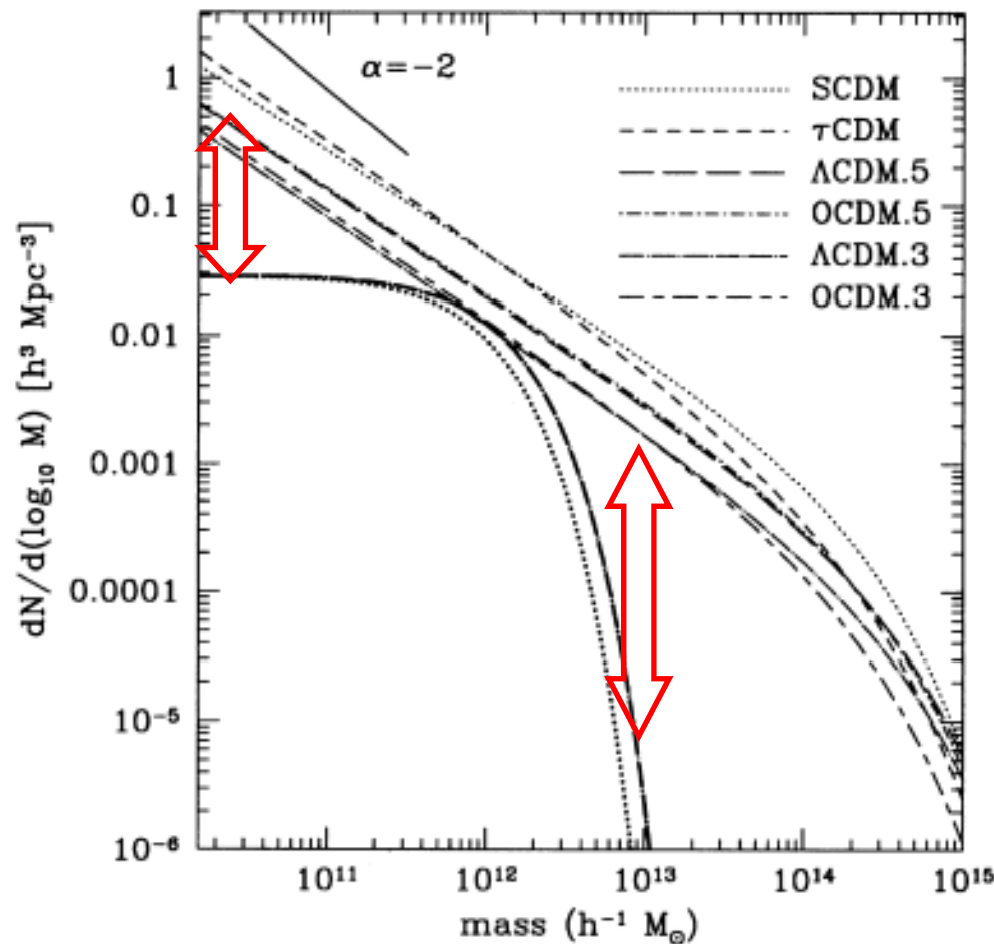
Galaxies are more localized within halos: **galaxy bias**

Galaxy bias depends on the physics of galaxy formation (and evolution); it differs depending on the population of galaxies (red and blue galaxies, luminous and less luminous, massive and less massive, optical and IR, etc.).

These characteristics are clearly reflected to the luminosity function and correlation functions of galaxies.

Halo mass function and luminosity function

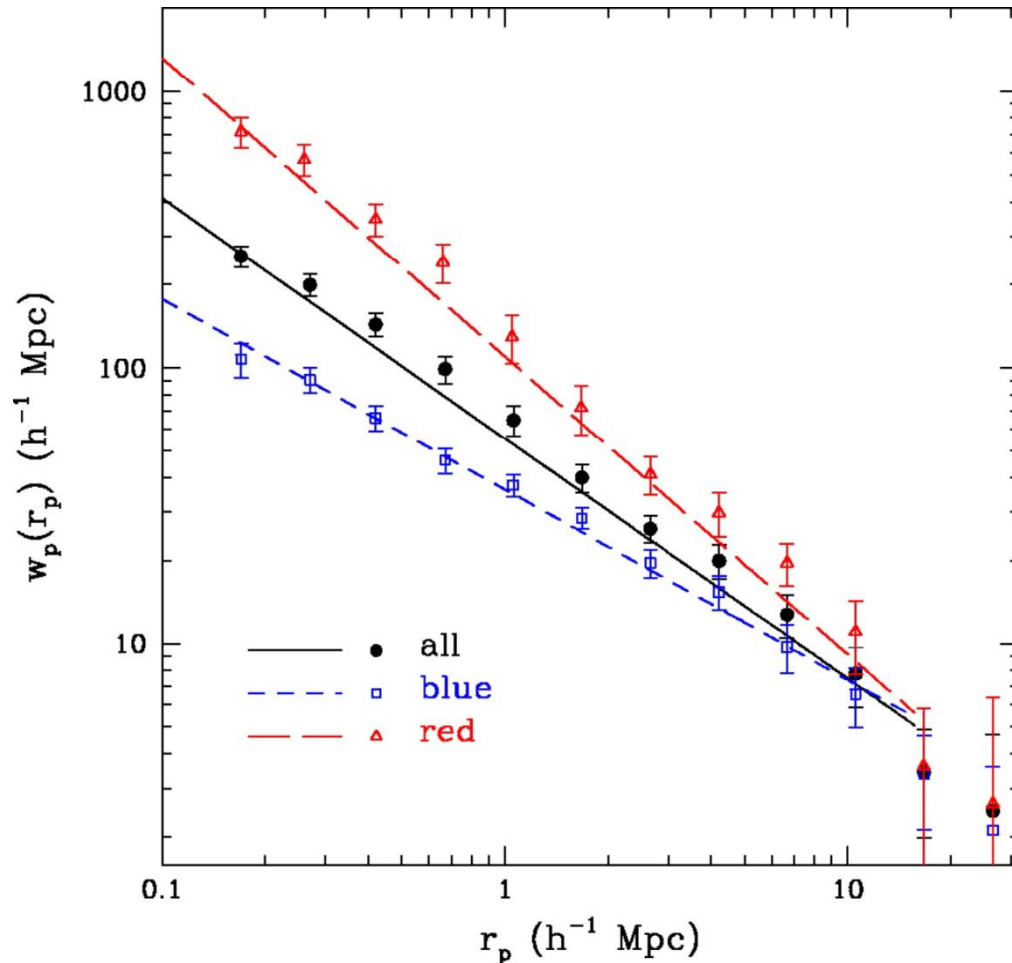
Halo mass function and galaxy luminosity function are very different in their shapes.



Related to the physics of galaxy formation

(Somerville & Primack 1999)

Clustering dependence on color (or equivalently, spectral type)



Bluer galaxies are less clustered than the whole population, while redder ones are more strongly clustered than the whole.

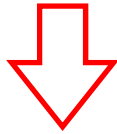


Thought to be related to the peak bias, since redder galaxies are believed to have formed in high- σ peaks.

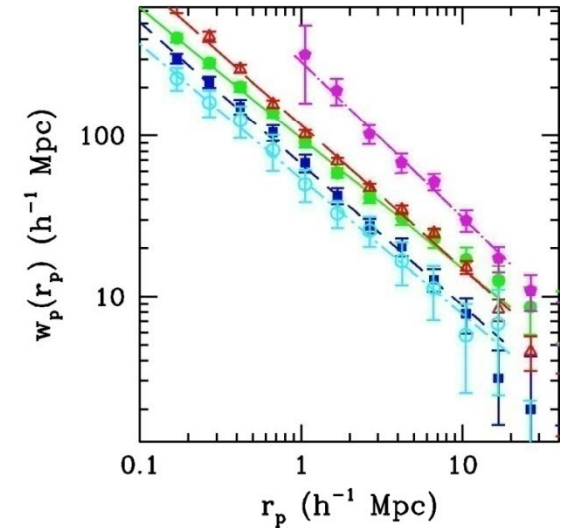
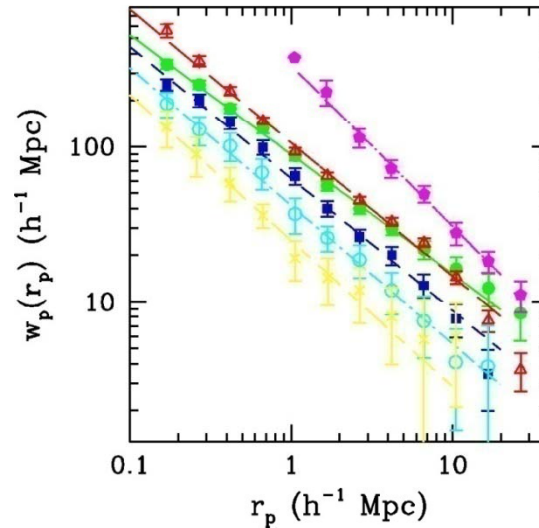
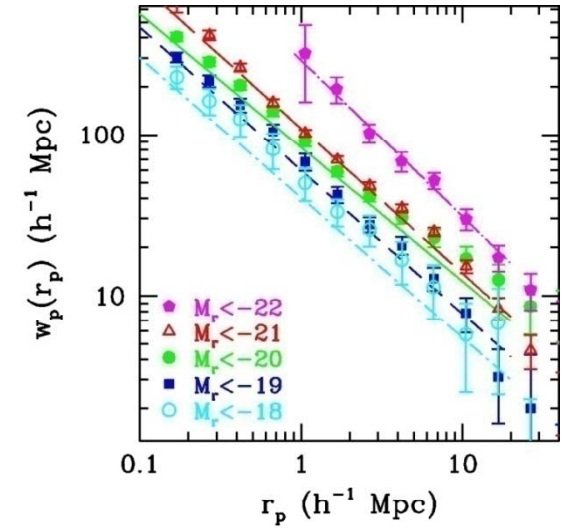
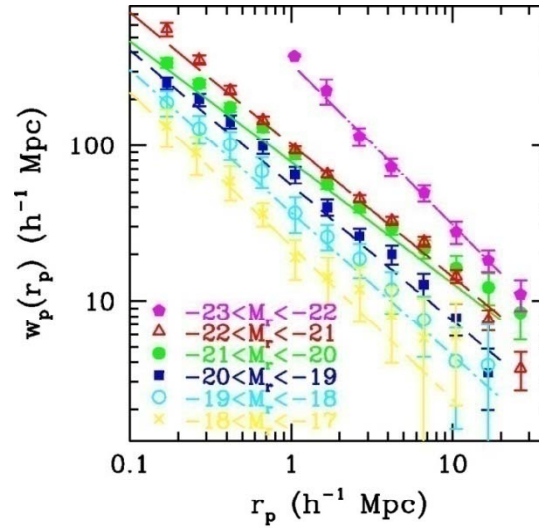
(Zehavi et al. 2005)

Clustering dependence on luminosity

The more luminous galaxies are, the more strongly clustered they become.



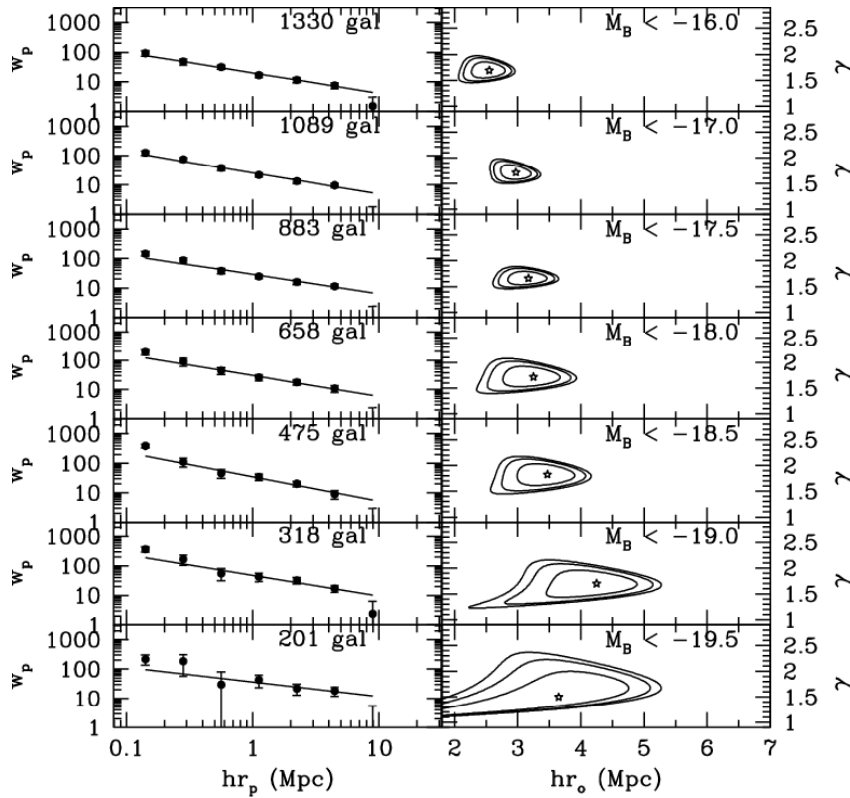
Also thought to be related to the peak bias.



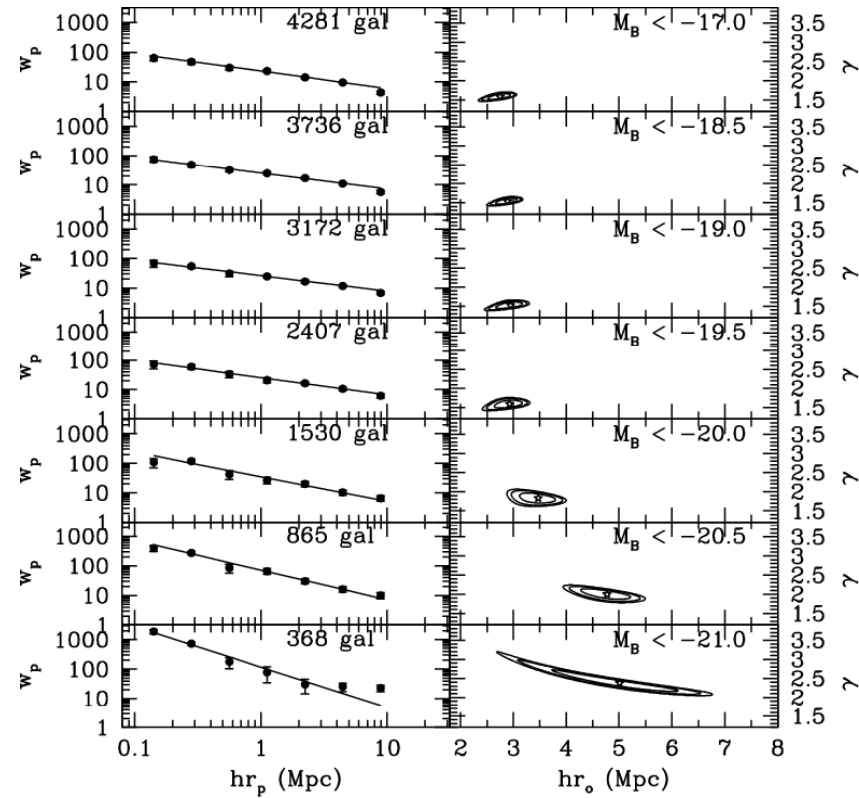
(Zehavi et al. 2005)

Clustering dependence on luminosity: evolution with redshifts

$z < 0.5$

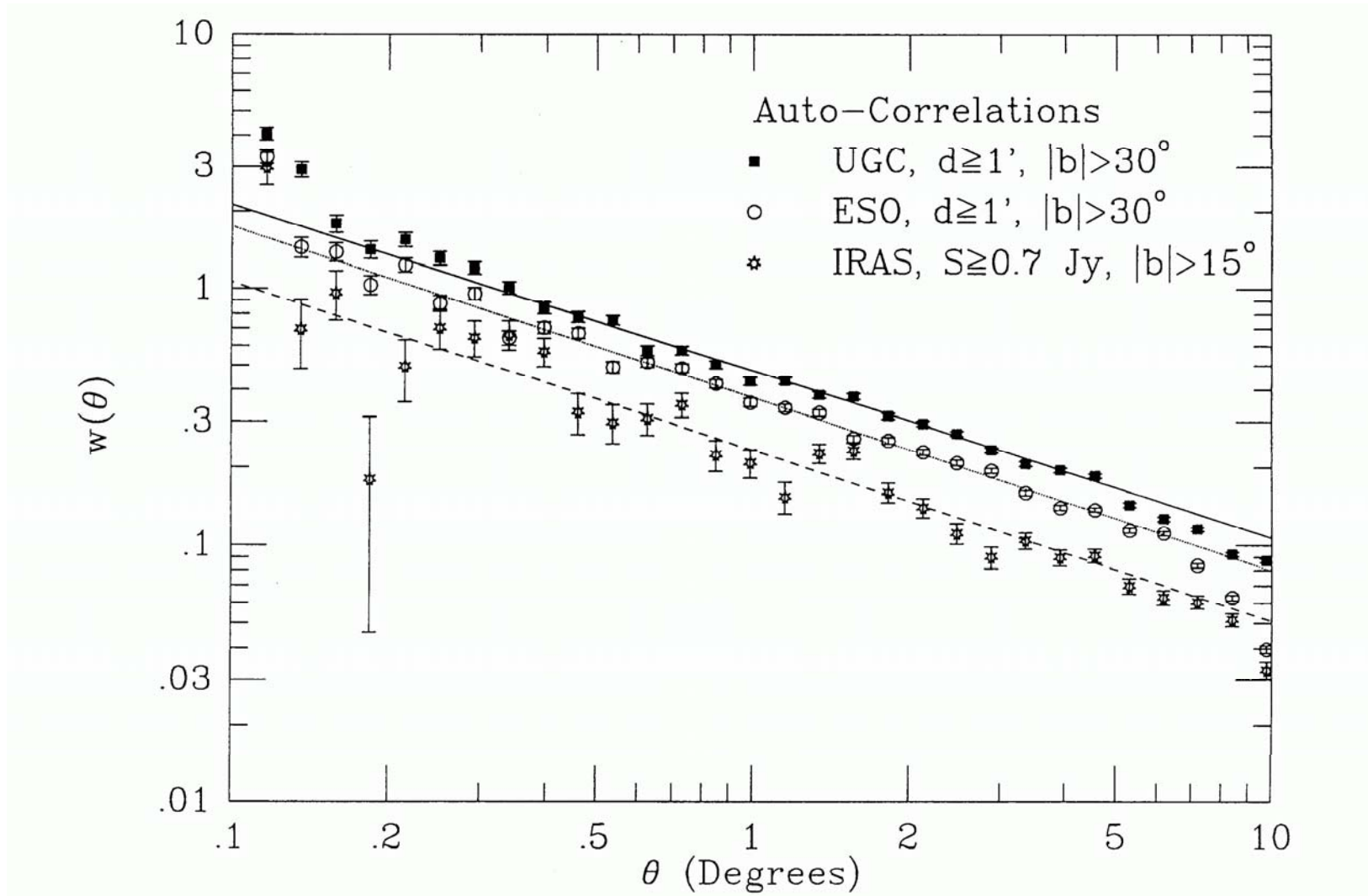


$0.5 < z < 1.2$



(Pollo et al. 2006)

Clustering dependence on wavelength (optical and IR)



(Lahav et al. 1990)

7. Galaxy Formation

7.1 Physics of galaxy formation

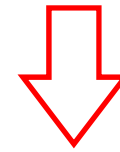
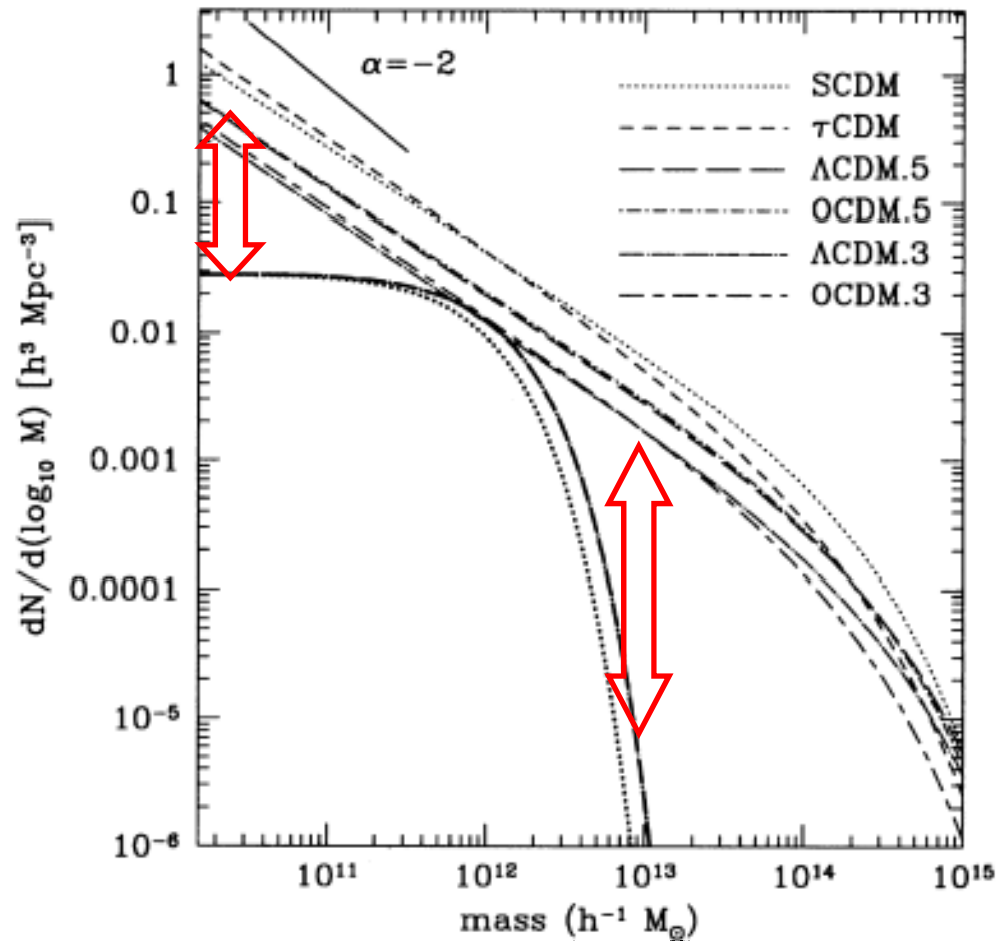
7.2 Formation of Population III stars

7.3 HI cosmology: prelude to SKA

7.1 Physics of galaxy formation

Halo mass function and luminosity function

The functional forms of the halo mass function and galaxy luminosity function are significantly different.



Related to the physics of galaxy formation

Somerville & Primack (1999)

Physics of galaxy formation

Halo \Rightarrow galaxies

Dark halo: purely gravitational

\Rightarrow dynamical evolution, merging

Baryons: hydrodynamics, electrodynamics, etc.

\Rightarrow cooling

star formation

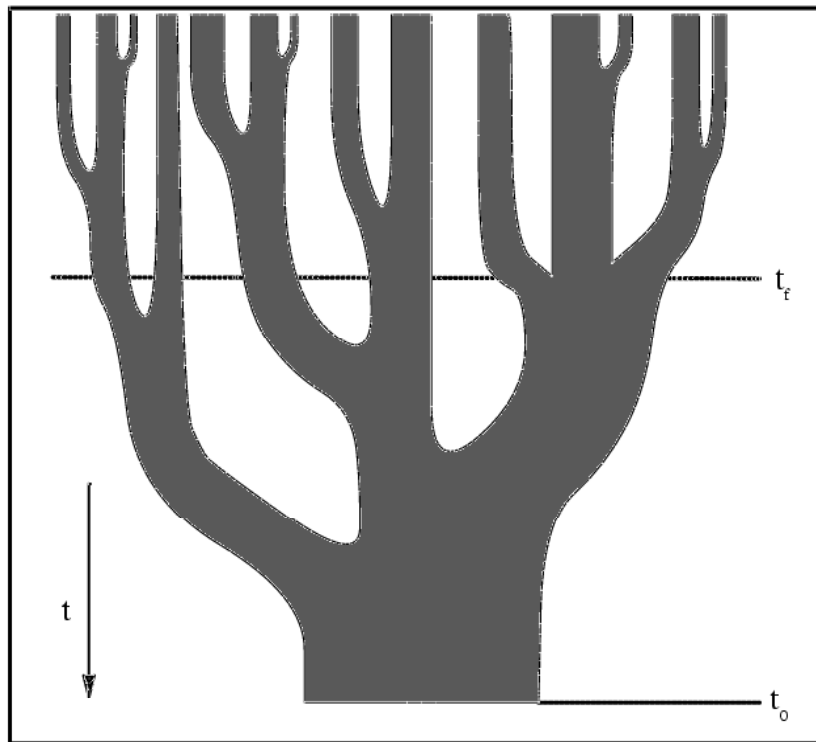
chemical evolution, formation of dust

feedbacks

blackhole formation, AGN formation

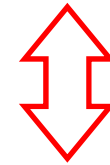
Merging

Dark halos of CDM form from smaller masses, and grow with time via merging and mass accretion to form larger mass objects: **hierarchical structure formation**



Lacey & Cole (1993)

(e.g., Searle & Zinn 1978)



A scenario to form a large object at once from the beginning:

monolithic formation

(e.g., Eggen et al. 1962)

Baryon cooling

When halos collapse or merge, a shock wave is generated in baryonic matter and **the gas will be heated.**



How to cool the gas to form galaxies?

Why do galaxies have only masses $\leq 10^{12} M_{\text{sun}}$, while there are halos with masses of $10^{15} M_{\text{sun}}$ (clusters of galaxies)?

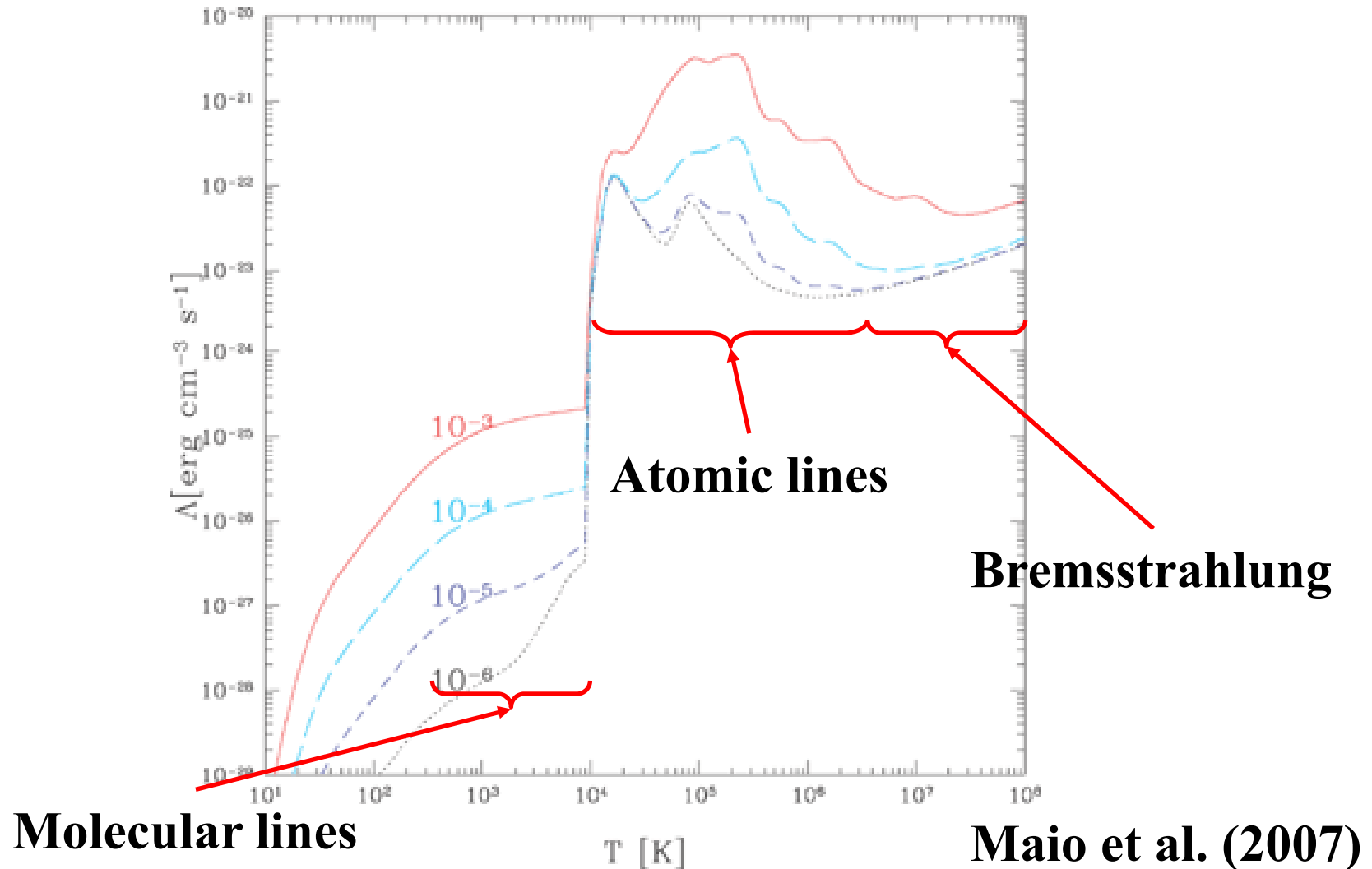
The gas temperature is typically an order of virial temperature

$$k_B T_{\text{gas}} \simeq k_B T_{\text{vir}} \simeq \frac{GMm_p}{r}$$

Galaxies: $T \sim 10^{4-5}$ K, clusters: $T > 10^7$ K (\Leftrightarrow 1 keV)

Cooling function

Cooling function Λ is a function of temperature and metallicity (see Sutherland & Dopita 1993).



Baryon cooling: why there is no galaxies with $M > 10^{13} M_{\odot}$



$10^{11} M_{\odot}$ halo with gas cooled



$10^{14} M_{\odot}$ halo with gas not cooled

Cooling time of cosmic objects

We can estimate the cooling time t_{cool} of a clump of baryonic gas by using the cooling function. Let n be the gas number density, we have

$$t_{\text{cool}} \simeq \frac{k_{\text{B}}T}{n\Lambda}$$

The dynamical time t_{dyn} of an object is estimated by the free-fall time,

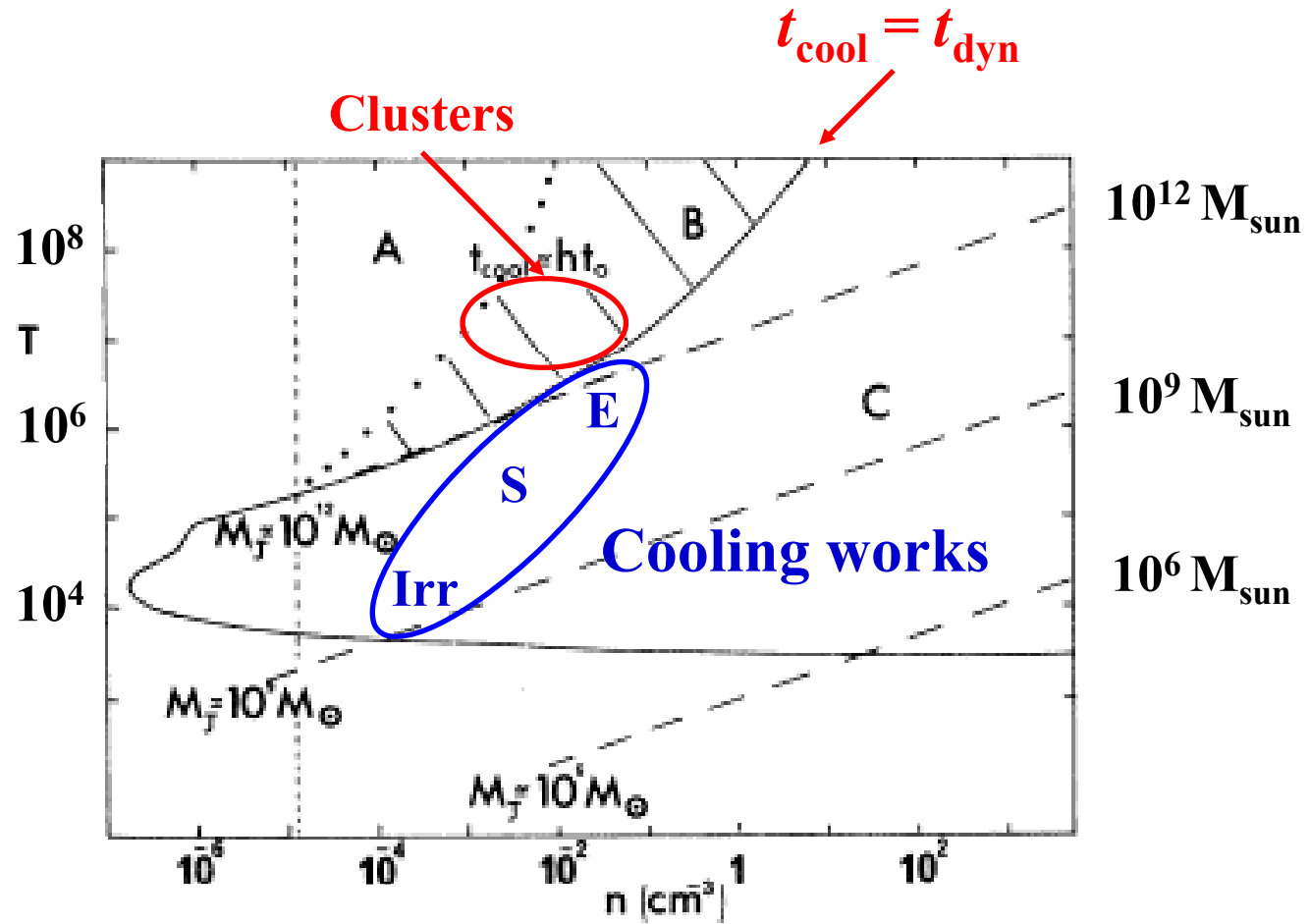
$$t_{\text{dyn}} \simeq \frac{1}{\sqrt{G\rho}}$$

Rees & Ostriker (1977)

$t_{\text{cool}} \ll t_{\text{dyn}}$: **baryons fall onto the halo center with a timescale of t_{dyn} before feeling the pressure generated by shock heating.**

$t_{\text{cool}} \gg t_{\text{dyn}}$: **baryons are supported by the pressure and dissipate their energy quasistatically.**

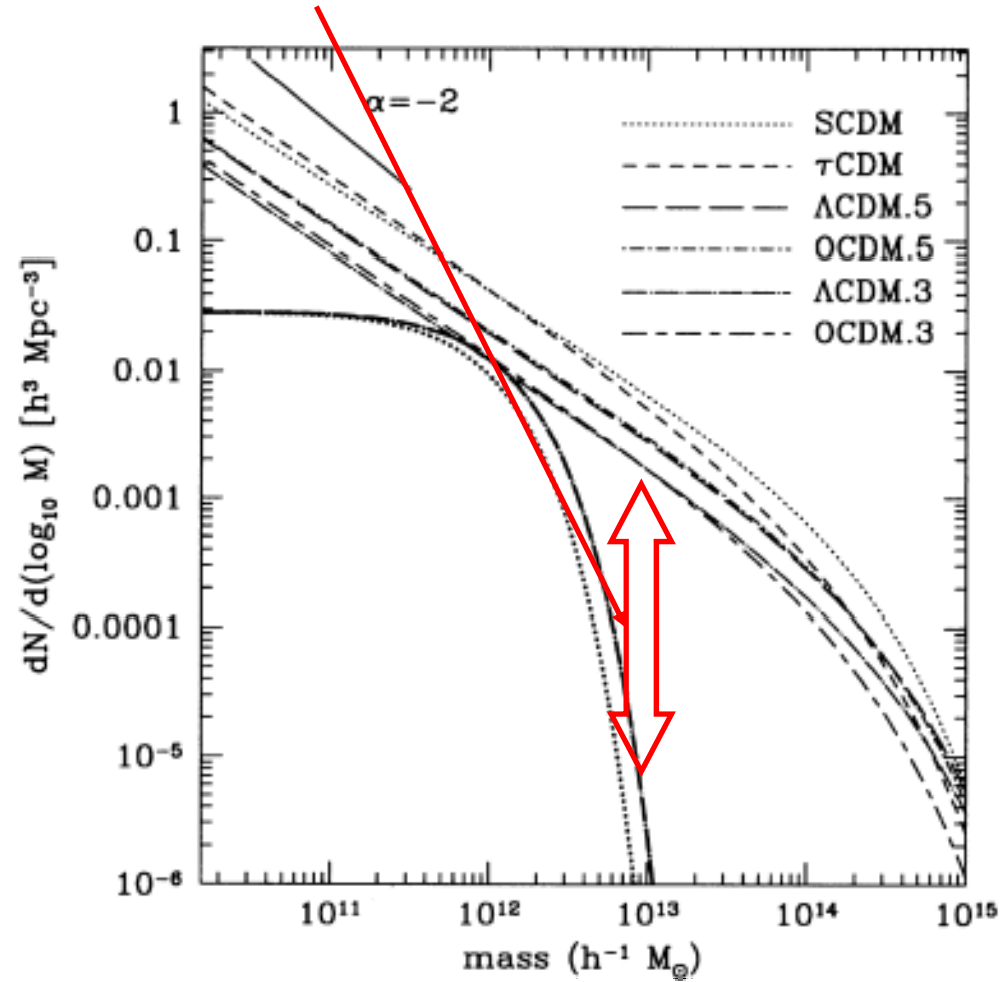
Cooling time of cosmic objects



Rees & Ostriker (1977)

Cooling time of cosmic objects

Cooling time explains this difference



Somerville & Primack (1999)

Cooling time of cosmic objects: recent progress

The above discussion is a well-established concept to explain the lack of galaxies with $M \sim 10^{15} M_{\odot}$ galaxies.

However, this is basically a one-zone argument. **Recent studies revealed that the gas cools efficiently at the center of clusters of galaxies if we consider the density profile properly.**

Cooling time of cosmic objects: recent progress

The above discussion is a well-established concept to explain the lack of galaxies with $M \sim 10^{15} M_{\odot}$ galaxies.

However, this is basically a one-zone argument. **Recent studies revealed that the gas cools efficiently at the center of clusters of galaxies if we consider the density profile properly.**



Overcooling problem has revived!

People are trying to solve the problem by **the feedback effect from AGNs at the center of clusters**, but it remains a matter of strong debate yet.

Star formation in galaxies

Gas cooled and fallen onto the halo center starts to be fragmented and contract, to form stars finally.

Jeans instability

hydrodynamic instabilities

magnetohydrodynamic instabilities etc.

In order to understand the physics of galaxy formation, we need to understand the formation process of first stars (Population III; Pop III). However, it is still poorly understood theoretically, and **only phenomenological methodology assuming properties of local galaxies is adopted (e.g., semi-analytic models).**

Dust formation

Most of galaxy formation and evolution models adopt oversimplified assumptions, e.g., the properties of dust extinction to be the same as those of the Milky Way.

Stellar species which supply dust change with galaxy evolution, from supernovae, novae, AGBs and RGBs (and planetary nebulae). There exist very few models which include the evolution of the source of dust supply, and even existing models are quite premature (e.g., Takeuchi et al. 2003, 2005; Asano et al. 2013a, b, 2014; Nozawa et al. 2015).

Feedback

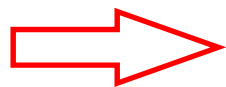
Star formation \Rightarrow supernova \Rightarrow galactic wind

Supernovae heat the ISM, and blow away the gas mechanically, and destroy molecular clouds by shocks.



Reduction of star formation activity

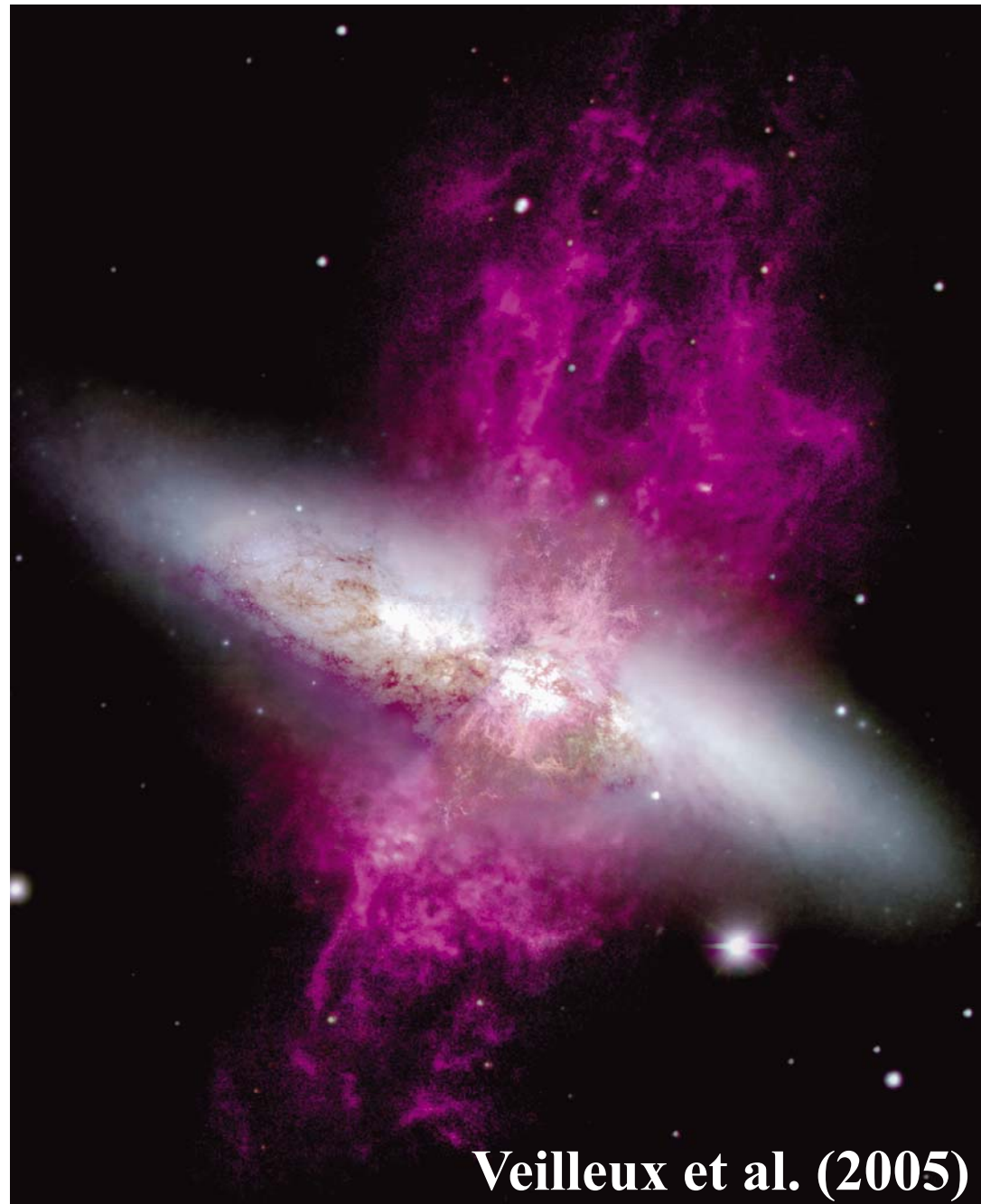
Since supernovae are originated from massive stars, the timescale is short (10^{6-7} yr).



Supernova rate \propto star formation rate

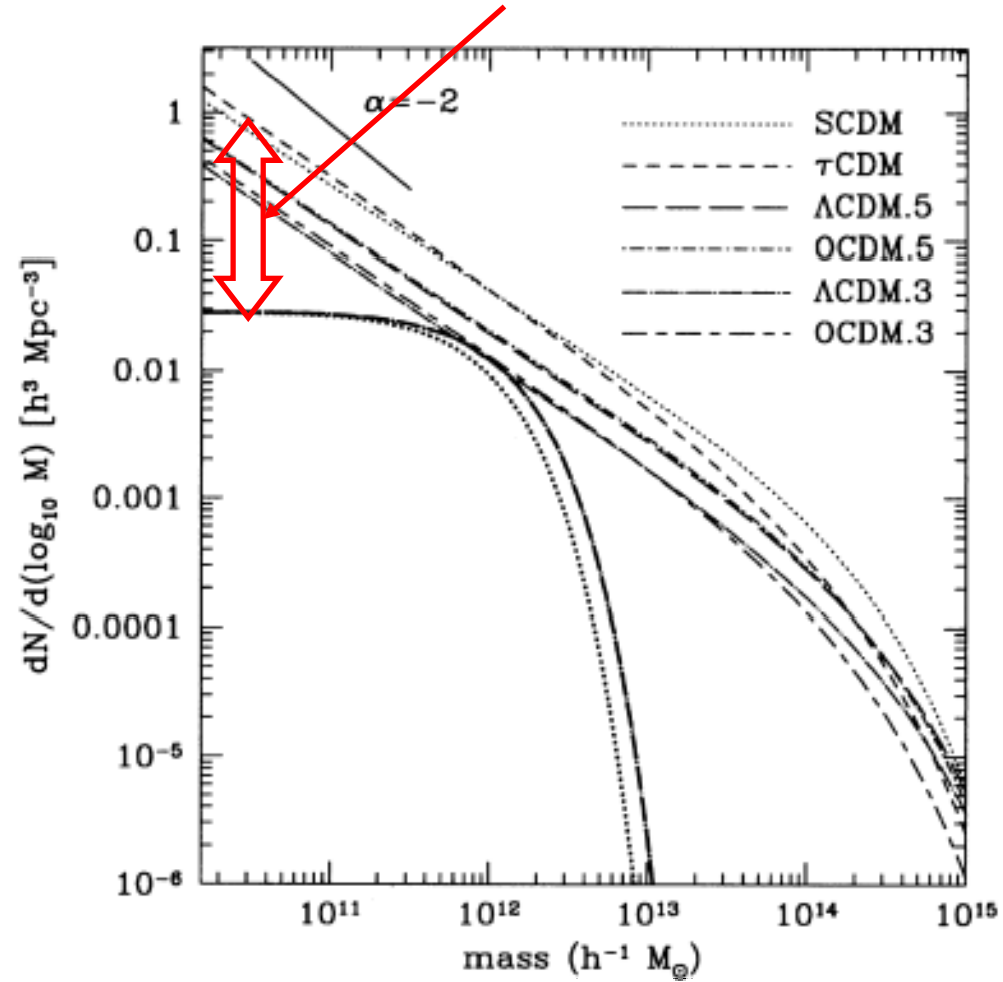
Many problems remain unsolved, e.g., how much energy is given to the ISM. The same as for AGN feedbacks (Dekel & Silk 1986; Mac Low & Ferrara 1999; Ferrara & Tolstoy 2000; Veilleux et al. 2005; NcNamara & Nulsen 2007).

Feedback



Feedback

Supernova feedback explains this difference??



Somerville & Primack (1999)

7.2 Formation of Population III stars

Basic properties of Population III stars

Population III

1. First stars formed from metal-free gas
2. Forms from the cosmological initial condition (no stellar feedback)

N.B., Some people call simply extremely metal-poor stars Pop III (e.g., $Z \sim 1/10000Z_{\odot}$).

Since metal-free gas cannot contract with metal line cooling, it is very difficult for them to collapse.



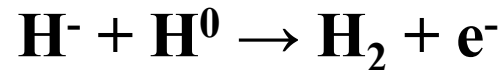
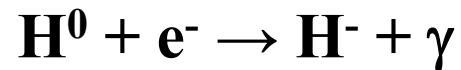
Cooling can proceed only via line emissions of hydrogen molecules (H_2 , HD)(e.g., Nishi et al. 1998).

Formation of molecular hydrogen in a gas phase

Formation of H₂ and HD in a gas phase:

Universe just after the recombination : ionized fraction $\sim 10^{-4}$

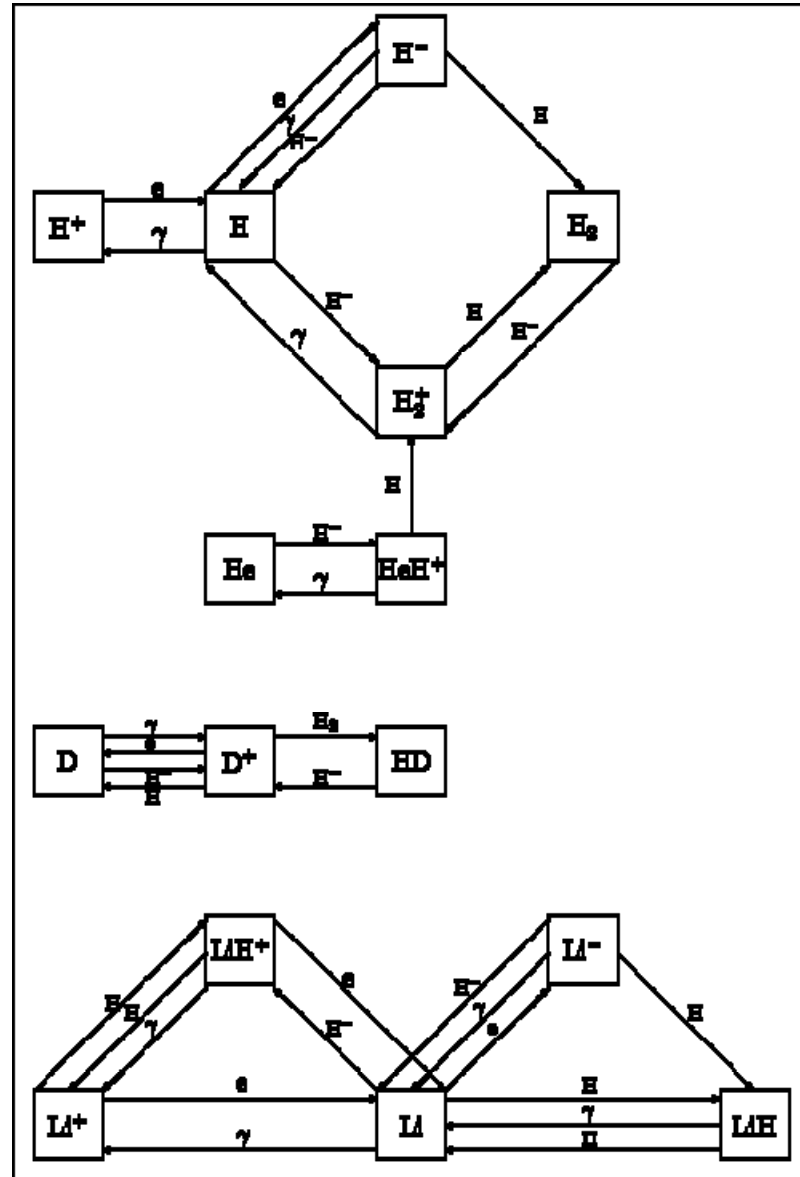
Basic reactions:



These reactions proceed with electrons being a catalyst. In the Universe after recombination, molecular hydrogen formation starts via relic electrons after the Big-Bang. To be precise, some tens of reactions proceed simultaneously in a very complicated way (e.g., Galli & Palla 1998).

Cf. In the ISM with a metallicity similar to solar, as the MW, H₂ formation proceed with **dust surface as a catalyst**. The H₂ formation on dust grains is more than 100 times more efficient than that in a gas phase.

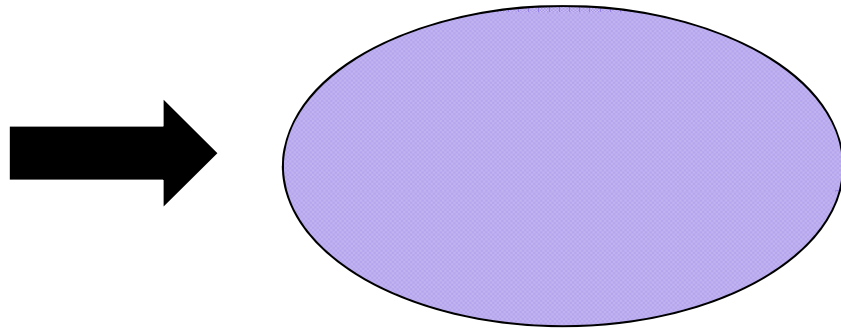
Reaction network in the pregalactic era



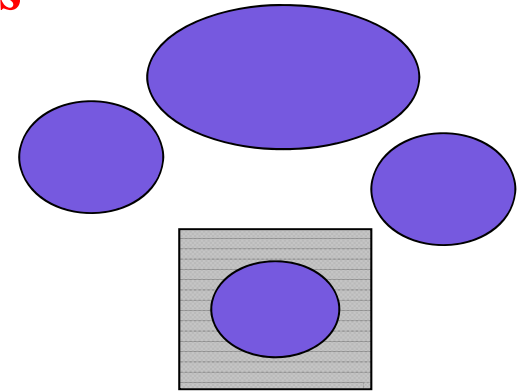
Galli & Palla (1998)

First collapse of Pop III

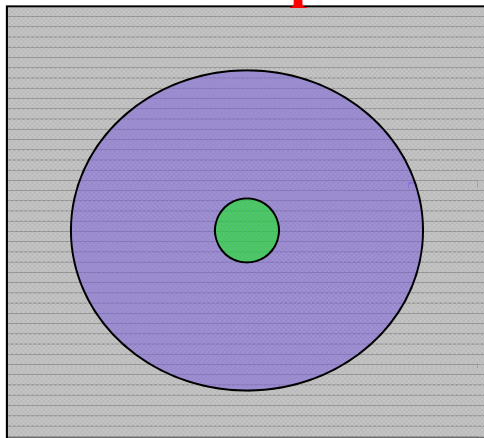
1. Formation of the first object



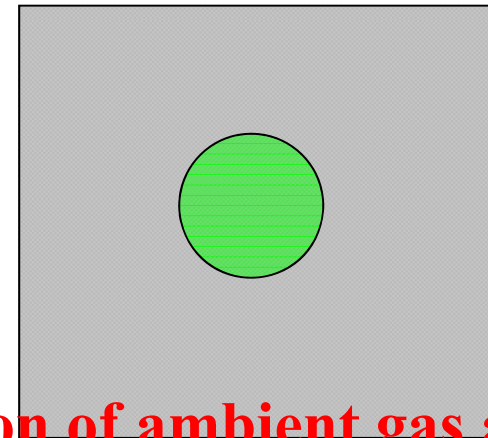
2. Fragmentation of the first objects



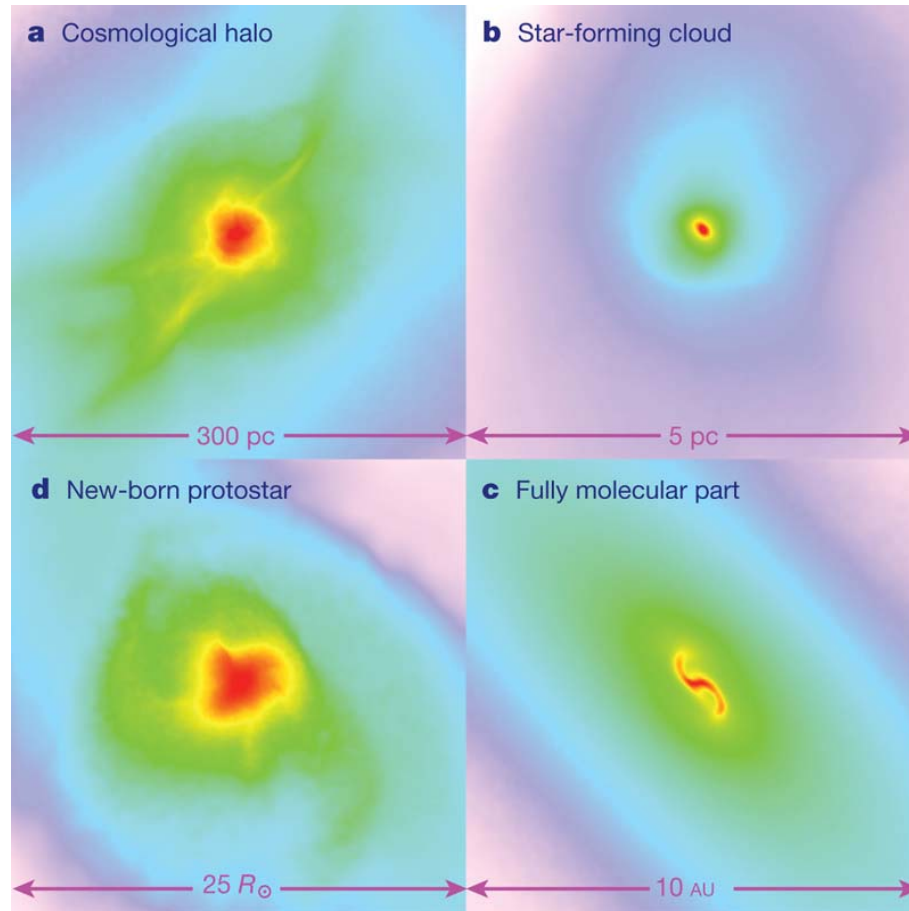
2. Collapse of dense cores:
formation of protostar



3. Accretion of ambient gas and
relaxation to main sequence star



Formation of the first object (minihalo)

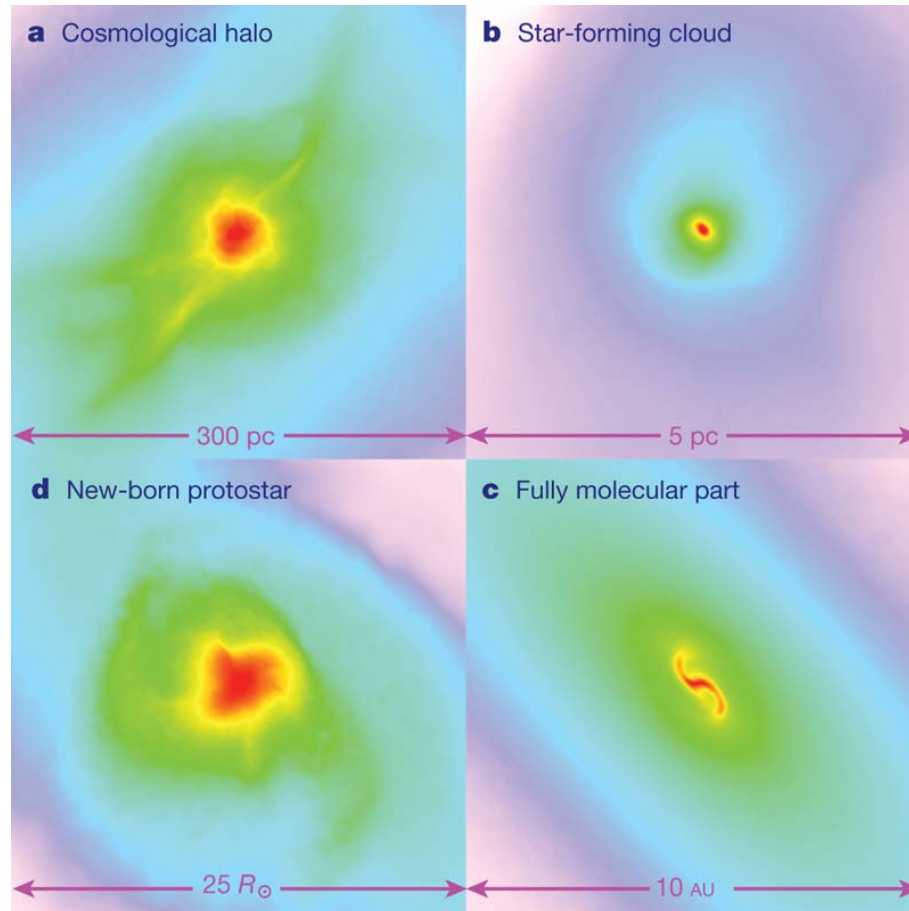


At $z = 20-30$, $3-4\sigma$ peaks of dark matter collapse to form minihalos ($M_{\text{halo}} \sim 10^6 M_{\odot}$ and the $T_{\text{vir}} \sim 10^3 \text{ K}$). These minihalos are the site of the first star formation.

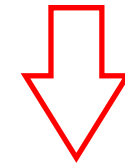
Since minihalos are predicted to be **strongly clustered** (halo bias), the feedback from the first star is very important in determining the state of surrounding gas clouds.

Bromm et al. (2009)

Formation of the first object (minihalo) II



The number of stars formed in a minihalo cannot be very large (one or a few at most), because the strong UV field dissociates the molecules around the first star (e.g., Omukai & Nishi 1999).



A Minihalo cannot form a galaxy.

Bromm et al. (2009)

Runaway collapse of dense cores: formation of a protostar

Primordial gas clouds undergo **runaway collapse** when sufficient mass is accumulated at the center of a minihalo. The minimal mass at the onset of collapse is determined by the Jeans mass

$$M_J = 500M_{\text{sun}} \left(\frac{T}{200 \text{ K}} \right)^{\frac{3}{2}} \left(\frac{n}{10^4 \text{ cm}^{-3}} \right)^{-\frac{1}{2}}$$

Typical fragmentation mass is \sim a few $\times 10^2$ - $10^3 M_{\odot}$.

The Jeans mass only gives an estimate of the stars formed. Standard star formation scenario predicts that **a tiny protostar forms first and subsequently grows by accreting the surrounding gas.**

Properties of the accretion to Pop III stars

1. **High accretion rate: for a zero-metal gas with $T \sim 300$ K,**

$$\dot{M} \approx \frac{c_s^3}{G} \approx T^{\frac{3}{2}} = 0.001 - 0.01 M_{\text{sun}} \text{yr}^{-1}$$

(Stahler, Shu, & Taam 1980)

\Rightarrow shorter formation timescale.

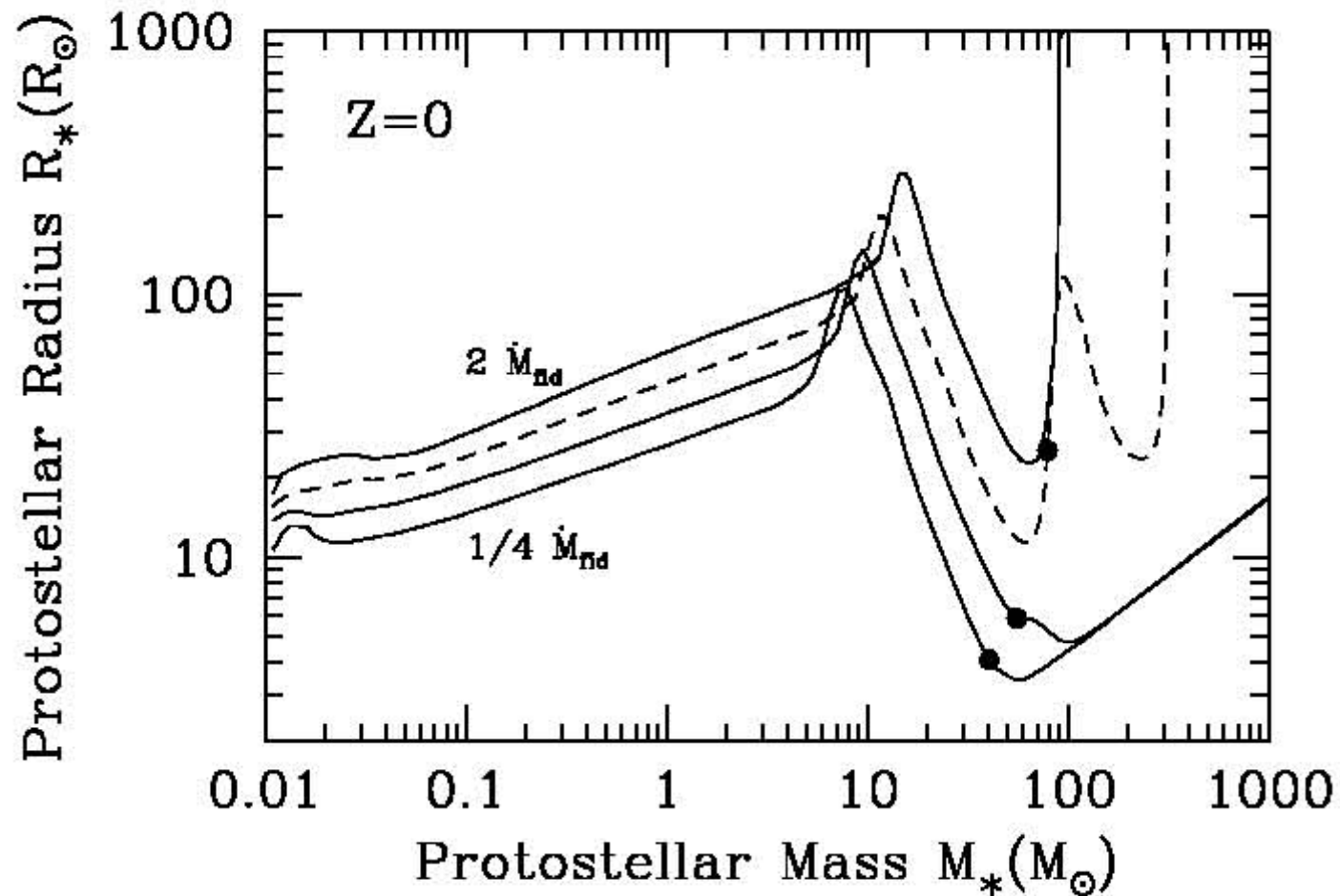
Cf. for a present-day star formation (Pop I),

$$\dot{M} \approx 10^{-6} - 10^{-5} M_{\text{sun}} \text{yr}^{-1}$$

2. **Low opacity of accreted matter because of no dust**

\Rightarrow weak radiative feedback from the accreting star.

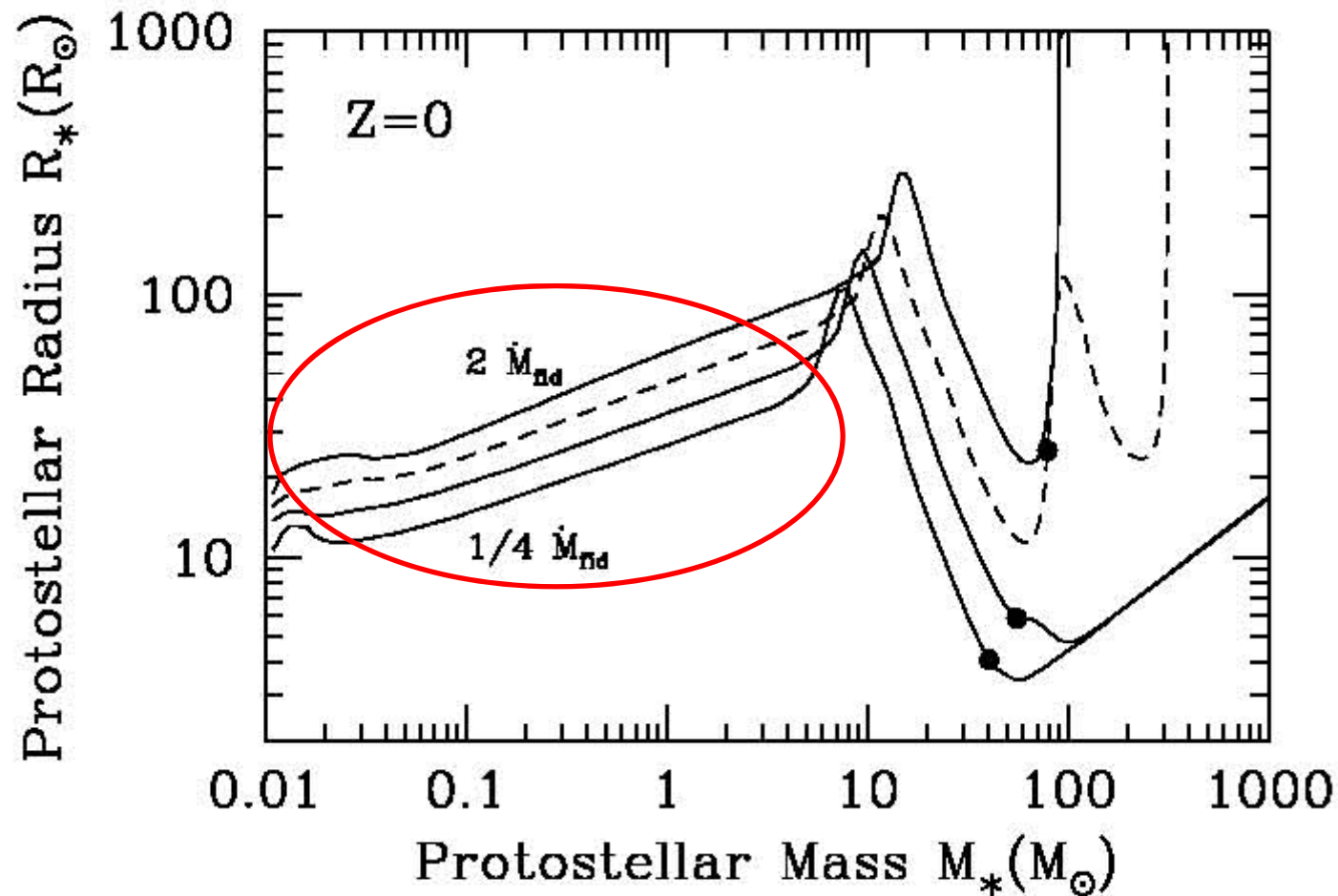
Protostellar evolution of Pop III stars with accretion



$$\dot{M} = 8.8, 4.4, 2.2, 1.1 \times 10^{-3} M_{\text{sun}} \text{ yr}^{-1}$$

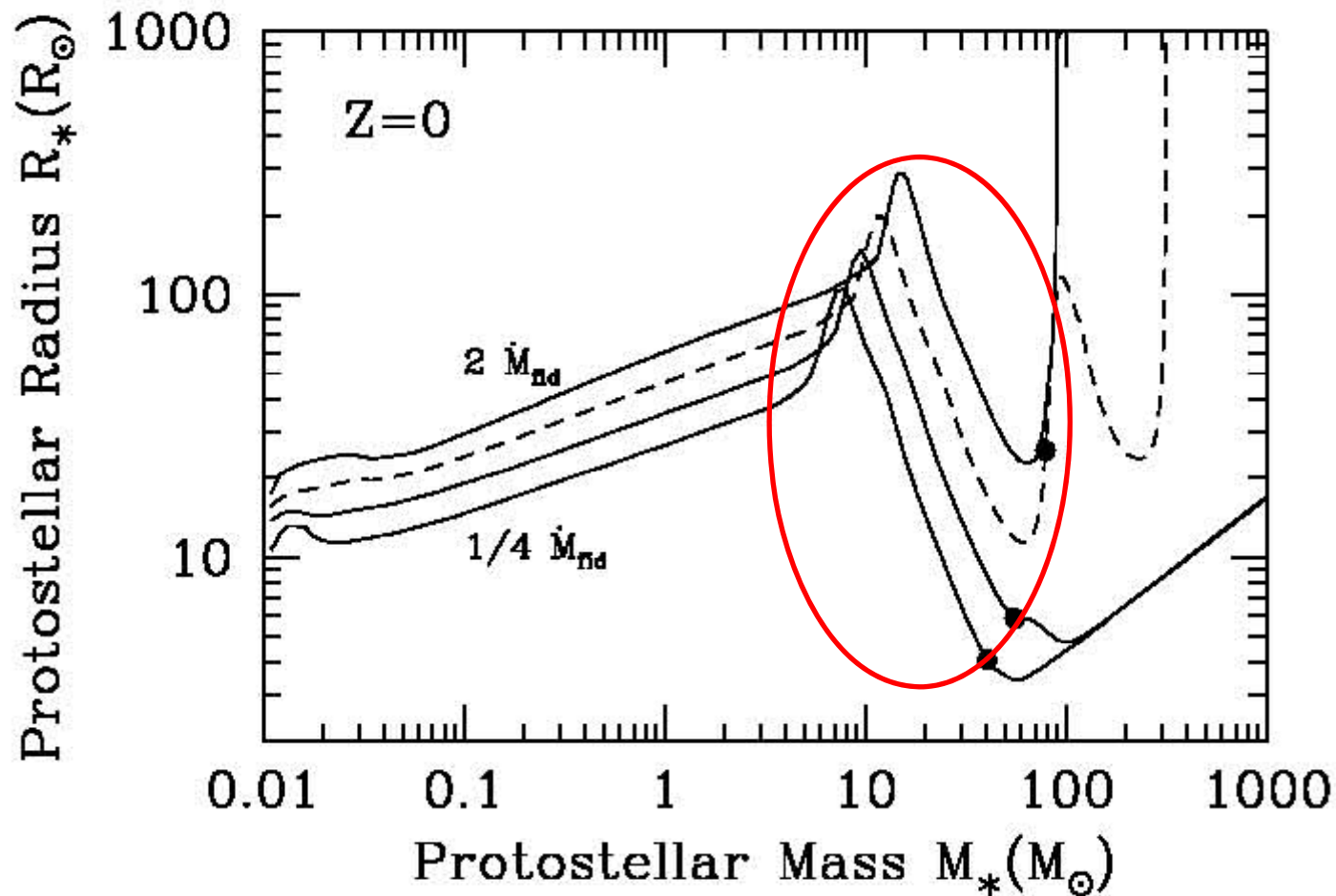
Omukai & Palla (2003)

Protostellar evolution of Pop III stars with accretion



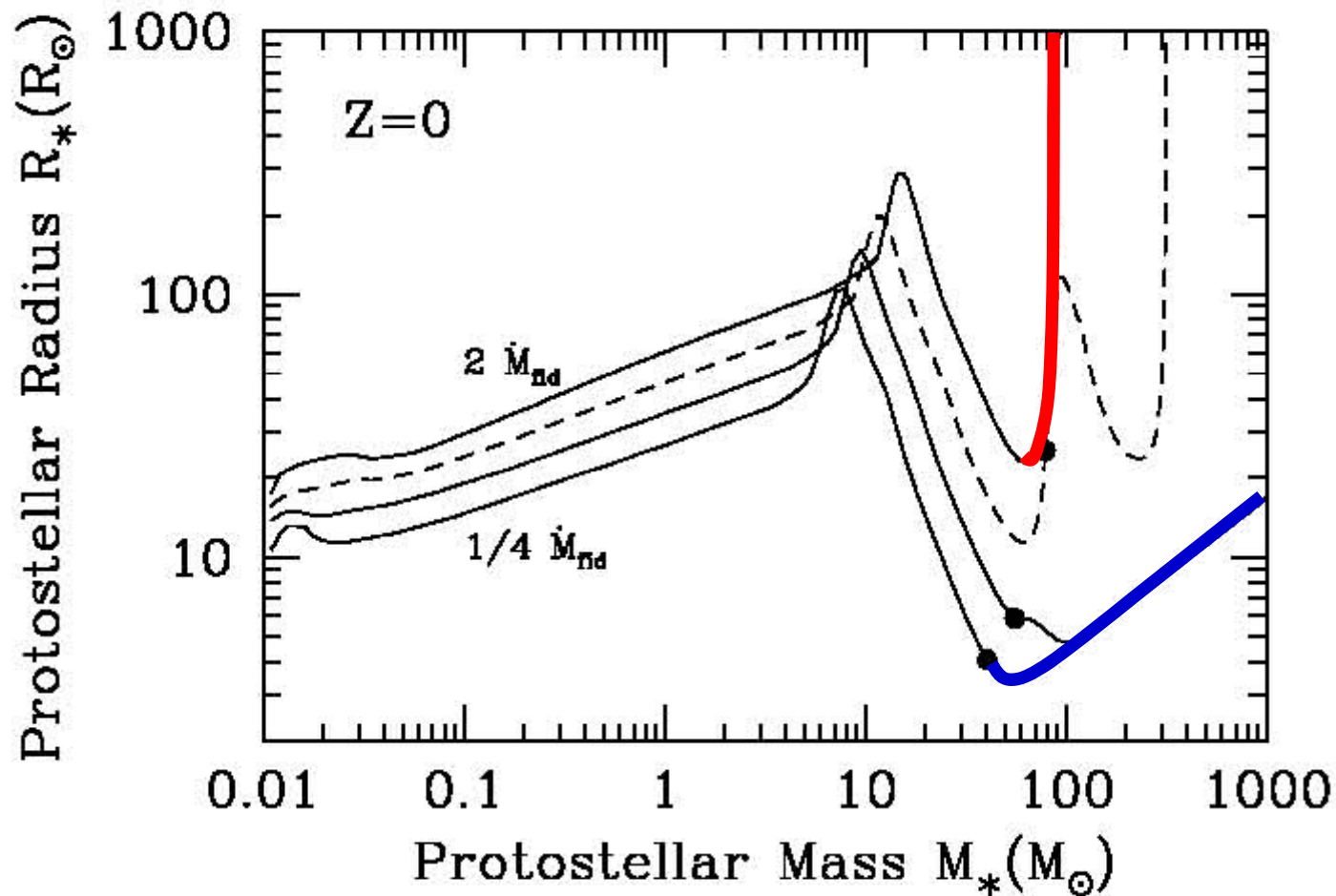
1. Adiabatic phase. A protostar expands gradually.

Protostellar evolution of Pop III stars with accretion



2. Kelvin-Helmholtz contraction phase. The gravitational attraction stops the expansion and contracts toward a main-sequence radius.

Protostellar evolution of Pop III stars with accretion



3a. Contraction proceeds and a protostar reaches the zero-age main sequence (ZAMS) phase. **3b.** Radiation pressure causes a sudden expansion and the outer layer is blown away.

Protostellar evolution of Pop III stars with accretion

1. Owing to the fast accretion, the star becomes massive before H burning (H burning via CN cycle starts at $40\text{-}100M_{\odot}$).
2. Accretion continues if the accretion rate is

$$\dot{M} < \dot{M}_{\text{crit}} = 4 \times 10^{-3} M_{\text{sun}} \text{yr}^{-1}$$

3. no stationary solution for $> 100M_{\odot}$ if the accretion rate is

$$\dot{M} > \dot{M}_{\text{crit}} = 4 \times 10^{-3} M_{\text{sun}} \text{yr}^{-1}$$

Omukai & Palla (2003)

Mass of Pop III stars

The mass of a Pop III star is determined by

$$M_* = \min(M_{\text{frag}}, \dot{M} \cdot t_{\text{OB}}, M_{\text{feedback}})$$

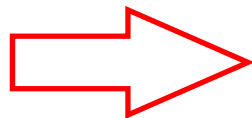
where

M_{frag} : fragmentation mass $\sim 1000M_{\odot}$

\dot{M} : accretion rate $\sim 10^{-3}M_{\odot} \text{ yr}^{-1}$

t_{OB} : massive star lifetime $\sim 10^6 \text{ yr}$

M_{feedback} : mass of star when the accretion is halted by stellar feedback $> 100M_{\odot}$



$$M_* = 100 - 1000M_{\text{sun}}$$

Thus, Pop III stars are predicted to be very massive.

Formation of the second generation Pop III stars (Pop III.2)

- 1. Initial condition in the formation is different from first generation (Pop III.1) stars:**

Ionization by Pop III.1 stars.

Density fluctuation induced by HII regions of the Pop III.1 and blast waves generated by the first SN.

- 2. Environment is different:**

External radiation field (UV from Pop III.1)

Cosmic rays

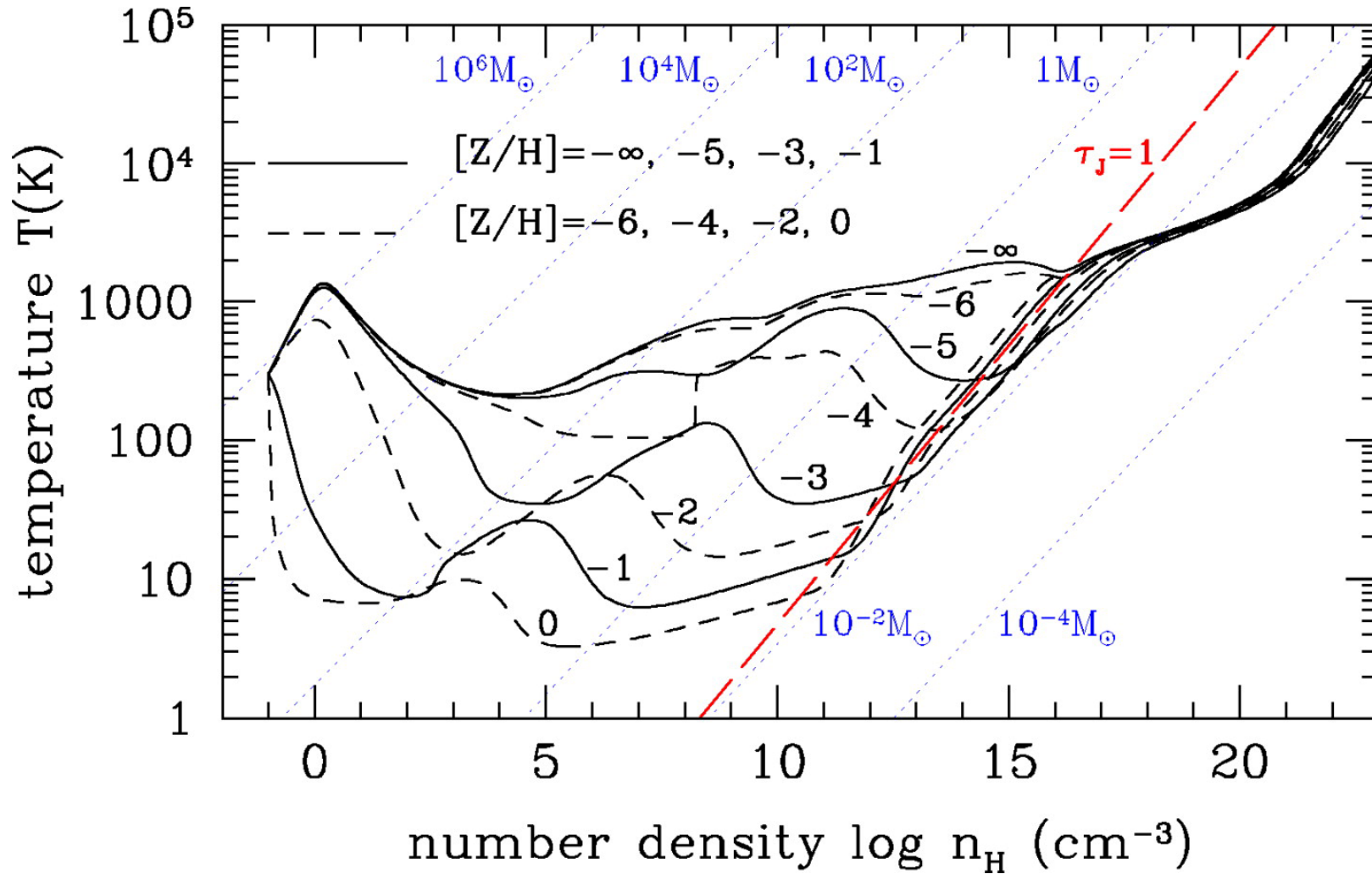
- 3. Abundance is different:**

Metal supply from Pop III.1 stars

Dust formation

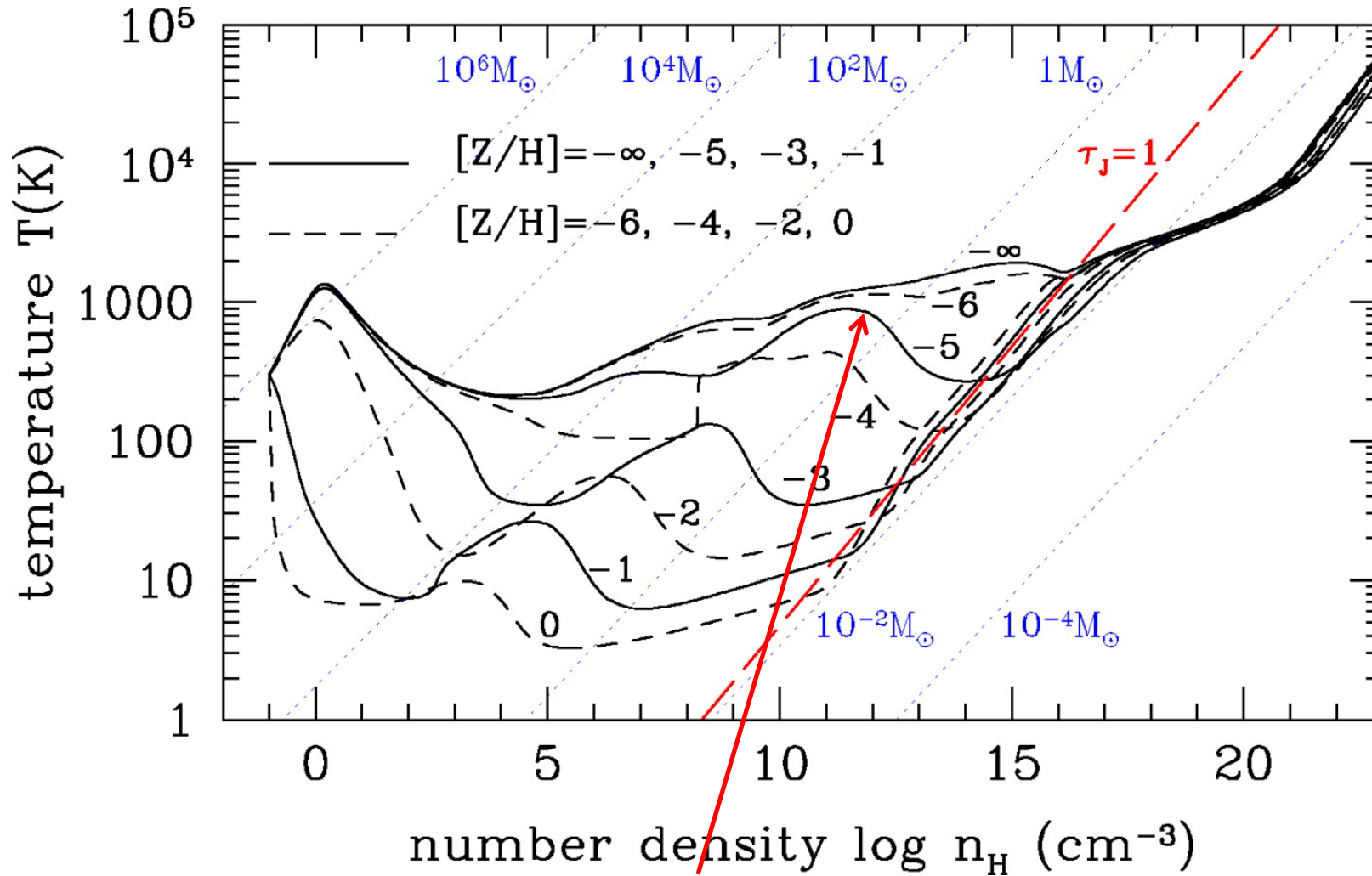
Due to these differences, the Pop III.2 stars do not become as massive as Pop III.1 stars.

Metallicity effect on the formation of Pop III



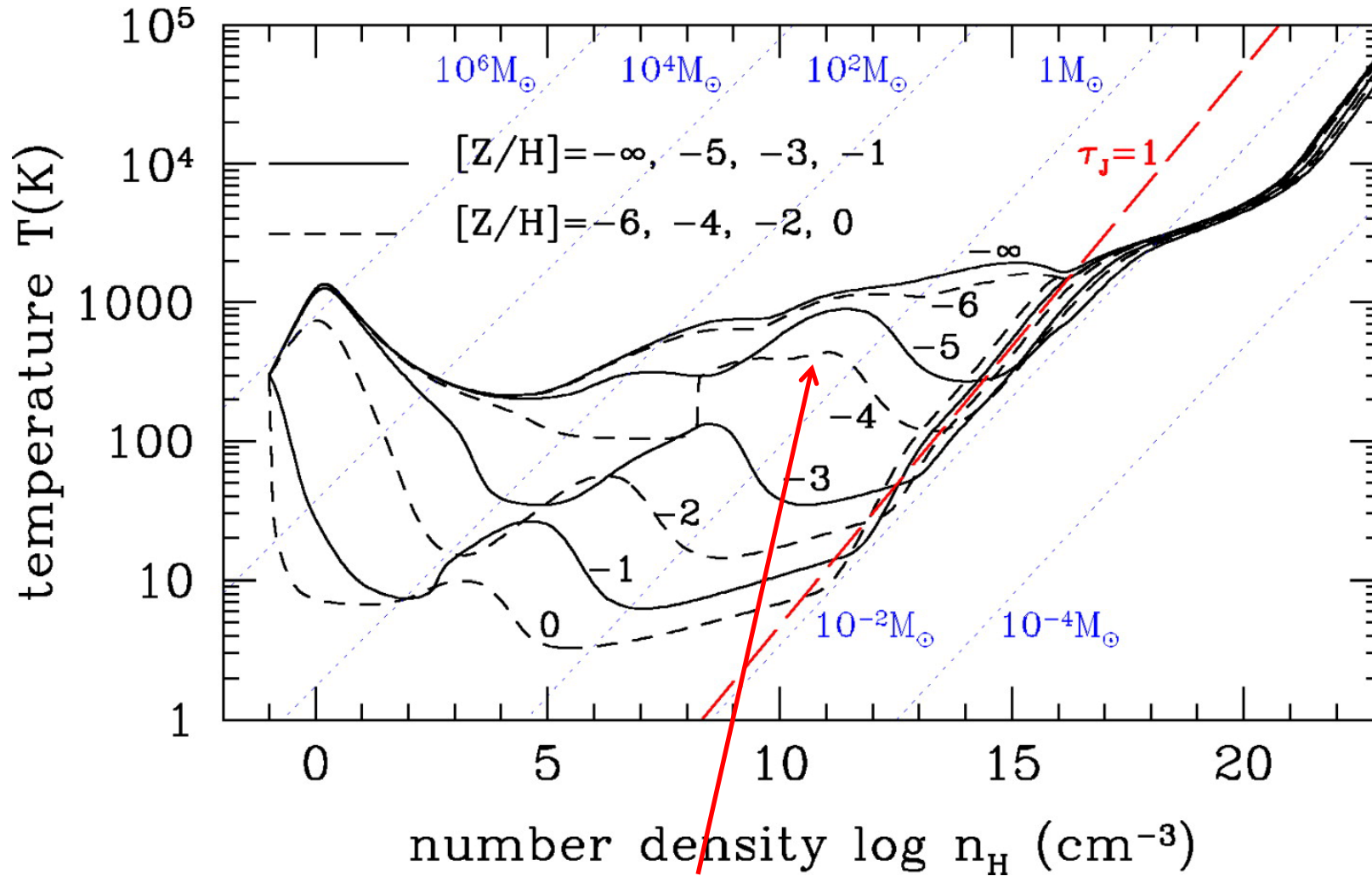
Omukai et al. (2005)

Metallicity effect on the formation of Pop III



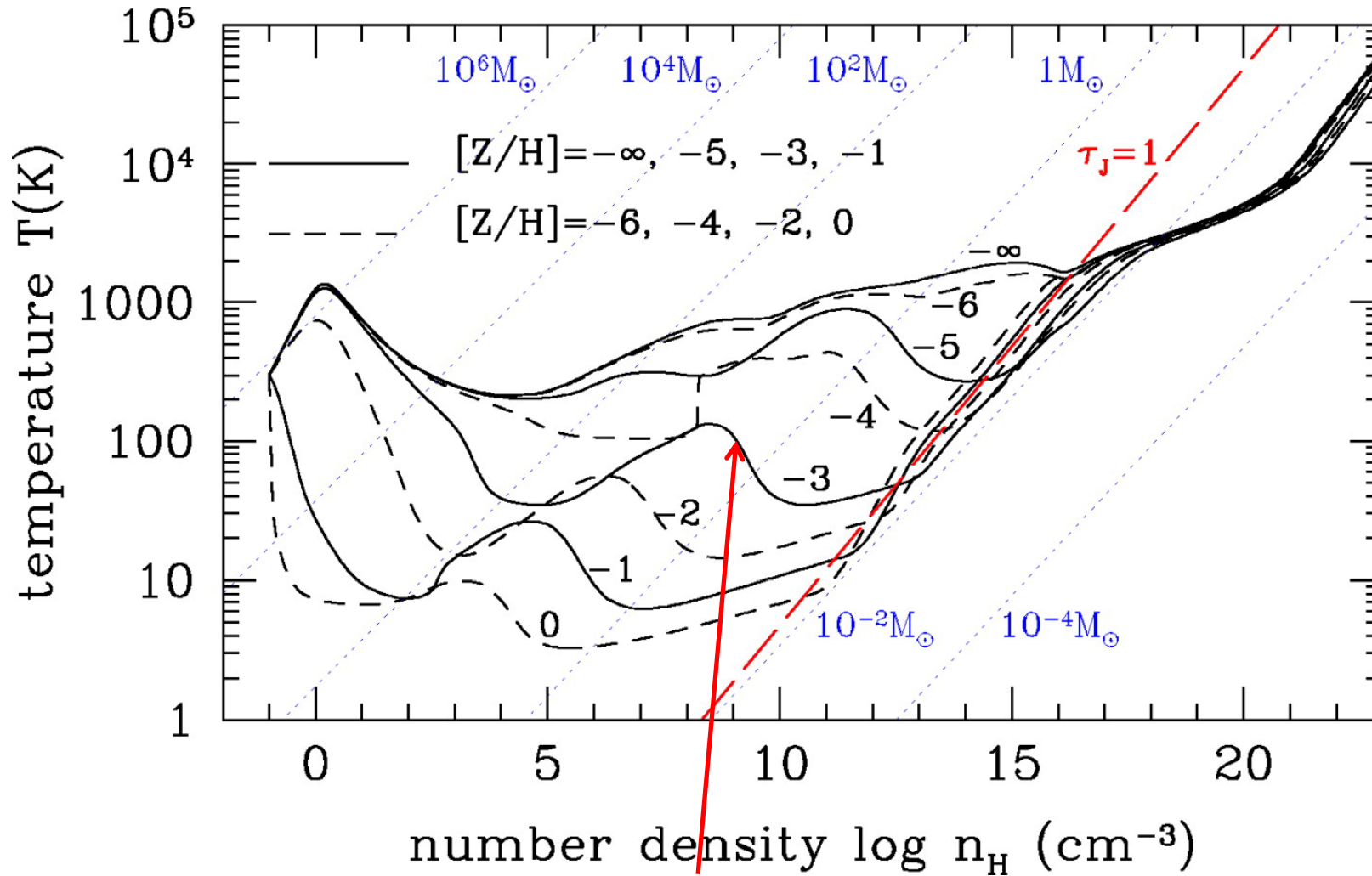
1. Cooling of gas by **dust emission** starts at $[Z/H] \approx -5$

Metallicity effect on the formation of Pop III



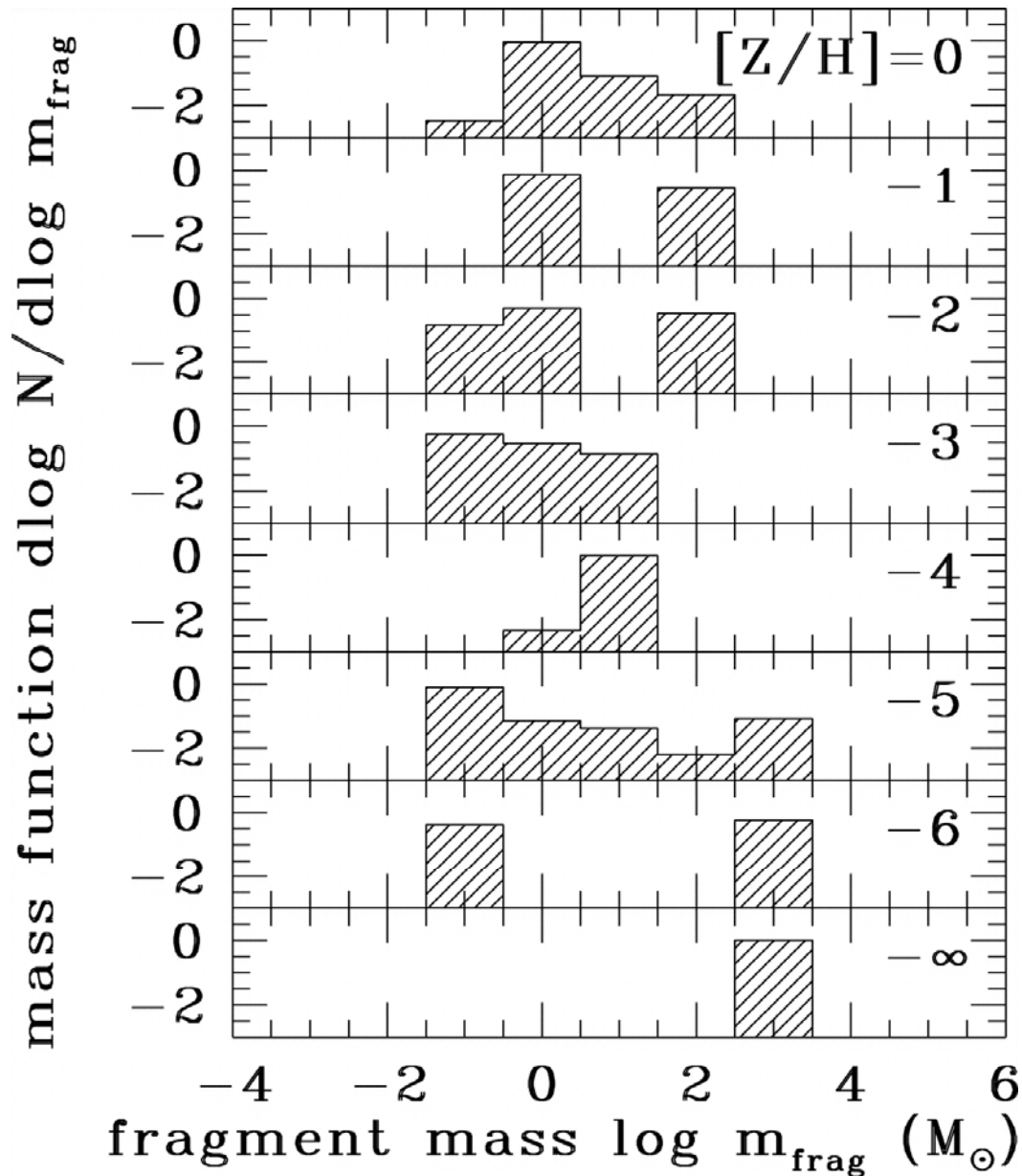
2. Formation of H_2 molecule on dust grains starts at $[Z/H] \approx -4$

Metallicity effect on the formation of Pop III



3. Gas cooling by **HD emission line** starts at $[Z/H] \approx -3$

Metallicity effect on the IMF of Pop III



The IMF of the fragments of gas with different metallicities.

With zero metallicity, the mode of star formation is that of Pop III.1 with which only very massive stars form. Then, with increasing metallicity, the Pop III.2-II mode becomes significant and low-mass star formation occurs.

Omukai et al. (2005)

Population III star formation: summary

1. Pop III stars

i. Pop III.1 (first generation)

Forms in minihalo, cooling only by H₂ molecules.

Typically very massive (100-1000 M_⊙)

ii. Pop III.2 (second generation)

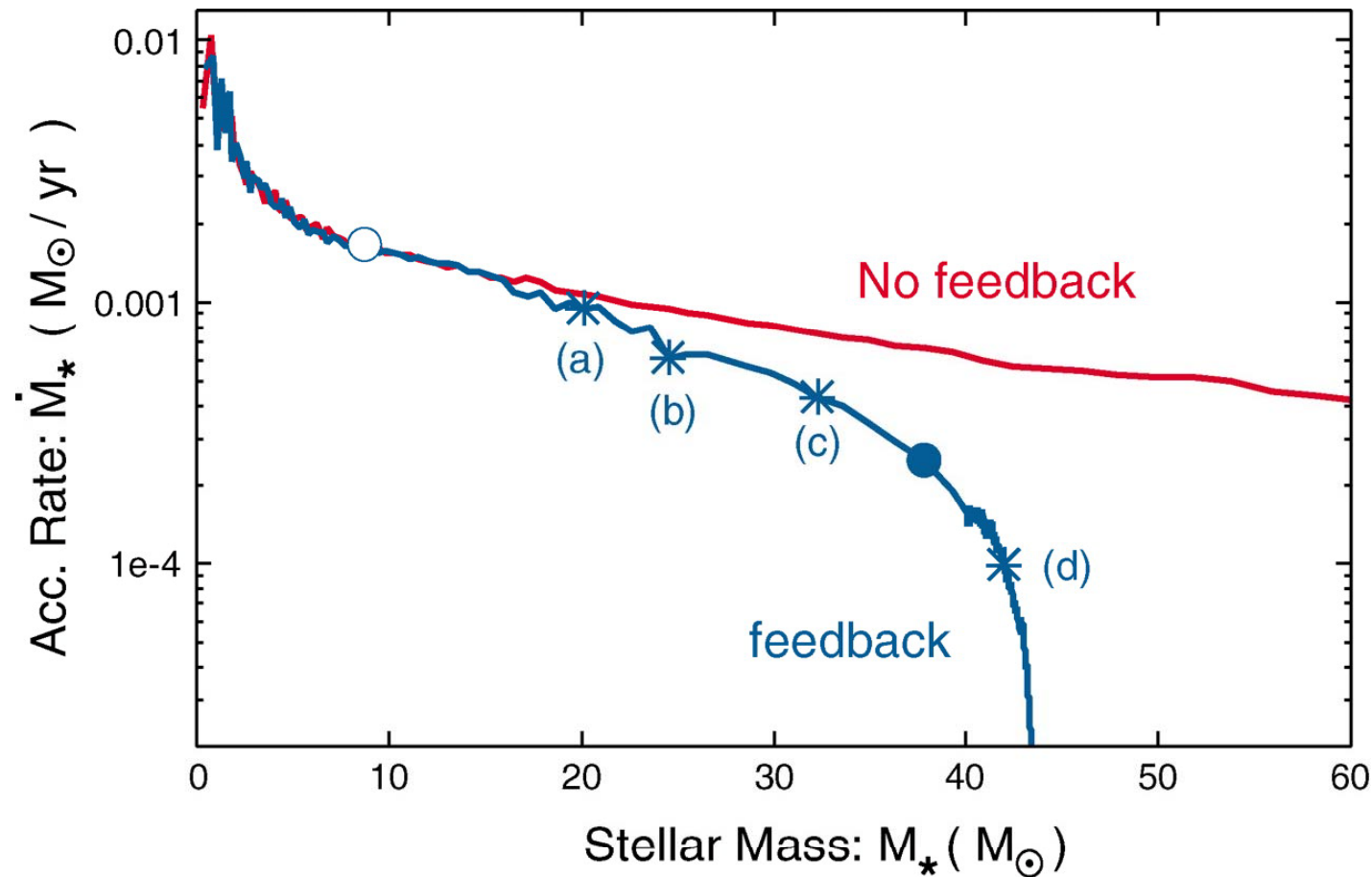
Cooling by HD, etc.

Less massive than Pop III.1.

2. Even a tiny amount of metals ($\sim 10^{-5}Z_{\odot}$) alters the mode of star formation from Pop III.1 to Pop III.2.

3. Because of two different modes in contraction, the IMF has a bimodality when the metallicity is low. With increasing metallicity, the two peaks of the IMF gradually merge and it becomes unimodal.

Population III star formation: latest result



However, Hosokawa et al. (2011) have shown that the feedback stops the mass accretion and the final mass of the Pop III stars cannot be high, only up to 40 M_\odot . Still there is a controversy.

7.3 HI cosmology: prelude to the SKA

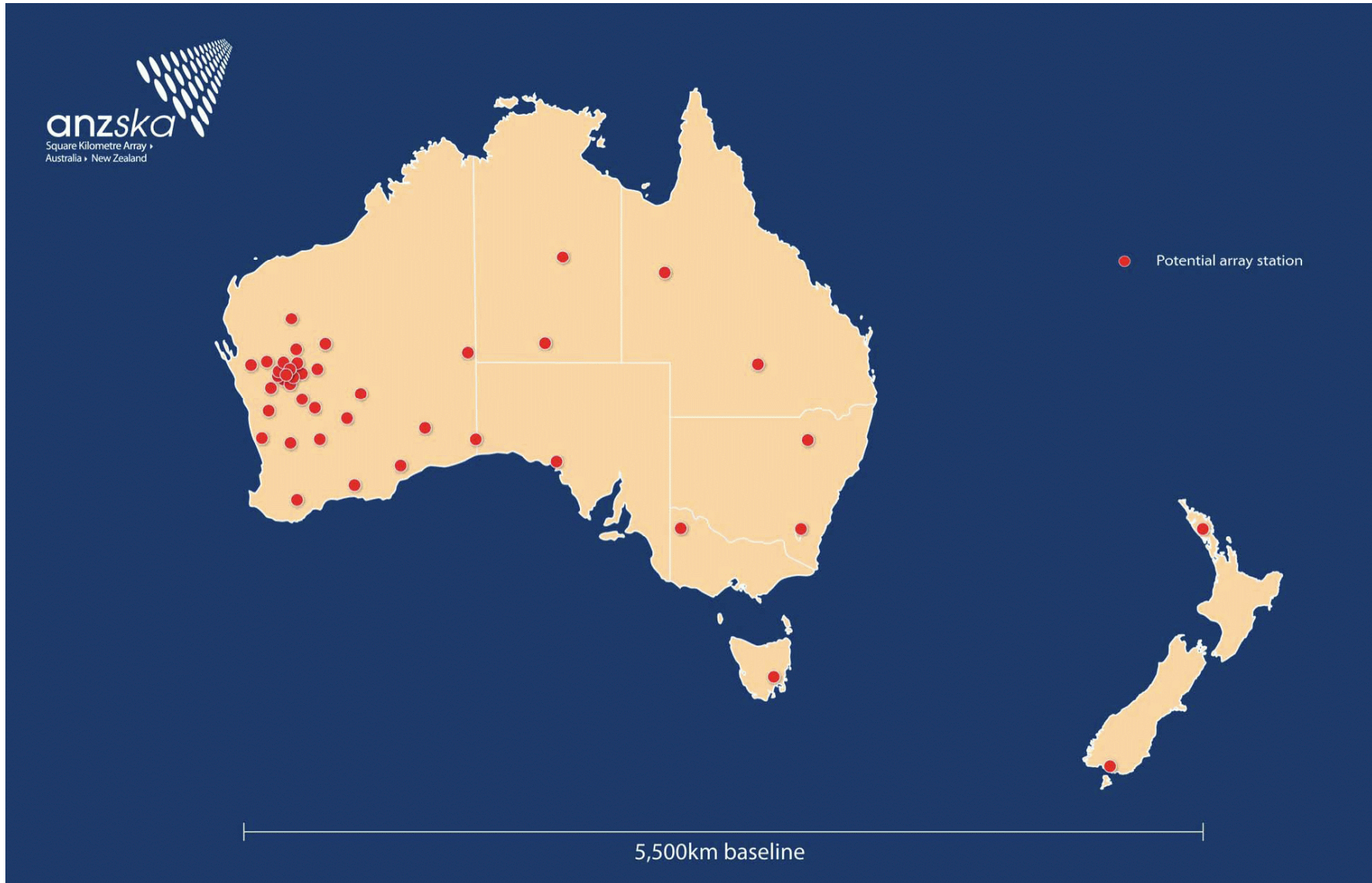
7.3.1 Square Kilometre Array (SKA)

- **A huge radio interferometer with a total antenna area of 1 km²**
 - **More than 10 countries joined officially, and 20 countries are interested in it.**
 - **Frequency: 0.1GHz - 10GHz (lower than ALMA)**
 - **Total antenna number: 15m antennas × 3000**
 - **Longest baseline: 3000 km**
 - **Location: Australia (SKA-low) and South Africa (SKA-mid)**
 - **Feature: high frequency resolution, high angular resolution, wide area, wide frequency coverage**
- ⇒ **Ultimate long-wavelength continental radio telescope!**

SKA-low: artist's view



SKA-low: location



SKA-mid: artists' view



SKA-mid: location



7.3.2 Specs of SKA

SKA1 (Phase 1)

- **About 10% of the ultimate specs of SKA**
- **Two topics are focused as the important themes of SKA1**
 - 1. History of HI from the dark age to the present.**
 - 2. Gravitational wave detection by pulsar observations.**

Parameter	Value
Frequency Range: Antennas	
SKA ₁ Low: (sparse aperture arrays)	70 – 450 MHz
SKA ₁ Mid: (dishes)	
Capability range	0.3 – 10 GHz
Initial baseline implementation	0.45 – 3.0 GHz
Baseline instrumentation	
SKA ₁ Low:	70 – 450 MHz 2000 m ² /K
SKA ₁ Mid:	0.45 – 3.0 GHz 1000 m ² /K
SKA ₁ Advanced Instrumentation Program	<i>e.g.</i> <i>High-frequency feeds,</i> <i>Field-of-view expansion</i> <i>technology,</i> <i>AA digital upgrades,</i> <i>Ultra-wide-band feeds etc.</i>
Frequency resolution (low-band):	1 kHz
Time resolution:	
Tied Array Beam (pulsars, VLBI)	1 nsec
Pulsar search equipment	0.1 msec
Max. baseline length from core	100 km

SKA2 (Phase 2)

Ultimate SKA. Final details will depend on the technical development and scientific requirement.

Parameters

Frequency range	70MHz ~ 10GHz
Sensitivity	5,000 m²K⁻¹ (400 μJy min⁻¹)
FoV	200 deg² (70 ~ 300 MHz), 1-200 deg² (0.3 ~ 1 GHz), max 1 deg² (1 ~ 10 GHz)
Angular resolution	< 0.1 arcsec
Bandwidth (simultaneous)	band center ± 50%
Spectral channels	16,384 per band per baseline
Precision of polarization	10,000:1

7.3.3 Comparison with present-day facilities

		JVLA	MeerKAT	SKA1- mid	ASKAP	SKA1- survey	LOFAR- NL	SKA1- low
A_{eff}/T_{sys}	m ² /K	265	321	1630	65	391	61	1000
Survey FoV	deg ²	0.14	0.48	0.39	30	18	6	6
Survey Speed FoM	deg ² m ⁴ K ⁻²	0.98×10 ⁴	5.0×10 ⁴	1.0×10 ⁶	1.3×10 ⁵	2.8×10⁶	2.2×10 ⁴	6.0×10 ⁶
Resolution	arcsec	1.4	11	0.22	7	0.9	5	11

A_{eff}/T_{sys}:

6xJVLA

6xASKAP

16xLOFAR

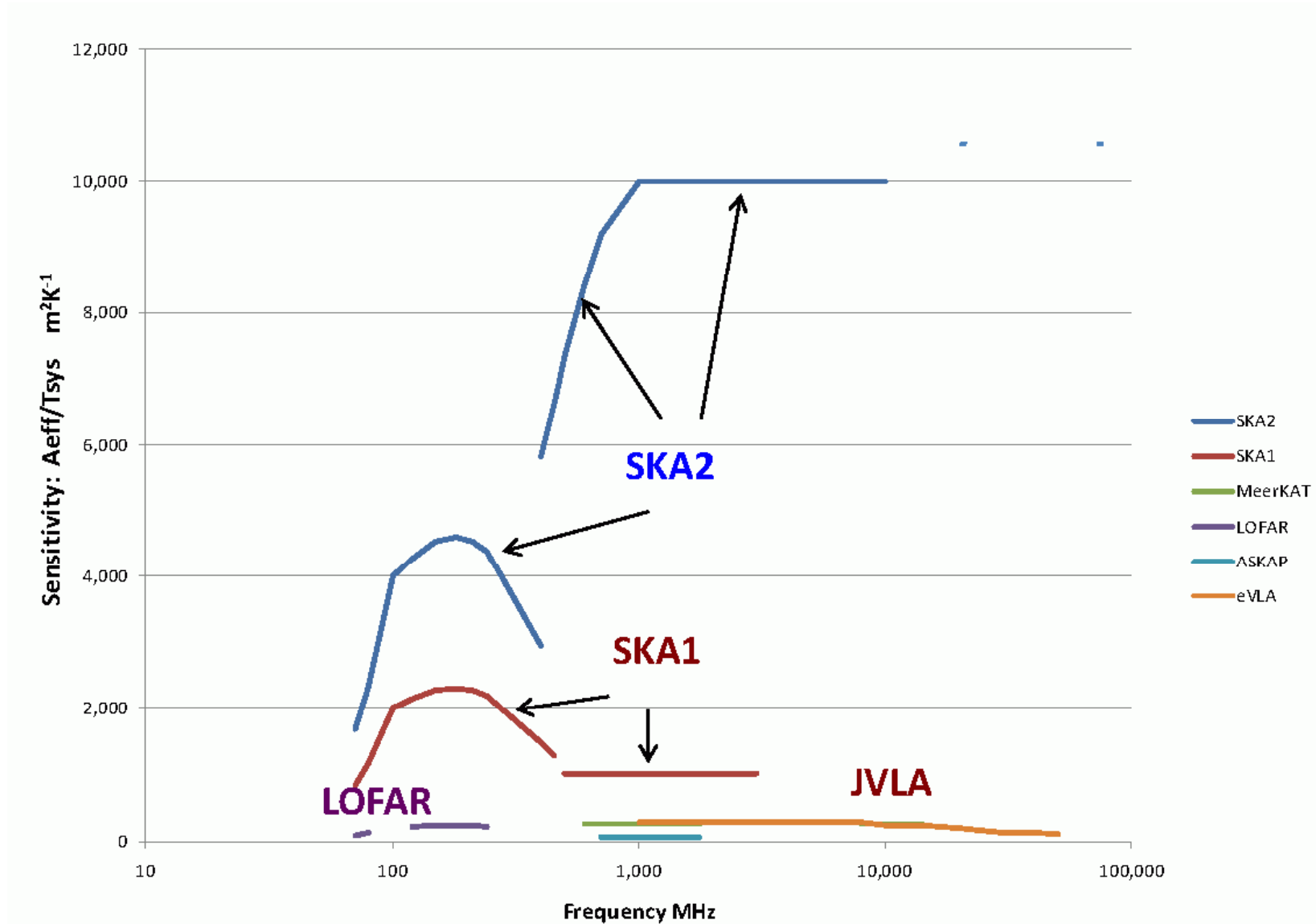
Survey Speed:

100x

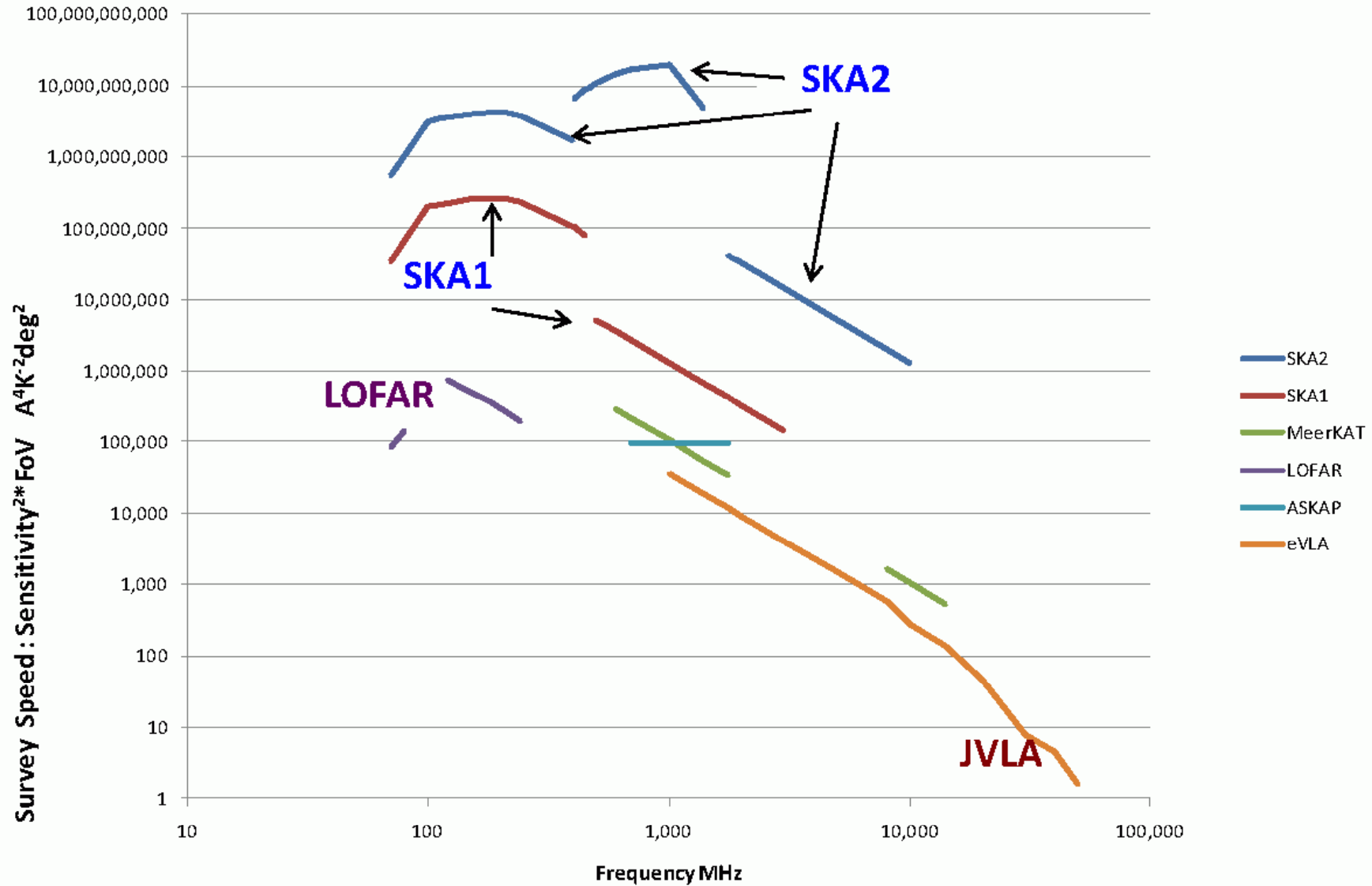
22x

270x

Comparison of SKA with other facilities: sensitivity

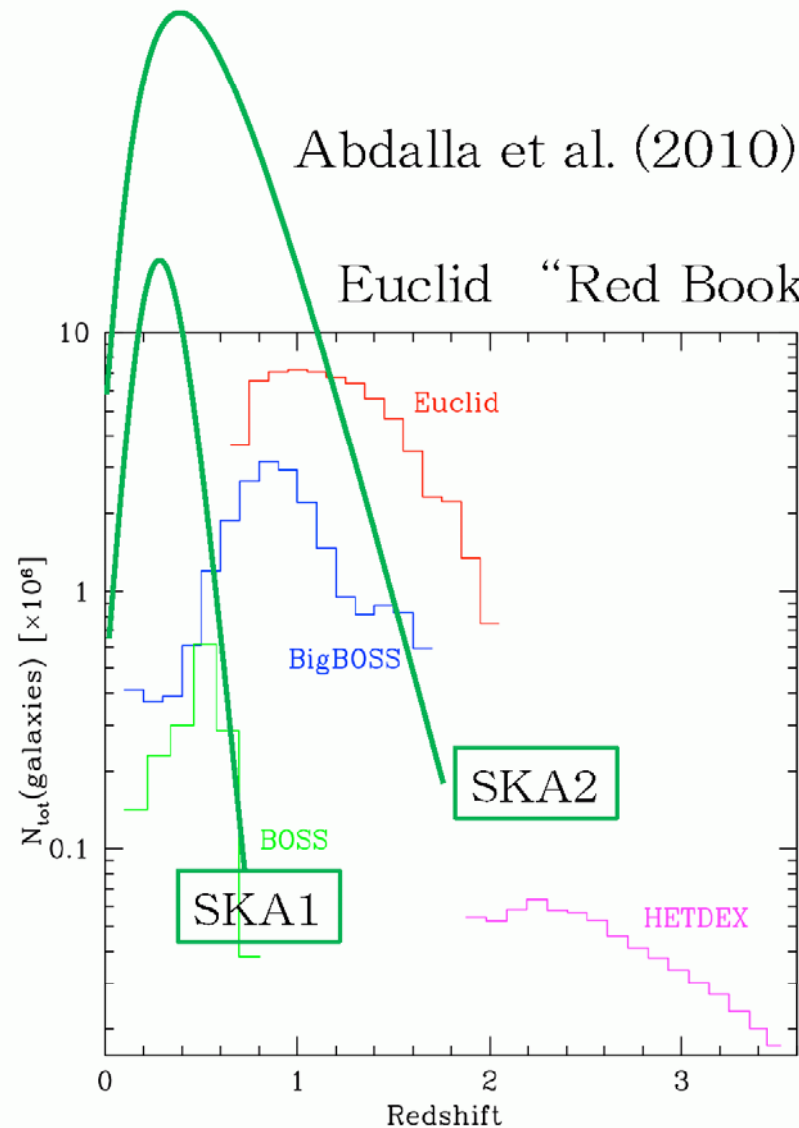


Comparison of SKA with other facilities: survey speed



7.3.4 Expected redshift distribution

Expected HI redshift distribution



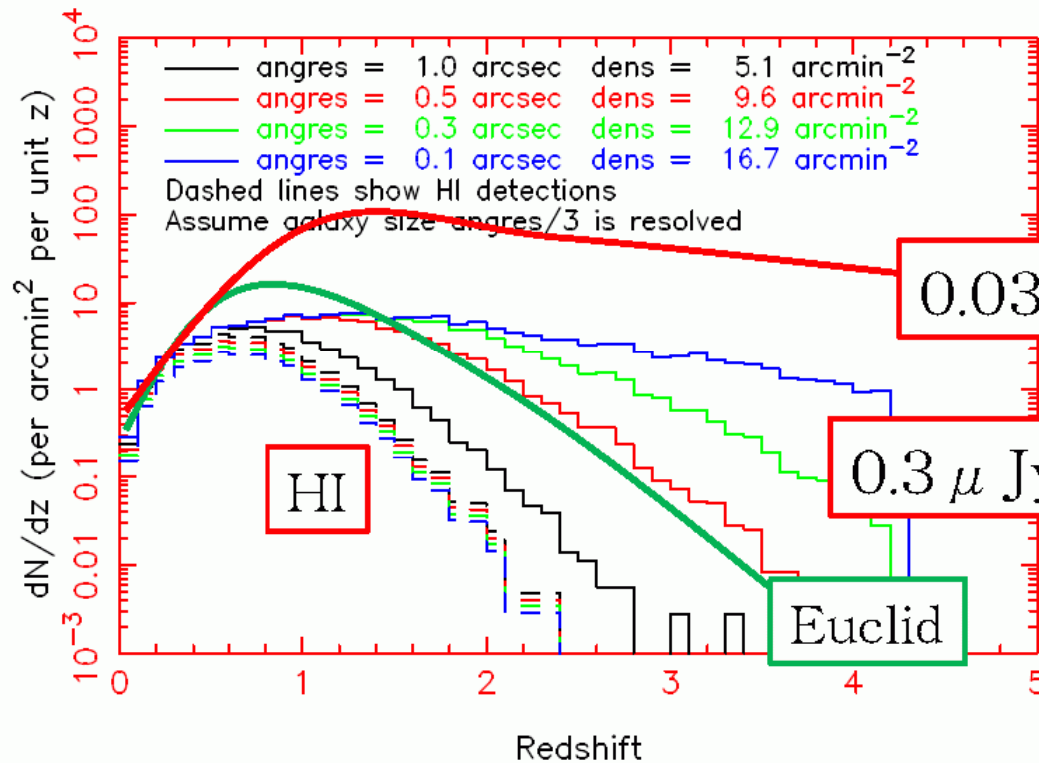
The redshift distribution of HI galaxies has a peak at $z \sim 0.4$ for SKA1 survey, and $z \sim 0.6$ for SKA2.

Most of the sources are at $z < 2$.

7.3.4 Expected redshift distribution

Expected radio continuum source redshift distribution

The redshift distribution of radio continuum sources is more extended toward high- z than HI.



(Blake et al. 2007)

N.B. However, this expectation is based on a certain galaxy evolution model, which is to be examined by SKA. See, e.g., Mancuso et al. (2015)

7.3.5 New topics in galaxy evolution

Galaxy evolution at SKA frequency

Existing HI surveys are shallow ($> \text{mJy}$), with poor angular resolution.

NRAO VLA Sky Survey (NVSS)

Sydney University Molonglo Sky Survey (SUMSS)

Faint Images of the Radio Sky at Twenty-cm (FIRST)

Westerbork Northern Sky Survey (WENSS)

The HI Parkes All Sky Survey (HIPASS)

The HI Jodrell All Sky Survey (HIJASS)

The Arecibo Legacy Fast ALFA Survey (ALFALFA)

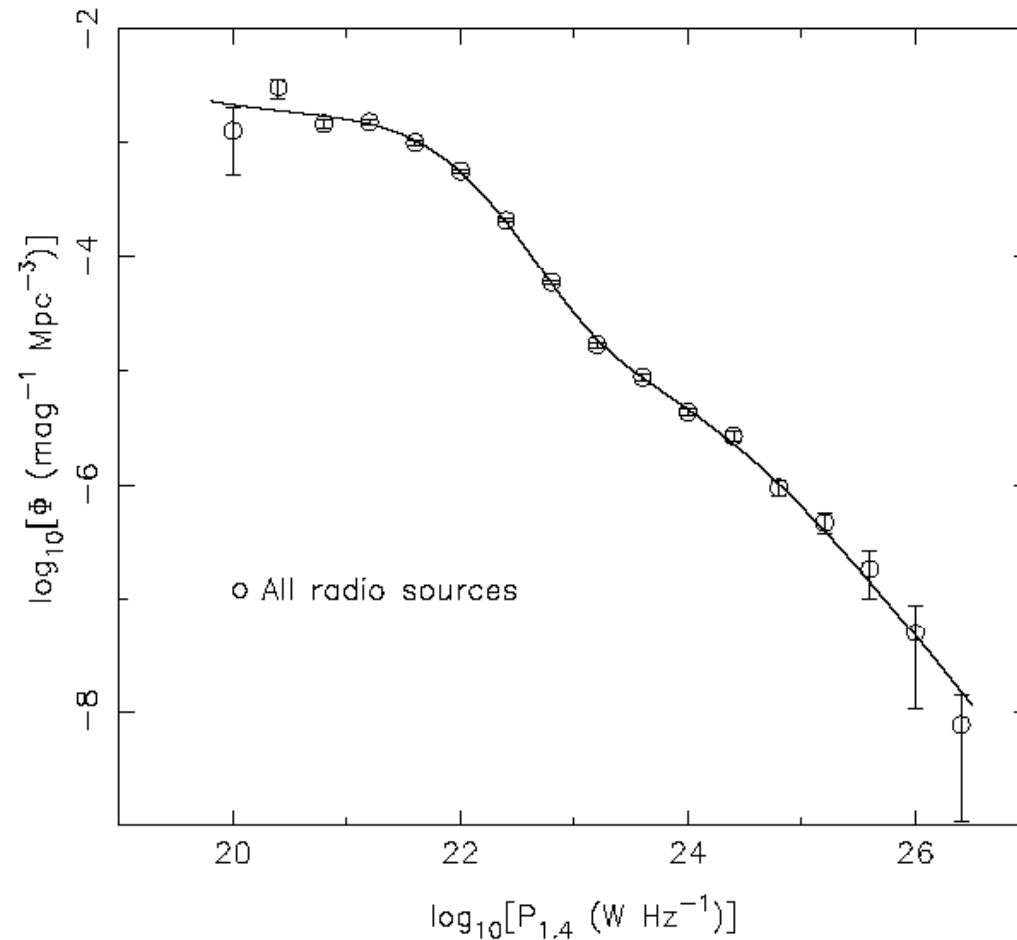
etc.

$\langle z \rangle \sim 0.01-0.06$

\Rightarrow We can examine the properties statistically only for nearby galaxies, and it is difficult to discuss their evolution.

Luminosity function at radio wavelengths

1.4 GHz continuum luminosity function



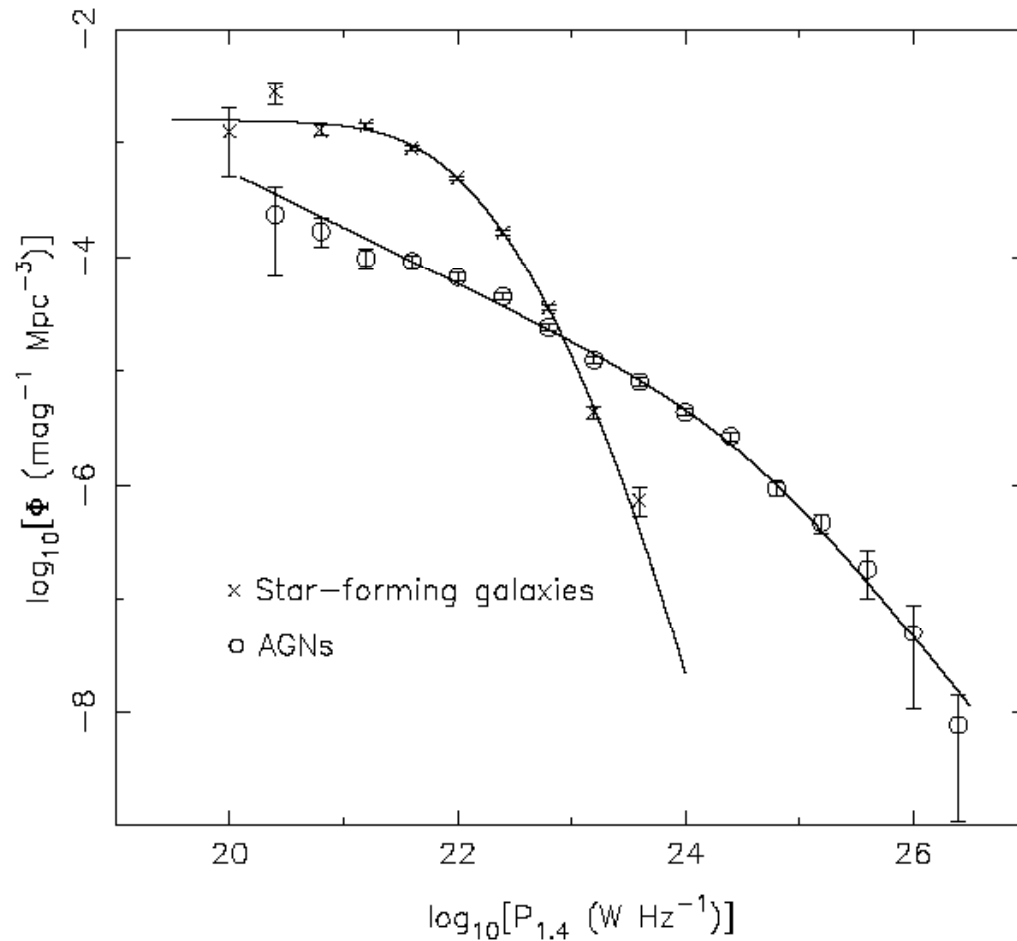
Galaxy LF at 1.4GHz by NVSS and 6dFGS.

We note that the radio LF cannot be well described by Schechter function, unlike optical, UV or NIR.

Neither by the double-power-law, unlike FIR or X-ray LF.

(Mauch & Sadler 2007)

1.4 GHz continuum luminosity function

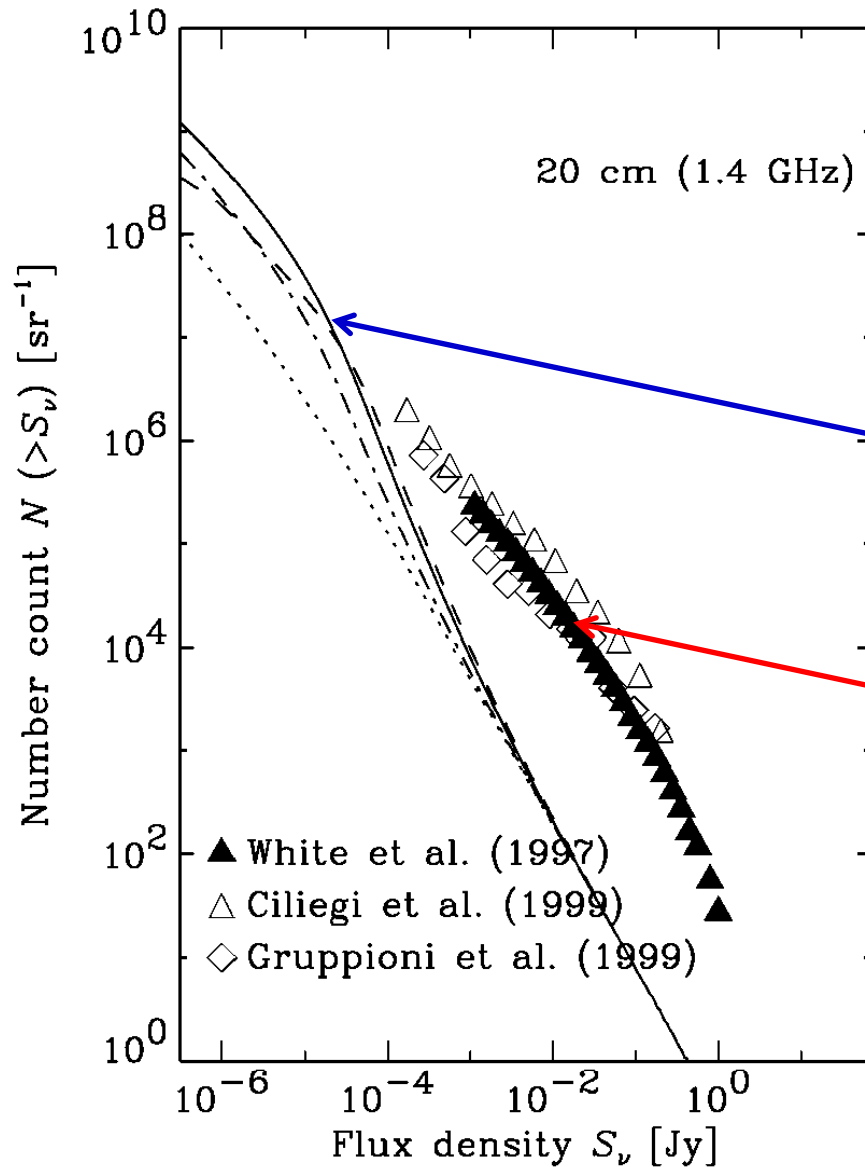


If we plot the LFs of SF galaxies and AGNs (radio galaxies), we find that there are two power-law function components (Machalski & Godlowski 2000; Mauch & Sadler 2007)

⇒ Do they evolve?

(Mauch & Sadler 2007)

Radio number counts



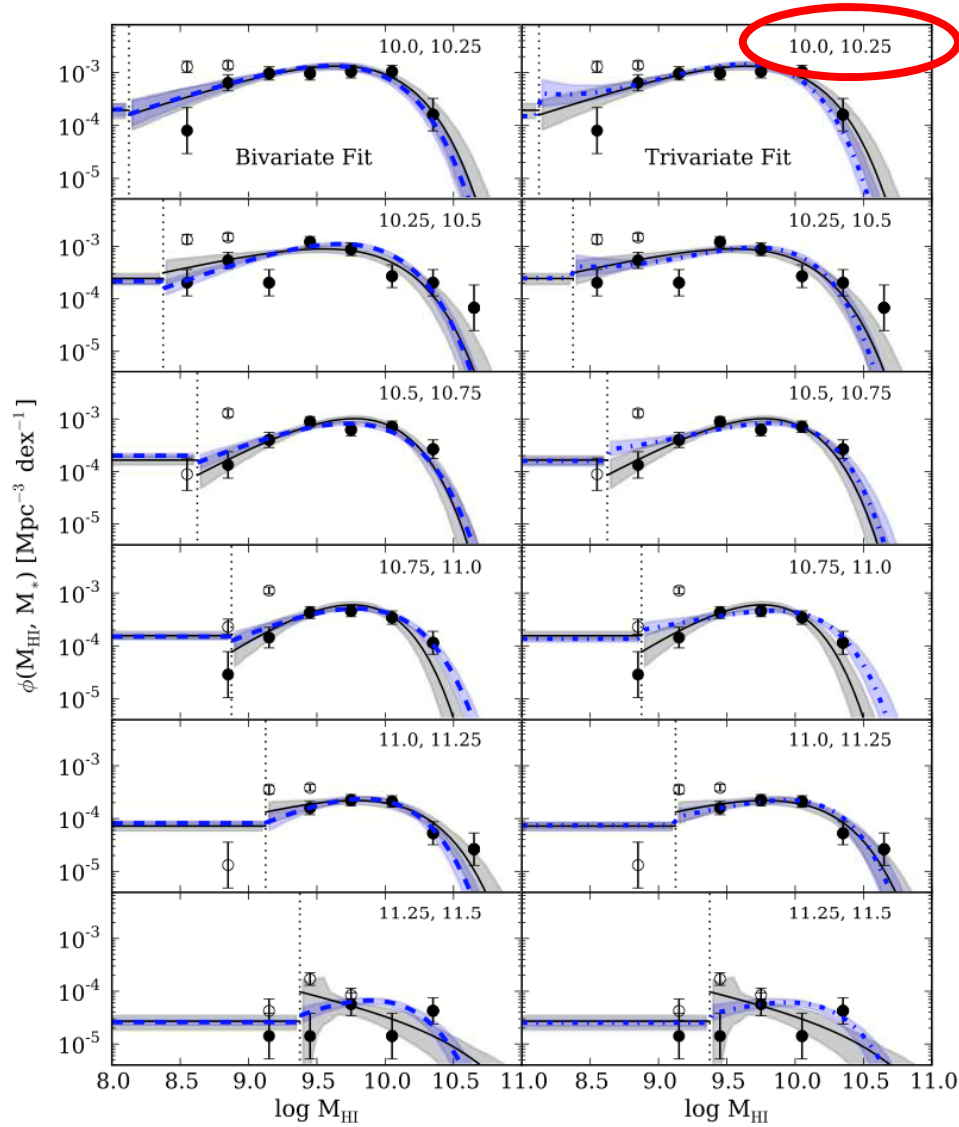
Different evolutions of SF galaxies and AGNs are suggested from number counts (Takeuchi et al. 2001).

Model NC of SF galaxies

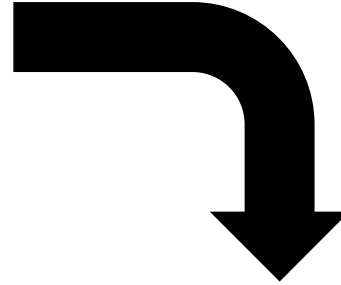
Observed: at bright fluxes, AGNs with developed lobes dominate the counts.

See also Mancuso et al. (2015)

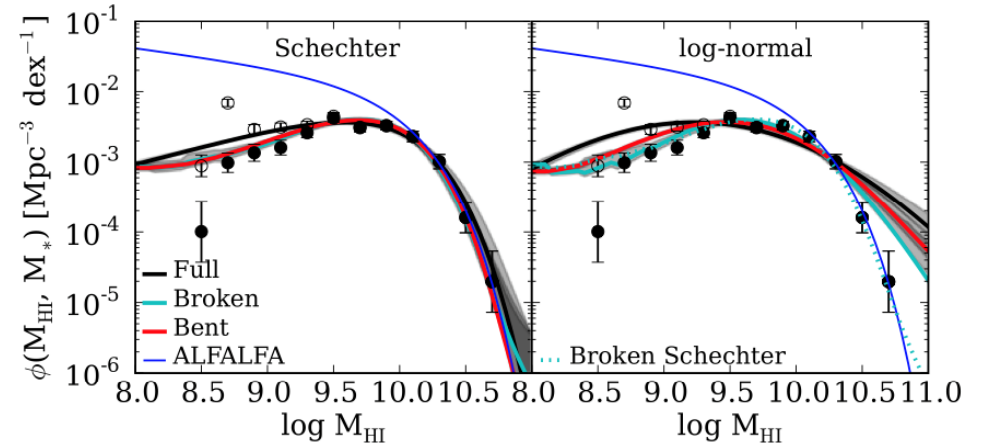
HI mass function (GASS)



Stellar mass range



HI mass function

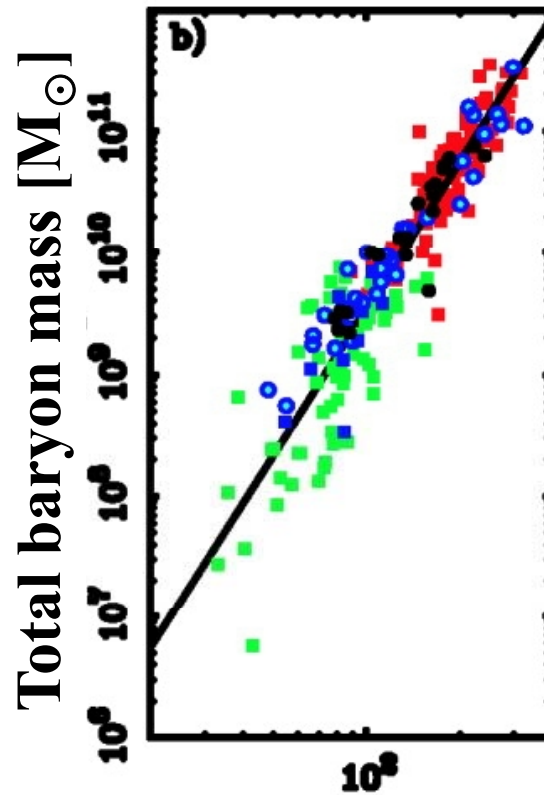
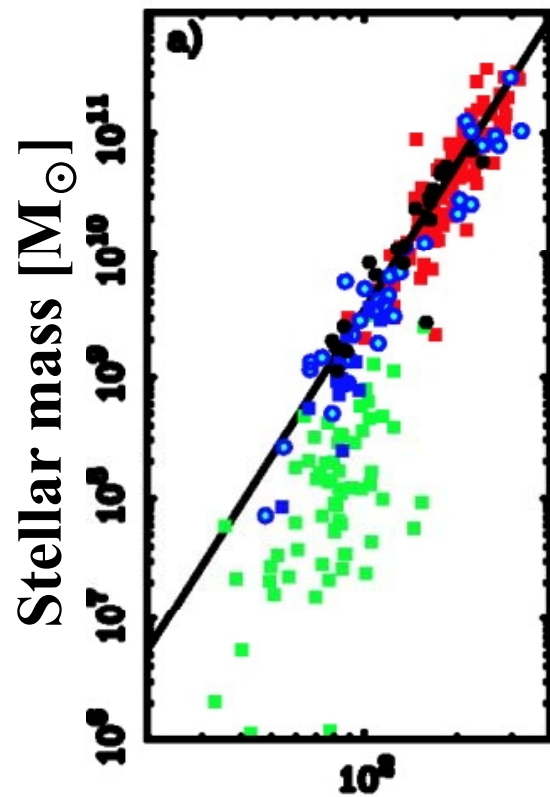


(Lemonias et al. 2013)

HI MF gives an important constraint on the theory.

Scaling laws including gas properties in galaxies

Baryonic Tully-Fisher (BTF) relation



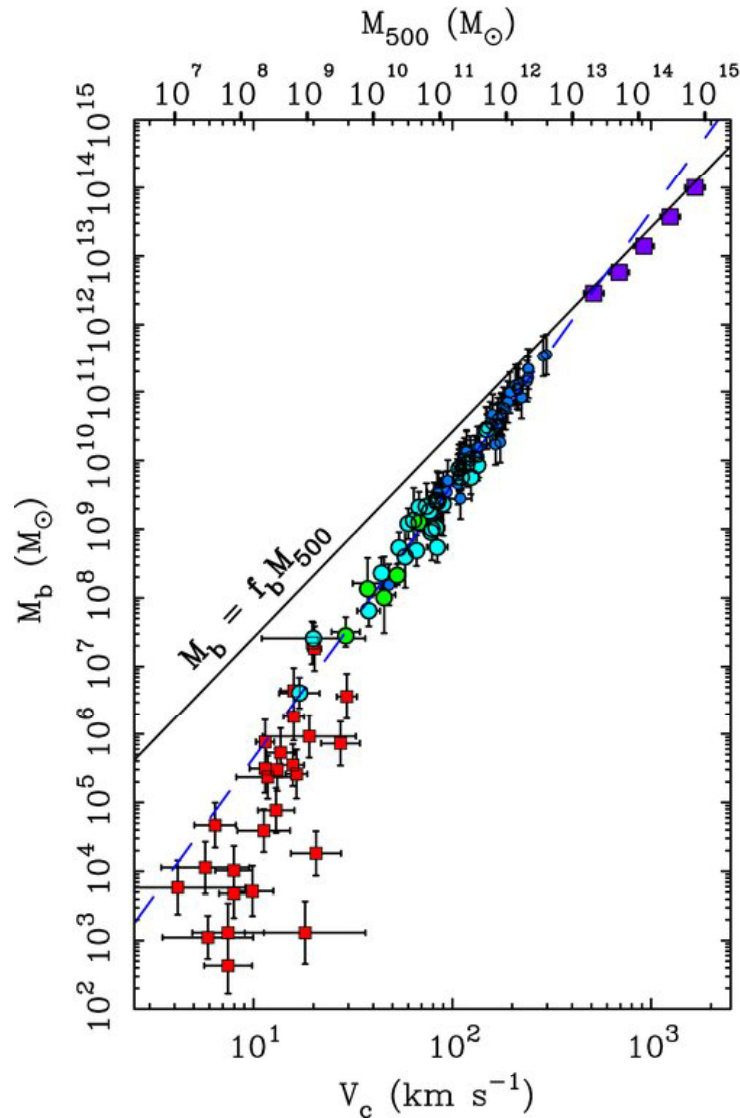
$$M_d = AV_c^b$$
$$b = 3.98 \pm 0.12$$

Circular velocity [kms⁻¹]

(McGaugh et al. 2000)

If HI mass is taken into account and we construct a relation between baryonic mass and circular velocity, linearity is recovered (McGaugh et al. 2000).

The “extended” BTF



(McGaugh et al. 2010)

In the extended BTF, the slope becomes shallower from dwarf spheroidals, normal galaxies, to clusters (clusters: violet symbols, giant galaxies: blue symbols, and dwarf spheroidals: red symbols).

⇒ Feedback?

However, this sample does not include gas-rich dwarf galaxies.

Toward lower HI masses!

Required sensitivity to examine the scaling relations of nearby galaxies

To detect the HI emission down to galaxies with HI mass = $10^3 M_{\odot}$ ($\sim M_{\text{baryon}}$ of dSph) at 3 Mpc, we need

$$S_{\nu} = 50 \left(\frac{M}{10^3 M_{\text{sun}}} \right) \left(\frac{v}{10 \text{ km s}^{-1}} \right)^{-1} [\mu\text{Jy}]$$

\Rightarrow SKA1 can achieve this sensitivity.

Star forming galaxy main sequence

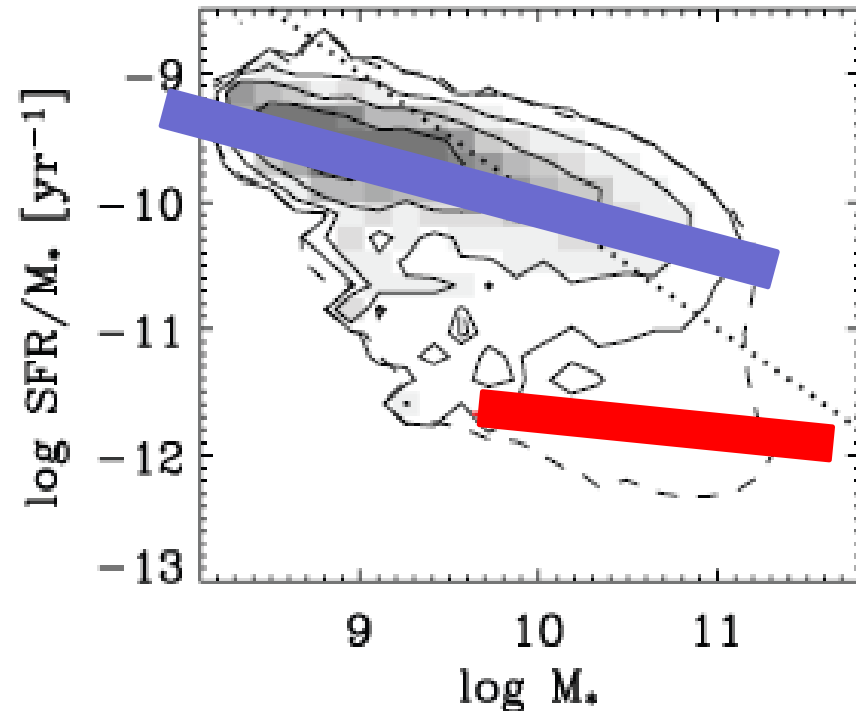
Since **the SFR** is the most interesting quantity, we want to examine the scaling relations including the SFR.

Specific star formation rate (SSFR)

$$\text{SSFR} = \frac{\text{SFR}}{M_*}$$

A prominent sequence of SF galaxies is found on the stellar mass-SSFR plane: **star-formation main sequence (SFMS)**.

cf. The SFMS corresponds to the blue cloud on the color-magnitude diagram.



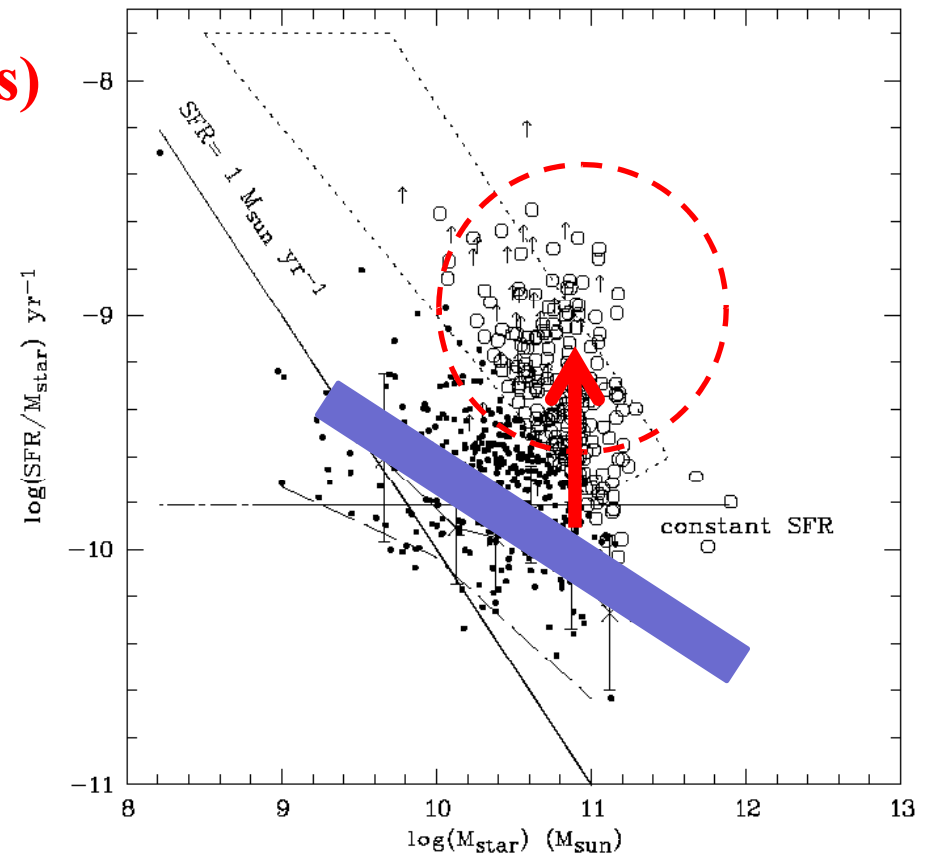
(Schiminovich et al. 2007)

Star forming galaxy main sequence

The SFMS is a sequence of galaxies with a secular evolution (i.e., not merger).

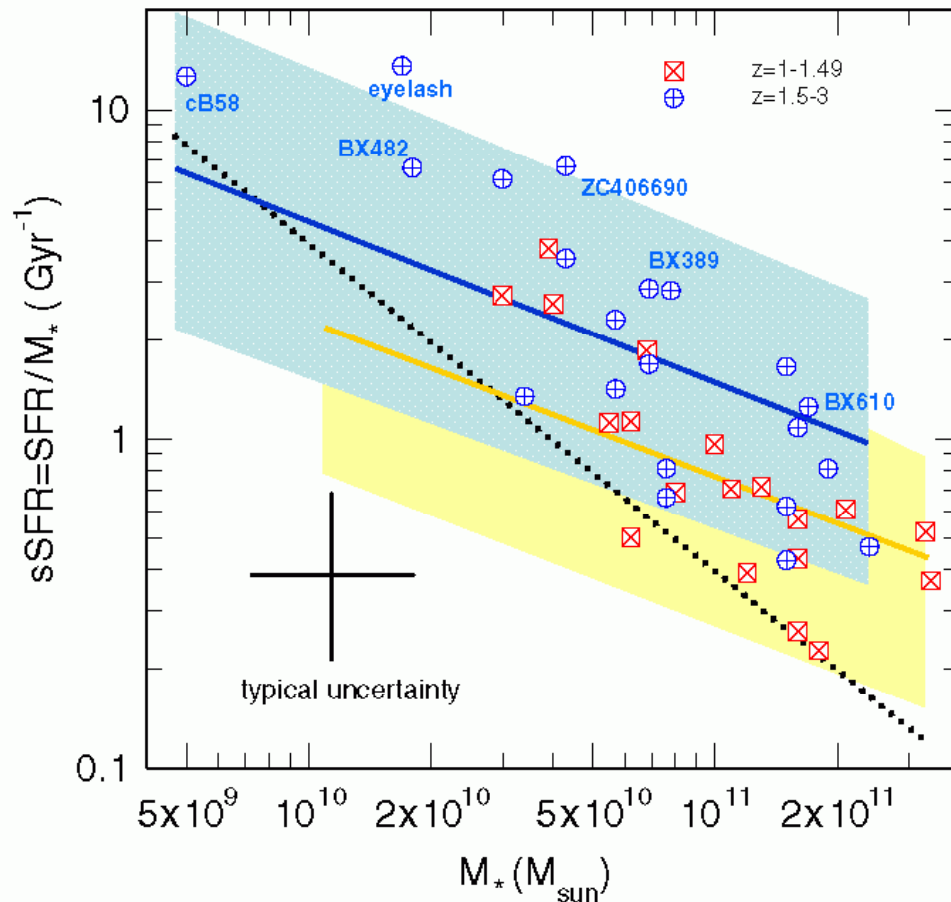
Starburst galaxies (e.g., ULIRGs) strongly deviate from the SFMS (e.g., Buat et al. 2007).

(Buat et al. 2007)



Star forming galaxy main sequence

The SFMS is a sequence of galaxies with a secular evolution (i.e., not merger).



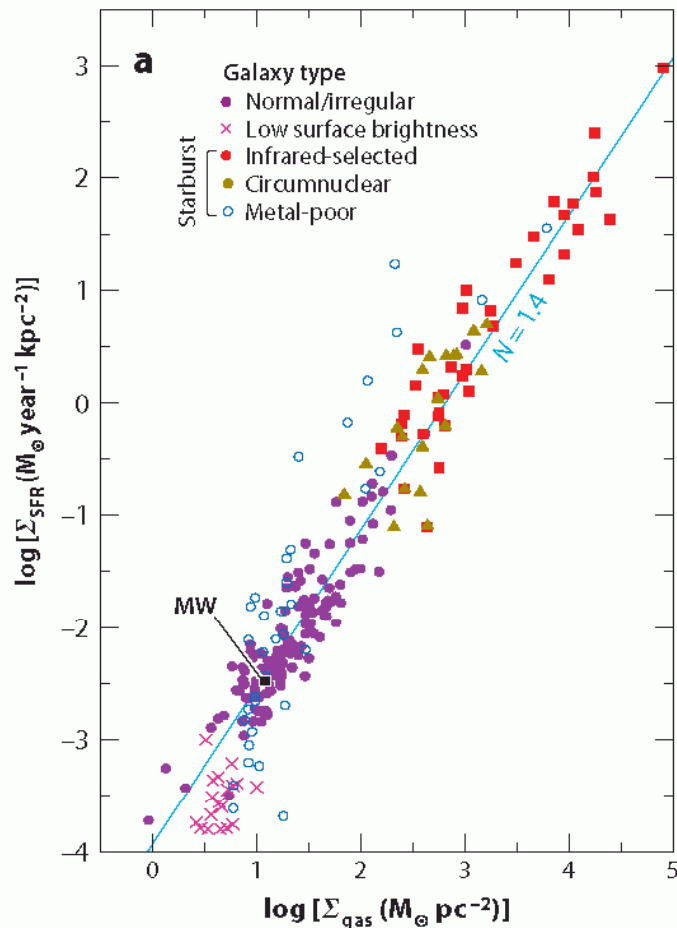
(Genzel et al. 2012)

Dependence on various quantities are examined (dust temperature, clumpiness, etc., particularly the relation to the molecular gas mass (Genzel et al. 2012; Magnelli et al. 2012).

Some CO observations reach redshifts of $1 < z < 2$, but not yet to be called a survey. HI is far behind it.

Schmidt-Kennicutt law

By considering **the size** of a galaxy, we can discuss the relation between surface densities of gas and SFR. This is known as **the Schmidt-Kennicutt law** (see also Samuel's lecture).



The classical Schmidt-Kennicutt law is the relation between **the surface densities** of gas and SFR.

A single power law is found in a wide range of gas surface density, but the slope is still a matter of debate.

(Kennicutt & Evans 2012)

Schmidt-Kennicutt law

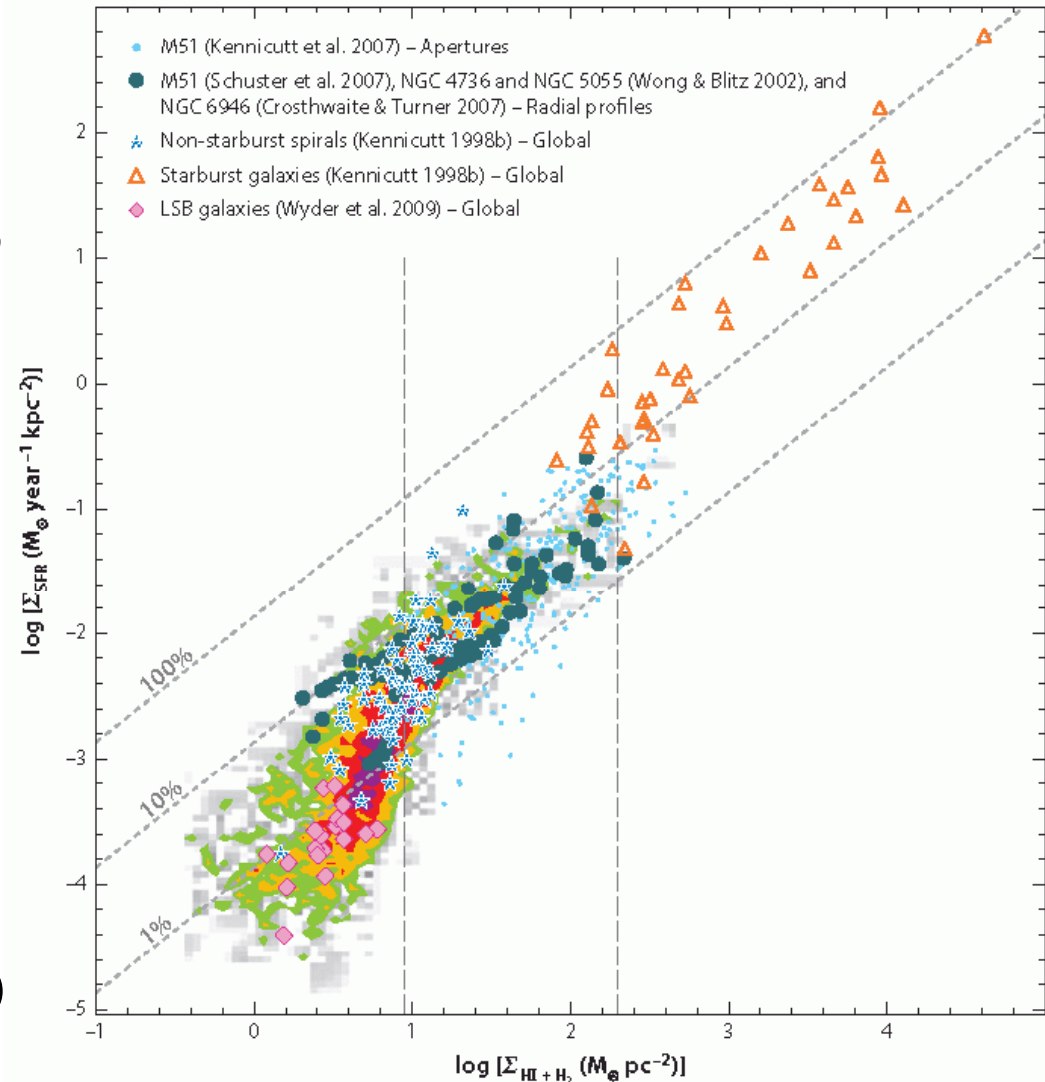
What the S-K law shows is the relation between total gas mass ($\text{HI} + \text{H}_2$) and SFR.

We need observations of HI as deep as CO ($1 < z < 2$), to explore the evolution of the S-K law.

⇒ SKA1 to SKA2

Synergy with observations of molecules is important!

(Kennicutt & Evans 2012)



Transition from HI to H₂ and star formation

Production

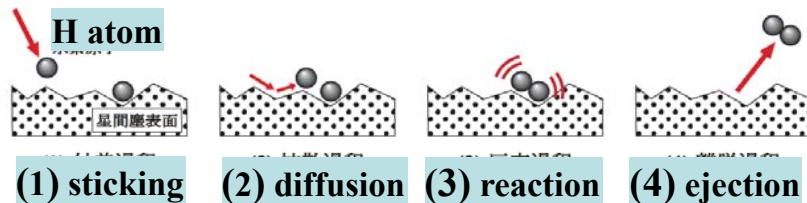
* 2-atom conjugate reaction

* 3-atom collision reaction



* Dust surface reaction

⇒ most efficient in galaxies



(Takahashi 2000)

Dissociation

* Photodissociation by UV

Not efficient in a dense dusty molecular clouds because of self-shielding.

* Dissociation by cosmic rays

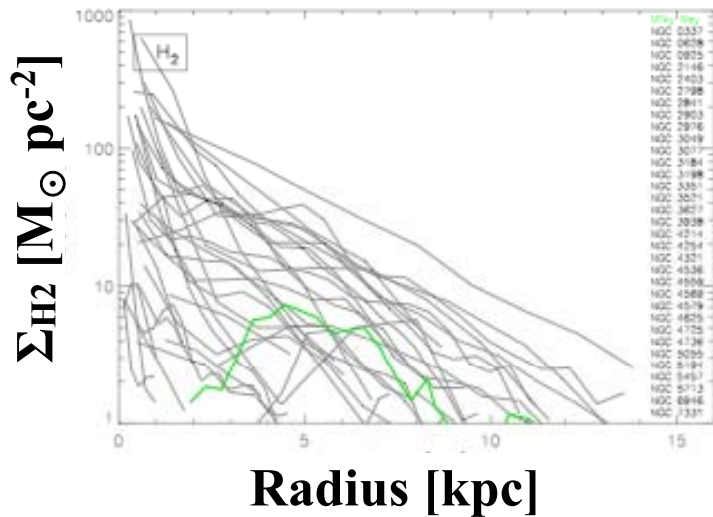
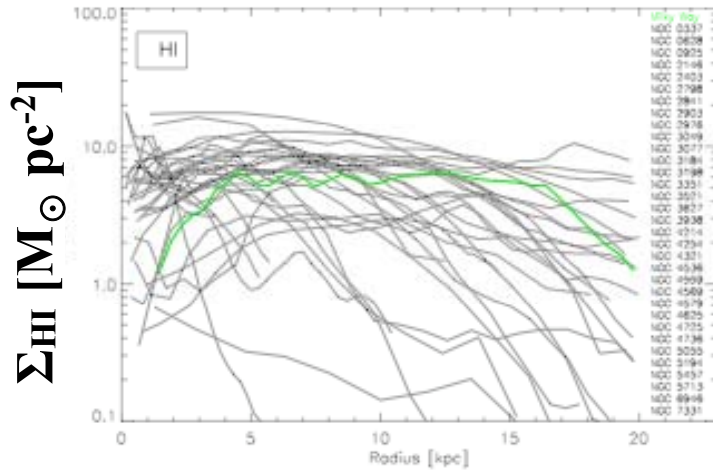
Dissociate H₂ in molecular clouds.

* Dissociation by collision

Contribution is small.

(e.g. Gould & Salpeter 1963;
Draine & Bertoldi 1996)

H₂ and HI in galaxies

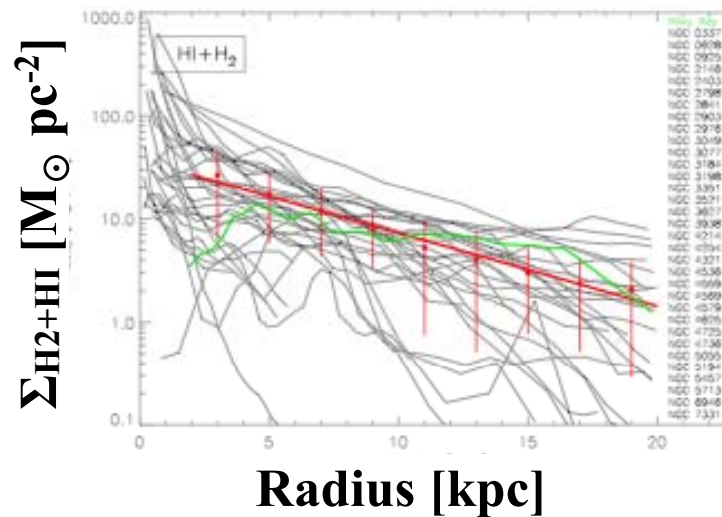


$$f_{\text{mol}} (= \Sigma_{\text{H}_2} / \Sigma_{\text{total}})$$

* For late types, $f_{\text{mol}} \sim 25\text{-}30\%$

* Radial decrease.

At galactic center, $f_{\text{mol}} \sim 1$



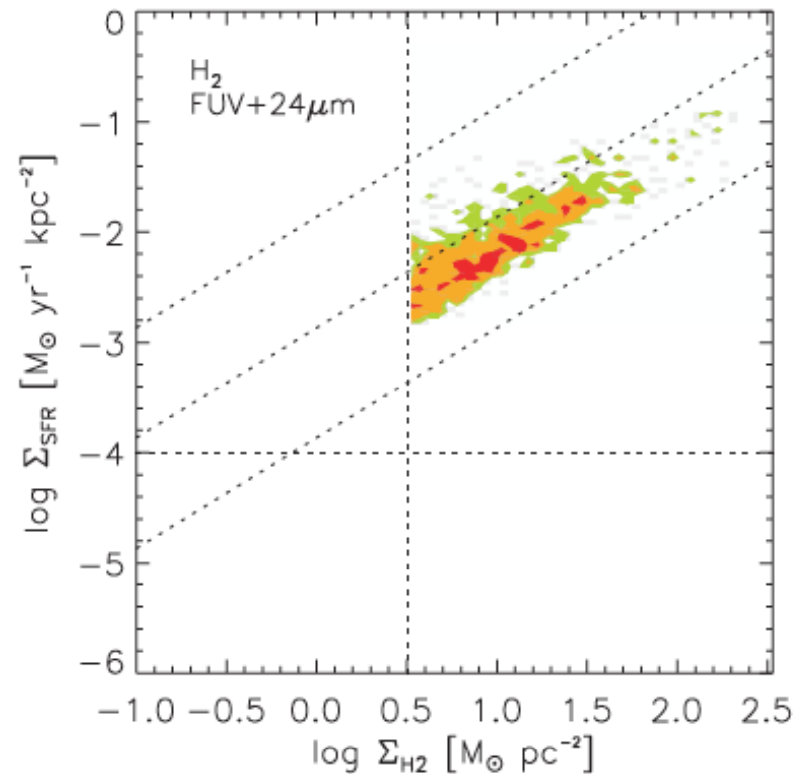
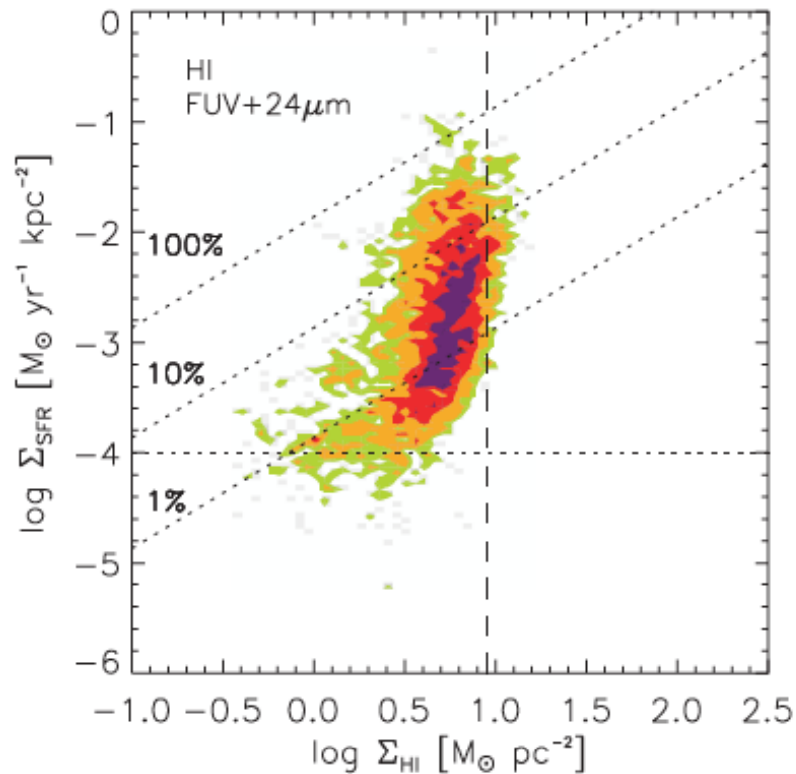
(Bigiel & Blitz 2012; Boselli et al. 2014)

Transition from HI to H₂

* Threshold density above which the photodissociation becomes efficient (Z_{\odot} is assumed):

$$\Sigma_{\text{H}_2} \sim 10 M_{\odot} \text{pc}^{-2}, N_{\text{HI}} \sim 10^{21} \text{cm}^2$$

Consistent with of local late-type galaxies.

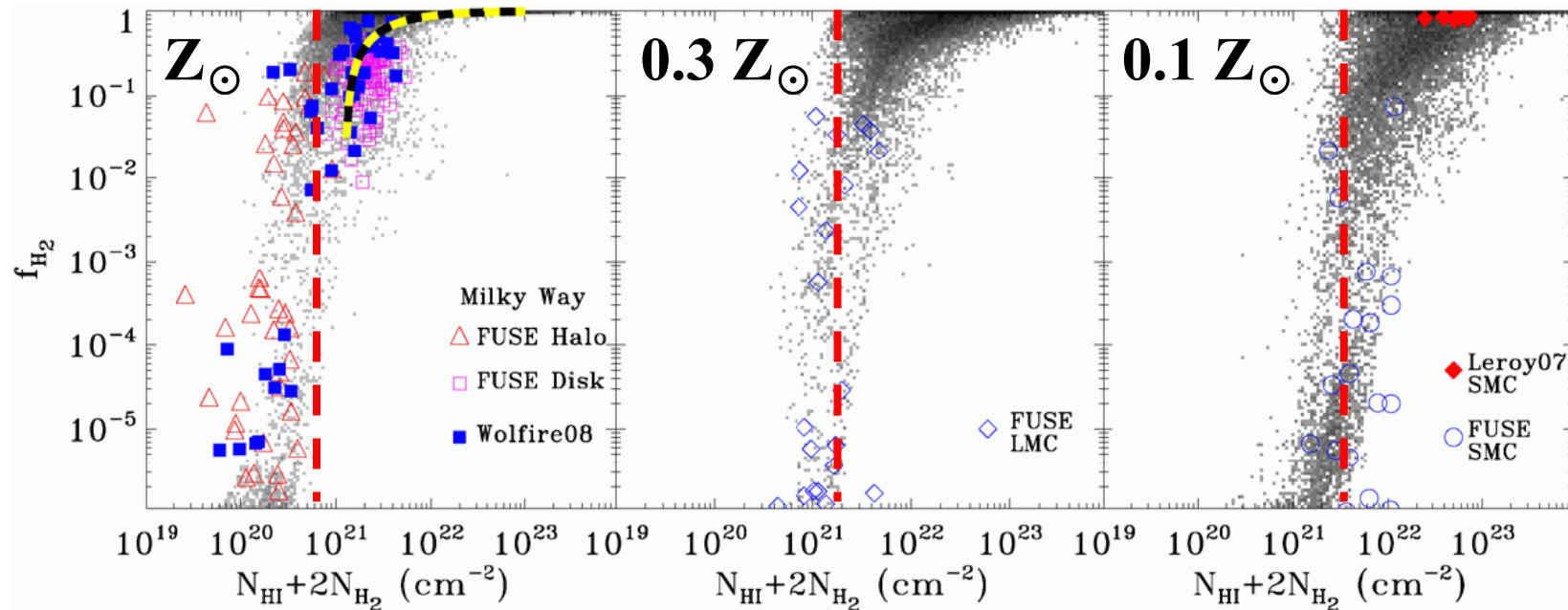


(Bigiel et al. 2008)

Transition from HI to H₂

* Transition column density is determined by **metallicity** (Gnedin et al. 2009).

Metal-poor molecular clouds do not contain much dust
⇒ **Critical N_{HI} becomes higher.**

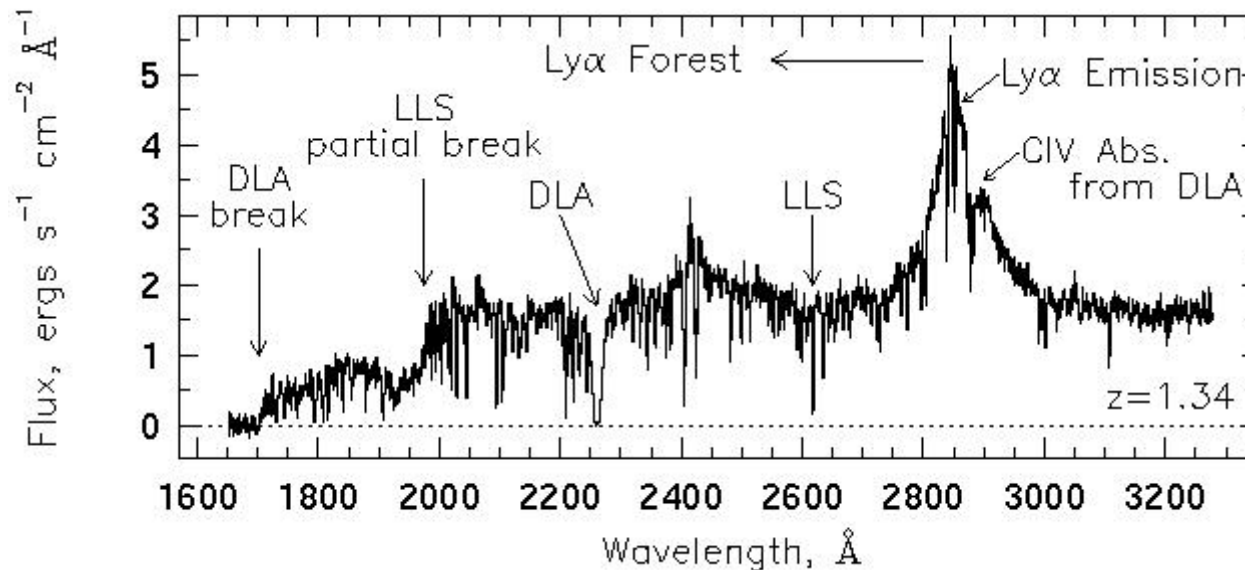
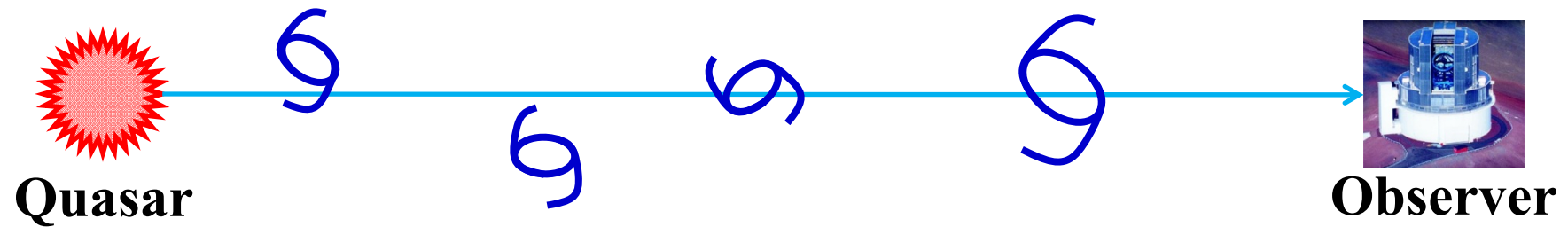


(Gnedin et al. 2009)

Exploration of galaxy formation via absorption

Observation of gas-dominated galaxies

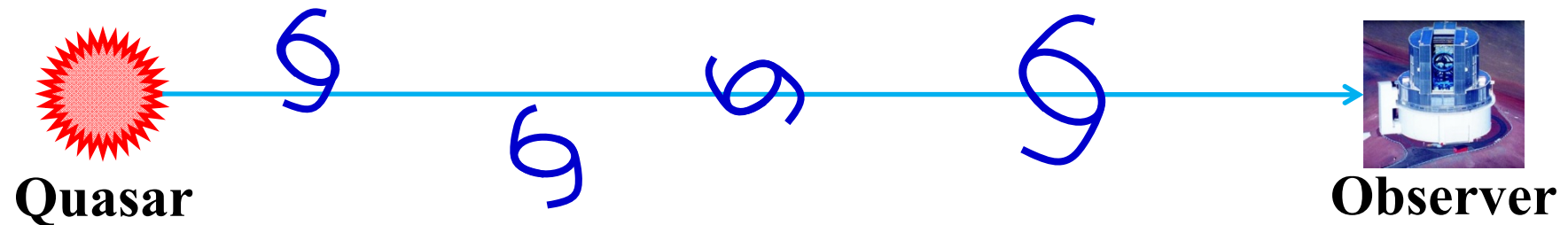
In optical, gas that is not yet turned into galaxies, or gas-dominant young galaxies can be efficiently detected through **QSO absorption lines**.



Exploration of galaxy formation via absorption

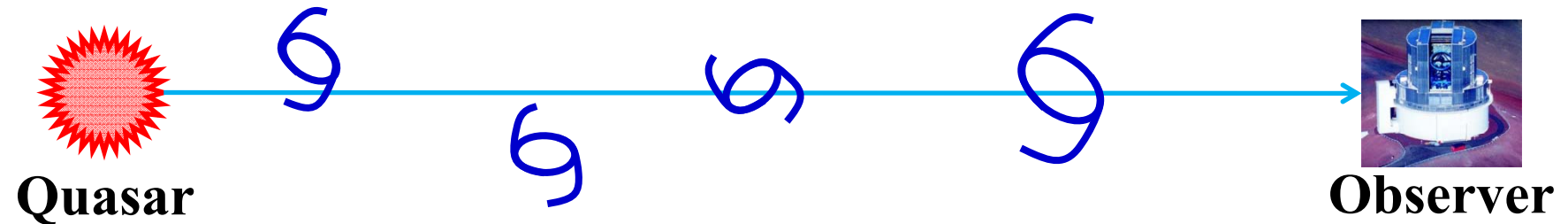
Observation of gas-dominated galaxies

In optical, gas that is not yet turned into galaxies, or gas-dominant young galaxies can be efficiently detected through **QSO absorption lines**.



QSO absorption line systems with particularly high H-column density are observed as **damped Lyman α systems (DLAs)**. Such systems are thought to be a **progenitor of present-day giant galaxies**.

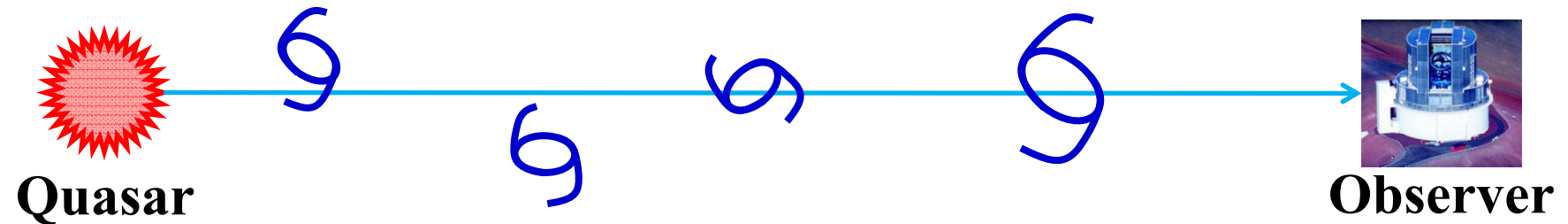
Observation of gas-dominated galaxies



Observations showed that these systems are gas-rich and metal-poor (e.g., Ledoux et al. 2003).

Also, DLAs can be a probe to explore the power spectrum of the large-scale structure at smaller scales.

Observation of gas-dominated galaxies

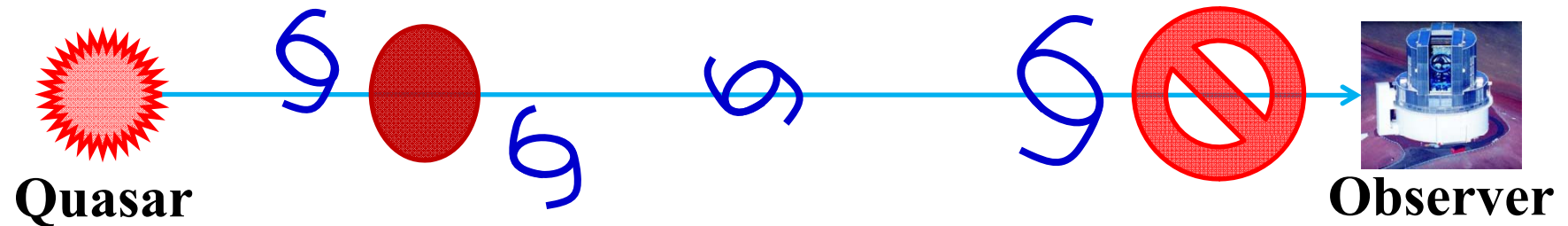


Observations showed that these systems are gas-rich and metal-poor (e.g., Ledoux et al. 2003).

Also, DLAs can be a probe to explore the power spectrum of the large-scale structure at smaller scales.

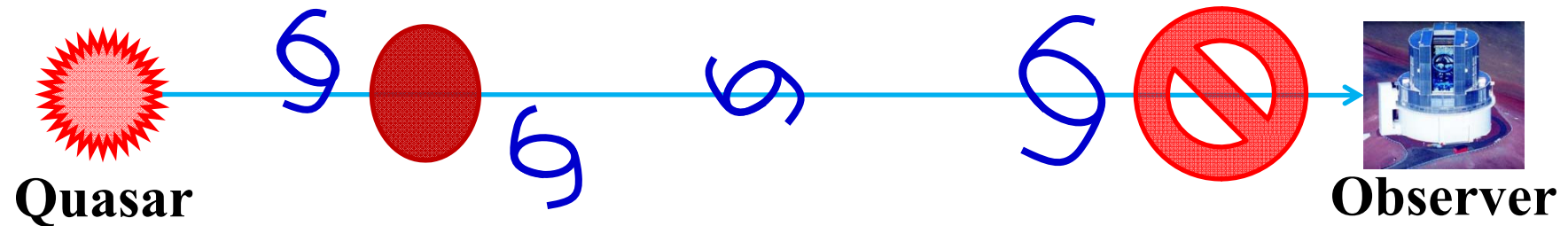
However, there is a fundamental problem in optical/UV-based observation!

Observation of gas-dominated galaxies



We want to detect absorption line systems. However, since the continuum emission from background quasars would be **very strongly extinguished through the systems with extremely high column density, such systems would be dropped from the initial selection (Vladilo & Péroux 2005).**

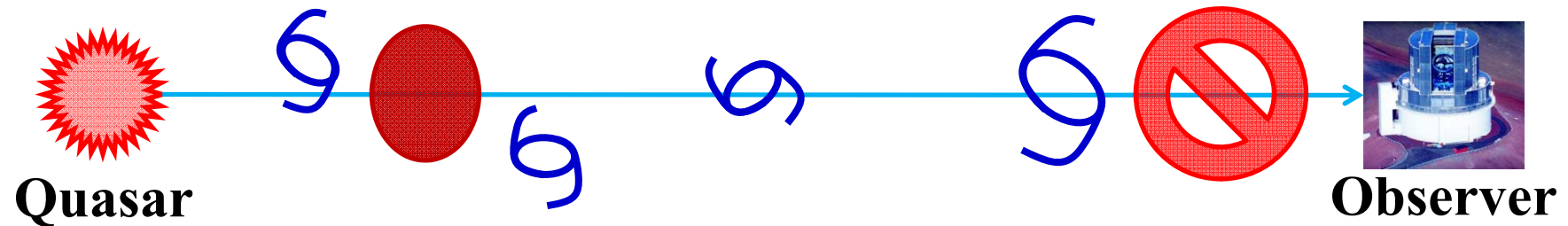
Observation of gas-dominated galaxies



We want to detect absorption line systems. However, since the continuum emission from background quasars would be **very strongly extinguished through the systems with extremely high column density, such systems would be dropped from the initial selection (Vladilo & Péroux 2005).**

But such a high column density systems are very possibly **just before the initial starburst.** Namely they are the systems fundamental to understand the cosmic SF history and what we indeed want to observe.

Observation of gas-dominated galaxies

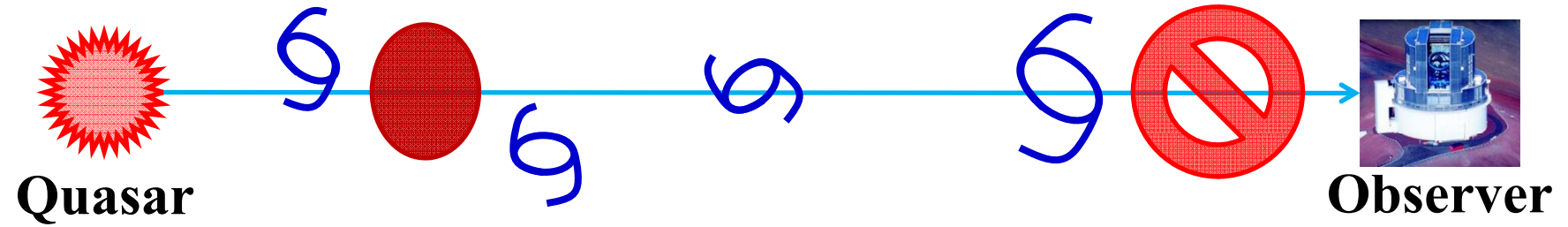


We want to detect absorption line systems. However, since the continuum emission from background quasars would be **very strongly extinguished through the systems with extremely high column density, such systems would be dropped from the initial selection (Vladilo & Péroux 2005).**

But such a high column density systems are very possibly **just before the initial starburst**. Namely they are the systems fundamental to understand the cosmic SF history and what we indeed want to observe.

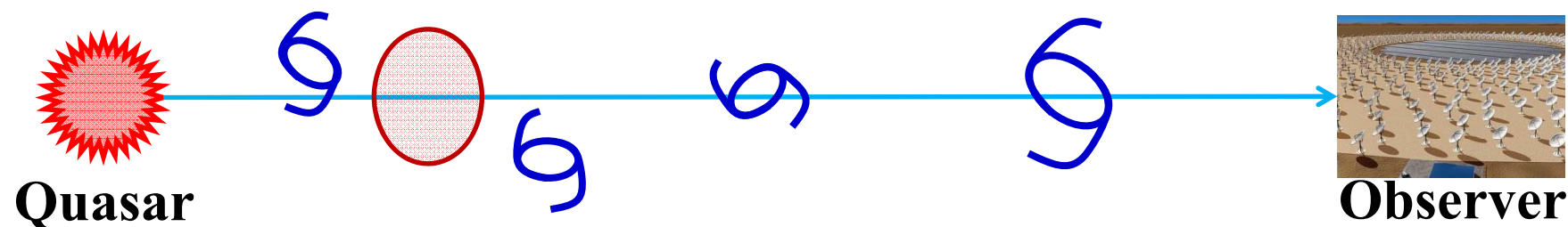
 **This selection bias is fatal!**

Observation of gas-dominated galaxies



How do we solve this fundamental problem?

Observation of gas-dominated galaxies



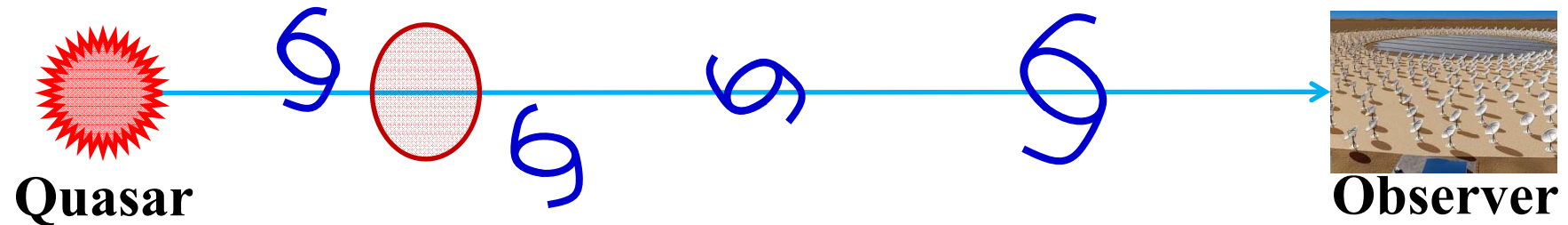
How do we solve this fundamental problem?

Select quasar continuum at radio, and explore 21-cm absorption line systems: best topic for SKA2!

Advantage to optical/UV absorption line observation:

1. At radio, **dust extinction is negligible.**
2. Because of small cross section, **very high column density systems can be observed.**

Observation of gas-dominated galaxies



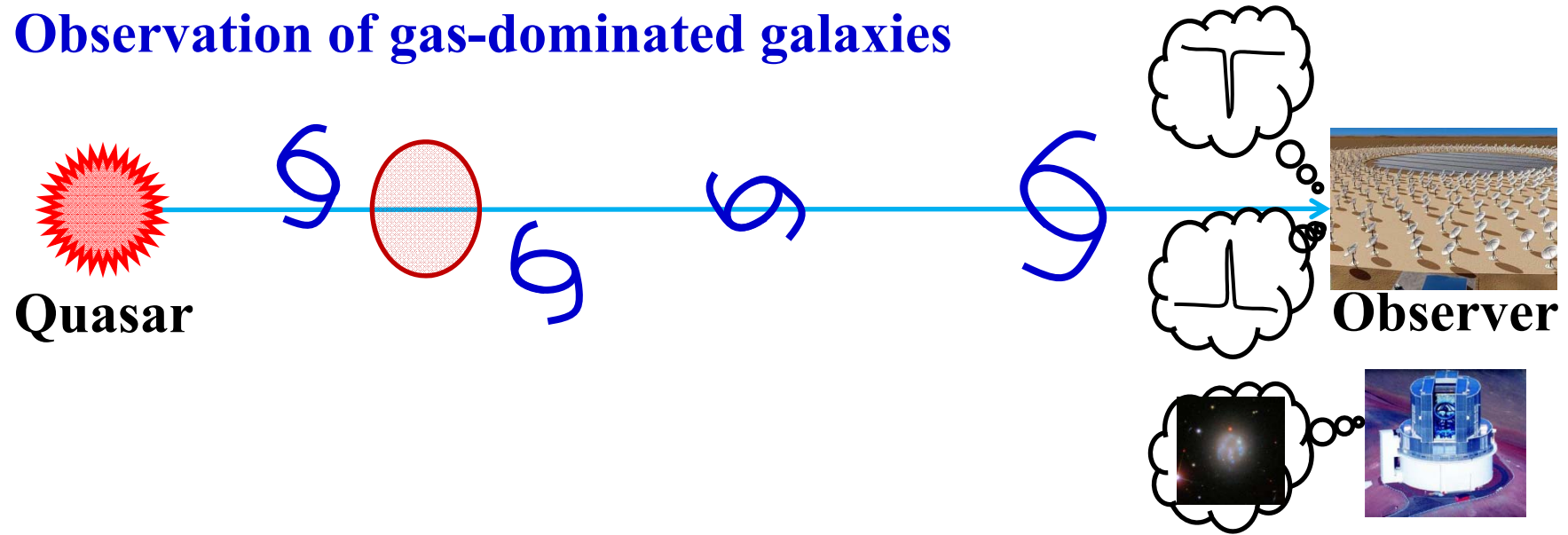
How do we solve this fundamental problem?

Select quasar continuum at radio, and explore 21-cm absorption line systems: best topic for SKA2!

Advantage to optical/UV absorption line observation:

1. At radio, **dust extinction is negligible.**
2. Because of small cross section, **very high column density systems can be observed.**

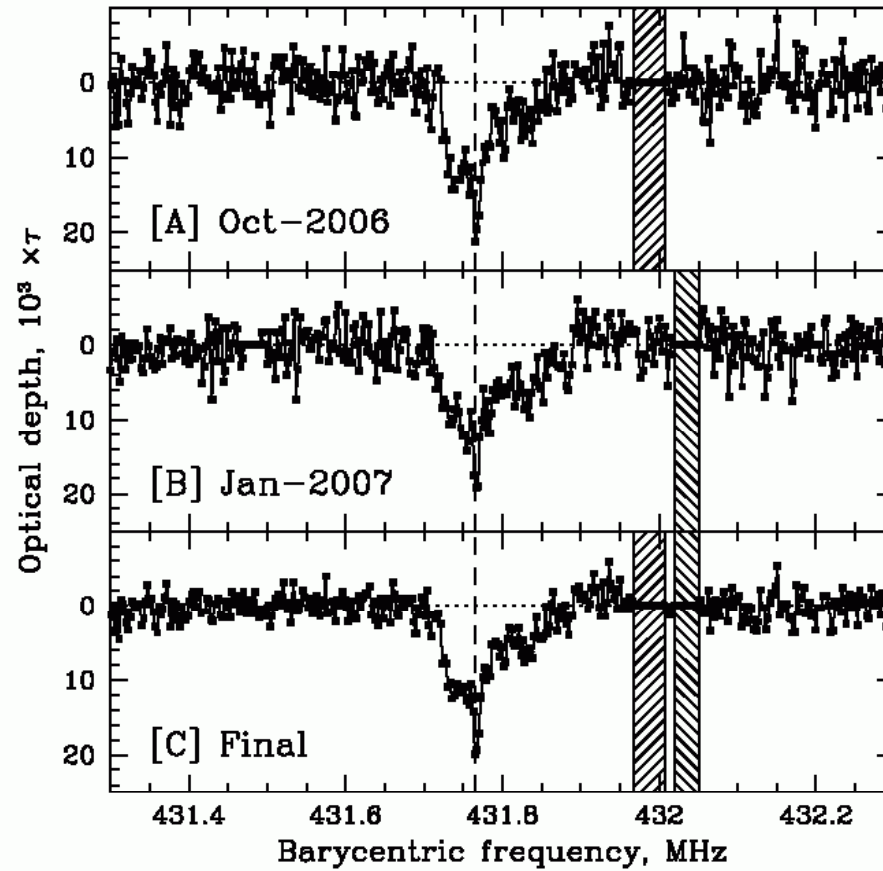
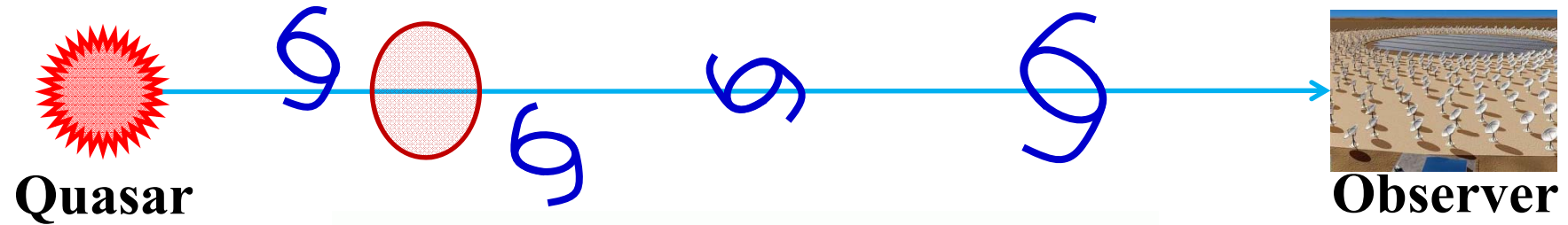
Observation of gas-dominated galaxies



Not only the continuum observation but also **ancillary observations like radio emission, optical etc.** will provide us with more information on the physics of the systems.

We are also developing theoretical models of galaxy evolution in parallel.

Observation of gas-dominated galaxies



(York et al. 2007)

Statistics of HI absorption line systems

Requirement for unbiased detection of DLAs:

1. For a typical QSO (100 mJy), **rms \sim 33 nJy is needed to detect $\tau \sim 0.001$.**
2. Since the noise level should be 1/3000 for a continuum, **the dynamic range must be 35 dB.**
3. **Pointed observation: to detect $\tau \sim 0.001$, a pointed observation with ~ 10 hr per one DLA by SKA-LOW is ideal.**



**Stay tuned to the SKA
As well as other wavelengths!**

